Modelling Integrated Scenarios of Land Use Change and Water Management in Two Mediterranean River Basins

Dissertation zur Erlangung des Doktorgrades an der Fakultät für Geowissenschaften der Ludwig-Maximilians-Universität München

vorgelegt von

Verena Huber García

eingereicht am 30. März 2020

1. Gutachter:	Prof. Dr. Ralf LUDWIG, Department für Geographie, Ludwig-Maximilians-Universität, München
2. Gutachter:	Prof. Dr. Karsten SCHULZ, Institut für Hydrologie und Wasserwirtschaft, Universität für Bodenkultur, Wien

Tag der mündlichen Prüfung: 24.06.2020

'People often ask, "What is the single most important environmental population problem facing the world today?" A flip answer would be, "The single most important problem is our misguided focus on identifying the single most important problem!'

Jared Diamond

Acknowledgements

I have long awaited this moment, but finally my thesis is coming to an end. Now it is time to thank the persons that have accompanied me in this journey.

First of all, I want to thank my supervisor Prof. Dr. Ralf Ludwig for offering me the opportunity to start this PhD project. While the progress of my work was not always straight-lined, Ralf always kept the view of the big picture, gave me good advice and offered pragmatic solutions. Despite his crowded agenda, he always tried to find a moment when I asked for it. I further appreciate Ralf's philanthropy, kindness and flexibility which made this collaboration really pleasant. I am well aware that this is not always the case and this is the reason I am so grateful for it.

I further want to thank Prof. Dr. Karsten Schulz for being my MICMoR mentor. It was always helpful to get some input from "outside". I appreciate also the numerous recommendation letters he wrote for me. Finally, I still profit from the very useful data analysis and R Statistics lessons during my master's programme.

Special thanks also to Dr. Kasper Kok and especially Peter Verweij from Wageningen University & Research for introducing me to iCLUE and helping me whenever I had questions.

I am grateful to all GLOBAQUA partners for their professional support to this thesis and the warm and amicable intercourse that prevailed in the project. I enjoyed the international and inter-disciplinary work a lot and hope to stay in contact.

A very warm thanks goes to Vera Erfurth, our caring secretary and 'working group mum'. Apart from solving all bureaucracy problems without me even noticing, she was always willing to chat, cheer us up and provided us with sweets and gossips.

Having occupied five different offices through the course of the years, the list of office mates I shared the room with is long: Dr. Swen Meyer, Dr. Janja Vrzel, Dr. Birgitta Putzenlechner, Amarachi Kalu, Fereshteh Kordrostami, Raul Wood, Florian Willkofer and Fabian v. Trentini. Even working in large shared offices is not always easy, I want to thank you for our professional discussions, chats and laughters. Thanks also for the colleagues I did not share the room with such as Michael Weber for the time spent at MICMoR events, Benjamin Müller for the help with R Statistics and Dr. Franziska Koch for lunch and coffee breaks spent together as well as for being an amazing climbing partner.

A special thanks goes to Dr. David Gampe, my office made for many years, co-MICMoR fellow and collaborator in GLOBAQUA. I enjoyed the time with you very much.

Thanks also to all other unnamed colleagues for the nice atmosphere which made work at LMU really pleasant for me.

I also want to thank the KIT research school MICMoR (Mechanisms & Interactions of Climate Change in Mountain Regions) in Garmisch-Partenkichen for giving me the possibility to take part in many interesting courses and conferences.

Finally, I thank my family for their support and their patience.

This work has been supported by the European Communities 7th Framework Programme Funding under Grant agreement no. 603629-ENV-2013-6.2.1-Globaqua.

Contents

List of Figures

List of Tables

List of Acronyms

AEI	Area Equipped for Irrigation
AIA	Actually Irrigated Area
CAPRI	Common Agricultural Policy Regional Impact
CEDEX	Centro de Estúdios y Experimentación de Obras Públicas
CGE	Computable-General Equilibrium
CHE	Confederación Hidrográfica del Ebro
CLC	CORINE Land Cover
CLUE	Conversion of Land Use and its Effects
CMI	Climate Moisture Index
CMIP	Coupled Model Intercomparison Project
CORDEX	Coordinated Regional Downscaling Experiment
DEM	Digital Elevation Model
EEA	European Environment Agency
EIM	European Irrigation Map
EPIC	Environmental Policy Integrated Climate
ESDB	European Soil Database
ESM	Earth System Model
ETC/ICM	European Topic Centre on Inland, Coastal and Marine Waters
EU-FP7	European Union 7th Framework Programme
EU-WFD	Water Framework Directive of the European Union
FAO	Food and Agricultural Organization of the United Nations
FSS	Farm Structure Survey
GCIA-CSI	GCIA Consortium for Spatial Information
GCM	Global Circulation Model
GDP	Gross Domestic Product
GEO	Global Environment Outlook

GIAM	Global Irrigation Area Mapping
GIR	Gross Irrigation Requirements
GMIA	Global Map of Irrigated Area
GTAP	Global Trade Analysis Project
GVA	Gross Value Added
HYDE	History Database of the Global Environment
IAM	Integrated Assessment Model
IAV	Impact, Adaptation and Vulnerability
IEA	Institut d'Estudis Andorrans
IIASA	International Institute for Applied System Analysis
INE	Instituto Nacional de Estadística
IPBES	Intergovernmental Science-Policy Platform on Biodiversity and Ecosystem Services
IPCC	Intergovernmental Panel on Climate Change
IUCN	International Union for Conservation of Nature
IWMP	Integrated Water Modelling Platform
JRC	Joint Research Centre
LAU1	Local Administrative Level 1
LPJmL	Lund–Potsdam–Jena managed Land model
LTM	Land Transformation Model
LUH1	Land Use Harmonization 1
LUH2	Land Use Harmonization 2
LUISA	Land Use-based Integrated Sustainability Assessment
LULCC	Land Use & Land Cover Change
LUMP	Land Use Modelling Platform
MAPAMA	Ministerio de Agricultura, Pesca, Alimentación y Medio Ambiente
MITECO	Ministerio para la Transición Ecológica
MDG	Ministry of Development of Greece
mHM	mesoscale Hydrological Model
MOLAND	Monitoring Land Use/Cover Dynamics
NCAR	National Center for Atmospheric Research
NSE	Nash-Sutcliffe Efficiency

NUTS	Nomenclature of Territorial Units for Statistics
OECD	Organization for Economic Co-operation and Development
PE	Partial Equilibrium
PESERA	Pan European Soil Erosion Risk Assessment
PIK	Potsdam Institute for Climate Impact Research
PoMs	Programmes of Measures
RBMP	River Basin Management Plan
RCM	Regional Climate Model
RCP	Representative Concentration Pathway
ScenarioMIP	Scenario Model Intercomparison Project
SIMPA	Sistema Integrado para la Modelización Precipitación Aportación
SLEUTH	Slope, Land use, Excluded land, Urban extent, Transportation and Hillshade
SPA	Shared Climate Policy Assumption
SRES	Special Report on Emissions Scenarios
SSP	Shared Socio-economic Pathway
SSW	Special Secretariat for Water, Greece
UFZ	Helmholtz-Zentrum für Umweltforschung
UNEP	United Nations Environment Programme
WCRP	World Climate Research Programme
WEI+	Water Exploitation Index Plus
WWTP	Waste Water Treatment Plant

Chapter 1

Introduction

1.1 Impacts of Land and Water Management

Since CRUTZER & STOERMER brought up the term "anthropocene" for the first time in 2000, it has become a widely used expression to emphasize the large impact human activities have on the earth and atmosphere in our current geological epoch (BRITISCH GEOLOGICAL SURVEY 2020, SIMPSON et al. 2019, SUBRAMANIAN 2019). With regards to the earth's surface, humans have by now induced land cover change on 18-29% of the ice-free land surface while an even larger part, 42-58%, has not been transformed but is still somehow managed to satisfy human needs (LUYSSAERT et al. 2014), see the global extend in figure 1.1.

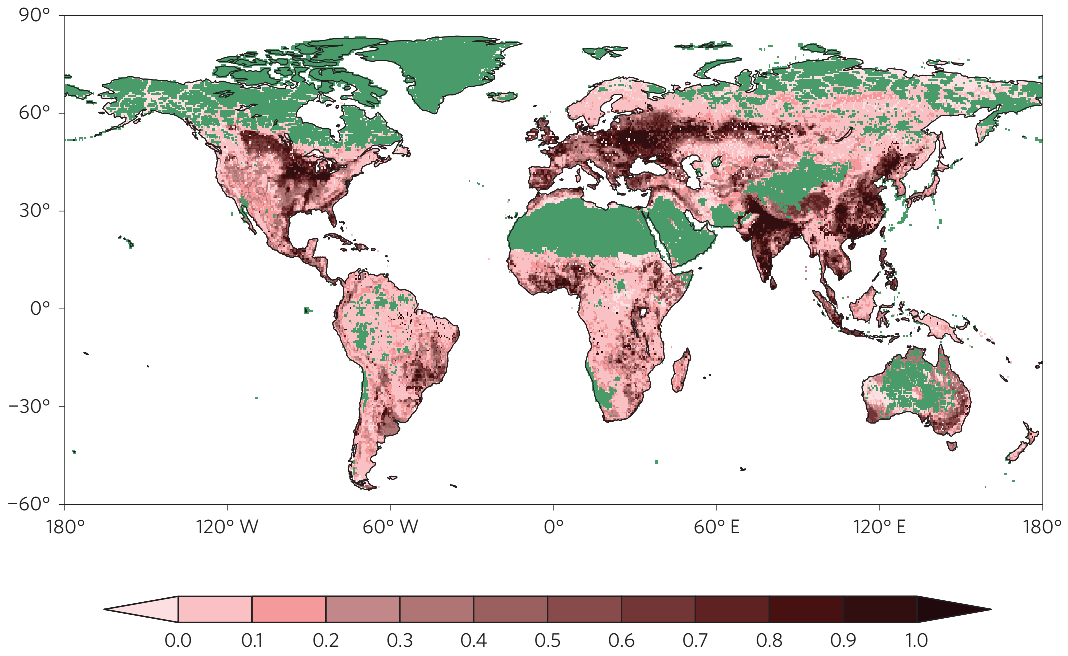

FIGURE 1.1: Spatial extent of land cover change and land management. The colour scale indicates which percentage of the cell's land cover was converted. Areas unaltered by humans such as wilderness and non-productive areas are displayed in green. Source: LUYSSAERT et al. (2014).

These modifications entail manifold consequences for almost any of the earth's spheres. They influence the global climate system by changing the biogeochemical composition of the atmosphere and the biogeophysical characteristics of the earth's surface (BROVKIN et al. 2013, LAWRENCE et al. 2016). Regarding the biosphere, Land

Use & Land Cover Change (LULCC), and in particular also the land management intensity (LAWRENCE et al. 2016, LUYSSAERT et al. 2014), is thought to be one of the main drivers of global biodiversity loss (HALLMANN et al. 2017, IPBES 2019, NEWBOLD et al. 2015). The intensification of agriculture has further come along with a strong increase in irrigation over the 20th century severely affecting the hydrological cycle (SIEBERT et al. 2015, WADA et al. 2014). Agriculture is nowadays by far the largest consumer of water accounting for 69% of global water extractions (FAO 2016a) and contributing to 40% of the global food production (FAO 2016b). Irrigated agriculture has led, however, to a variety of problems such as soil salinisation, erosion, reduced water quality and quantity, damage to aquatic ecosystems, groundwater depletion and salt water intrusion, to mention just a few (DOUGHERTY et al. 1995, WRIEDT et al. 2009a). Besides, the overexploitation of water resources for irrigation is considered to be one of the main drivers of water scarcity combined with a rising population (KUMMU et al. 2010).

Also in Europe, irrigation is a major water consumer accounting for over 60% of the total water abstractions (WRIEDT et al. 2009a). The Mediterranean region is particularly vulnerable to water scarcity due to a strong seasonal and spatial precipitation variability (RAMOS et al. 2012). According to the Water Exploitation Index Plus (WEI+), an indicator designed by the European Environment Agency (EEA) to assess water scarcity across Europe by relating true water abstraction with renewable water resources (ZAL et al. 2017), almost all European river basins considered water scarce during summer, i.e. with an WEI+ above 20%, are located in the Mediterranean (EEA 2018). Many of them reach values way beyond 40%, the threshold indicating severe water scarcity.

Meanwhile, many studies agree that the Mediterranean region will suffer from increased water scarcity in the future caused by a combination of higher water demands and a simultaneous reduction of the water availability due to climate change (FADER et al. 2016, FORZIERI et al. 2014, GAMPE et al. 2016, IPCC 2014a, KONZMANN et al. 2013, VAUTARD et al. 2014). This implies that the pressure on water resources in the Mediterranean will increase in the future and lead to an even stronger overexploitation of resources which will exacerbate the competition on water uses and may even raise the risk for conflicts (DU et al. 2014).

As a consequence, it is of utmost importance to find solutions for a sustainable management of water resources if we want to guarantee a good quantity and quality of water in the future for all uses. In Europe, a tool for integrated river basin management already exists: The Water Framework Directive of the European Union (EU-WFD) adopted in 2000 (EUROPEAN COMMISSION 2019c). One of its aims is to promote the sustainable use of water through so called River Basin Management Plans (RBMPs). But are the existing plans sustainable enough? Are the measures really effective and adaptive to dynamic changes that lay ahead? And what about the influence specific measures have on the environment?

To answer such questions, scenario analysis is an indispensable tool. Widely used in environmental sciences, it allows to test several alternative futures under a set of simple conditions (VELDKAMP & LAMBIN 2001), analyse their impact and finally be able to give recommendations on the best management strategies. At present, nearly all climate change impact, adaptation and vulnerability (IAV) studies working with scenarios are based on the current Representative Concentration Pathways (RCPs) and Shared Socio-economic Pathways (SSPs) promoted by the Intergovernmental Panel on Climate Change (IPCC), which allow for comparability and consistency. They provide, however, only global scenarios and storylines which are difficult to apply to regional studies. Besides, they do not take into consideration the already existing specifications in the various RBMPs and vice-versa. This is, however, needed to provide policy relevant information and inputs for further IAV studies. The presented thesis contributes to closing this substantial gap in land use change and water resources research.

The downscaling of these global scenarios and the modelling of integrated land and water use scenarios for two Mediterranean river basins, the Ebro in Spain and Evrotas in Greece, build the core of this thesis. Integration in this respect means that both climate and socio-economic projections were taken into account. The downscaling was achieved by introducing also recommendations from experts and local stakeholders into the basin specific scenarios. This information was used to run the land use change model iCLUE (VERWEIJ et al. 2018) and produce spatially distributed land use maps for two different scenarios in each of the test sites for the time horizon 2050. The maps were combined with water use statistics and projections reported in the RBMP, in case of the Ebro, and by the Greek Ministry of Development, in case of the Evrotas. By this means, it was possible to distribute the official statistics in space and evaluate the present situation. Furthermore, the feasibility of two opposed future scenarios was analysed and, in case of the Ebro, also contrasted with the expected water availability in both scenarios represented by the Climate Moisture Index (CMI) and already available runoff modelling results.

The river basins presented in this thesis are part of a wider set of catchments investigated in the EU-FP7 project GLOBAQUA, which deals with the management of the effects of multiple stressors, such as climate change and land use change, on aquatic ecosystems under water scarcity (NAVARRO-ORTEGA et al. 2015). The project provided the thematic frame and funding for this thesis.

1.2 Motivation and Scope of this Thesis

The above mentioned consequences of the over-exploitation of water resources combined with the expected reduction of water availability in southern Europe leads me to my first hypothesis:

1. Under conditions of climate and land use change, current water management practices and even long-term RBMPs are insufficient to meet the goals of the EU-WFD in Mediterranean river basins.

In case of the Ebro, the hydrological plans have been repeatedly subject to criticism for being unsustainable: The Spanish National Hydrological Plan of 2001 (Ley 10/2001, 5th of July) - by now overruled - foresaw water transfers from the Ebro to other regions to promote irrigation (BISWAS & TORTAJADA 2003). The RBMPs of the 1st (2010-2015) and 2nd (2015-2021) cycle have been largely criticised for not addressing substantial environmental problems such as the poor water quality, the inadequate regulation and protection of the delta and the building of new dams in the Pyrenees which negatively affect the population, biodiversity, natural flood protection and water quality (FRANQUET I BERNIS 2009, MARCOS FERNÁNDEZ 2016, PIÑOLS 2016). Besides, the long-term irrigation plans reported in the RBMP 2015-2021 sum up to additional 47% of irrigated area and a related 30% increase of the water demand (CHE 2015). Already now, the long-term mean annual WEI+ lies around 21% and is therefore considered to be water scarce (ETC/ICM 2016).

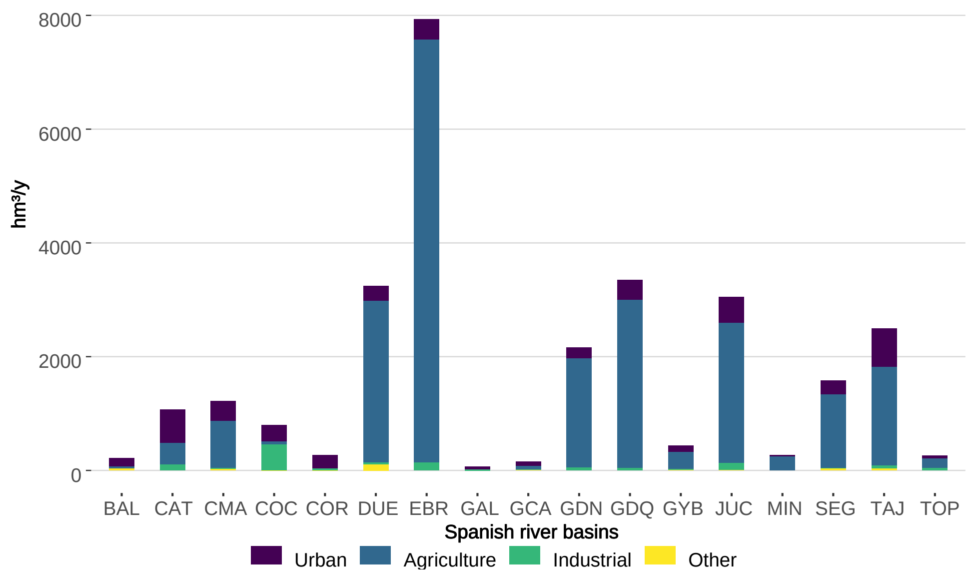

FIGURE 1.2: Water used per sector [hm^3/year] to satisfy the demands of Spanish river basins for the hydrological year 2016/2017. The Ebro River Basin is abbreviated with "EBR". "DUE" stands for Duero. Source: MINISTERIO PARA LA TRANSICIÓN ECOLÓGICA (MITECO, 2018).

As figure 1.2 impressively demonstrates, the water used for agriculture in the Ebro, 99% of it for irrigation (CHE 2013, Annex III), exceeds by far the water used in other Spanish river basins while it is only the second largest catchment after the Duero (MAPAMA 2007).
At the same time, a study commissioned by the Spanish Ministry for Agriculture, Fishery, Nutrition and Environment (MAPAMA) recommends to take into account climate change related runoff reductions in the RBMPs for 2039 of -5% as compared to the period 1940-2006 in case of the Ebro for a moderate scenario (RCP 4.5) and 9% in an extreme scenario (RCP 8.5) (CEDEX 2017). For the far future the reductions to take into consideration are even higher. The consequences of future water scarcity for the Ebro River basin, highly specialised on irrigated agriculture, can therefore be expected to be substantial.

In case of the Evrotas, it is difficult to quantify the WEI+ due to a lack of comparable data. Nevertheless, it seems to be clear that the irrigation expansion to olive trees, which has increased the irrigation demand by 70% since the beginning of the 1990s (SKOULIKIDIS et al. 2011), now gives cause for drying out large parts of the river network during summer which priorly did not (NIKOLAIDIS et al. 2009).

Trajectories of future land and water use at the basin scale are highly uncertain. While many assumptions can be and are often easily made, meaningful and reasonable projections must be embedded in wider narratives of global change to remain traceable, explainable and logically consequential. However, the methodological framing to conduct this ambitious task is largely missing. Thus, my second hypothesis addressing the applied method reads as follows:

2. The future projection of land and water uses at the basin-scale requires the downscaling of global change narratives and the modelling of integrated scenarios of climate and land use change.

It is important to develop sustainable land and water management practices adapted to more difficult future conditions and study the impacts of future changes. As KEBEDE et al. (2018) point out, "site-specific and policy-relevant integrated assessments need information at finer resolution" which the global scenarios defined by RCPs and SSPs mentioned above, however, are not able to provide.
Many land use and water modelling activities already exist. But why are they not sufficient to carry out regional or local IAV studies? With regards to spatially explicit water use or irrigation maps, there are only very few products available that go beyond recording the current state and also providing future projections, as the examples in chapter 2.5.3 will show. It is further difficult to find datasets taking into account not only agricultural water uses but also other sectors. Besides, at this stage there is not a single product including simulations for several different future scenarios which are necessary to carry out scenario analyses. In addition, the definition of the scenarios does not follow the RCP-SSP-scenario framework, which was a main objective of the GLOBAQUA project and of the present study. The situation is better for land use/cover simulations since the Land Use Harmonization 2 (LUH2) dataset is available that provides future simulations for most RCP-SSP combinations (HURTT et al. in prep.). However, being a global dataset, the resolution is too coarse for detailed analyses at the basin-scale or below. This equally applies to most available water use or irrigation maps.

Besides, the uncertainty of future land use projections across models is substantial (RIAHI et al. 2017). ALEXANDER et al. (2017) come to the same conclusion both for global and European land use models as figure 1.3 illustrates. The differences in absolute values already for the historic period for cropland, forest and especially pasture displayed in the upper part of the figure are noticeable. Also after normalising the starting point to historic Food and Agricultural Organization of the United Nations (FAO) values, the spread of results from different models and scenarios remains remarkable. These discrepancies are caused by different model assumptions underlying global land use models (POPP et al. 2017). MEIER et al. (2018) report that large differences exist also between global irrigation maps. For this reason, it is necessary to downscale global scenarios and model them at smaller scale to be able to adapt them to the local characteristics of each study area.

The third hypothesis results from this requirement:

3. Combining sectoral water use statistics with land use change models provides an efficient and transferable method to deliver projected water use maps as planning tools for

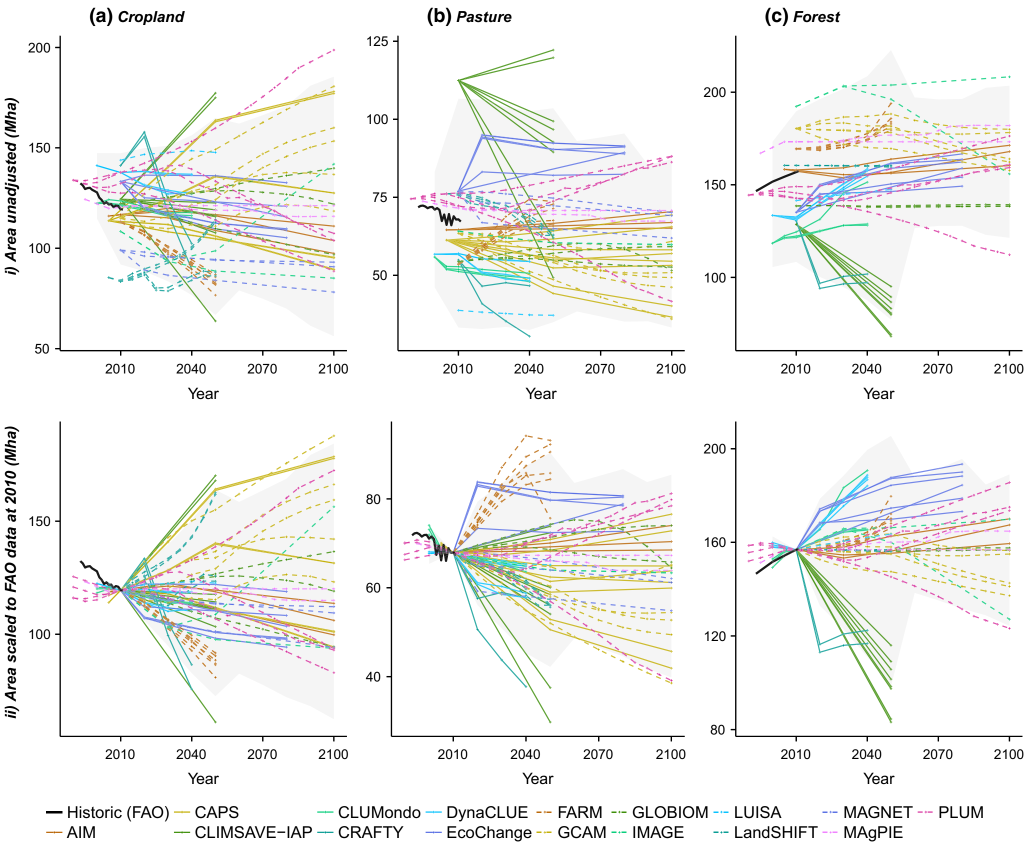

FIGURE 1.3: European land cover modelled with 16 models over a total of 64 scenarios for the EU27 member states. The absolute areas are shown in (i) and the areas scaled to match the historical data in 2010 are shown in (ii). Source: ALEXANDER et al. (2017).

users and policy makers.

Being developed at the global scale, the datasets and scenarios described in chapter 2.5.2 and 2.5.3 are not able to include more detailed information on the special characteristics of the study area, such as local stakeholder knowledge or basin-specific water use statistics. As a consequence, they lack local relevance and may be meaningless as policy support since they do not refer to the RBMPs and consequently neither to the EU-WFD. Since official water statistics are, however, available for the GLOBAQUA case studies, the attempt was made to use this information for making a point on the sustainability of the adopted plans in each of the case studies.

The scope of this study is therefore to provide spatially explicit land and water use maps, differentiated by sectors, that match the following criteria:
a) meet the methodological standards of the climate and water research community
b) utilize the RCP-SSP scenario framework to develop and provide regional scenarios of global change at the river basin scale
c) comply with the regulatory framework of the EU-WFD.

1.3 Structure of this Thesis

As shown in figure 1.4, the scenarios modelled rely on the global RCPs and SSPs which were further regionalised to meet the characteristics of the GLOBAQUA project. Besides, the regional EURO-CORDEX climate data, again realisations of the RCPs, were downscaled and bias-adjusted as part of the GLOBAQUA project and served as input to the land use modelling with the iCLUE model. The basin specific scenarios, defined through local stakeholder workshops carried out by a project partner, provided useful information for the parametrisation of the land use model, in particular for the future land use demand, see chapter 5.2. A further important part of this thesis is the derivation of water use maps by using official water use statistics, described in chapter 5.4. The resulting land and water use maps can be found in chapter 7. Finally, for the Ebro the attempt is made to compare the water use maps to the expected water availability represented by the CMI and spatially distributed runoff modelled by a GLOBAQUA project partner, see chapter 7.8 and HUBER GARCÍA et al. (in prep.). To test the transferability of the approach, it was also applied to the Evrotas. The results of this validation experiment are summarised in chapter 8. Chapter 9 provides a reflection on the research objectives and hypotheses differentiating between Ebro and Evrotas. Besides, it discusses the transferability of the approach in space and scale and gives some final recommendations for the EU-WFD.

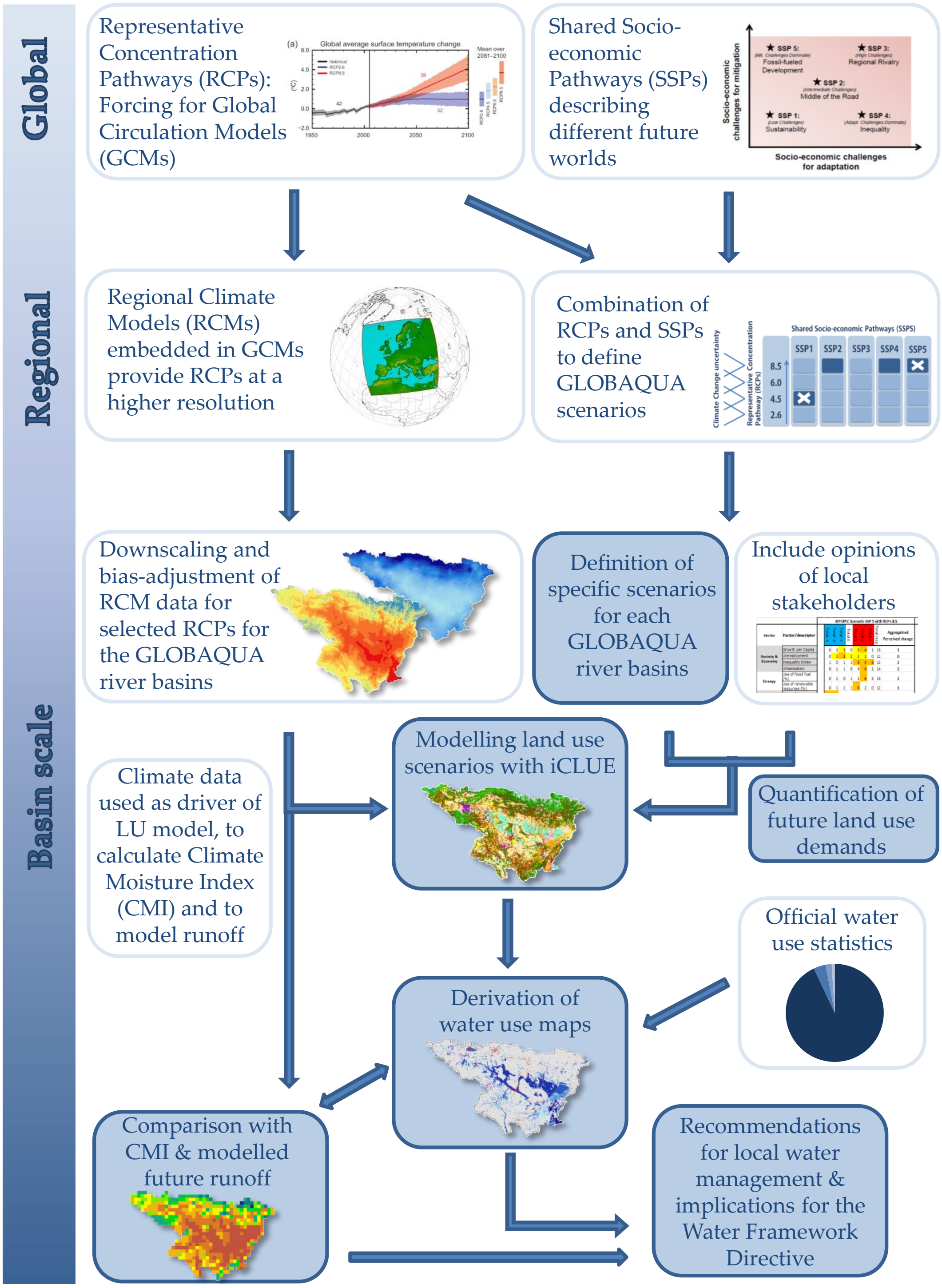

FIGURE 1.4: The location of this thesis relative to the global scenario framework and the work carried out in GLOBAQUA as well its workflow. The boxes highlighted in blue constitute the present study.

Chapter 2

Framing this Thesis

2.1 Definition of Important Terms

There are several terms repeatedly coming up in this thesis that have to be clarified first:

Water scarcity is the imbalanced relation between the water needed to satisfy the demand of different human activities (drinking, irrigation, industry etc.) and the availability of exploitable water (ZAL et al. 2017). It is closely related to the consequences of water management (FAERGEMANN 2012, ZAL et al. 2017).

Water demand is the quantity of water of a specific quality required for different human activities assuming that water availability is not a limiting factor. This is therefore a theoretical term that is estimated or calculated (FAERGEMANN 2012).

Water use is used hereafter as synonym for water demand as the exact definition of these terms is often unclear. According to FAERGEMANN (2012) it is rather a synonym for water consumption, i.e. the consumptive use of water. Other authors like GONZÁLEZ-CEBOLLADA 2016 understand 'water use' as the water withdrawn from the system and used for various purposes, out of which a share may return to the system.

Water consumption is the water consumed by the end users. This excludes the water going back into the system such as return flows from agriculture or recycled water (FAERGEMANN 2012).

Land cover summarises all properties of a land surface at a given location (e.g., biophysical, morphological, topographical) and is usually described by the vegetation growing at this point and the soil characteristics (rocks, sand etc.) (PONGRATZ et al. 2018).

Land use: relates according to PONGRATZ et al. (2018) "to the purposes or functions that humans assign to a given location and how humans interact with the land". 'Land cover' and 'land use' are often not clearly separated in the literature. This is also the case for the CORINE Land Cover (CLC) datasets often referred to hereafter which mixes land *covers* like various forest types and 'sclerophyllous vegetation' with 'permanently irrigated land' or 'sport and leisure facilities', which clearly indicate land *uses*. For the purpose of the present thesis I stick to the term 'land use' to describe the result maps.

For the present thesis, I will stick to the unit hm^3, i.e. $1 \times 10^6\ m^3$, for total water volumes (demands, renewable water resources) widely used in water management. The final water use maps are in mm/y to allow for comparability with spatially distributed variables of the water balance such as precipitation or modelled runoff.

2.2 The EU Water Framework Directive

Land and water management is greatly influenced by various regional, national or international laws and policies. An important tool is the Water Framework Directive of the European Union (EU-WFD) adopted in 2000 that promotes the sustainable use of water "based on a long-term protection of available water resources" and "gives priority to environment conservation through participatory and consultative programs" (EUROPEAN COMMISSION 2007, EUROPEAN COMMISSION 2019c). The directive initially aimed at achieving a good qualitative and quantitative status of all ground and surface waterbodies in Europe by 2015. As part of the a EU-WFD, river basin districts were established as planning units which means that water management is carried out according to the natural geographical and hydrological boundaries of a river basin, rather than administrative borders (EUROPEAN COMMISSION 2019b). Individual River Basin Management Plans (RBMPs) collect all the measures to be applied in order to achieve the aims of the EU-WFD (RICHTER et al. 2010). They are specially geared to the needs of each river basin. In 2009, the first management cycle started establishing also the first RBMPs which have to be revised and updated every six years, see the timeline in figure 2.1.

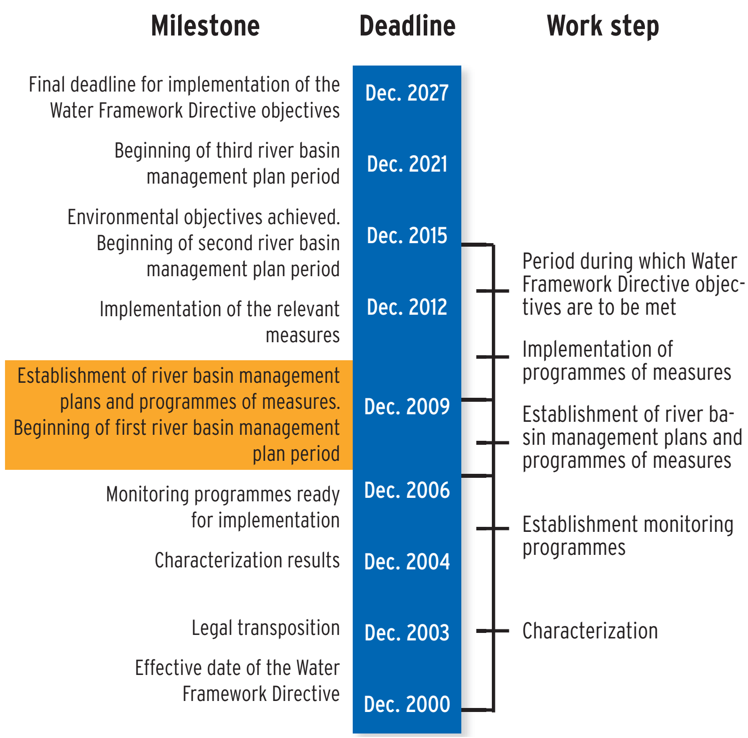

FIGURE 2.1: The implementation timeline of the EU Water Framework Directive. Source: RICHTER et al. (2010).

Generally speaking, substantial efforts have been made to implement the EU-WFD and improvements are visible all across Europe (EUROPEAN COMMISSION 2019a). Nevertheless, by February 2019 less than half of all European surface waters were in good status and the achievements very heterogeneous. This shows that the path towards full compliance of the EU-WFD until the end of the third cycle in 2027, which was set as final deadline for reaching a good water quality and quantity status, is now very challenging (EUROPEAN COMMISSION 2019d).

2.3 The Water Exploitation Index Plus

The Water Exploitation Index Plus (WEI+) introduced in 2012 is one of the main indicators that the European Environment Agency (EEA) uses to regularly assess water scarcity across Europe as insufficient water quantity is one of the main issues which Europe has been encountering (ZAL et al. 2017). The aim is to inform policy makers on the severity of water scarcity. It is calculated as follows:

$$WEI+ = \frac{Abstractions - Returns}{Renewable\ Water\ Resources} \tag{2.1}$$

Abstractions are the totality of water withdrawn from freshwater resources for human uses and *returns* the water returned back to the environment, usually accompanied by a certain decrease in quality (ZAL et al. 2017). The difference between abstraction and return is referred to hereafter also as "water consumption" see chapter 2.1. Regarding the denominator of the equation, there are several ways to define the *renewable water resources* depending on the data availability. The easiest is to set it equal to the natural outflow of a given territory (FAERGEMANN 2012) which was also done hereafter.
The WEI+ can be calculated for various spatial units and also for any desired time frame such as annual averages as well as on seasonal or monthly basis (ZAL et al. 2017). So far, there are no commonly agreed thresholds, so the ones proposed by RASKIN et al. (1997) are used where a water consumption to resource ratio above 20% indicates water scarcity whereas values above 40% designate severe water scarcity.
The policy relevance of the WEI+ is high, particularly in light of the EU-WFD which requires Member States to promote the sustainable use of water (FAERGEMANN 2012, ZAL et al. 2017). Nevertheless, until now no formal quantitative targets have been pronounced in relation to the WEI+ (ZAL et al. 2017).

2.4 The GLOBAQUA Project & its Case Studies

The GLOBAQUA project was designed to analyse how future water-related management practices and policies, in particular the EU-WFD described in chapter 2.2, need to be adapted "to minimise the ecological, economical and societal consequences of ongoing global change" (NAVARRO-ORTEGA et al. 2015). More precisely, the project focused on the impacts multiple stressors have on aquatic ecosystems, such as for example changes of land and water use (NAVARRO-ORTEGA et al. 2015).

The project was funded by the European Union 7th Framework Programme (EU-FP7) and ran from February 2014 to January 2019. Under the title "managing the effects of multiple stressors on aquatic ecosystems under water scarcity" GLOBAQUA gathered an international and interdisciplinary team of researchers from various fields such as hydrology, chemistry, biology, geomorphology, economy and sociology.

To investigate the value of different adaptation measures, various GLOBAQUA specific integrated scenarios were developed for the future and the implications for interlinked multiple stressors simulated (NAVARRO-ORTEGA et al. 2015). The spatially distributed land use and water management scenarios developed as part of this thesis and described hereafter were the basis for the whole modelling chain.

The GLOBAQUA case studies included six river basins in Europe and Northern Africa displayed in figure 2.2: The Adige in Italy, the Anglian in the UK, the Ebro in Spain, the Evrotas in Greece, the Souss-Massa in Morocco and the Sava in South-eastern Europe. Out of these, the experimental and modelling activities in the project focused on the ones located on the European continent. Consequently, site-specific land and water use scenarios were developed for the Adige, Ebro, Evrotas and Sava taking into account the very divergent characteristics and scales of each river basin. The present work will focus on the scenarios developed for the Ebro, a rather large river basin covering 85000 km^2, where the implementation showed good results. The Evrotas, with 2410 km^2 considerably smaller, was as validation site to demonstrate the spatial and multiscale transferability of the applied methods. The data availability is good for both river basins and they share characteristics such as the predominant Mediterranean climate and the high water use for irrigation. For the Adige and Sava, the derivation of water use maps did not work as well due to missing data or inconsistencies described in HUBER GARCÍA et al. (2018), which is the reason the results will not be presented hereafter.

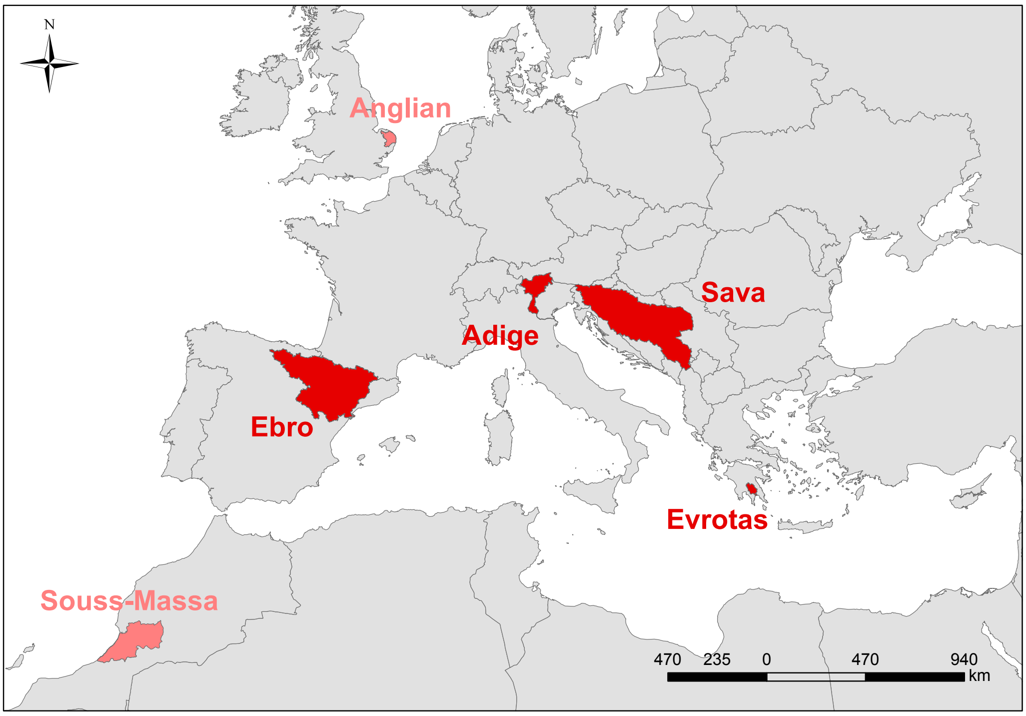

FIGURE 2.2: The GLOBAQUA case studies. The darker colour indicates the experimental study areas.

2.5 State of the Art

Modelling allows testing different hypotheses or scenarios and is therefore one of the key elements in climate impact research. The lack of spatially distributed and high resolution data is, however, a common problem among modellers that often limits the explanatory power of the model outcomes. This is even more the case when analysing scenarios as projections for many variables are often missing. The input data needed to run a model vary substantially depending on the study's purpose, whereas land and water use information is usually indispensable for environmental studies (HUBER GARCÍA et al. 2018). The following chapters give an overview of current land and water use modelling activities as well as of scenarios used in environmental and climate sciences.

2.5.1 Scenario Development

As stated by MOSS et al. 2010, "the goal of working with scenarios is not to predict the future, but to better understand uncertainties in order to reach decisions that are robust under a wide range of possible futures". In the last decades scenarios, and in particular global long-term scenarios, have become an indispensable tool in climate change and environmental research to analyse complex systems and possible future developments (O'NEILL et al. 2017). In fact, as VAN VUUREN et al. (2014) point out, it is necessary to apply a common set of scenarios in the research community analysing climate change IAV to facilitate the integration between research disciplines, simplify the access to literature independently from the discipline, scale or region and provide a valuable basis for scientists that do not have the capacities to develop their own scenarios. Many of the well-known international institutions have also used alternative futures for their analyses resulting in some of the most prominent sets of scenarios of the past years such as the United Nations Environment Programme (UNEP) Global Environment Outlook (GEO) scenarios (UNEP 2004), the Millenium Ecosystem Assessment (ALCAMO et al. 2005) or the IPCC Special Report on Emissions Scenarios (SRES) (NAKICENOVIC et al. 2000). The latter ones have provided the basis for climate model projections in Phase 3 of the Coupled Model Intercomparison Project (CMIP) (MEEHL et al. 2007) and a wide range of climate impact studies that have found entrance into the IPCC Fourth Assessment Report (NAKICENOVIC et al. 2000). Similar to previous scenarios, the SRES scenarios were developed following a forward approach handing on the results from one research community to the next: Socio-economic scenarios were developed first to further derive emission scenarios which provided the basis for radiative forcing and climate modelling. Finally, the climate scenarios were used to carry out IAV studies (MOSS et al. 2010). This, however, is a lengthy process that leads to inconsistencies in the results of the different research groups due to time delays (MOSS et al. 2010).

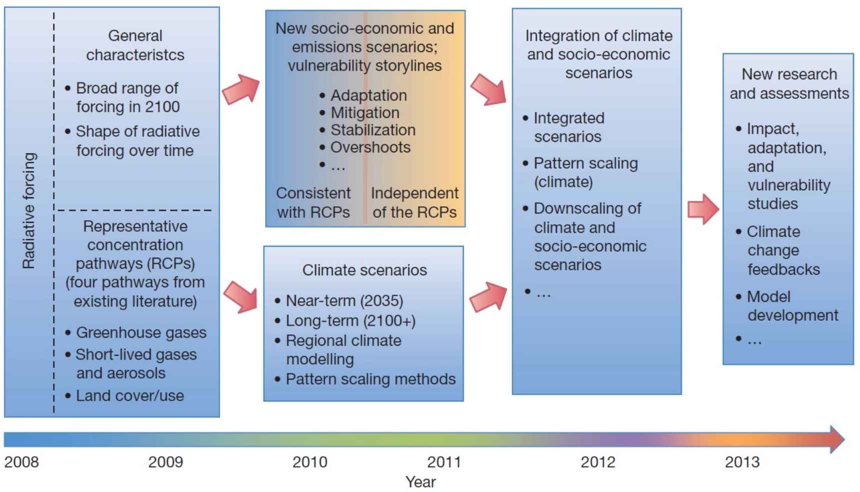

FIGURE 2.3: The parallel scenario development process. Source: MOSS et al. (2010).

Slowly, the SRES scenarios started to become outdated with more and more new data and observations being available. Besides, the interest in climate scenarios that analyse also possible mitigations to climate change was huge, a feature that the ‘no climate policy’ SRES scenarios did not address (MOSS et al. 2010). Eventually, in 2006 the IPCC called on the research community to develop a new set of global integrated scenarios following the IPCC’s principle of being policy-relevant without being policy-prescriptive (IPCC 2010, MOSS et al. 2010). To overcome the disadvantages of the old forward approach, the new generation of scenarios was developed using an inverse and parallel approach, see figure 2.3, where the interesting outcomes for climate change research were identified first (O’NEILL et al. 2014, VAN VUUREN et al. 2014). This means, that the process started with the selection of four scenarios of future radiative forcing from literature which represent alternative trajectories of the concentrations of greenhouse gases and aerosols in the atmosphere (VAN VUUREN et al. 2011). The actual levels of radiative forcings were modelled with Integrated

Assessment Models (IAMs) resulting in the new Representative Concentration Pathways (RCPs) (VAN VUUREN et al. 2011). They are expressed as the relative change in radiative forcing between the year 2100 and pre-industrial times (year 1750) in net energy flux into the climate system per unit of area (KEBEDE et al. 2018). A new central feature of the RCPs is that they are not linked to a specific set of socio-economic conditions, "but can result from different combinations of economic, demographic, policy and institutional futures" (MOSS et al. 2010). The word "pathway" was further chosen deliberately to emphasize that apart from the long-term concentration also the trajectory over time is of interest (MOSS et al. 2010). In the second, parallel phase of the scenario development process, sketched in figure 2.3, climate modelers produced RCP-based climate change projections as part of CMIP Phase 5 (O'NEILL et al. 2016, VAN VUUREN et al. 2014) which were the basis for the IPCC Fifth Assessment Report (IPCC 2013). At the same time, alternative future societal scenarios were developed in a collaborative effort by researchers of various disciplines (MOSS et al. 2010, O'NEILL et al. 2016). The resulting five qualitative storylines, the so called Shared Socio-economic Pathways (SSPs), were modelled with IAMs and are composed of qualitative and quantitative elements (O'NEILL et al. 2017).

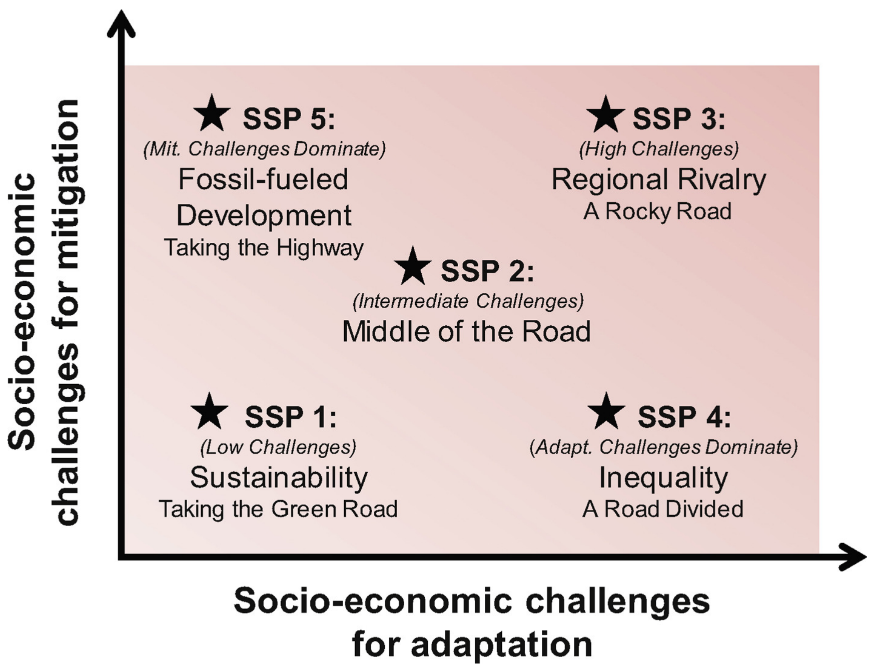

FIGURE 2.4: The five Shared Socio-economic Pathways (SSPs) in their 'challenges space' with different levels of mitigation and adaptation challenges. Source: O'NEILL et al. (2017).

The SSPs "describe plausible alternative trends in the evolution of society and natural systems over the 21st century at the level of the world and large world regions" and are supposed to serve a wide range of research disciplines (O'NEILL et al. 2014). Unlike the old SRES scenarios, they are designed to represent societies with different levels of mitigation and adaptation challenges without considering climate change explicitly, see figure 2.4 (O'NEILL et al. 2014). These storylines were accompanied by tables summarising the assumed developments of key elements of the SSPs in the fields of demographics, human development, economy & lifestyle, policies &

institutions, technology and environment & natural resources. Examples for these elements are population growth, inequality, globalization or energy intensity (O'NEILL et al. 2017). Meanwhile, the IAM community started to quantify socio-economic variables based on the SSPs including also emission scenarios and changes in land use/cover for different countries (O'NEILL et al. 2017). Some of their results such as Gross Domestic Product (GDP) and population growth projections are now available at country level through the SSP Database (`https://secure.iiasa.ac.at/web-apps/ene/SspDb/dsd?Action=htmlpage&page=about`). The SSP-based IAM scenarios consist both of baseline scenarios, which do not consider any climate mitigation strategies, and mitigation scenarios which in turn look at the effects of such policies (O'NEILL et al. 2016). For each SSP, which was run with several IAMs, one realisation was chosen as "marker scenario".
To overcome the lack of policy actions in the SSPs, they may be extended by Shared Climate Policy Assumptions (SPAs) developed in addition to them which represent the third dimension of the scenario framework (KEBEDE et al. 2018, KRIEGLER et al. 2014). These SPAs are meant to depict global mitigation and adaptation policies for the whole century. However, they are not yet fully developed and therefore implemented only in a few studies such as FRAME et al. (2018).
Finally, in the third phase of the scenario development process, see figure 2.3, the SSPs and the RCP-based climate change scenarios are combined in an integrated framework spanning a scenario matrix which "should guide the development and use of new scenarios" for the climate change research community (VAN VUUREN et al. 2014). For regional or sectoral studies in the climate change and IAV research fields, the scenarios and especially the SSP narratives need and are supposed to be extended, as has already been done in various recent publications (FRAME et al. 2018, KEBEDE et al. 2018, MALEK & VERBURG 2018). Also the integrated scenarios developed in GLOBAQUA, which provide the basis for the present work, build on the new generation of scenarios (KER RAULT et al. 2018). They are not only widely used in the scientific community but represent also the scenarios used by the IPCC which show the relevance they have also for a broader public including stakeholders and policymakers. For the purpose of this work, the climate and socio-economic scenarios were downscaled to the basin-scale. A detailed description of the selection and building process can be found in chapter 4.

For the sake of completeness, it has to be mentioned that by now the next CMIP Phase 6 is already in place (O'NEILL et al. 2016). The primary activity within CMIP6 is the Scenario Model Intercomparison Project (ScenarioMIP) which will use alternative emissions and land use change scenarios modelled with IAMs to provide multi-model climate projections (O'NEILL et al. 2016). Unlike prior phases, the climate projections of CMIP6 produced with a new generation of climate models, are driven by SSP-based scenarios which in turn are run with updated versions of IAMs (O'NEILL et al. 2016). As part of ScenarioMIP, an expanded set of now eight concentration pathways has been identified including new "gap scenarios" not covered by prior RCPs such as RCP 2.6, 3.4, 7.0 and an overshoot scenario of RCP 3.4 (O'NEILL et al. 2016). A further novelty is the fact that each of the eight forcing pathways was combined to a specific SSP on which to base the emissions and land use scenarios. As O'NEILL et al. (2016) state, the rationale behind is that "differences in climate outcomes produced by different scenarios for the same global forcing pathway are likely small relative to regional climate variability, uncertainty across climate models, and uncertainty in impact models used to investigate outcomes of interest to the IAV community".

2.5.2 Land Use Modelling and Future Projections

Land Use & Land Cover Change (LULCC) models per se are not a novel development. Some applications date back to the 1940s or 1960s, economy based models originate even from von Thünen's land rent theory published in 1826 (DANG & KAWASAKI 2016, VON THÜNEN 1826). The land use modelling community as we know it today emerged mainly in the 1990s and 2000s as part of the larger land change or land system sciences, a discipline aiming at understanding land use dynamics (DANG & KAWASAKI 2016, TURNER et al. 2007). The interest in this interdisciplinary research field was encouraged by the increased awareness of the need for a sustainable future land management that arose at that time (DANG & KAWASAKI 2016). The progress in computing power and the availability of extensive satellite data in space and time necessary for monitoring land changes further propelled the developments in this field (DANG & KAWASAKI 2016, TURNER et al. 2007). As DANG & KAWASAKI (2016) mention, the main goal in land system science is currently to project changes of land use/cover to help resource managers and decision- makers choose long-term sustainable alternatives. At present, a large variety of LULCC models simulating scenarios is in use following different purposes and applying various techniques, and the options to categorise them are manifold.

An attempt to classify LULCC models is according to their modelling scale. At global level, IAMs play an important role in modelling integrated scenarios and the IPCC relies heavily on them (HURTT et al. 2011). They are often linked to computable-general equilibrium (CGE) or Partial Equilibrium (PE) models that are based on economic optimization approaches and also provide estimates of future LULCC, either for nations, regions or even gridded land use maps (ALEXANDER et al. 2017). The implementation of LULCC scenarios in global integrated scenario analyses has been extended substantially in the past years. The CMIP5, which provided standardised simulations for the IPCC Fifth Assessment Report (IPCC 2014b), was the first one to include spatially explicit fractional land use information in the Earth System Models (ESMs) to simulate the combined biogeochemical and biogeophysical effects of anthropogenic LULCC and greenhouse gas emissions on the climate system (HURTT et al. 2011). The dataset prepared by the Land Use Harmonization 1 (LUH1) project was the first to include historical land use data, based on the gridded maps of crops and pasture data from the History Database of the Global Environment (HYDE) 3.1 for 1500-2005 (KLEIN GOLDEWIJK et al. 2010), were harmonized with future LULCC projections derived from the IAMs to serve the requirements of the ESMs (HURTT et al. 2011). For the ongoing CMIP6, a new version of this dataset, the LUH2, has been prepared providing a higher resolution (reaching now 0.25°), updated input and additional agricultural and management layers for the period 850-2100 (HURTT et al. in prep.). The scenarios of future LULCC that find their way into the LUH2 are simulated for most combinations of the RCP-SSP-framework by different IAMs, all driven by the same projections for economic growth and population (POPP et al. 2017). Since November 2018 the LUH2 dataset is readily accessible through the LUH2 homepage: `http://luh.umd.edu/faq.shtml`.

For regional studies, a 0.25° (approx. 27.6 km x 27.6 km at the equator) resolution is, however, too coarse. There have been other LULCC modelling attempts in the past years that provided global LULCC simulations at a finer resolution such as 5′ x 5′ (approx. 6 km x 9 km in Central Europe) with the LandSHIFT model (SCHALDACH et al. 2011) or the future land use simulation (FLUS) model (1 km x 1 km, LIU et al. 2017). VAN ASSELEN & VERBURG (2013) simulated global land system change, a combination of land cover, livestock, and land-use intensity, with the CLUmondo model on a 9.25 km x 9.25 km grid. Even the spatial resolution is better than the one provided by the LUH2 dataset, the thematic resolution is often coarse for, in case of LIU et al. (2017), or incompatible with, in case of VAN ASSELEN & VERBURG (2013), the objectives of the present study. Besides, the scenarios of these studies are outdated and do not reflect the current RCP-SSP-framework.

LULCC simulations have also been carried out specifically for Europe. The Land Use-based Integrated Sustainability Assessment (LUISA) is a platform run by the Joint Research Centre (JRC) "designed to assess LU impacts of European policies by providing a vision of possible futures and quantitative comparisons between policy options" (LAVALLE et al. 2016). LUISA is built around the EU-ClueScanner100, which was also the core fo the former Land Use Modelling Platform (LUMP) of the JRC, but with substantial modifications and expansions (LAVALLE et al. 2016). It provides LULCC simulations for one European reference scenario at a 100 m x 100 m resolution and for decadal time steps from 2010 to 2050. A recent study by MALEK & VERBURG (2018) modelled land system changes in the Mediterranean region including the northern part of Africa under different irrigation efficiency and water availability scenarios up to 2050 with the CLUmondo model. The socio-economic and climate scenarios are based on the SSP2 marker scenario and CMIP5 simulations for RCP 4.5, respectively, and are therefore up to date (MALEK & VERBURG 2018). Still, they elaborate only on one RCP-SSP-combination and do not confront several ones as in the present study.

Countless other LULCC models exist that have been applied to regional or local case studies. They are based on a large variety of modelling approaches according to their scope. DANG & KAWASAKI (2016) group them in the following categories according to the main technique:

1. Cellular automata
2. Markov chains models
3. Economic based models
4. Statistical based models
5. Artificial neural networks
6. Agent-based analysis models
7. System dynamic models
8. Hybrids of the previous categories also in combination with CGE and PE models.

In cellular automata the landscape is divided into cells and the model is trained by transition rules to simulate spatial patterns (CHAUDHURI & CLARKE 2013, DANG & KAWASAKI 2016). This approach works well for urban sprawl which is the reason why models like the Slope, Land use, Excluded land, Urban extent, Transportation and Hillshade (SLEUTH) model or Monitoring Land Use/Cover Dynamics (MOLAND) model have been often applied to urban areas (CHAUDHURI & CLARKE 2013, CROLS et al. 2017). Pure Markov chains models are not spatially explicit and are therefore usually combined with other techniques such as cellular automata as it is the case for the Dinamica EGO model (DANG & KAWASAKI 2016, MAS et al. 2014). In economic based models the demand for and allocation of land is driven by economic variables following the aim of maximizing profit (DANG & KAWASAKI 2016). A widely used example for this model category is the Global Trade Analysis Project (GTAP) model which, however, does not take into account climate and biophysical factors affecting the distribution of land as other economic models (HERTEL & TSIGAS 1997). Statistical based models use mathematical relationships between the spatial distribution of land uses and a large variety of biophysical and socio-economic drivers to derive the probability of land use change at a certain location (DANG & KAWASAKI 2016). Models like FORE-SCE or from the Conversion of Land Use and its Effects (CLUE) framework such as CLUE-S, Dyna-CLUE, the above mentioned CLUmondo or the new iCLUE are based on such statistics (SOHL & SAYLER 2008, VERBURG & OVERMARS 2007, VERBURG & OVERMARS 2009, VERWEIJ et al. 2018). The CLUE modelling framework represents empirical, data-driven models that apply rather a top-down approach determining first the scenarios with the overall demand which is then allocated in a second step (VERWEIJ et al. 2018). DANG & KAWASAKI (2016) argue that the weakness of statistical based models lies in the extrapolation of trends for calculating demands which is not suitable for long-term scenario analysis according to the authors. The Land Transformation Model (LTM) is an example for a combination of artificial neural networks with GIS (PIJANOWSKI et al. 2002). Artificial neural networks are able to combine data from different sources. At the same time, they are not self-explanatory and have to be treated as black-boxes (DANG & KAWASAKI 2016). Agent-based models are a useful tool to integrate the knowledge of stakeholders in the modelling process while they neglect other important factors (DANG & KAWASAKI 2016). System dynamic models take into account feedback loops in the land system but do not provide spatially explicit outputs (DANG & KAWASAKI 2016). There are countless examples of hybrid LULCC models that combine two or even three techniques, DANG & KAWASAKI (2016) collected some of them. For instance, BRITZ et al. (2011) presented a combination of the spatial downscaling module of the Common Agricultural Policy Regional Impact model (CAPRI-Spat), an IAM for agricultural policies that simulates changes in crop area and yield, herd sizes, feeding and fertilizing practices, with the statistical model Dyna-CLUE for the land use allocation. Changes in agricultural land at national level are derived from the combined economic and IAM GTAP-IMAGE.

This incomplete list of LULCC models gives an idea of the variety of models that exist. Depending on the scope of the study, a different model may be suitable. For the present study, the iCLUE model mentioned above was used (VERWEIJ et al. 2018). Compared to other models listed here, iCLUE combines several advantages explained in more detail in chapter 5.1.

2.5.3 Spatially Distributed Estimation of Water Uses

Regarding spatially distributed water use maps, several products exist covering the last decades and applying different approaches: SIEBERT et al. (2005) and SIEBERT et al. (2013) produced the Global Map of Irrigated Area (GMIA) which displays the area equipped for irrigation (AEI) around the year 2005. The GMIA was developed combining and harmonising statistics from a wide range of sources such as the FAO, World Bank or national institutions and downscaling them to a 5′ grid. The Global Irrigation Area Mapping (GIAM) project (THENKABAIL et al. 2009) is also widely known. It estimated the total area available for irrigation and the annualised irrigated areas, which consider the intensity of irrigation, around the year 2000 at a 10 km x 10 km resolution relying on remote sensing techniques (THENKABAIL et al. 2009). Other global irrigation maps were developed by SALMON et al. (2015) and PORTMANN et al. (2010), the latter one provides monthly irrigation information. Several products are available for Europe such as the European Irrigation Map (EIM) (WRIEDT et al. 2009b) or the gross and net irrigation requirements as well as real irrigated area modelled with a combination of the models WATERGAP3 and LPJmL by AUS DER BEEK et al. (2010). Net irrigation requirements in mm over Europe were also estimated by WRIEDT et al. (2009a) using the Environmental Policy Integrated Climate (EPIC) model. A few datasets exist that account also for other water uses such as the reconstructions of global monthly sectoral water withdrawals for 1971-2010 by HUANG et al. (2018) or the estimates of global thermoelectric and manufacturing water use by VASSOLO & DÖLL (2005). As these - by no means exhaustive - examples show, the research focus lies on irrigation, which is reasonable considering how much water is used for irrigation worldwide, 69% out of the total global water consumption (FAO 2016a).

When it comes to the time span, the mentioned examples describe the situation around the years 2000 to 2005 or further back in the past in case of AUS DER BEEK et al. (2010). The studies providing also spatially explicit future simulations of water uses, however, are very rare. The gridded sectoral (domestic, energy, irrigation, livestock, manufacturing) water abstraction maps provided by the JRC (`http://data.jrc.ec.europa.eu/collection/water`) can be mentioned here. They were modelled using the LISFLOOD hydrological model for 2006 and 2030 at a 5 km x 5 km resolution (EUROPEAN COMMISSION & JOINT RESEARCH CENTRE 2011). The 2030 land use projection is a baseline scenario originating from the LUMP model. Within the EU SCENES project SCHALDACH et al. (2012) modelled the mean annual net irrigation requirements in mm and % share of irrigated area per cell under different integrated socio-economic and climate scenarios at a 5′ resolution over Europe. The modelling chain included the ecohydrological and agro-ecosystem Lund–Potsdam–Jena managed Land model (LPJmL) (for estimating potential crop yield), WATERGAP3 (modelled the impact of climate and LULCC on net irrigation water requirements) and LandSHIFT for modelling LULCC. Four different socio-economic scenarios were combined with climate data for one climate scenario, the SRES A2, from two different Global Circulation Models (GCMs) (SCHALDACH et al. 2012). DE ROO et al. (2012) modelled several water quantity and quality scenarios for continental Europe using the Integrated Water Modelling Platform (IWMP) maintained by the JRC that include the following models: the agricultural Common Agricultural Policy Regional Impact (CAPRI) model, LUMP, LISFLOOD for water quantity, EPIC for water quality and LISQUAL as combined water quantity, quality and hydro-economic model (DE ROO et al. 2012). Similar to the other datasets provided by the JRC mentioned above, simulations are carried out for 2006 and 2030 at a 10 km x 10 km grid. The EPIC model calculates the irrigation water requirements for the five dominant crop types of each cell (DE ROO et al. 2012). Based on this study, DE ROO et al. (2016) modelled the water demand under future climate and land use scenarios specifically for the Sava River basin using the same modelling platform, however, replacing the LUMP model by the more recent LUISA platform (see chapter 2.5.2). For future climate projections, they used Coordinated Regional Downscaling Experiment (CORDEX) data for RCP 4.5 and 8.5. (DE ROO et al. 2016). Results are provided for 2006, 2010, 2030 and 2050. While this study includes several scenarios for crop irrigation, there is only one future LULCC simulation (DE ROO et al. 2016). Simulations of the effects of water allocation schemes in Europe for different sectors were carried out within the CLIMSAVE project (HARRISON et al. 2015). Also here, the future horizon is 2050. The spatial resolution is only at river basin scale. FADER et al. (2016) simulated several irrigation scenarios providing also quantified Gross Irrigation Requirements (GIR) over the Mediterranean for four warming levels and 19 GCMs using the LPJmL. This gets very close to the aims of the present study. The modelling resolution, however, is only 30′ and therefore very coarse. Finally, the study mentioned above by MALEK & VERBURG (2018) elaborated spatially explicit maps of cropland cover, irrigation and intensity under different irrigation techniques (drip, sprinkler, deficit irrigation) and water withdrawal scenarios. Quantified water uses per pixel are, however, not reported in this study.

To sum up, water use and mainly irrigation maps can be derived either by downscaling of statistical data, remote sensing or modelling (PORTMANN et al. 2010). However, none of the above mentioned examples meets the requirements for the present study either regarding the resolution, the up-to-dateness of the scenarios or even their lack. For this reason an own scenario downscaling and modelling approach had to be developed.

Chapter 3

The Case Studies

3.1 The Ebro River Basin

The following sections partly coincide with the case study descriptions published in HUBER GARCÍA et al. (2018).

3.1.1 General Characteristics

The Ebro catchment comprises 85600 km^2 and is located in North-eastern Spain including the whole territory of Andorra (468 km^2) and a very small part of France. It accounts for approx. 17% of the Spanish national territory. The Cantabrian Range and the Pyrenees (maximum altitudes >2000 m and 3000 m a.s.l., respectively) build the northern hydrographic boundaries, the Iberian mountains (maximum altitude 2000-2300 m a.s.l.) enclose the large Ebro depression to the South and the Coastal Range (maximum elevation 1000-1200 m a.s.l.) to the East, parallel to the Mediterranean coast (LÓPEZ-MORENO et al. 2013).

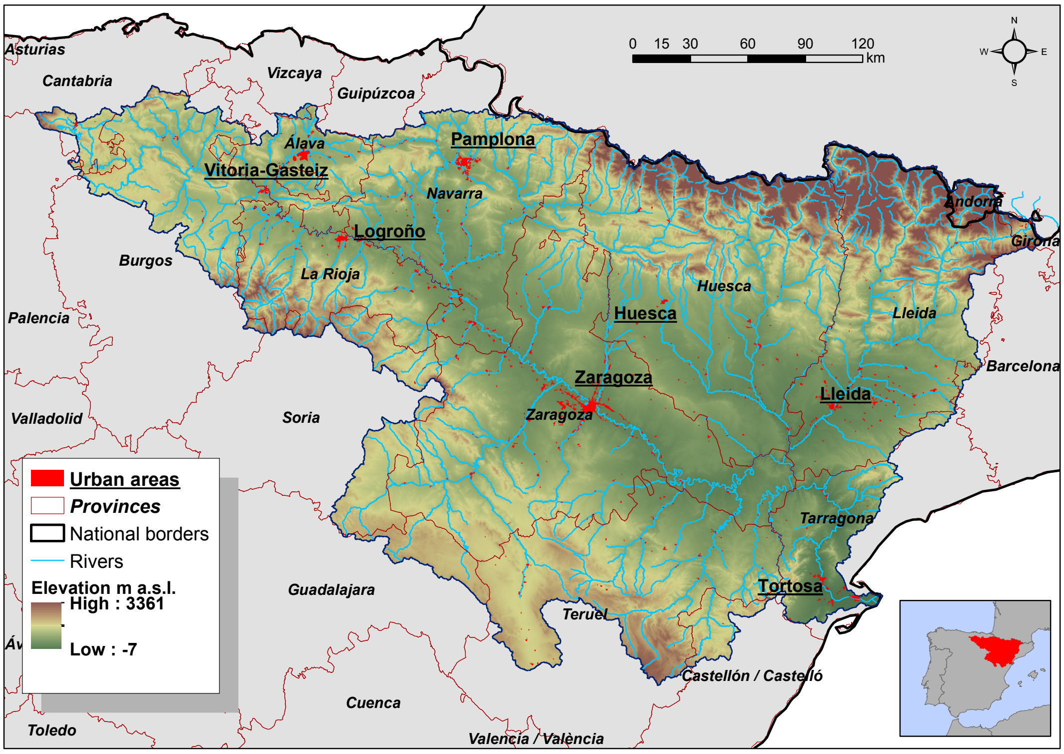

FIGURE 3.1: The Ebro River basin.

The altitude ranges from over 3400 m a.s.l. in the Pyrenees to sea level where the Ebro enters the Mediterranean forming a vast delta, see figure 3.1. The wetlands of the delta are important in terms of their environmental value and are part of the NATURA 2000 Network (VALDEMORO et al. 2007).

3.1.2 Climate

Due to the topography, the climate varies considerably within the basin. Figure 3.2 illustrates the differences by confronting the Walter-Lieth climate diagrams for three different locations in the Ebro indicated also in the map in figure 3.1. The mountain ranges to the North are influenced by an oceanic climate and annual precipitations of up to 1500 mm are not unusual (CHE 2015). Also in Vitoria-Gasteiz, in the north-western part of the basin just south of the Cantabrian Range, the mean annual precipitation for the period 1981-2010 is 749 mm (AEMET 2020a), see figure 3.2. The largest part of the basin is, however, dominated by a Mediterranean climate showing a large variety of manifestations, from mountainous to semi-arid in the central valley as for example in Zaragoza, upper right diagram in figure 3.2. The low-lying central valley is, in fact, the driest part of the catchment with approx. 400 mm/y annual precipitation sum, but values below 100 mm/y have been measured and a strong seasonal and interannual variability is typical for the region (CHE 2015). Close to the Mediterranean coast in Tortosa the mean annual precipitation turns to be higher (lower diagram in figure 3.2). All over the catchment there are two distinct precipitation peaks, visible also from the climate diagrams, one in spring and one in autumn (LÓPEZ-MORENO et al. 2013). The mean annual precipitation over the whole catchment is 618 mm/y for the period 1980/81-2005/06 (CHE 2015).
Also temperatures vary considerably throughout the basin. For the period 1981-2010 the mean annual temperature in Vitoria-Gasteiz is only 11.7°C while it rises up to 17.7°C close to the sea in Tortosa (AEMET 2020a, AEMET 2020b). The mean annual temperature over the whole catchment for the period 1940/41-2005/06 is 12.5°C while it lies above 15°C in the dry central depression causing an elevated water deficit there (AEMET 2020c; CHE 2013, Annex II; LÓPEZ-MORENO et al. 2013).

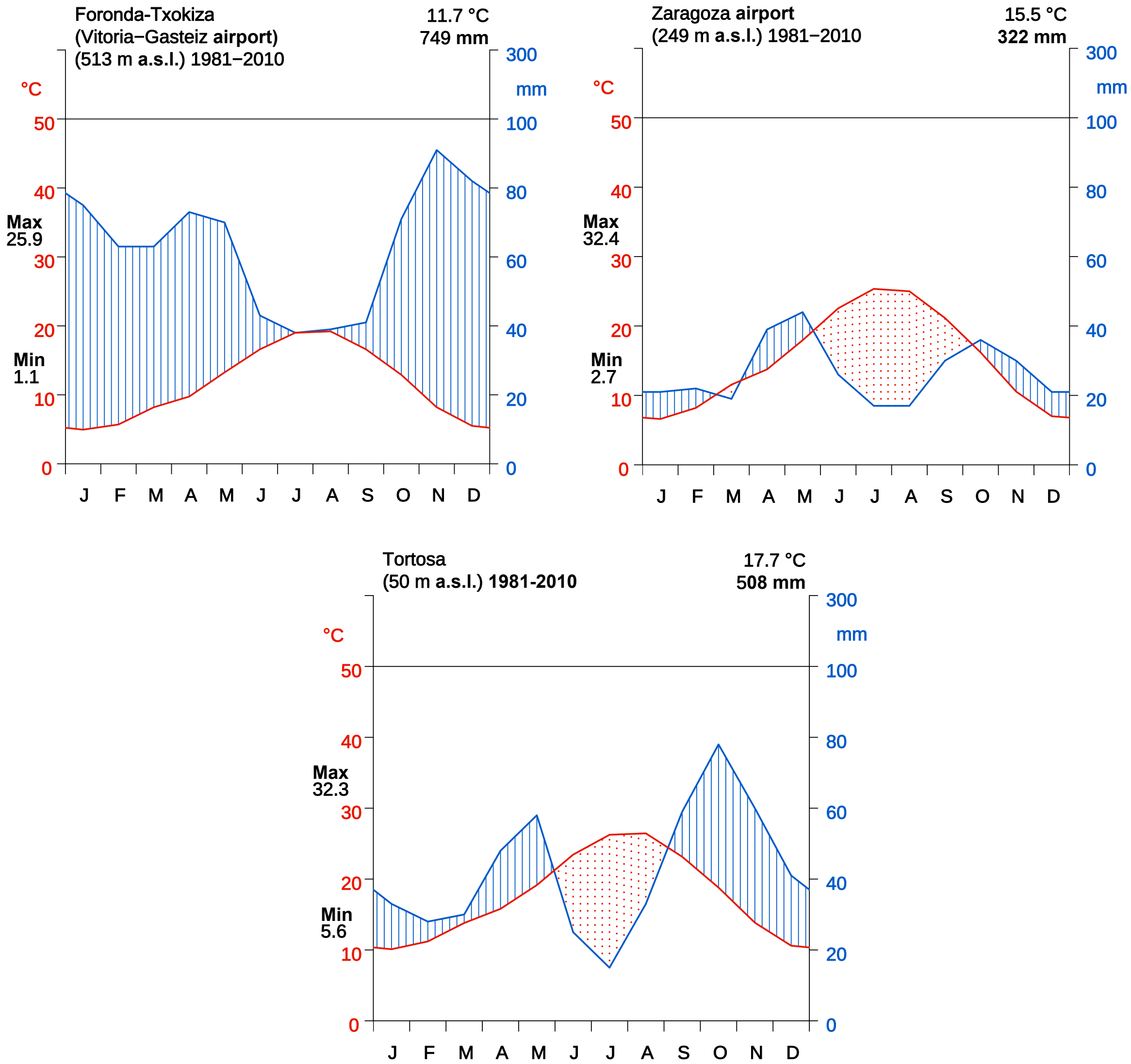

FIGURE 3.2: Climate diagrams for Foronda Txokiza (Vitoria-Gasteiz airport) (left), Zaragoza airport (right) and Tortosa (bottom). Data source: AEMET 2020a, AEMET 2020b, AEMET 2020c.

3.1.3 Land Cover and Land Use

Due to different climatic influences and altitudes, the land cover in the Ebro basin is very heterogeneous. According to the RBMP 2015-2021 (CHE 2013, Annex III), forest and shrubs cover 54% of the Ebro basin. Grasslands and coniferous forests dominate in the Pyrenees; broadleaved forests are prevalent in the western mountain regions, see figure 3.3. The vast plains of the inner Ebro valley are used for agriculture. Approx. 22% are non-irrigated agriculture according to the CLC map of 2006, see figure 3.3, additional 7% are occupied by the large irrigation systems, but the total irrigated area sums up to 10% of the whole watershed (CHE 2015). Between 1995 and 2009 an increase of agricultural surface authorized for irrigation was registered mainly in the already highly technologised areas (CHE 2015). The Ebro basin further comprises the famous Rioja vine region located in the western part of the watershed, a purple pattern in figure 3.3, which makes up the largest part of the vineyards (1% of the total area). Urban and industrial areas together make up only 1% of the basin. The main cities located in the basin are Zaragoza, Vitoria-Gasteiz and Pamplona, see figure 3.1.

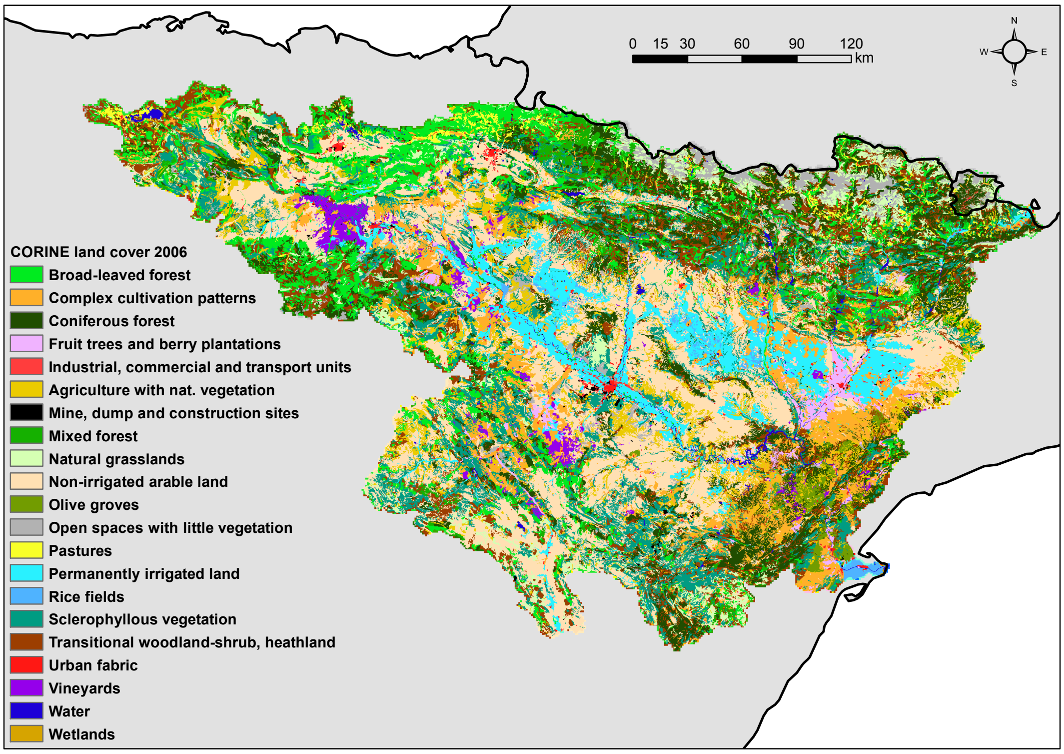

FIGURE 3.3: CORINE Land Cover 2006 in the Ebro reclassified to 21 classes.

3.1.4 Hydrology and Water Use

The main course of the Ebro has a length of 970 km. The Centro de Estúdios y Experimentación de Obras Públicas (CEDEX) simulated the mean annual runoff under natural conditions at 16448 hm^3/y for the period 1940/41-2005/2006 with the Sistema Integrado para la Modelización Precipitación Aportación (SIMPA) hydrological model (CHE 2018). For the period 1980/81-2005/06, they modelled 14623 hm^3/y. The hydrology of the Ebro is largely influenced by man, counting 187 dams and reservoirs built in the 20th century that have affected the hydrology and the sedimentary regime (R. J. BATALLA et al. 2004). Due to the strong variability of its climate, the discharge of the Ebro also varies considerably from year to year. Table 3.1 illustrates that the discharge of a particular year may well be only 50% of the one of the previous year, here taking the example of the city of Zaragoza.

TABLE 3.1: Measured annual discharge sums [hm^3/y] of the Ebro River in Zaragoza for various periods. Source: MITECO (2018).

	Mean 1980/81-2011/12	Mean last 5 years	Mean last 10 years	2014/15	2015/16	2016/17
Discharge	6003	7749	6552	9337	6450	3220

As it is the case for many Mediterranean rivers, the mean discharge has been decreasing in the last decades. In the case of the Ebro by even 40% in 50 years (DELGADO et al. 2010). The reduction is mainly attributed to the abandonment of, in its majority mountainous, marginal agricultural land due to demographic changes, low economic viability and a lower guarantee of water being supplied (CHE 2015). This process was followed by a regrowth of forest. At the same time, the Spanish Government and the European Union have promoted reforestation (DELGADO et al. 2010). The larger forest areas have led to higher transpiration rates and by this means reduced the runoff. It is assumed that also climate change plays a role in the observed runoff reduction (CHE 2018). For the future, the basin authorities are to plan with a runoff reduction of 5% for the 2039 horizon (CHE 2018).

The vast valleys of the Ebro and of its main tributaries are intensively used for agricultural practices. Irrigated agriculture accounts for approx. 10% of the total area of the Ebro basin. Out of the 8190 hm^3/y of water consumed in the Ebro 94% (7681 hm^3/y) are attributed to the agricultural sector and again 99% out of it to irrigation, only 1% to livestock farming directly (CHE 2015). The urban demand, including industries supplied by the urban supply networks, lies around 359 hm^3/y (4.4%), while the purely industrial demand accounts for 147 hm^3/y (1.8%). Urban water consumption is driven by the number of inhabitants, which fluctuates around 3.2 million in the Ebro catchment (CHE 2015). Another 200 hm^3/y are transferred to supply metropolitan areas outside the catchment, the largest consumers being the metropolitan area of Bilbao and the coastal municipalities of the province of Tarragona (CHE 2013, Annex III). Another 60 hm^3/y are transferred outside the basin for industrial uses. Also the water consumption of the tourism sector is reported in the RBMP reaching highest values in July and August (CHE 2018). However, at the present stage the share of this sector does not carry much weight. In general, the urban demand has been decreasing over the past decades due to a higher water efficiency (CHE 2018).

3.1.5 Agriculture and Livestock Farming

The Ebro shows a higher percentage of agro-industrial activities than the rest of Spain, mainly focused on food production (CHE 2015). 31% of the Spanish production of sweet fruits is located in the Ebro as well as 28% of vineyards and 35% of fodder (CHE 2018), while it accounts only for 17% of the Spanish territory. In fact, crop cultivation, and in particular irrigated agriculture, is strongly interlinked with livestock farming since the prior produces fodder for the livestock which in turn provides large amounts of manure as organic fertilizer for the fields (CHE 2018). For this reason, large-scale livestock farms are often located around the large irrigation systems in the Ebro (CHE 2018). Even if only 25% of the approx. 3 million ha of cultivated land are irrigated, they account for 65% of the total gross value added (GVA) of agricultural goods produced in the Ebro (CHE 2018). The irrigation techniques have undergone

a modernization process in the past years. Rather traditional techniques such as channel irrigation have been transformed to more efficient sprinkler or localized irrigation techniques, for example drip irrigation (CHE 2015). This has certainly led to higher irrigation efficiency. However, a reduction of the water used for irrigation has not been reported until now (CHE 2015). Instead, the opposite is the case: The irrigation modernisation in Spain has led to an increase in water and, in particular, also energy consumption needed to supply the new pressurised irrigation systems (GONZÁLEZ-CEBOLLADA 2016).
Also the meat industry, including milk and eggs, of the Ebro has a large weight at national level: It accounts for 28% of the total Spanish GVA of this sector (CHE 2018). The lion's share has to be attributed to the meat industry (94%) and out of that mainly to pigs (65%). The number of pigs has been growing substantially over the past 10 years. Meanwhile, milk and eggs account only for 6% of the GVA of the longtime mean (CHE 2018). In general, livestock units have increased 70% in 20 years between 1989 and 2009 (CHE 2015). Still, this increment constitutes a marginal factor for the water use since it represents less than 1% of the total water consumed in the Ebro for agriculture. Nevertheless, it may be relevant regarding water pollution since it increases the diffuse pollution (CHE 2015).

3.2 The Evrotas River Basin

3.2.1 General Characteristics

The Evrotas River basin is entirely located in Greece on the southern Peloponnese and drains in the Laconic Gulf of the Mediterranean (GAMVROUDIS et al. 2015). It is a rather small river basin covering 2412 km^2. In terms of management, the Evrotas is addressed in the RBMP of the Eastern Peloponnese and accounts for 28.6% of the total area of this district (SSW 2013). The altitude ranges from 0 m at sea level to 2407 m in the Taygetos Mountains which delineate the Evrotas valley to the west, see figure 3.4. The highest peak of the Parnonas Mountains, located to the east of the central depression, reaches 1935 m. GAMVROUDIS et al. (2015) state that only 11% of the catchment has slopes with less than 5% inclination which depicts the rugged character of the basin.

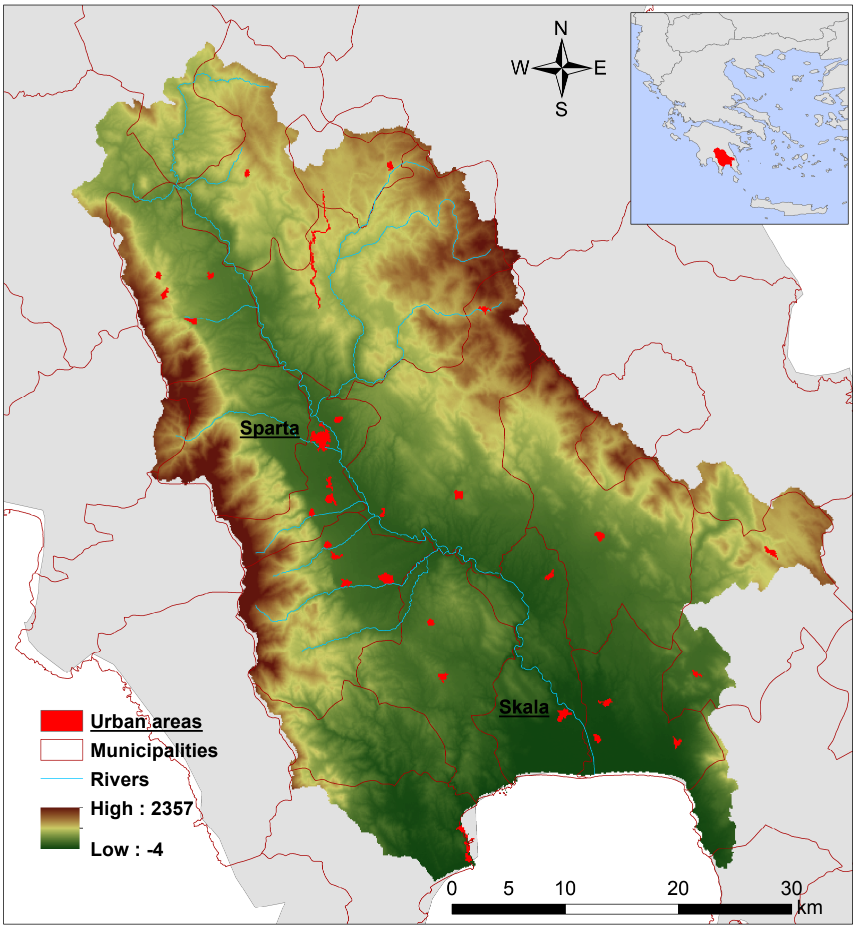

FIGURE 3.4: The Evrotas River basin.

3.2.2 Climate

The Evrotas is characterised by a Mediterranean climate with wet and cool winters (November to March) and hot and dry summers (April to October) (GAMVROUDIS et al. 2015). The mean annual temperature is 16°C, on average 4-11°C in the winter months and 22-29°C in summer (TZORAKI et al. 2013). The annual precipitation sum for the period 2000-2008 was 803 mm on average (NIKOLAIDIS et al. 2009). In the rainiest areas in the western mountains annual precipitations of 1300-1600 mm have been measured while near the coast the annual sum does not exceed 500-550 mm (VERNOOIJ et al. 2011).

3.2.3 Land Cover and Land Use

The majority of the basin is covered with sclerophyllous vegetation and agriculture with natural vegetation according to the CLC maps (together about 48%, approx. 1200 km^2 of the total area). This classes are especially dominant in the mountainous regions, as also coniferous forests. The totality of land covered by semi-natural vegetation including forests sums up to 61% (SKOULIKIDIS et al. 2011). Olives (approx. 15% or 350 km^2) are the main crop grown in the basin followed by fruits, mainly citrus, that are more located in the low lands of the basin. In fact, the two main industrial activities in the Evrotas are the production of olive oil and orange juice (DEMETROPOULOU et al. 2010). These two crop types cover about 90% of the agricultural area which in total accounts for 38% (SKOULIKIDIS et al. 2011). VERNOOIJ et al. (2011) report that most of the agricultural land in the basin is irrigated even this may not be directly deduced from CLC data. Only areas located far from the river without access to springs and groundwater are rain fed. Urban areas make up only a very small part, less than 1%.

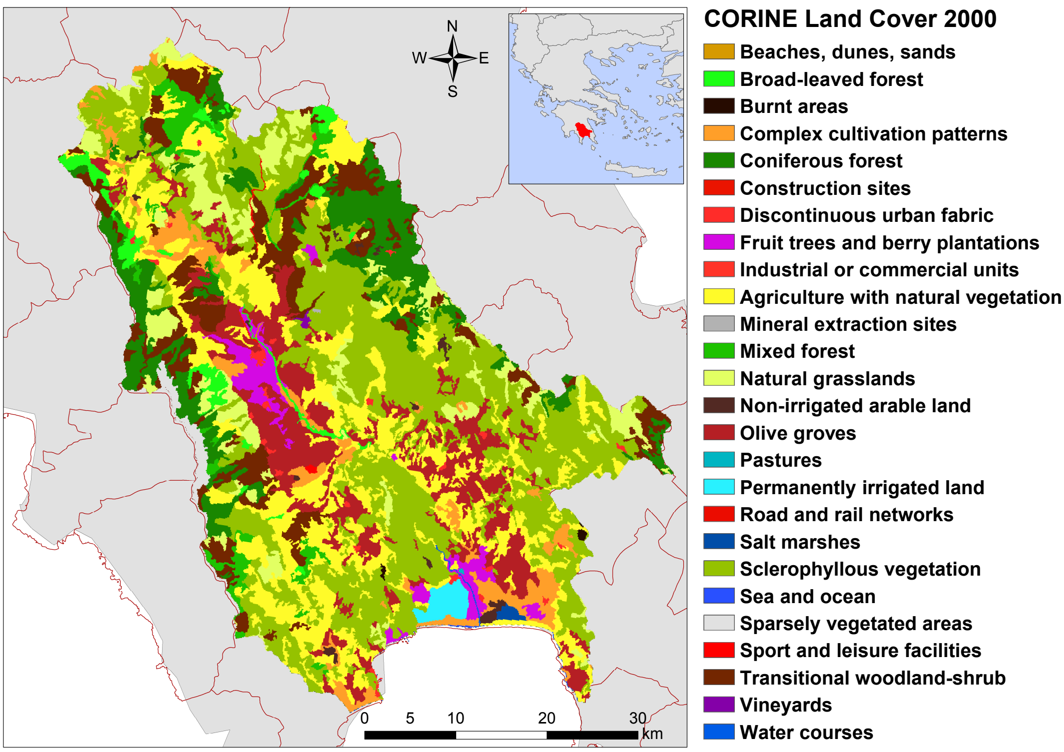

FIGURE 3.5: CLC 2000 map of the Evrotas River basin.

3.2.4 Hydrology and Water Uses

Due to its complex geology, the Evrotas River system is fed by various karstic and alluvial springs (SKOULIKIDIS et al. 2011). In summer, numerous intermittent and ephemeral streams can be found in the catchment and also the main course of the Evrotas dries partly out (NIKOLAIDIS et al. 2009). Historical analysis have revealed that in the past the Evrotas main course carried water throughout the whole year, but in the last decades water abstractions for irrigation affected the regime of the river (NIKOLAIDIS et al. 2009). Other authors like VERNOOIJ et al. (2011) mention that the intermittency is partly caused by the karstic systems in the watershed.

Formerly, all crops except olive trees were irrigated, the irrigated areas mainly concentrating in the areas around Sparta and close to the coast (SKOULIKIDIS et al. 2011). After a severe drought period in 1989-1993 permanent irrigation was extended also to olive trees out of which 2/3 are irrigated now (SKOULIKIDIS et al. 2011). This has led to a massive increase in water consumption of around 70% (SKOULIKIDIS et al. 2011). According to data from the Ministry of Development of Greece (MDG,

2005) the irrigation demand in 2001 was around 76.8 hm^3.
GAMVROUDIS et al. (2015) state that the water balance in the Evrotas is generally positive, irrigation and drinking water needs are usually met. Domestic water use accounts for approx. 6.4 hm^3/y, the total population being 68400 inhabitants (MDG 2005). Problems occur, however, in dry periods during summer due to the increased irrigation demands. There are 150 public wells and around 3550 private wells through which water is abstracted (GAMVROUDIS et al. 2015), but SKOULIKIDIS et al. (2011) point out that there are numerous, mainly illegal, surface water abstractions. The over-exploitation of ground and surface water then leads to the dessication of vast parts of the river system during drought periods (GAMVROUDIS et al. 2015, SKOULIKIDIS et al. 2011). Apart from increasing the pressure on water resources, this comes along with several further negative effects such as the lowering of groundwater tables, the rapid deterioration of water quality, the degradation of habitats and massive fish mortality (SKOULIKIDIS et al. 2011).

Chapter 4

Scenario Development within GLOBAQUA

The scenarios developed within GLOBAQUA are based on the new scenario framework currently used in climate change research described in chapter 2.5.1. This new framework is organised in a scenario matrix architecture, see figure 4.1, a key assumption being that the users are free to combine a SSP with different RCPs since the SSPs are neither linked to a specific climate policy action nor to a level of climate change (VAN VUUREN et al. 2014). It has to be noticed, however, that some combinations may be inconsistent. VAN VUUREN et al. (2014) further elaborate on the need to combine SSPs and RCPs for building scenarios as 'pathways' describe only one component whereas 'scenarios' combine different pathways with other information. This means that the final scenarios applied by the researchers which then include the impacts of climate change and possible policy interventions will slightly differ from the original assumptions in the SSPs (VAN VUUREN et al. 2014), as it is the case also for the GLOBAQUA scenarios presented here. Concerning this matter, O'NEILL et al. (2017) consider the SSPs as being basic storylines which should be extended by the users to fit the needs of their research keeping in mind the consistency with the basic SSPs. O'NEILL et al. (2017) further make clear that the quantitative parts of the basic SSPs do not include the outcomes of the scenarios such as emissions or land use change, but that the quantification of these outcomes is left to the scenarios. The present study addresses exactly these need by projecting land use and water management under different scenarios. In addition, also the uncertainties related to climate modelling are taken into account in this study, see the left part of figure 4.1. They are described in chapter 4.4.
The reference period of the GLOBAQUA scenarios is defined by the project description being 1980-2010. Regarding the future period, a compromise had to be made between socio-economic assumptions and a period relevant for climate impact studies. Socio-economic developments can hardly be estimated in detail throughout several decades. In contrast to that, the climate forcing of the RCPs does not diverge notably until 2035 as MOSS et al. (2010) state. Consequently, 2036-2065 was chosen as future period for the climate input and the 2050 as final scenario horizon, which lies exactly in between.

4.1 Selection of SSP-RCP Combinations

For GLOBAQUA, four RCP-SSP combinations were chosen and their basic storylines adapted and downscaled to fit the purposes of the project. The full scenario matrix spanned by SSPs and RCPs can bee seen in figure 4.1, the fields highlighted in dark blue represent the four GLOBAQUA scenarios, the ones marked with a cross the two scenarios modelled as part of this study. The selection and development of the GLOBAQUA specific scenarios was a joint effort of different project partners from various disciplines such as environmental modellers, economists, sociologists and scenario experts as well representatives from the partner projects MARS (`http://www.mars-project.eu`) and IMPRESSIONS (`http://www.impressions-project.eu`). The complete storylines for the SSPs used in this study can be found in the Appendix B. The two scenarios relevant for the present study are described in more detail hereafter.

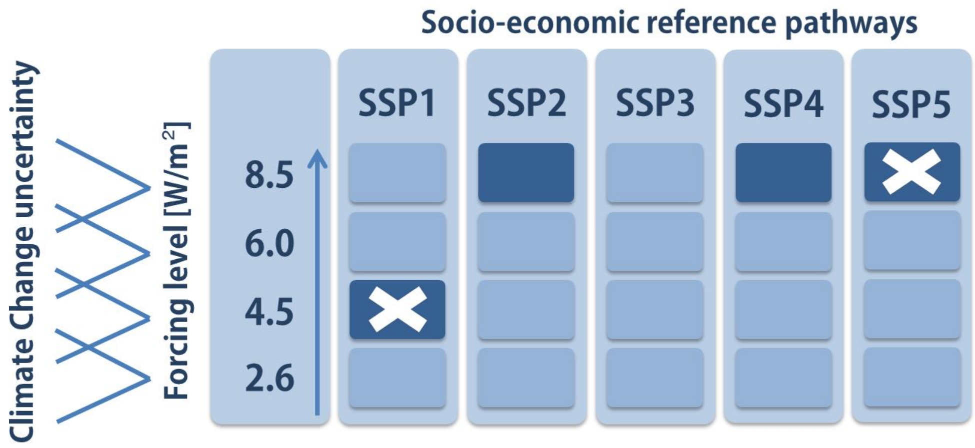

FIGURE 4.1: The RCP-SSP scenario matrix including uncertainties of climate change. The dark blue fields represent the combinations chosen as GLOBAQUA scenarios. The two white crosses mark the two scenarios modelled in this study. Adapted from VAN VUUREN et al. (2014).

Already by their location in the scenario matrix in figure 4.1 it becomes clear that these two scenarios are opposed to each other. The intention here was to maximise the variations in the results creating one more economy-friendly and another more environment-friendly scenario. The final SSP-RCP combinations are thought to have adverse effects on land and water uses spanning a wide range of possible futures. Regarding the combination of SSPs and RCPs, it was important to be consistent and allow for scientific credibility as some combinations are very unlikely.

For the climate forcing levels, RCP 2.6 was discarded as it assumes the lowest radiative forcing rates only reachable with very strict and effective climate mitigation actions at global scale. None of the old SRES scenarios reaches CO_2 concentrations as low as RCP 2.6, as also figure 4.2 demonstrates, because the SRES scenarios did not include explicit mitigation policies (VAN VUUREN & CARTER 2014). RCP 6.0 was excluded due to its position in between the RCP 4.5 and 8.5 which span the largest forcing level range left. Consequently, RCP 8.5 and 4.5 were selected to form the scenarios in GLOBAQUA. These two forcing levels are widely used in the scientific literature (LEVIS et al. 2018, THOBER et al. 2017, HSIANG et al. 2017, KIM et al. 2013) and the hits on Google Scholar show the prevalence of RCP 8.5 and 4.5: RCP2.6 - 10400 hits, RCP4.5 - 17800 hits, RCP6.0 - 4920 hits, RCP8.5 - 23000 hits (checked 18/03/2020).
RCP 8.5 can be considered a 'worst-case' scenario regarding climate change characterised by increasing greenhouse gas concentrations reaching high levels at the end

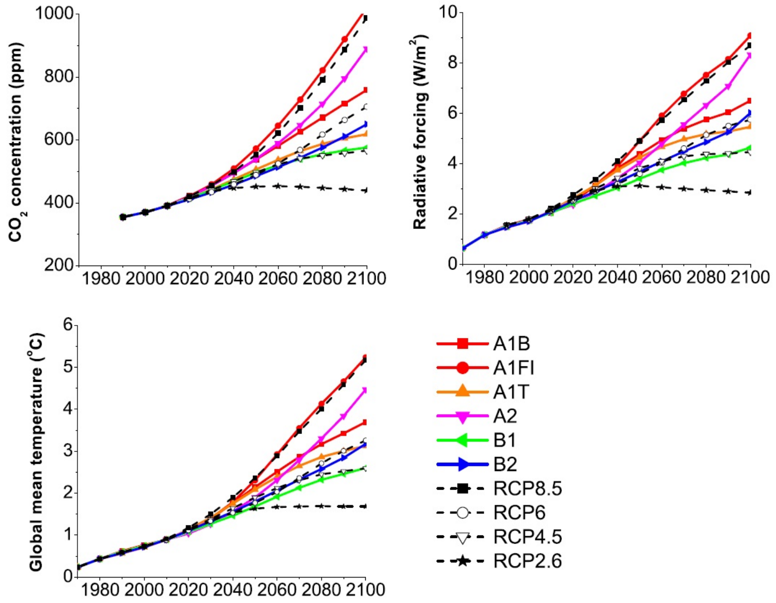

FIGURE 4.2: Trends of CO_2 concentrations, radiative forcing levels and global mean temperature until 2100 for the RCPs and IPCC SRES based on the MAGICC model (VAN VUUREN & CARTER 2014).

of the 21st century and consequently a strong increase in global temperature (VAN VUUREN et al. 2011), see figure 4.2. It becomes clear that its development is in line with the fossil fuel intensive A1FI scenario from the old SRES set. In contrast to that, RCP 4.5 is a stabilisation scenario where the total radiative forcing stabilises shortly after 2100 (VAN VUUREN et al. 2011). It corresponds to the B1 world of the SRES scenarios. RCP 8.5 fits well to SSP 5 which describes an economy driven future with "resource and energy intensive lifestyles around the world" (O'NEILL et al. 2017). Also KEBEDE et al. (2018) that only SSP 5 is fully compatible with RCP 8.5 and able to lead to the emission levels of this RCP. It is an optimistic scenario with strong economic growth and a high globalisation level. Technical measures are applied successfully to adapt to climate change. In contrast, the society experiences high mitigation challenges.

Regarding SSP 1, there is a clear correspondence to the former SRES B1 scenario according to RIAHI et al. (2017). SSP 1 describes a development towards a society that acts more and more sustainable and has little challenges to both mitigation and adaptation, see figure 2.4. Consequently, this was combined with the stabilisation pathway RCP 4.5, a combination also recommended by VAN VUUREN & CARTER (2014). Both SSP 1 and 5 assume low population growth rates and a fast economic development at the global scale, mainly driven by "rapid improvements in education, fast income growth, and rapid urbanization, leading to relatively rapid declines in fertility in high fertility countries" (O'NEILL et al. 2017). Despite these similarities at global level, the assumed developments of the basic SSPs differ depending on the countries, subdivided into a low, middle and high income group according to the World Bank's definition (O'NEILL et al. 2017). For the GLOBAQUA case studies, all located in high income or at least upper middle (Serbia and Bosnia & Herzegovina in the Sava River basin) income countries, this manifests in a medium economic growth in SSP 1 while it is high for SSP 5. By contrast, VAN VUUREN & CARTER (2014) state that the quantitative projections of population for the Organization for

Economic Co-operation and Development (OECD) region carried out with IAMs are very similar all across the scenarios. A more detailed description of SSP 1 and SSP 5 is included in Appendix A.

4.2 Definition of Scenarios and Scenario Descriptors

The detailed scenario definition was carried out on the grounds of the above mentioned RCP-SSP combinations with a focus on water management as it constitutes the key aspect of the GLOBAQUA project as well as of the present study. The combination of RCP 8.5 and SSP 5 was given the name "MYOPIC scenario" while RCP 4.5 and SSP 1 together were called "SUSTAINABLE scenario". They will be named this way hereafter.
The scenario were developed in a joint effort by a transdisciplinary team of GLOBAQUA partners and in consultation with the partner projects MARS and IMPRESSIONS as they aimed at developing regional scenarios for Europe, too.

Similar to the basic SSPs, the final scenarios consist of two elements: a qualitative storyline and a table indicating the expected trends of key elements, called "descriptors" in the GLOBAQUA context. The first out of several steps was to elaborate the qualitative narratives for each of the scenarios. These storylines had to cover the fields of society & economy, energy, environment, policies and water management. For each of these sectors a short paragraph was drafted delineating its future development in each of the scenarios. This represents a first effort to downscale the global SSPs as the narratives were defined for the domain of the GLOBAQUA project, i.e. Europe, or even more precisely, Southern Europe. The narratives of the SUSTAINABLE and MYOPIC scenario read as follows (KOUNDOURI et al. 2016):

> ***SUSTAINABLE scenario (SSP 1 - RCP 4.5):***
>
> ***Society & Economy:*** *The GDP per capita is growing at a faster rate than the 25-year average. As the societal emphasis shifts from economic growth per se towards an increase in equity, social capital and especially natural capital, this growth slows down over the long term. The overall level of globalisation is relatively high with markets being globally connected. However, the focus is on regional production and low material growth trying to reduce the resource and energy intensity. Economic growth allows for investments in environmental technologies and human capital, which in turn enhances the development of efficient and internationally collaborating institutions. All these factors result in relatively low challenges to both mitigation (high mitigation capacity) of and longer-term adaptation to climate change effects.*
>
> ***Energy:*** *Investments in environmental technologies together with the phase-out of subsidies for fossil fuels and lower taxes make renewable energies more attractive. Fossil fuels are used less and less reducing also the CO_2 emissions compared to the present. As a result of the overall trend to reduce energy and resource use, the resource efficiency and energy efficiency reaches a higher level. Still, the energy demand keeps on increasing in the near future. Eventually, the measures taken lead to an overall decrease in energy demand in the far*

future.

Environment: *Environmental sustainability is prioritised. The increasing effectiveness of institutions and a stronger cooperation and collaboration at different levels help improving the management of local and global environmental issues over the longer term. Environmental impacts such as air and water pollution decrease and environmental conditions improve overall. Land use is strongly regulated to avoid negative environmental impacts.*

Policies: *The awareness of the society regarding the social, cultural and economic costs of environmental degradation is expressed in policies (e.g. directives), which try to assign financial incentives (e.g. subsidies, taxes) to development and sustainability goals. There is a strong focus on environmental protection and strong regulations e.g. regarding land use.*

Water Management: *Complementary to civil protection and water supply, the management of water resources is triggered by a strong will to achieve high environmental standards. Ecosystem services related to water are considered to be of high value. Integrated long-term management is applied addressing local as well as regional water issues. The economic situation allows the use of technical measures in water resources management, although non-technical measures of selfregulation are preferred.*

MYOPIC scenario (SSP 5 - RCP 8.5)

Society & Economy: *GDP per capita is growing at a faster rate than the 25-year average. Economic growth allows investment and growth in human capital. This enhances institutional building and social equity and produces technological advances that enhance adaptation to climate change, but places no emphasis on mitigation. This has a negative effect on the quality and quantity of stock and flows of natural capital (NC). This negative effect is not integrated in production and consumption decisions and relevant policies (i.e. environmental externalities are not considered by any stakeholder group in the country). In summary, economic growth is driven by substituting natural capital with physical capital (technological development).*

Energy: *Energy demand increases and in response energy supply increases, but only in terms of making available more fossil fuel based energy. Increased supply is driven by technological advances making all fossil fuel resources cheaply accessible. Fossil fuel based energy (conventional and non-conventional, excluding uranium) prevails, because policies are not incentivising green energy. Investments in alternative energy sources and mitigation measures exist, but are limited. The rate of growth of C02 emission increases, compared to 2012.*

Environment: *Governmental environmental regulation is myopic (i.e. does not take into account long-run effects), while adaptation measures are reactive to only local concerns. Provisioning services are considered relevant as long as they are supporting profitable energy production. Other ecosystem services (i.e. regulating, supporting and cultural) are only of local short-run economic*

> *relevance and rank low in the global political agenda.*
>
> ***Policies:*** *Policies are myopic and driven by technological advancements, aiming to maintain GDP growth, without considering the medium and long-run effects on natural capital and human well-being. Environmental policies rank low in the political agenda and their enforcement diminishes as time passes.*
>
> ***Water Management:*** *Water management is fragmented and does not integrate the effects of water services on water resources. Water is considered valuable, and hence managed with care, only as input in income generating production processes, civil protection and water supply. All its non-use (passive) values are ignored.*

These qualitative storylines describe well the respective future worlds. The information they provide is, however, not sufficient to be used for modelling purposes and quantitative values are needed instead. The next step to take was splitting the storylines into different descriptors similar to the SSP key elements mentioned in chapter 2.5.1 and attributing an expected change to each of them according to the following scale:

- Significant increase: +++
- Moderate increase: ++
- Slight increase: +
- No change compared to present: 0
- Significant decrease: ---
- Moderate decrease: --
- Slight decrease: -

The trends may range from a significant increase, shown as +++, to a significant decrease (---). If no change is expected with respect to the current situation it is indicated by "0".
Some descriptors were directly adopted from the SSP elements, others were chosen to address the needs of the GLOBAQUA project. The division of SSP elements in low, middle and high income countries helped defining the descriptors with a more regional focus and distinguishing the scenarios further at this spatial scale. Following the example mentioned in chapter 4.1, the economic growth rate was set to be medium for the SUSTAINABLE scenario and high for the MYOPIC one. The complete descriptor table can be found in Appendix B. These European scenarios are, however, still too coarse to reflect the characteristics of each of the GLOBAQUA case studies. For this reason, the scenarios had to be further downscaled to the basin scale. The applied procedure is described in the next chapter. The quantification of descriptor trends for use in modelling is elaborated in more detail in chapter 5.2.3.

4.3 Downscaling of Scenarios to the River Basin Scale

4.3.1 Downscaling of Qualitative Scenarios by Stakeholder Participation

For in depth analysis and modelling activities at the catchment scale, the level of detail of the scenarios presented here is not yet sufficient. At this point, the GLOBAQUA scenarios do not account for regional differences inside Europe and the particular characteristics of each case study. Besides, the same cause may have diverging manifestations in different areas. As for example RIAHI et al. (2017) explain, SSP 1 "depicts a reversal of historical trends" including a "pervasive expansion of forests" at global scale. This is opposed to the trend observed in the Mediterranean in the last decades where a regrowth of forest has taken place due to the abandonment of marginal farmland mainly in mountainous regions (REY BENAYAS et al. 2007, LASANTA-MARTÍNEZ et al. 2005). A reversal of the trend in this case would mean a reactivation of abandoned agricultural land and consequently a reduction in forest cover. For this reason, the scenarios have to be further downscaled to the catchment level. As ROUNSEVELL & METZGER (2010) point out, a crucial tool in this context is stakeholder participation to ensure the scenarios address local needs and fit to the characteristics of each region. For GLOBAQUA, workshops were held in each of the case studies and local stakeholders were asked to translate the MYOPIC and SUSTAINABLE scenario to their river basin and to estimate the trends of the descriptors applying the same scale, see chapter 4.2, as earlier by the project partners in the scenario definition process. The trends of all stakeholders were averaged resulting in a second case study specific descriptor table reflecting the stakeholders' opinion. Table 4.1 shows exemplarily for the Ebro how often a change was expected by the stakeholders and the aggregated perceived changes.

In addition, GLOBAQUA internal case study experts were asked to estimate if a descriptor is a relevant stressor in their river basin having in mind the aquatic ecosystems as core of the project. If possible, the experts should give insides on the concrete effects. This information is summarised for the Ebro in Appendix C.

4.3.2 Downscaling Quantitative Socio-Economic Variables

The above described trends estimated by the stakeholders were helpful for setting up the land use change model. However, quantitative information is indispensable. GLOBAQUA partners from the Athens University of Economic and Business downscaled national projections of population growth and GDP growth provided by the SSP database mentioned before to the river basin scale. Regarding population growth, a single realisation developed by the International Institute for Applied System Analysis (IIASA) and National Center for Atmospheric Research (NCAR) is available for each SSP through the database (KC & LUTZ 2017). For GDP growth, three different modelling groups (IIASA, Potsdam Institute for Climate Impact Research (PIK) and OECD) have produced projections. The models coincide in their basic assumptions while the methodology and outcomes differ. Similar to the common practice in climate change research, this allows to consider uncertainties of GDP assumptions in impact modelling studies. In case not all model projections can be used, it is recommended to stick to the OECD projections which was chosen as "illustrative" case (IIASA 2016). This is the case for the present study and consequently the reason why only the GDP projections from the OECD were considered.

TABLE 4.1: Individual and aggregated perceived changes of stakeholders for the descriptors of the two GLOBAQUA scenarios in the Ebro river basin. The numbers represent the frequency of each notation. The highest frequency is highlighted in orange and the second highest in yellow only if first and second highest score are separated by 1 rank. Source: KER RAULT 2017.

		MYOPIC Scenario SSP 5 with RCPs 8.5									SUSTAINABLE Scenario SSP 1 with RCP 4.5								
Sector	Factor/descriptor	Total-3	Total-2	Total-1	Total0	Total1	Total2	Total3	Total resp	Aggregatred Perceived change	Total-3	Total-2	Total-1	Total0	Total1	Total2	Total3	Total resp	Aggregatred Perceived change
Society & Economy	Growth per Capita	0	2	3	0	3	4	1	13	1	1	1	1	3	4	1	0	11	0
	Unemployment	0	2	3	2	2	2	0	11	0	0	1	3	1	4	0	1	10	1
	Inequality Index	1	0	1	1	3	3	3	12	2	0	4	5	1	1	1	0	12	-1
	Urbanisation	0	1	1	0	4	6	2	14	2	0	4	3	5	1	0	0	13	-1
Energy	Use of fossil fuel (%)	0	1	0	1	2	6	3	13	2	2	8	3	1	0	0	0	14	-2
	Use of renewable resources (%)	0	1	2	1	6	2	0	12	1	0	1	0	0	1	8	4	14	2
Environmental Effects	Air Quality	5	5	1	1	1	1	0	14	-2	0	0	0	0	5	7	2	14	2
	Biodiversity	6	5	2	0	1	0	0	14	-2	0	0	0	1	5	6	2	14	2
	Invasive species	0	2	0	1	4	4	2	13	1	0	6	2	2	3	0	0	13	-1
	Deforestation	1	2	1	2	2	5	0	13	1	1	5	4	2	1	0	0	13	-1
	Soil Degradation	2	1	1	0	3	6	1	14	2	1	5	3	2	2	1	0	14	-1
	Water Scarcity (quantity/quality)	1	1	1	1	0	8	2	14	2	0	5	3	2	3	1	0	14	-1
Water management	Technical Measures	0	0	3	0	3	5	1	12	2	0	1	3	2	3	2	1	12	1
	Non-Technical Measures	0	2	6	2	2	0	0	12	-1	0	0	2	2	5	2	1	12	1
Agriculture	Irrigated surface area (ha)	0	1	3	2	3	4	1	14	1	0	1	6	4	2	0	1	14	-1
	Industrial agriculture (yield levels)	0	0	2	1	4	5	1	13	1	2	0	4	2	3	2	0	13	0
	Organic agriculture (yield levels)	1	1	1	3	5	1	0	12	1	0	1	0	0	4	7	2	14	2
	Meat production	0	2	0	4	3	4	1	14	1	1	1	5	5	2	0	0	14	-1
	Use of pesticides	0	2	1	2	1	5	3	14	2	2	5	4	2	1	0	0	14	-2
	Area cover with water intensive crops (ha)	0	0	3	1	4	4	2	14	1	1	1	6	2	2	1	1	14	-1
	Organic fertilizers	1	0	2	3	6	2	0	14	1	0	1	2	2	3	5	1	14	1
	Mineral fertilizers	0	0	2	3	4	4	1	14	1	2	1	5	3	2	1	0	14	-1
	Reuse of manure and by-products	0	2	4	2	4	1	1	14	0	0	0	0	0	6	6	2	14	2
	Abandonment of land	1	1	1	1	6	3	1	14	1	2	1	4	2	3	1	0	13	-1
	Crop rotation	0	2	6	1	2	1	0	12	-1	0	0	0	1	4	6	2	13	2
	Erosion prevention	2	4	4	2	0	1	0	13	-1	0	0	1	0	8	3	2	14	1
	Soil Salinization	0	2	1	2	2	6	0	13	1	0	2	5	5	0	1	0	13	-1
Industry	Investment in technology to emission reductions	2	3	0	1	4	3	0	13	1	0	1	1	0	2	6	3	13	2
	Level of emissions	0	1	1	0	3	3	6	14	2	1	4	3	1	4	1	0	14	-1
Residential	Water consumption/demand	0	1	0	1	6	5	1	14	1	0	4	5	2	2	1	0	14	-1
Tourism & recreation	Mass tourism	1	0	2	1	6	4	0	14	1	1	3	4	3	3	0	0	14	-1
	Selected tourism	1	2	2	2	4	3	0	14	0.5	0	1	2	2	5	4	0	14	1
Policies	Protected areas	1	4	2	2	4	1	0	14	-1	0	0	0	1	3	6	3	13	2
	Water quality standards	1	4	3	4	2	0	0	14	-1	0	1	1	1	5	4	2	14	1
	Food security	1	2	5	1	4	0	0	13	-1	0	0	1	0	7	5	1	14	1
	Desalination for irrigation	0	2	2	4	3	1	0	12	0	0	2	5	3	3	0	0	13	-1
		Total-3	Total-2	Total-1	Total 0	Total 1	Total 2	Total 3	Total resp	Aggregatred Perceived change	Total-3	Total-2	Total-1	Total 0	Total 1	Total 2	Total 3	Total resp	Aggregatred Perceived change

For downscaling the national population and GDP growth projections first the average growth rates of these two variables were determined based on statistics of the last decades. More precisely, the growth rate of all countries GLOBAQUA case studies are located in and the growth rates of the study areas themselves based on statistics from the RBMPs were estimated. The ratio of the average growth rate of a river basin to the average growth rate of the corresponding country was then calculated.This ratio was assumed to be constant over time also for the future. The value was then multiplied with the national projections (e.g. Spain) of GDP and population growth for each of the SSPs to obtain a case study specific growth rate (e.g. the Ebro). The observed time period and data sources for calculating the ratios differ depending on the river basin. More detailed information on the procedure can be found in the GLOBAQUA sub-deliverable 9.2 (KOUNDOURI et al. 2016).

4.4 Uncertainties in Climate Change Projections

Besides socio-economic projections also climate projections are subject to large uncertainties. For the same radiative forcing level the projected climate change may differ greatly depending on the climate model (VAN VUUREN et al. 2014). These uncertainties mainly derive from three sources (DESER et al. 2012, HAWKINS & SUTTON 2009): i) The internal variability of the climate system is responsible for the natural fluctuations that occur independently from the radiative forcing. ii) The response uncertainty arises from differences in physical and numerical formulations of the climate models causing each model to simulate slightly different changes to the same external forcing. iii) Finally, the forcing or scenario uncertainty has to be attributed to our incomplete knowledge of the factors influencing the climate system such as future trajectories of greenhouse gas emissions or land use change. As stated by VAN VUUREN et al. (2014), it is important to address the uncertainties related to climate change projections in impact studies. According to these authors, climate uncertainty can be considered another axis of the scenario matrix. The approach in GLOBAQUA depicted in figure 4.1 takes this into account.

To cope with uncertainties related to climate modelling, the use of multi-model projections has become more and more popular in IAV studies (ARAÚJO & NEW 2007, GRAHAM et al. 2007, NAJAFI & MORADKHANI 2015). Multi-model ensembles provide climate projections from various combinations of Global Circulation Models (GCMs) and Regional Climate Models (RCMs). To allow for comparability, the World Climate Research Programme (WCRP) has established the CMIP, which is already in its sixth phase (CMIP6), to organise and coordinate the setup of GCMs developed by various research groups (TAYLOR et al. 2012). The output of the GCMs is then used by other researchers to run RCMs and downscale the GCM data to the scale relevant for impact studies (WILCKE & BÄRRING 2016). Similar to CMIP, also the RCM simulations are coordinated in frameworks such as Coordinated Regional Downscaling Experiment (CORDEX) which aims at providing regionally downscaled climate projections for IAV studies (GIORGI et al. 2009).

However, the use of ensemble projections is not always feasible due to computational constraints. As a consequence, the climate models to be used in impact studies have to be chosen carefully (VAN VUUREN et al. 2014). For GLOBAQUA, a clustering method (WILCKE & BÄRRING 2016) was applied for selecting different GCM-RCM combinations out of the EURO-CORDEX ensemble, its spatial domain being Europe (KOTLARSKI et al. 2014). The clusters were built based on the climate change signals, i.e. the difference between the future (2035-2065) and reference (1980-2010) period, of different climate variables at annual and seasonal level (HERRERO et al. 2018). After several steps the simulation closest to the centre of the cluster was selected. Three final GCM-RCM combinations were chosen for the GLOBAQUA project, keeping most of the spread of the whole ensemble over the project's case studies and by this means also of the uncertainty (GAMPE et al. 2016). These combinations are: HadGEM2-ES-RCA4 (hereafter referred to as RCA4), ECEARTH- RACMO22E (RACMO22E) and

EC-EARTH-CCLM4-8-17 (CCLM4).

In order to be used for subsequent modelling, a bias-adjustment had to be carried out to reduce the systematic deviations compared to observations of a reference period climate simulations usually show (DOSIO 2016). In this case, a distribution-based scaling approach (YANG et al. 2010) was applied to the climate data using the regional reanalysis dataset MESAN (HÄGGMARK et al. 2000) as reference for precipitation and mean air temperature (HERRERO et al. 2018). As the resolution of the bias-adjusted simulations of 0.11° (approx. 12 km) is too coarse to reflect the heterogeneity of the GLOBAQUA case studies, the data was further downscaled using the SCALMET algorithm (MARKE 2008) to a 1 km grid (HERRERO et al. 2018). The resulting bias-adjusted and downscaled precipitation and air temperature projections for the three GCM-RCM combinations were used as dynamic input to the land use modelling described in chapter 5.

4.5 The Water Use Scenarios

Since the GLOBAQUA project focused on the effects of stressors on aquatic ecosystems under water scarcity, it was necessary to elaborate in more detail on the future water uses in the two scenarios. A project internal group of experts developed river basin specific water use scenarios in collaboration with the case study leaders. The water statistics reported by the RBMPs provided the basis for their assumptions. If available, already existing scenarios on the future water demand in a catchment were taken into account. Table 4.2 summarises the changes in the overall water use set for the different scenarios in the two GLOBAQUA test sites analysed hereafter.

The water consumed for irrigation makes up by far the largest part in both watersheds (CHE 2015, SKOULIKIDIS et al. 2011). Consequently, it dominates the reasoning regarding the scenarios. The 30% rise in the MYOPIC scenario in the Ebro is based on the changes reported in the RBMP 2015-2021 (CHE 2013, Annex III). They expect an increase of 27.5% of water used for irrigation until the year 2033. These changes fit best to the MYOPIC scenario as they reflect an optimistic attitude regarding the economic development of the region and the future water availability. The change in the SUSTAINABLE scenario was set to -30% to create a scenario which gets along with notably less water as it is currently the case, knowing that water scarcity is a problem already present in some parts of the basin (BOITHIAS et al. 2014). Regarding the Evrotas, SKOULIKIDIS et al. (2011) report that the irrigation has been expanded to olive trees only recently. This trend is assumed to continue in the MYOPIC scenario, which accounts for a +15% in the total water use. Meanwhile, it

TABLE 4.2: Percentage changes of the overall water demand in a scenario for the Ebro and Evrotas GLOBAQUA sites and values of sectoral water uses in the present (reference period) according to the RBMPs in $hm^3/year$.

	MYOPIC	SUSTAINABLE	PRESENT				
			Total	Domestic	Industry	Irrigation	Livestock
Ebro	30% (10641)	-30% (5730)	8186	358	147	7623	57
Evrotas	15% (106)	-30% (64)	92	7	1	83	1

was reduced in the SUSTAINABLE scenario by 30% to return to a situation where olive trees are not irrigated. Even though the water abstractions prior to the irrigation of olive trees were estimated to be 70% less than the present (SKOULIKIDIS et al. 2011), such a reduction for the future was valued as being unrealistic to happen.

Chapter 5

Land and Water Use Modelling

5.1 Selection of a Land Use Change Model

There are several reasons why iCLUE was selected as the most suitable model for the present study. First of all, it was indispensable to be able to model spatially explicit land use changes, i.e. to have a raster-based model. Besides, iCLUE is freely available. Out of all spatial land use models the main advantage of iCLUE lies in the fact that it allows simulating an unlimited number of land use classes simultaneously while there is no restriction on the type of the classes (VERWEIJ et al. 2018). Besides, there are no restrictions regarding the spatial resolution or the extent of the study area.

Furthermore, iCLUE is able to handle more land use classes and drivers than prior versions (VERWEIJ et al. 2018). A further improvement is the automation of many manual steps necessary in previous CLUE versions which makes the whole modelling less prone to errors. As input the model accepts any kind of drivers, both biophysical or socio-economic factors influencing the land use distribution (VELDKAMP & FRESCO 1996), which can be supplied as spatially explicit maps to the model (VERWEIJ et al. 2018). iCLUE also allows to implement yearly changing dynamic driving factors and by this means shape different scenarios (VERWEIJ et al. 2018). Its speedy calculations allow doing many model-runs, tests, validations and model adaptations during a day (HUBER GARCÍA et al. 2018).

5.1.1 The iCLUE model

iCLUE is a land use change model originating from the CLUE modelling framework formerly developed by VELDKAMP & FRESCO (1996) and more precisely from the spatially explicit CLUE-S model version (Conversion of Land Use and its Effects at Small regional extent) which enables analyses at the regional scale (VERBURG et al. 2002). CLUE is wellknown in the land use modelling community and has been applied in various forms to an abundance of study areas since its first release (FOX et al. 2012, KOK 2004, MEHDI et al. 2015, VERBURG et al. 2006). The version used in this study has been recently upgraded conceptually, methodologically and technically by VERWEIJ et al. (2018) and integrated into the QUICKScan software (VERWEIJ et al. 2016). QUICKScan is a participatory modelling tool used in workshops which allows to combine stakeholder knowledge, spatial and statistical data and provides many analysis tools (VERWEIJ et al. 2016).

To simulate changes in land use the iCLUE model combines empirically quantified relations between a land use class and its drivers with dynamic modelling of the competition between different land use classes (HUBER GARCÍA et al. 2018, VERBURG et al. 2002). Drivers are, as mentioned earlier, spatially explicit variables that influence the land use distribution such as soil type, climate, slope, distance to roads and cities, population density etc.. They are used to describe the suitability S of a location i for a certain land use lu at time t (VERWEIJ et al. 2018). Suitabilities are obtained by relating the driving factors to each land use by means of statistical relationships (HUBER GARCÍA et al. 2018). Out of several statistical methods supported by the model, a stepwise logistic regression was used in this study (HEDDERICH & SACHS 2012). Together with the "ease of change" E, the neighbouring land use N and the demand weight D, the total probability P of a land use lu to occur at a certain location i and time t is calculated as follows:

$$P_{\mathrm{i,lu,t}} = S_{\mathrm{i,lu,t}} + E_{\mathrm{i,lu,t}} + N_{\mathrm{i,lu,t}} + D_{\mathrm{i,lu,t}} \tag{5.1}$$

The "ease of change" is a value describing how easily a land use may be transformed into another (HUBER GARCÍA et al. 2018). It is further described in chapter 5.2.5. The influence of neighbouring land uses is not part of the iCLUE model used in this study, but was implemented indirectly for example for urban areas by included "distance to cities" as a driver. S and E in equation 5.1 are represented by numbers from 0 (low) to 1 (high) (VERWEIJ et al. 2018). The demand weight D stands for the difference between the future demand and the actual area covered by a land use. The demand weight is not constant but changes for each iteration depending on the difference between the allocated and the required area (VERWEIJ et al. 2018). Its value is derived from a sigmoid function between -1 (the actual area has to shrink strongly) and 1 (the area has to increase) and is larger the larger the difference is (VERWEIJ et al. 2018).

The sum of all these factors, resulting in a location-specific probability distribution across the potential future land use classes, provides the basis for the land use allocation algorithm that distributes land use classes in space in an iterative process. The probability is used to allocate each location to a single specific land use type (VERWEIJ et al. 2018). If the total allocated area of a land use class does not pass the acceptability tests, i.e. it deviates considerably from the required land use demand, the combined probability value for this land use is adapted in the next iteration by modifying the demand weight (VERWEIJ et al. 2018). How the future land use demands were determined is explained in more detail in chapter 5.2.3.

In addition, it is possible to define so called conversion rules which determine "if and under which conditions a conversion from one land use to another is allowed" (VERWEIJ et al. 2018). To be able to run, the model further needs an initial land use map for the starting year and the land use demand for each land use class at least for the first and last year of the simulation. All inputs and factors influencing iCLUE are displayed in figure 5.1. The Ebro and Evrotas specific model setups are explained in more detail hereafter.

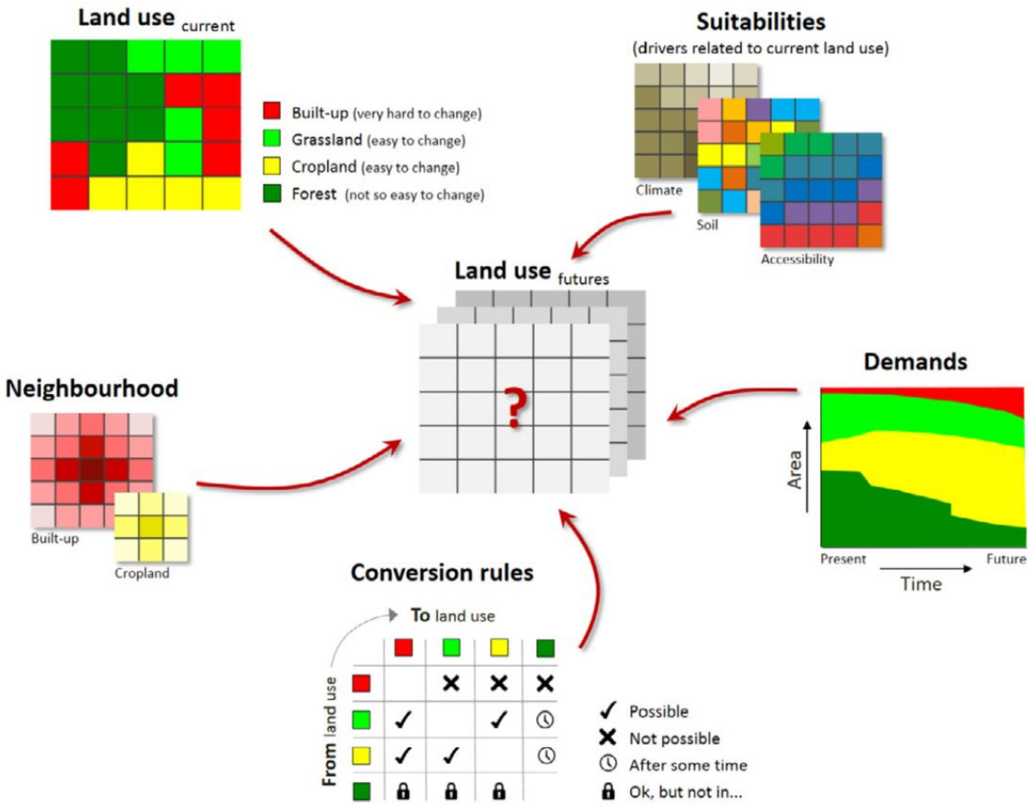

FIGURE 5.1: Factors determining the land use projections by the CLUE model. Source: VERWEIJ et al. (2018).

5.2 iCLUE Model Setup - Ebro River Basin

5.2.1 Preprocessing of LULCC Input

Several regional, national and international land use/cover databases were evaluated with regard to their suitability for the use in the present study. In general, the CORINE Land Cover data, called CLC data hereafter, provided by the EEA were found most adequate. First, CLC data is available for most European countries and therefore provides a more or less homogenous classification of land use/cover all over Europe which allows for comparisons between different case studies. Second and more importantly, CLC data were produced for several years covering now a range of about 28 years (1990 (EEA 2013a), 2000 (EEA 2013b), 2006 (EEA 2013c), 2012 (EEA 2016a), and 2018 (EEA 2018)). The existence of such a long-term LULCC inventory is of particular importance for deriving the land use demands for iCLUE described in chapter 5.2.3. Besides, it allows to evaluate the simulation results as shown in chapter 7.3. Even though national land use maps might provide a more detailed spatial or thematic resolution, the CLC data present a decent compromise with a 100 m x 100 m resolution and 44 land cover classes over Europe. In HUBER GARCÍA et al. (2018) an overview is given of the pre-analysis of land use data carried out for the Ebro compared to the one for the other GLOBAQUA test sites.

With regards to the Ebro, the CLC map of 1990 was chosen as start of the iCLUE simulations. This map, however, does not cover the territory of Andorra, located to a 100% in the Ebro River basin, nor do the other CLC observations. To fill this gap the

1990 map was merged with a national land cover map of Andorra provided by the Institut d'Estudis Andorrans (IEA) from 1995 (IEA 1995). These two maps had to be adjusted also thematically.
As mentioned in HUBER GARCÍA et al. (2018), the model performance of iCLUE is influenced by the number of modelled land use classes. Theoretically, iCLUE is able to handle an infinite number of land use classes. However, too many classes hamper the simulation as the model struggles in finding solutions for the allocation of all land uses, in particular for very small ones. The aim of the present study was to model as many classes as possible in order to be able to derive detailed information on water uses without reducing the model performance. For this reason, the number of classes was reduced from 41 present in the Ebro in the CLC 1990 map to 13. Special emphasis was put in preserving information related to water uses and grouping together only classes that are expected to cause similar water consumptions (HUBER GARCÍA et al. 2018). For this purpose, the GLOBAQUA internal Ebro experts were asked to evaluate the importance of each land use regarding the aim of the project, i.e. its potential to cause negative effects on aquatic ecosystems. This assessment was used for a subsequent reclassification and simplification of the land use/cover information to focus on the most relevant classes resulting in the 1990 land use map displayed in figure 7.12. The reclassified CLC maps containing 13 classes are called CLC 1990, CLC 2000 and CLC 2006 hereafter.

5.2.2 Protected Areas

Taking into account spatial restrictions is widely used in land use modelling whereas the exact implementation differs (FOX et al. 2012, LUO et al. 2010, MALEK & VERBURG 2018, SOHL et al. 2012). Also in the present study, some restrictions were included in the modelling setup for protected areas such as national parks. It was assumed that protected areas are not allowed to change and consequently stay constant over time. The national designated areas dataset made available through the EEA was used to identify the correct locations (EEA 2014a). The dataset reports the International Union for Conservation of Nature (IUCN) protected areas management categories to which also MALEK & VERBURG (2018) refer. Areas with a high protection standard - including the categories Ia, Ib, II and III - were masked out from all iCLUE input maps prior to the simulations. The result maps were merged with the CLC 2006 map to cover the missing areas. In total, 1329 km^2 are treated as restricted areas which accounts for approx. 1.5% of the area modelled in the Ebro basin setup (87364 km^2).

5.2.3 Quantification of the Land Use Demand

One of the core inputs to the iCLUE model is the land use demand, i.e. the exact number of pixels belonging to each land use class, for the first and final year of the simulation, in this case 1990 and 2050. To help the model finding results more easily and align historic land use simulations to observations, iCLUE allows to include also land use demands for arbitrary years in between the start and end year. By now, land use demands are available for the RCP-SSP-framework through IAMs presented in POPP et al. (2017). However, the spatial aggregation is way to coarse for local impact studies as it is the case here. Furthermore, the problem of a huge range of outcomes of global models regarding future land uses remains as mentioned priorly in chapter 1.2.

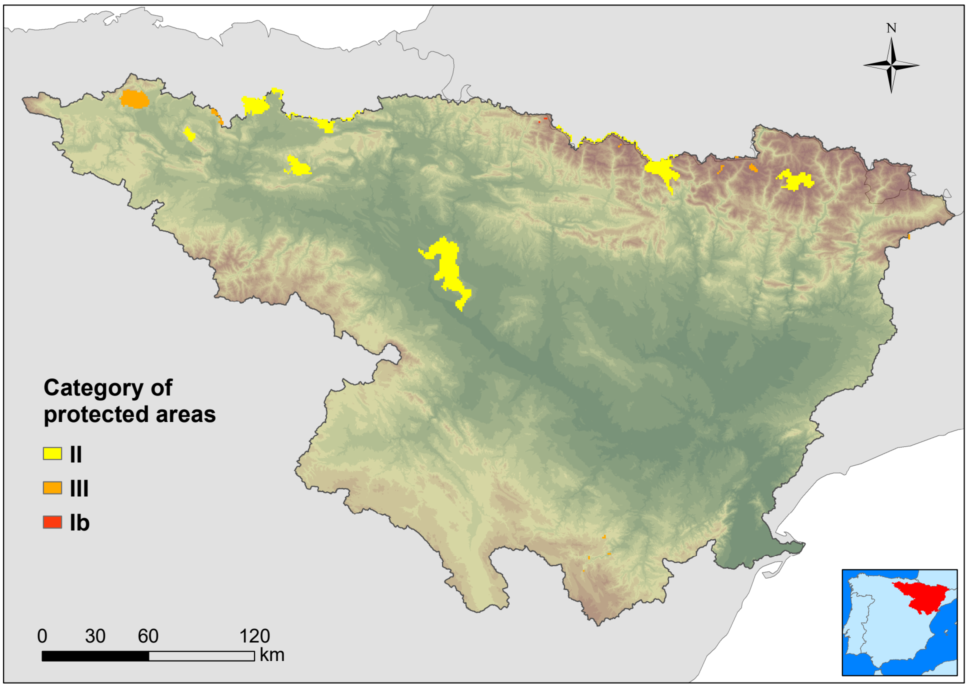

FIGURE 5.2: Protected areas in the Ebro River basin. Datasource: EEA (2014a).

In case of the Ebro, the land use demands between 1990 and 2006 were handed to the model at a yearly basis to mimic the observed development as good as possible. Yearly values were achieved by interpolating the existing CLC maps over time. As only a land cover map of the year 1995 is available for Andorra, actual land use/cover in this area could not be quantified. iCLUE may, however, model change also there. The interpolation period was not expanded further since the CLC 2012 map presents considerably classification differences compared to the previous ones and was therefore excluded. The sudden change from *complex cultivation patterns* to *permanently irrigated land* in some areas in 2012 is thought to be caused by diverging classification schemes rather than by actual land use changes. Uncertainties in CLC data are a well-known issue also addressed by ZOMLOT et al. (2017).
After 2006, the demands are defined for five year time steps starting from 2010 until 2050. Until 2017 the land use evolves equally in both scenarios to make sure that the past development is the same. For this purpose, the overall trend between 1990 and 2006 is extrapolated for each land use class.

From the GLOBAQUA scenario development process a large amount of qualitative information was available summarised in Table 5.1 including the descriptors for the GLOBAQUA large scale scenarios developed by a group of project internal experts, the downscaled case study specific descriptors defined during the stakeholder workshops and the relevance of descriptors according to GLOBAQUA case study experts. For being fed into the land use model this information had to be quantified, which means translated into actual numbers first, as also stated by MALLAMPALLI et al. (2016). To do so, it was combined with data collected in an extensive literature review. In case of the Ebro, the RBMP was particularly helpful as it provides some assumptions on the future development of irrigated area in the basin aiming at an increase of approx. 50% until the 2033 while the water used for irrigation purposes

TABLE 5.1: Scenario descriptor table for the Ebro for both scenarios including the global scenario definitions, the downscaled scenarios according to the stakeholders and the relevance of the descriptors for the case study according to GLOBAQUA experts.

Descriptor	Global scenario - Experts' opinion	Downscaled scenario - Stakeholders' view	Final factor	Relevance for Ebro
Growth per capita	MYO:+++ SUS:++	MYO:+/++ SUS:0/+	MYO:+2 SUS:+1	yes
Urbanisation	MYO:+++ SUS:+	MYO:++ SUS:0/-	MYO: +2.5 SUS: 0	yes
Irrigated surface area	MYO:++ SUS:- -	MYO:+/++ SUS:-	MYO: +1.5 SUS: -1	yes, very important
Industrial agriculture	MYO:++ SUS:-	MYO:+/++ SUS:-	MYO: 1.5 SUS: -1	yes, very relevant
Organic agriculture	MYO:- - SUS:+++	MYO:+ SUS:++	MYO: -0.5 SUS: +2.5	yes, less relevant
Area covered with water intensive crops	MYO:- - SUS:- - -	MYO:+/++ SUS:-	MYO: 0.5 SUS: -2	yes, very relevant
Abandonment of land	MYO:+ SUS:-	MYO:+ SUS:-	MYO: +1 SUS: -1	yes
Deforestation	MYO:++ SUS:-	MYO:+/++ SUS:-/- -	MYO: +1 SUS: -1.5	yes

will increase approx. 30% compared to the year 2013 (CHE 2013, Annex III). Figure 5.3 shows a map of the present (light green) and planned (dark green) irrigation systems in the Ebro.

In terms of numbers, the RBMP takes as reference an irrigated area of 9657 km^2 for the years 2009-2015, even though the entirety is not permanently irrigated. The discrepancy between AEI and actually irrigated area (AIA), which may vary strongly between years and over the growing season, is a well known problem when trying to estimate spatially distributed irrigated land (AUS DER BEEK et al. 2010). According to the FEDERACIÓ ECOLOGISTES EN ACCIÓ DE CATALUNYA (2012), the targeted increase will account for 14100 km^2 of irrigated land in the Ebro (total basin area modelled: 87364 km^2). From an ecological point of view, this is a quite negative development driven rather by economic interests, which is the reason why it was used as reference for the MYOPIC scenario. It further implies the idea of unlimited water resources and fits therefore well to the technological optimism of SSP 5 (KEBEDE et al. 2018). The land use demands of the other land use classes were built around it. The SUSTAINABLE scenario was developed in contrast to the MYOPIC one trying to reduce the agricultural water needs. A detailed description of the quantification of the demands follows hereafter.

5.2.3.1 *Permanently Irrigated Land, Fruit Trees & Olives*

MYOPIC: The area of the class *permanently irrigated land* according to CLC is smaller than the one assumed by the RBMP. Since also the class *fruit trees & olives* is mainly located in areas which are irrigated when comparing the CLC map of 2006 with the map in figure 5.3, also this class was expected to be irrigated for the land use demand calculations. This is due to the intensive irrigation of fruit trees, mainly peaches and pears, and less to olives (CHE 2013, Annex III). However, only 25% of the total 50% increase of irrigated land was attributed to this class and 75% to *permanently irrigated land* to underline the prevalence of the latter one. The land use demands for these

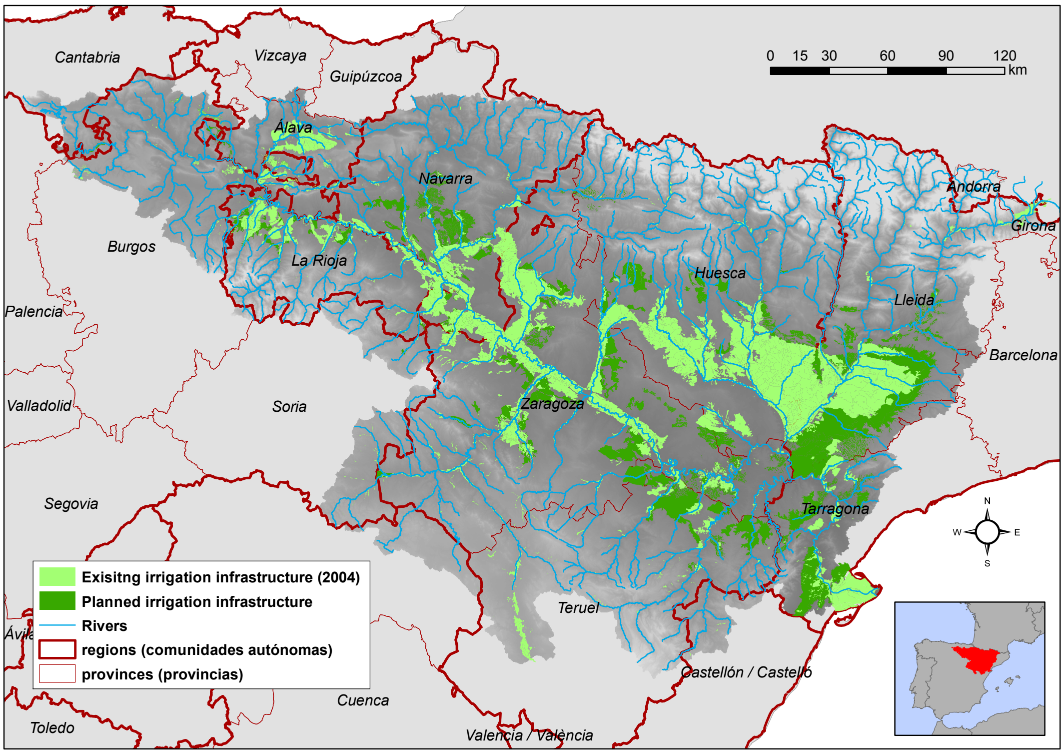

FIGURE 5.3: Long term irrigation plans in the Ebro basin according to the RBMP with present (light green) and planned irrigation infrastructure (dark green). Adapted from CHE (2015).

classes grow until 2033 increasing together by around 50% as suggested in the RBMP. Until the end of the simulation in 2050 the demand increases further by another 5% compared to 2033.
Herbaceous plants such as alfalfa, maize, wheat and barley are cultivated on 70% of the irrigated land in the Ebro River basin, a substantial part of it dedicated to fodder and therefore to the meat industry (CHE 2013, Annex III). The growth of this sector in the MYOPIC scenario is in line with the global trend in SSP 5 which expects an increased meat consumption (O'NEILL et al. 2017). The draft for the next RBMP confirms both that the amount of livestock and the irrigated area producing fodder has expanded lately (CHE 2018).

SUSTAINABLE: A reduction of 25% until 2033 was set for this scenario for both land use classes. From 2033 to 2050 the demands are reduced by another 5% of the value in 2033.

5.2.3.2 *Non-Irrigated Arable Land, Complex Cultivation Patterns, Agriculture with Significant Areas of Natural Vegetation, Transitional Woodland & Shrubs & Sclerophyllous Vegetation*

MYOPIC: The increase in irrigated area in the MYOPIC scenario described above has to be compensated with the decrease of other land use classes. But which land uses are they and how is the loss distributed between them? Two things were considered:

1. Which land uses are located in the planned irrigated areas (dark green) in figure 5.3 according to the RBMP?

2. Which percentage of the total area of a class will be transformed into irrigated land and will consequently belong to the planned irrigated areas in the RBMP?

As a result, the 45% of the new irrigated land was taken from the class *non-irrigated land*, 35% from *complex cultivation patterns* and 15% from *agriculture with significant areas of natural vegetation*. The remaining 5% are translated as a loss in *transitional woodland & shrubs & sclerophyllous vegetation*.

SUSTAINABLE: Due to its location in the wide plains of the Ebro catchment, *non-irrigated arable land* has to be considered to be intensively managed. This way of managing the land can be expected to decrease in a sustainable world as defined by the GLOBAQUA scenarios in table 5.1 and based on SSP 1 with healthy diets, reduced meat consumption and limited food waste (RIAHI et al. 2017). Consequently, the slightly negative trend between 1990 and 2006 according to CLC data was extrapolated until 2050. *Complex cultivation patterns* and especially *agriculture with significant areas of natural vegetation*, which are considered to represent small scale agriculture with high variety in crops and species, were expected to grow 10% and 15% until 2050 compared to 2017, respectively. *Transitional woodland & shrubs & sclerophyllous vegetation* increases 5% until 2050.

5.2.3.3 *Sealed Area*

MYOPIC + SUSTAINABLE: The demand for this class was calculated using a regression model that relates the sealed area with GDP and population growth data similar to the one used by REGINSTER & ROUNSEVELL (2006):

$$L_{\text{is}} = a_1 + a_2 G + a_3 P + e \tag{5.2}$$

where L_s represents the sealed area in the Ebro in km^2, G is the annual real GDP growth [%], P the annual population growth [%] and e an error term. For calculating the regression coefficients, GDP and population data for the period 1996-2013 from the Instituto Nacional de Estadística (INE) were used. The future GDP and population growth projections for the different SSPs used are the ones downscaled for the GLOBAQUA project, see chapter 4.3.2. The resulting demand of sealed area until 2050 is visible in figure 5.4, the red curve represents SSP 5 (MYOPIC) and the black one SSP 1 (SUSTAINABLE). The urban demands according to the CLC maps are marked with small dots in the graph. CLC 2012 and 2018 were excluded from calculations as it shows notable classification differences compared to the previous maps. This causes the urban demand in 2012 to be considerably higher than in the years before. Following this trend would have meant an extreme increase of urban area which was discarded as being unrealistic.

According to RIAHI et al. (2017) the urbanisation, i.e. the shift from rural to urban population, is assumed to be fast both in SSP 1 as in SSP 5 due to high income growth. This, however, does not mean that the urban areas grow at the same pace. In SSP 1 "urban areas are desired given the high efficiency that compact urban areas may achieve" (RIAHI et al. 2017) while the increase in urban area will be larger in SSP 5.

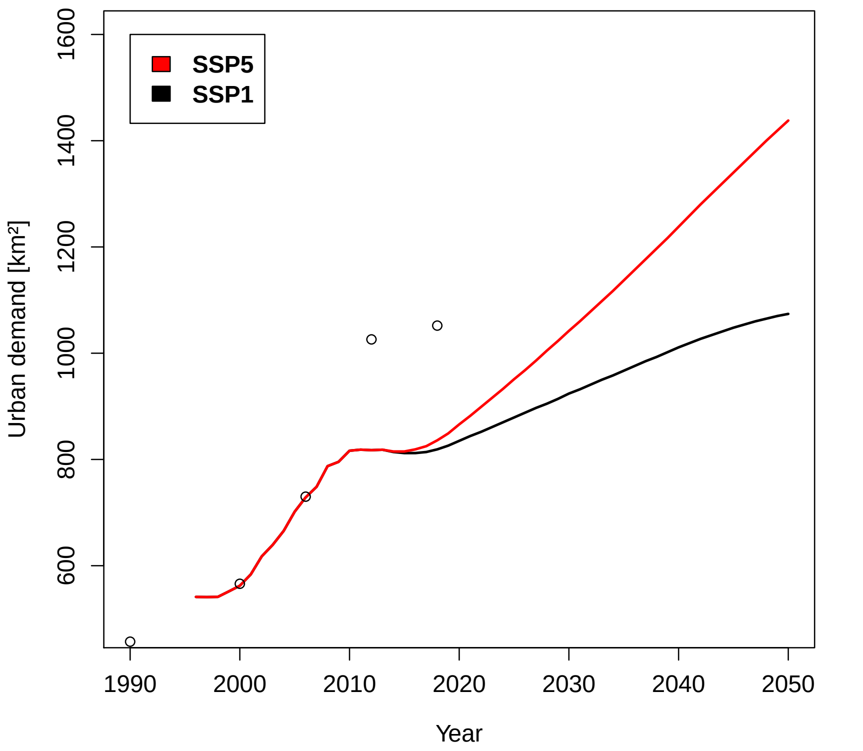

FIGURE 5.4: Calculated demand of sealed area [km^2] in the Ebro from 1990 to 2050 for the MYOPIC scenario (SSP 5, red) and the SUSTAINABLE scenario (SSP 1, black). The dots represent the sealed area according to CLC data (1990, 2000, 2006 (version 17), 2012 and 2018).

5.2.3.4 *Broadleaved Forest, Coniferous & Mixed Forest*

The scenario descriptors 'deforestation' and 'abandonment of land' have to be considered when looking at the demand for the forest classes. In case of the Ebro, they describe opposed trends and 'neutralise' each other at the catchment scale. At short term, the latter descriptor is rather equivalent to the expansion of shrubs, while it leads to an increase of forested area in the long term. Looking at the trends for the GLOBAQUA scenarios in Table 5.1 that means:

MYOPIC:
Deforestation (++) - Abandonment of land (+) = Trend: (+), Forest demand goes down

SUSTAINABLE:
Deforestation (-) – Abandonment of land (-) = Trend: (0), Forest demand stays constant/goes up slightly

For the SUSTAINABLE scenario the negative trend of 'abandonment of land' was rather interpreted as a clear out of *transitional woodland & shrubs & sclerophyllous vegetation* located on former agricultural areas abandoned during the last decades (DELGADO et al. 2010) and now revaluated for regional agriculture, than a clear cut of forest stands. Consequently, the overall trend of forest demand was expected to slightly grow (+). In the MYOPIC scenario, the forest area until 2050 will be reduced (-).

Orientation values to translate the '+' and '-' signs to numbers were found in KANKAANPÄÄ & CARTER (2004), where they constructed European forest scenarios based on the old SRES scenarios. For Italy, Greece, Portugal and Spain they estimate a decrease of 10-15% in the A1 scenario, while for the more sustainable B1 scenario they expect an increase of around 10-15%. Since the change in forest area in the GLOBAQUA scenarios, see Table 5.1, is less marked (only one +/-), a difference of up to 5% between the historic (CLC 2006) and future (2050) was assumed. For the MYOPIC scenario, the slightly negative trend in forest area in the CLC data from 1990-2000-2006 was extrapolated until 2050, resulting in a 3.5% and 2.2% reduction of *broadleaved forest* and *coniferous & mixed forest*, respectively. In the SUSTAINABLE scenario both forest classes gain 5% in 2050 compared to the values in 2017.

5.2.3.5 *Vineyards*

By far the largest and most important wine-cultivating region in the Ebro is the Rioja region located in the North-eastern part of the catchment. In a recent publication by ANTOÑANZAS VILLAR et al. (2015) they analyse the possibilities of expansion of vineyards in the Rioja region until 2030 presenting 5 different scenarios summarised in Table 5.2.

TABLE 5.2: Five scenarios of the expansion of vineyards in the DOC Rioja region. Shares in % relate to production. Adapted from ANTOÑANZAS VILLAR et al. (2015).

Baseline scenario	**Scenario 1**		**Scenario2**	
Production constant at value of 2015	+1% per year		+1.8% per year	
	Scenario 1A	**Scenario 1B**	**Scenario 2A**	**Scenario 2B**
	+1% until 2030	+1% until 2021, than constant	+1.8% until 2030	+1.8% until 2021, than constant

MYOPIC: Scenario 2A in Table 5.2, the one with the strongest increase, 1.8% yearly growth until 2030, was used as reference for the MYOPIC scenario in the Ebro. 1.8% was the mean yearly production increase between 2008 and 2015 (ANTOÑANZAS VILLAR et al. 2015). In this wealthy world the focus is set on global trade, so the demand for vineyards can be expected to grow substantially.

SUSTAINABLE: In this scenario, a less globalised world is assumed and more self-sufficiency. As a consequence, the wine production may not grow as much as in the MYOPIC scenario. Scenario 1B from ANTOÑANZAS VILLAR et al. (2015) with 1% yearly increase in production until 2021 was therefore chosen as reference: The trend in vineyard area between 1990-2006 from CLC data was extrapolated until 2021, which is equivalent to a yearly increase of 0.9%. It has to be noticed, that the production growth rates in ANTOÑANZAS VILLAR et al. (2015) are specified in litres of wine. For the land use change modelling in GLOBAQUA, these values were directly applied on the land use demands.

5.2.3.6 *Open Spaces with Little or no Vegetation*

The development of this land use class is difficult to interpret. In the Ebro, it can mostly be found in high mountain areas covering only a small part which is the reason it is less relevant for water issues analysed in GLOBAQUA. On the one hand, considering climate change, the treeline may be shifted upwards, meaning that it would cover an even smaller area only on the mountain tops. On the other hand, more forest fires are expected due to climate change, which would expand the area of *open spaces with little or no vegetation* also in the lowlands.

MYOPIC: From 2017 on, the trend 1990-2006 from CLC data was reversed since more forest fires are expected, resulting in an 4% increase in 2050 with respect to 2006.

SUSTAINABLE: The trend 1990-2006 from CLC data was extrapolated until 2050 causing a reduction of 5.5% compared to 2006.

5.2.3.7 *Grassland & Pastures*

Also in this case, it is difficult to estimate how this land use may develop in the two scenarios. Eventually, it was adapted depending on the developments of the other classes since the sum of all demands has to sum up to the same amount of pixels for each year.

5.2.3.8 *Water*

The demand for water is left constant all over the simulation period in both scenarios.

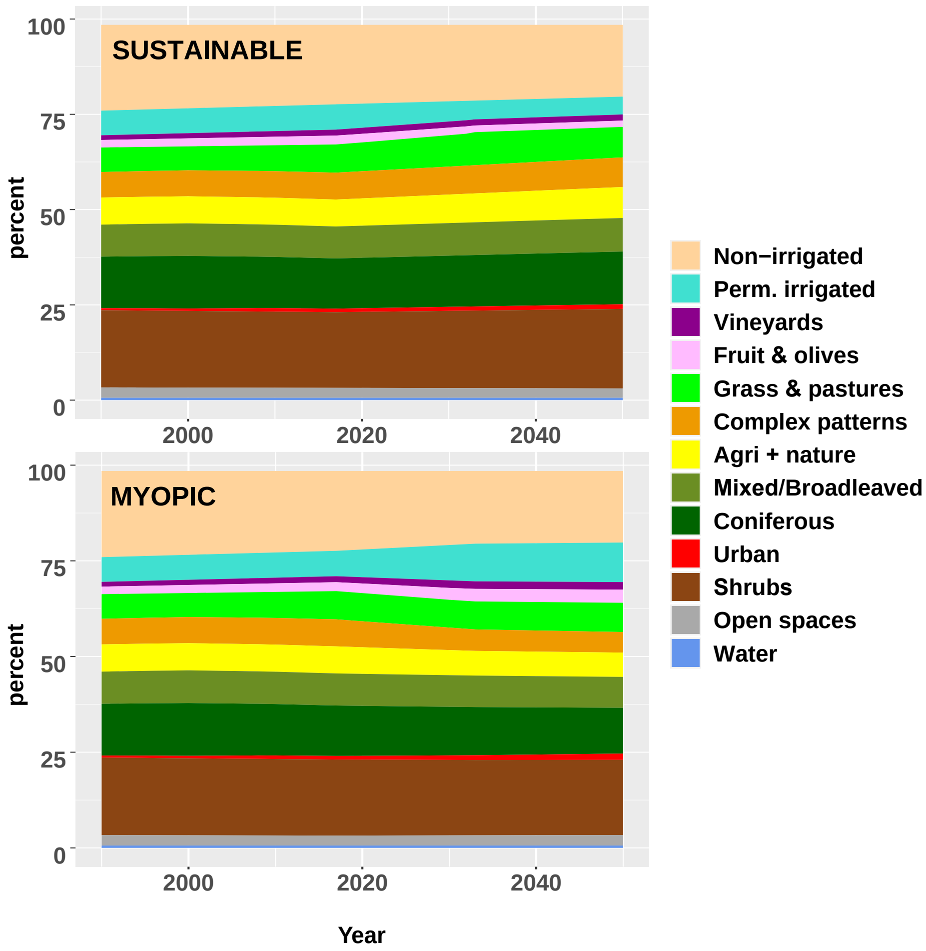

FIGURE 5.5: Land use demand for the Ebro in the SUSTAINABLE (top) and MYOPIC (bottom) scenario 1990-2050.

Taking everything into account, the land use demands for the Ebro until 2050 in the two scenarios come to be as in figure 5.5. The most striking difference, the increase of irrigated land in the MYOPIC scenario vs. the reduction of that class in the SUSTAINABLE, is clearly visible. The differences between the other land use classes are less pronounced. However, also the way land is managed plays a crucial role in the GLOBAQUA scenarios. This is defined in more detail through the water use scenarios in chapter 5.4.

5.2.4 iCLUE Drivers

Due to its large extent, the Ebro River basin was modelled at a 1 km^2 resolution to reduce the calculation time. Besides, many of the input drivers were only available at 1 km^2 and therefore increasing the modelling resolution would not have meant to include more information.
The iCLUE results are largely influenced by the drivers used to run the model as they have a large weight in the allocation of land. When considering past developments in the region, the underlying reasons mentioned most frequently in literature are social and economic changes that caused a rural exodus and made farming unprofitable

under certain conditions, whereas it concentrated economic activities in other areas (GARCÍA-RUIZ et al. 2011). Some of these driving forces are difficult to capture in numbers and, even more, distribute spatially on a map. This is, however, the input format that iCLUE needs. Nevertheless, the aim was to gather a wide range of different influencing factors available as spatially explicit information. All drivers used for the Ebro setup are summarised in table 5.3. The variables include physical properties of the land (slope, lithology, aspect, erosion levels), climate variables (annual precipitation sum, mean minimal temperature) as well as demography (population density) and economic factors (employees in different sectors, GDP). Distance measures to the main infrastructure were included to represent the distance to markets and transport costs, a widely used approach in land use change science (VERBURG & OVERMARS 2007). Other drivers than the ones in table 5.3 had been tested before in iCLUE but were excluded since they worsened the simulation results or were eliminated by the model due to high correlations with other drivers (HUBER GARCÍA et al. 2018).

iCLUE calculates a new land use map at yearly time steps based on previously created probability maps. The probability maps are adapted in each time step, i.e. as the demand for a land use class increases/decreases or drivers change. In fact, the model allows including dynamic drivers changing at each time step to be able to describe changing conditions. For the present setup, the mean annual temperature and annual precipitation sum were included as dynamic drivers for the whole modelling period 1990-2050. The data are bias-adjusted climate projections originating from the EURO-CORDEX project and downscaled to a 1 km^2 resolution for use in GLOBAQUA as described in chapter 4.4. The SUSTAINABLE scenario was run with projections for RCP 4.5 whereas the MYOPIC included RCP 8.5 projections. To analyse the sensitivity of iCLUE to different climate inputs, each scenario was run with climate data from three different combinations of GCMs and RCMs, abbreviated RCA4, RACMO22E and CCLM4, priorly selected within the GLOBAQUA project and explained in more detail in chapter 4.4.
As regards socio-economy, it was possible to create spatially distributed drivers of the population density from national statistics for the period 1992-2013. Population numbers are available through the INE at municipality level. For the years 1990 and 1991 the map of 1992 was used. Unfortunately, no projections of the future development of the spatially distributed population density at this aggregation level were available and the SSP database provides only national values so the information could neither be derived from there. Consequently, for modelling future scenarios the population density in 2013 was held constant until 2050. Nevertheless, population and GDP projections are indirectly included in the model as they are used to calculate the demand of urban areas described in chapter 5.2.3.

TABLE 5.3: Drivers used for setting up iCLUE in the Ebro River basin and their sources.

Driver	Source
Ratio of employees in manufacturing industry to total employees at municipality level	Census 1991, INE, http://www.ine.es/inebmenu/indice.htm
Ratio of employees in agriculture to total employees at municipality level	Census 1991, INE
Euclidean distance [m] to: - Channels - Towns >10,000 inhabitants - Towns >20,000 inhabitants - Towns >50,000 inhabitants - Main rivers - All roads (categories 1-8) - Largest roads (category 1& 2) - Roads of categories 1 to 3, 1 to 4, and 1 to 7 - Wells for water extraction	Calculated from data obtained from: - Geoportal Confederación Hidrográfica del Ebro (CHE) (http://iber.chebro.es/geoportal/)
- Coasts	- Natural Earth (http://www.naturalearthdata.com/downloads/)
Presence of hydrogeological units	Geoportal Confederación Hidrográfica del Ebro (CHE)
Digital Elevation Model (DEM) [m]	SRTM 90 (CGIAR-CONSORTIUM FOR SPATIAL INFORMATION 2015)
Aspect	Calculated from the DEM
Slope [%]	Calculated from the DEM
Dynamic population density [persons/km^2] per municipality 1992-2013, calculated from population data	data 1990–1995, INE (http://www.ine.es/dynt3/inebase/es/index.htm?padre=583&dh=1) data 1996–2006, INE (http://www.ine.es/dynt3/inebase/es/index.html?padre=517&dh=1)
Dynamic annual mean temperature [°C] Dynamic annual precipitation sum [mm]	Downscaled and bias-adjusted EURO-CORDEX data (JACOB et al. 2014)
Erosion levels 1 to 8	For Spain from Geoportal CHE For Andorra and Garona River from the European Soil Database (ESDB) (http://eusoils.jrc.ec.europa.eu/ESDB_Archive/ESDB_Data_Distribution/ESDB_data.ht)
Population 2011	GEOSTAT 2011 grid (http://ec.europa.eu/eurostat/web/gisco/geodata/reference-data/population-distribution-demography)
Nominal GDP at provincial level 2007	INE (http://www.ine.es/jaxi/tabla.do?path=/t35/p010/a2004/l0/&file=02001.px&type=pcaxis&L=0) Data for Andorra: (http://www.estadistica.ad/serveiestudis/web/index.asp)
Lithology of the upper layer, 22 classes	OneGeology (http://www.europe-geology.eu/onshore-geology/geological-map/onegeologyeurope/)
Irrigation density	Geoportal CHE
Soil erosion	Pan European Soil Erosion Risk Assessment (PESERA) (https://esdac.jrc.ec.europa.eu/content/pan-european-soil-erosion-risk-assessment-pesera)
Landscape values based on Flickr	Environmental Geography, University Amsterdam (https://www.environmentalgeography.nl/site/data-models/data/)

5.2.5 Further Model Specifications

5.2.5.1 *Ease of Change*

In addition, there are several other parameters for the fine tuning of iCLUE which are also used to calibrate the model (HUBER GARCÍA et al. 2018). The first one is the ease of change which determines how easily a land use class can be transformed into another. The following categories exist: "Very easy", "easy", "hard", "very hard" and "cannot change". For the Ebro, *Non irrigated arable land*, *agriculture with natural vegetation*, *transitional woodland & shrubs & sclerophyllous vegetation* and *open spaces* obtained the value "easy" since these classes are not equipped with large infrastructures and their transformation can be carried out with little physical and economic effort. *Complex cultivation patterns* and *frui trees & olives* were set to "hard", while the rest of the classes was considered to be very hard to transform to other classes. This includes all forest types which would need to be cleared before transforming it, agricultural classes with high investments in infrastructure such as *permanently irrigated land* or *vineyards* as well as urbanised areas. The reason why *grassland & pastures* is thought to be difficult to change is due to its remote location mainly in mountain areas. *Water* was the only class which was not allowed to change at all since it is supposed to stay constant. The modelling resolution of 1 km^2 is too coarse to actually capture fluctuating water bodies.

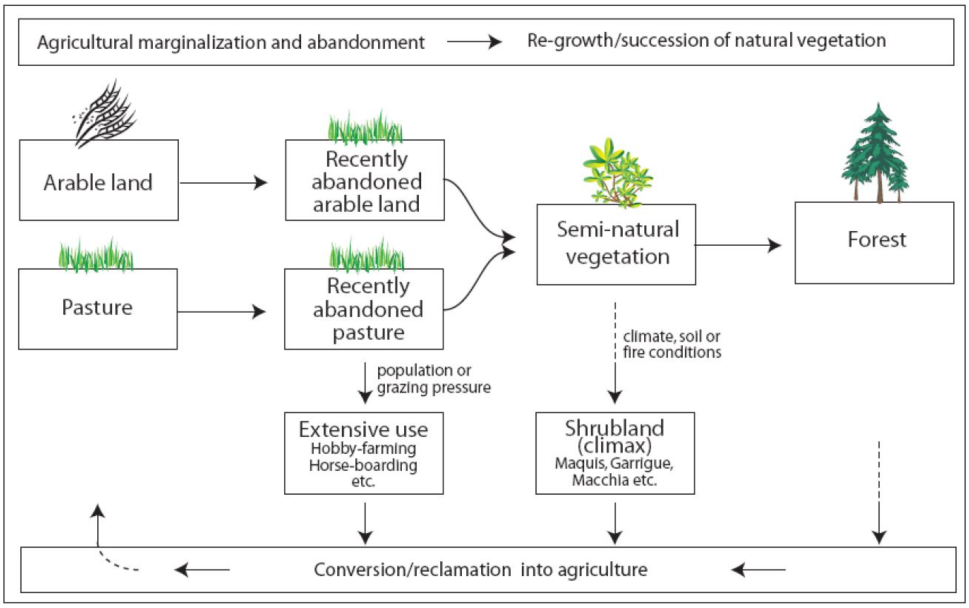

FIGURE 5.6: Schematisation of the land use/cover transitions upon abandonment of agricultural land. Source: VERBURG (2010).

5.2.5.2 *Conversion Rules*

Adapting the conversion rules allows to control which land use transitions are allowed to take place, where and when (HUBER GARCÍA et al. 2018). It also allows forcing transitions to happen in a certain order, e.g. following the example in figure 5.6 from VERBURG (2010) to imitate a natural vegetation succession following the abandonment of agricultural land. Similar rules are used by MALEK & VERBURG

(2018) in their application of the CLUMondo model. To imitate such a development, *grassland & pastures* were allowed to change to *transitional woodland & shrubs & sclerophyllous vegetation* only after three years and this class to either types of forest only after another 10 years of persistence. *Open spaces* remain constant for two years before they can be turned into *grassland & pastures* and *transitional woodland & shrubs & sclerophyllous vegetation*. Also for *non irrigated arable land* it takes to years two change to *sealed area* or *complex cultivation patterns*. In turn, *sealed area* is not allowed to change to any of the other 12 land use classes. There are also restrictions for *permanently irrigated land* which is not allowed to change to *agriculture with natural vegetation*, *transitional woodland & shrubs & sclerophyllous vegetation*, *grassland & pastures*, neither forests.

5.2.5.3 *Allowed Demand Deviation*

To facilitate the process of finding a solution, the iCLUE user can set a value indicating to what extent the simulated demand is allowed to deviate from the target demand passed to the model. The deviation may be specified as absolute value (cell counts) or percentage deviation for each land use class individually. According to VERWEIJ (June 2015), the deviations should constitute 5% of the demand of a class at maximum, whereas small classes should be allowed to deviate relatively more than large classes. For the Ebro setup, the deviation was indicated in absolute terms. Table 5.4 summarises the values set for each of the land use classes.

TABLE 5.4: Allowed deviation [%] from the targeted land use demand for the Ebro setup.

Land use	Allowed Deviation
Non-irrigated arable land	0.9
Permanently irrigated land	1.8
Vineyards	2.8
Fruit trees & olives	2.9
Grasslands & pastures	1.8
Complex cultivation patterns	1.7
Agriculture with natural vegetation	2.4
Broad-leaved forest	2.7
Coniferous & mixed forest	1.7
Sealed area	3.3
Trans. woodland&shrubs&sclerophyllous	1.1
Open spaces with little or no vegetation	1.1
Water	0

The ease of change, the conversion rules and the allowed deviation were used to tune the model in the calibration process. Besides, there are two further parameters that can be set in iCLUE: the sample size percentage and the correlation threshold. The first one defines the percentage of pixels that is used to carry out the stepwise regression to calculate the suitability maps, it was set to 0.2 (default is 0.1). The correlation threshold specifies the threshold above drivers should be excluded from the regression due to their high correlation with the land use distribution.

5.3 iCLUE Model Setup - Evrotas River Basin

5.3.1 Preprocessing of LULCC Input

CLC maps for the Evrotas basin, entirely located in Greece, are available for the years 1990, 2000, 2012 and 2018 whereas the last one was not taken into consideration since it is not yet fully validated. As for the Ebro, the last version of CLC data shows considerable differences to previous versions which are thought to be changes caused by divergent classification rules rather than actual changes. Due to its small extent, the modelling resolution of the Evrotas could be set equal to the original resolution of the CLC data, i.e. 100 m^2. The CLC classes were reclassified to seven classes representing well the heterogeneity of the catchment while reducing the model complexity. The 1990 reclassified map of the Evrotas is displayed in figure 5.7.

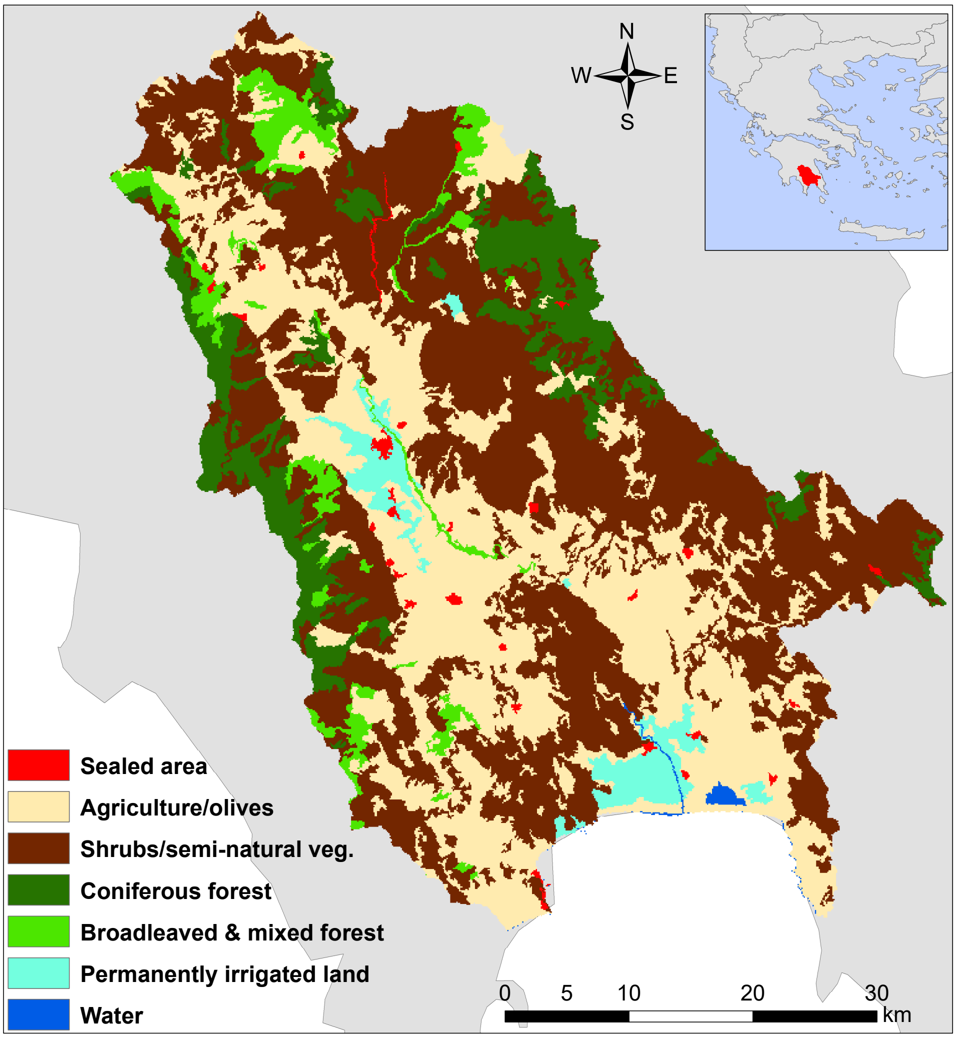

FIGURE 5.7: Reclassified CLC map of the Evrotas in 1990.

5.3.2 Implementation of Riparian Forests

Evrotas experts from the Hellenic Centre on Marine Research in Sparta, a GLOBAQUA partner institution, consulted on the future scenarios emphasised the importance of riverbank protection or restoration as a measure for improving water quality in the catchment. The high modelling resolution permitted to take this into account and incorporate riparian forests in the SUSTAINABLE scenario. Except for the stretch close to the sea, the river network in the Evrotas basin cannot be distinguished from the CLC maps as it is surely narrower than a 100 m, i.e. the pixel resolution, and therefore classified as the surrounding land cover. The assumption was made that for the main rivers below 500 m of altitude, a 100 m wide pixel could represent the river plus river bank vegetation on both sides. The limit regarding the elevation was set for two reasons: 1) agriculture is mainly carried out in the low lying parts (areas where river bank protection makes sense to reduce erosion and diffuse pollution); 2) to include only wider river stretches their width can be represented approximately with a 100 m pixel. First, the land use change model was run without any restrictions regarding the river banks. The riparian forest was "burned" into the final land use map afterwards by changing all pixels along the river below 500 m to *mixed & broadleaved forest* which did not belong already to this class or to *coniferous forest* or *shrubs & semi-natural vegetation*. By this means, a possible measure from a Programme of Measures was included into the modelling process.

5.3.3 Quantification of the Land Use Demand

Table 5.5 summarises the trends attributed to the scenario descriptors for the general GLOBAQUA scenarios by the experts and by the Evrotas stakeholders for the case study specific scenarios. The final factor is the approximate mean of the two trends. These final factors were used to calculate the final land use demands. In case of the Evrotas, the simulation of both scenarios is equal until 2017, after which they divert. The final factors in table 5.5 were multiplied by 5% and define in most cases the trend between 2017 and 2030. For 2030 to 2050, half the increase/decrease as in the previous period was usually assumed.

TABLE 5.5: Scenario descriptor table for the Evrotas for both scenarios including the global scenario definitions, the downscaled scenarios according to the stakeholders and the relevance of the descriptors for the case study according to GLOBAQUA experts.

Descriptor	**Global scenario - Experts' opinion**	**Downscaled scenario - Stakeholders' view**	**Final factor**	**Relevance for Evrotas**
Growth per capita	MYO:+++ SUS:++	MYO:+ SUS:+	MYO: +2 SUS: +1.5	Yes
Urbanisation	MYO:+++ SUS:+	MYO:+ SUS:-	MYO: +2 SUS: 0	No
Irrigated surface area	MYO:++ SUS:- -	MYO:++ SUS:+	MYO: +2 SUS: -1	No changes expected
Industrial agriculture	MYO:++ SUS:-	MYO:++ SUS:-	MYO:+2 SUS: -1	Yes
Abandonment of land	MYO:+ SUS:-	MYO:++ SUS:0/-	MYO: +1.5 SUS: -0.5	yes
Deforestation	MYO:++ SUS:-	MYO:+/++ SUS:-	MYO: +1.5 SUS: -1	Yes, Wildfires in dry years

5.3.3.1 *Sealed Area*

A regression model as for the Ebro could not be applied for estimating the development of *sealed area* in the Evrotas, because the available data for the past were not sufficient for a satisfactory result. Consequently, the trends for the scenarios were chosen according to the descriptor 'urbanisation' in Table 5.5.

MYOPIC: The final factor is +2, so an increase of 10% was expected until 2030 and a 5% increase of sealed area from 2030 to 2050.

SUSTAINABLE: The final factor for this scenario is 0. As sealed area is very unlikely to disappear, the demand for this land use was left constant after 2017.

5.3.3.2 *Permanently Irrigated*

MYOPIC: Both experts and stakeholders expect the irrigated area to increase considerably, so a trend of +10% until 2030 was set. Since this class is relatively small in extent compared to others, another +10% was assumed until 2050.

SUSTAINABLE: -5% compared to 2017 until 2030, -2.5% until 2050 compared to 2030. Adding the riparian forests makes this class shrink by approximately 11% between 2017 and 2050. It is the class most affected by this measure, at least in relative terms.

5.3.3.3 *Coniferous Forest, Mixed & Broadleaved Forest*

These two land use classes were treated equally. For deriving the future trends of these classes, the descriptor 'deforestation' was considered.

MYOPIC: Due to an increased deforestation activity and possibly more frequent wildfires caused by bad management and climate change, forests are expected to decrease in the MYOPIC scenario. A reduction of 7.5% for both classes until 2030 is expected and a further reduction of 5% from 2030 to 2050.

SUSTAINABLE: 5% increase both for the period 2017 to 2030 and 2030 to 2050 for *coniferous forest*. The trend was not reduced for the latter period as reforestation is a slow process and changes may take long. *Mixed & broad-leaved forests* are set to increase only 5% until 2050 for the modelling. By burning in the riparian forests in the final map, this class rises by 16.4% in 2050 compared to 2017.

5.3.3.4 *Shrubs & Semi-natural Vegetation*

In some regions of the Evrotas basin, it is very hard to differentiate forests from *shrubs & semi-natural vegetation* in aerial photography as done in the processing of CLC data. According to all available CLC maps for Greece, the two forests classes plus *shrubs & semi-natural vegetation* cover 61% of the total basin area. This coincides with the 68% of semi-natural vegetation stated by SKOULIKIDIS et al. (2011). Nevertheless, for calculating the land use demand, *shrubs & semi-natural vegetation* were treated independently from forests. This was done to be able to better capture the factor 'abandonment of agricultural land'.

MYOPIC: The abandonment of land is expected to be considerable in the MYOPIC scenario. Therefore, a 5% increase was expected from 2017 to 2050. Since this class is very large in size with respect to the others, the factor 1.5 was not translated in 7.5 but only 5% increase.

SUSTAINABLE: According to both experts and stakeholders, the abandonment trend will be stopped or slightly reversed in a sustainable scenario. Consequently, the demand for this class was left constant after 2017.

5.3.3.5 *Agriculture & Olives*

This class was used to compensate the changes occurring to the other classes.

MYOPIC: A total reduction of -4.8% from 2017 to 2050 takes place. A decrease for this scenario is inline with the observed trend of abandonment of marginal agricultural land in many Mediterranean regions mentioned already. It is assumed that in the future the cultivation of olives will be concentrated even more on profitable land.

SUSTAINABLE: The final land use map for this scenario after the transformation of riverine pixels to *mixed & broadleaved forest* shows a reduction of -3.7% of agriculture compared to 2017.

5.3.3.6 *Water*

As for the Ebro, the class *water* was set constant at the value of 1990.

The development of the demands in the two scenarios are visualised in figure 5.8. The two scenarios seem the same at the first glance. This is related to the intension to develop plausible scenarios and not extreme ones. In both scenarios, *shrubs & semi-natural vegetation* increase whereas *agriculture* decreases. The trends are stronger in the MYOPIC scenario. At second sight one can also see the increase of forests in the SUSTAINABLE scenario while in the MYOPIC scenario *sealed area* and *permanently irrigated land* expand.

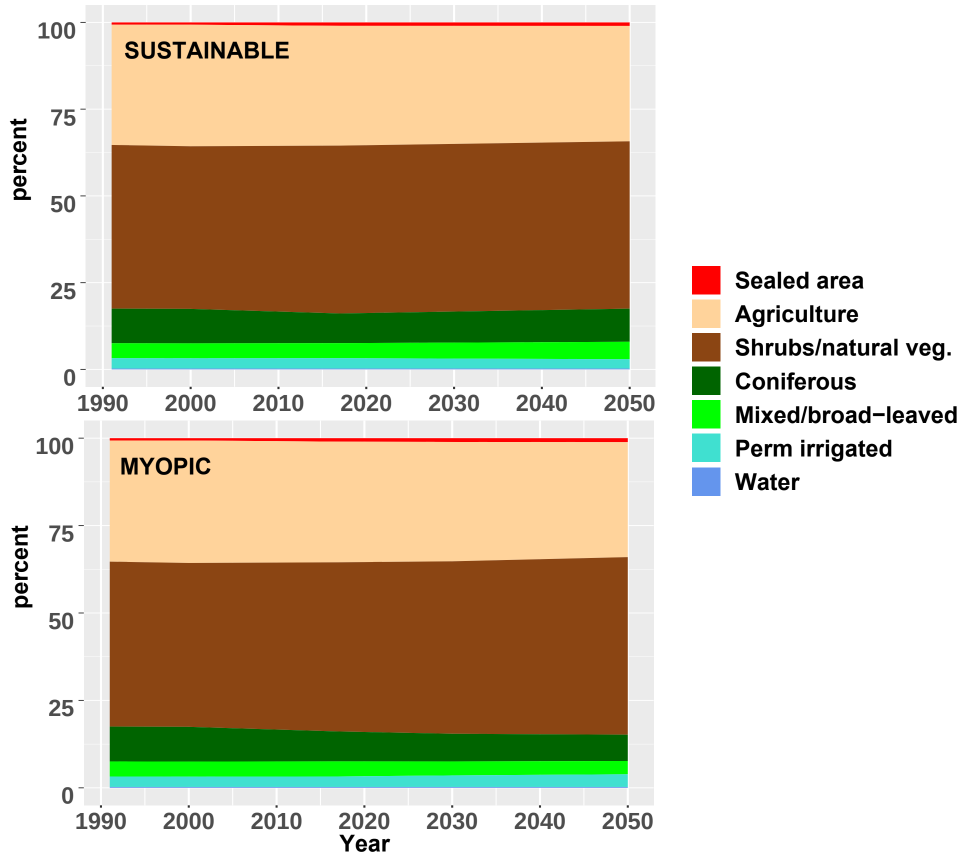

FIGURE 5.8: Land use demand for the Evrotas in the SUSTAINABLE (top) and MYOPIC (bottom) scenario 1990-2050.

5.3.4 iCLUE Drivers

Table 5.6 summarises the drivers used to set up iCLUE for the Evrotas River basin. Similar to the Ebro, the list includes only the drivers actually part of the setup but not other data tested previously and rejected. The annual mean temperature was included in iCLUE as dynamic driver. Other climate variables were not considered as the model discards them due to high correlation coefficients.

5.3.5 Further Model Specifications

5.3.5.1 *Ease of Change*

In case of the Evrotas, the ease of change was set to "very hard" for *sealed area*, to hard for *agriculture*, *coniferous forests*, *mixed & broadleaved forests* and *permanently irrigated land*. *Shrubs & semi-natural vegetation* is the only class that can easily be transformed to other classes. As for the Ebro, *water* was not allowed to change.

5.3.5.2 *Conversion Rules*

Sealed area is not allowed to change to any of the other land use classes. The conversion from *agriculture* to *shrubs & semi-natural vegetation* is parametrised to take four years. In turn, *shrubs & semi-natural vegetation* to *mixed & broadleaved forests* and *coniferous forests* will happen after 13 and ten years, respectively.

TABLE 5.6: Drivers used for setting up iCLUE in the Evrotas River basin and their sources.

Driver	**Source**
Population density 2011	Hellenic Statistical Authority (ELSTAT 2011)
Labour 2001 at Local Administrative Level 1 (LAU1)	ELSTAT 2001
Overnight stays tourism 2009 at LAU1	ELSTAT 2009b
Euclidean distance [m] to:	Calculated from data obtained from:
- Oil mills	- Digitalised from TZORAKI et al. (2008)
- Largest roads (category 1)	- OpenStreetMap data GEOFABRIK GMBH (2018)
- Water abstractions	ELSTAT 2011
- Large rivers	
- Coasts	
- Settlements	
DEM [m]	SRTM 90 (GCIA-CSI 2015)
Slope [%]	Calculated from the DEM
Aspect	Calculated from the DEM
Number of livestock per municipality (2009): - Cattle - Sheep - Goats - Poultry - Pigs	ELSTAT 2009a
Nature 2000 areas	EEA 2014b
Dynamic annual mean temperature [^{c}ircC]	Downscaled and bias-adjusted EURO-CORDEX data (JACOB et al. 2014)
Irrigation Requirement per municipality 2001	MDG 2005

5.3.5.3 *Allowed Demand Deviation*

For the Evrotas, the allowed deviations for the land use demands are the following:

TABLE 5.7: Allowed deviation [%] from the targeted land use demand for the Evrotas setup.

Land use	**Allowed Deviation**
Sealed area	3.1
Agriculture	1.2
Shrubs & semi-natural veg.	1.8
Coniferous forest	1.7
Mixed & broad-leaved forest	1.9
Permanently irrigated	2.1
Water	0

5.4 Derivation of Water Use Maps - Ebro River Basin

Table 4.2 summarises the changes in total water use defined for the two future scenarios compared to the reference period 1980-2010 for the Ebro and Evrotas. These values represent, however, merely the overall water demand and do not specify the changes for sectoral water uses, which may differ considerably from the total amount of water used. Besides, it does not provide any information on the spatial distribution of water uses or differing amounts across the basin. For both case studies it was possible to retrieve information on sectoral water uses either from the RBMP or national institutions for subunits of each catchment. The dimensions of these units, however, vary substantially from site to site. To obtain spatially explicit water use maps, the priorly produced land use maps were combined with the water statistics. The water abstractions of a sector were linked to the land use class of the final simulated map representing the sector best. As for retrieving future maps, the pixel values of the reference map were multiplied by factors to fit in sum to the future overall demands defined in table 4.2. The general procedure of deriving spatial water use maps for the reference scenario in all four basins is explained in more detail in HUBER GARCÍA et al. (2018).

5.4.1 Water Uses Statistics for the Ebro

As regards the Ebro, the statistics and values mentioned refer to the official basin defined by the CHE, called Ebro basin hereafter, which slightly differs from the natural watershed (CHE 2015): The Ebro CHE limitation includes the headwaters of the Garona River belonging to Spain while the rest of the river runs through France and empties into the Bay of Biscay. Statistics in the RBMP for this area are mainly listed apart. The CHE basin shape and statistics exclude, however, a small area located in France, the headwaters of the Segre River, a tributary to the Ebro. Statistics for Andorra, whose national territory lies completely in the natural Ebro catchment as well as in the CHE basin, are not reported. Since its area of 468 km^2 is small compared to the whole Ebro catchment (85600 km^2) the area of Andorra was considered part of the downstream main tributary, the Segre, for calculations.
It is further worth noting that the statistics available for the Ebro do not differentiate clearly between water use, water demand and water supply. The RBMP 2015-2021 reports two reasons for that (CHE 2015): First, until now it has been possible to provide the largest part of the requested water even if this situation may change dramatically in the future. Consequently, the water demand, or water use, equalled the water supply without taking into account return flows. Secondly, the obtained numbers are mainly estimations and in most cases only demands were estimated, not water supply. Consequently, the terms “use”, “demand” and “supply” will be used as synonyms in the following chapters as already explained in the introduction.

5.4.2 Linking Water Uses to Land Uses

The RBMP of the Ebro differentiates agricultural, subdivided into irrigation and livestock, industrial and urban water uses, the latter one including also industries supplied by the urban supply networks (CHE 2015). The water demands for urban and industrial uses were added and attributed to the land use class *sealed area*, which represents both urban and industrial areas according to the classification introduced above used for modelling with iCLUE. Linking agricultural water uses to a land use class is more complex. Based on the used CLC input map, it is not possible to localise livestock production in space. The water consumption related to this activity is probably very concentrated on the farm buildings while the resolution of the CLC maps of 1 ha and even more the modelling resolution of 1 km^2 is far too coarse to represent it correctly. Considering the fact that irrigation accounts for 99% of the agricultural water demand in the Ebro (CHE 2015), the inaccuracy introduced by

merging livestock and irrigation demands was considered negligible. A substantial part of the irrigation systems produce fodder for the cattle in the Ebro valley and receive in turn manure as organic fertiliser. As a result, farms are located nearby the fields which is another argument in favour of combining irrigation and livestock demands (CHE 2015).
Regarding the land use classification for the Ebro, the class *permanently irrigated land* certainly makes up for a good part of the irrigation demand in the Ebro. According to the CLC nomenclature 'permanently irrigated' stands for "crops irrigated permanently or periodically, using a permanent infrastructure" (BOSSARD et al. 2000). However, comparisons of CLC data with the map in figure 5.3 have shown that also the categories *complex cultivation patterns* and *fruit trees & olives* are probably irrigated to some extent since their location coincides with areas of existing irrigation infrastructure. The RBMP also reports irrigation amounts for fruit trees and partly also for olives, however, to a smaller extent (CHE 2013, Annex III). The term *complex cultivation patterns* was adopted from the original CLC nomenclature and represents landscapes with high spatial variability, which does not exclude irrigated agriculture at smaller scale (BOSSARD et al. 2000). Furthermore, the 7680 hm^3 (7623 hm^3 for irrigation + 57 hm^3 for livestock, see 4.2) agricultural demand reported by the RBMP for around the year 2010 and used for calculations hereafter were simulated assuming an irrigated area of 9657 km^2, a rather high value considering that the actually irrigated area in 2005 was estimated to lie rather around 7000 km^2 (CHE 2013, Annex III). In fact, the RBMP 2015-2021 reports several numbers from various sources ranging from 6621 km^2 in 2005 according to a farmers' survey to the already mentioned 9657 km^2 (CHE 2013, Annex III). In the draft for the next RBMP 2021-2027 7455 km^2 can be found as estimation for the year 2014 (CHE 2018). For the derivation of water use maps, 9657 km^2 was interpreted as AEI and consequently a value overestimating the actually irrigated area. Still, it was necessary to find a balance between all values and to "choose" an irrigated area large enough to avoid obtaining unrealistic high values when calculating the water use per pixel. Since 5740 km^2 *permanently irrigated land* and 1909 km^2 *fruit trees & olives* together in the CLC 2006 map are considerably less, it makes sense to include 20% of *complex cultivation patterns* obtaining a theoretical irrigated area of 8854 km^2 for the year 2006.

The statistics mentioned above are reported in the RBMP (CHE 2015) as values for the whole Ebro CHE basin but also for different kind of subunits. A rather fine division of the catchment is obtained by dividing the area in 49 so called agricultural demand units. A coarser disaggregation describes the 18 exploitation units which are of varying sizes, see map in figure 7.17. Despite the coarser spatial resolution the statistics for these latter units were used for calculations as they provide information for all main water consuming sectors (agriculture, industry, urban) and, in addition, report present values (2013) as well as future estimations for 2033 (CHE 2015). The values for 2013 and 2033 in the RBMP 2015-2021 are equal to the values reported in the prior RBMP 2010-2015 (CHE 2015) for the years 2007 and 2027, respectively. Consequently, the values for 2007/2013 were used to represent the GLOBAQUA reference period (1980-2010) and are assumed to be an estimation for around the year 2010.

5.4.3 Deriving Spatial Water Uses in the Ebro

For deriving spatial maps a very similar approach to the one applied by MALEK & VERBURG (2018) was used where the water demand of a sector in each exploitation

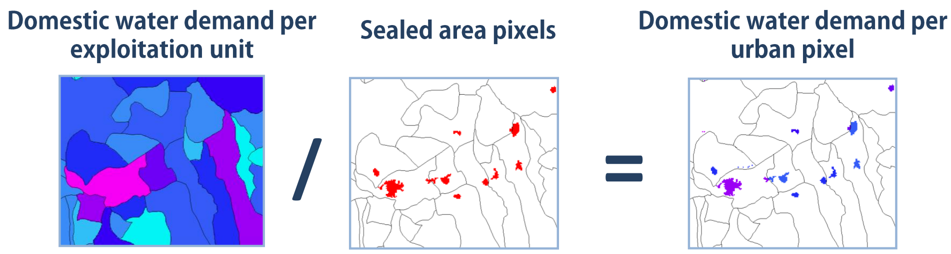

FIGURE 5.9: Procedure to obtain water use values per pixel from statistics for subunits.

unit was distributed to all pixels of the land use class priorly related to this sector. For the urban water demand this means that the demand per exploitation unit was divided by all *sealed area* pixels in this unit and the obtained value attributed to each pixel as mean water consumption per pixel in this area, as figure 5.9 illustrates. For agriculture, the agricultural demand was divided by the sum of pixels of all irrigated classes *permanently irrigated land*, *fruit trees & olives* and 20% of the class *complex cultivation patterns*. The reason to consider only 20% of the area of this class is that it is thought to represent irrigated area only to some extent. The obtained value was attributed to the first two classes without any changes whereas *complex cultivation patterns*, again, only obtained 20% of the water the other ones got per pixel to consider the fact that this class might be less intensively irrigated. SALMON et al. (2015) apply a similar approach to account for the fact that a single satellite remote sensing pixel covering 500 m x 500 m includes a mixture of land use classes. By this means, water use maps representing the end of the reference period were obtained by combining water use statistics for the Ebro representative for the period 2007-2013 with the CLC 2006 map.

5.4.4 Introducing Thresholds

In some cases, the CLC 2006 map shows only very few or no pixels of water consuming land use classes while the RBMP reports a substantial amount of agricultural water demand for the same area (CHE 2013, Annex III). This results in an unrealistically high value when divided by the amount of pixels. To spot those, the mean and standard deviation of all water-uses-per-pixel-values (excluding outliers) was calculated. Values lying below or above the mean +/- twice the standard deviation were identified as extreme values. These values were excluded and the mean of the remaining units calculated again. All priorly excluded exploitation units were replaced by this mean value, 0.73 hm^3/km^2. In a slightly different way, also MALEK & VERBURG (2018) introduced a threshold on maximum water withdrawal in their calculations of irrigation scenario to account for actual available water resources.

5.4.5 Future Water Demands

For obtaining future water use maps, the reference maps were modified by multiplying the mean water consumption per pixel with a factor. The factor was set to be the same all over the Ebro catchment, while it differed for each water consuming land use. The reference values were adapted in a way that the sum of all pixels and all water demands in the Ebro equalled the future change defined for each scenario in table 4.2.

For the Ebro, the factors for each land use in the two scenarios are summarised in table 5.8.

TABLE 5.8: Factors applied to the water demand per pixel for the reference period to obtain values for the two future scenarios in the Ebro.

FACTOR	MYOPIC	SUSTAINABLE
Sealed area	0.85	0.80
Perm. irrigated, fruit trees & olives	0.9	0.85
Complex cultivation patterns	0.8	0.8

Multiple scenario specifications had to be taken into account when setting the factors, as there are for example 1) the increase/decrease of total water demand for each scenario set for the GLOBAQUA project, 2) the wide margin of water demand and irrigated area values reported by the RBMPs for the present and 3) the credibility of the resulting water demand per pixel. After the introduction of a threshold, these values set the boundary conditions for calculating the water demand per pixels. The allocation of irrigated pixels is controlled by the iCLUE model. The water use sum over the whole catchment may change depending on the location of these pixels in different exploitation units since the mean values per pixel vary strongly between the units. Knowing that iCLUE simulations are subject to a certain amount of randomness the exact percentage of increase/decrease fluctuates depending on each model run. The factors in table 5.8 were set in a way that the future demand increase/decrease of a specific scenario, +30% in case of the Ebro, is reached approximately by all model runs.

The factors applied reduce the water consumption per pixel with respect to the present in both scenarios. This might be surprising at first sight, however, both the MYOPIC and the SUSTAINABLE scenario experience an increase in irrigation efficiency by definition, see scenario descriptors in Appendix A. This may occur for various reasons: In the MYOPIC scenario, a very high technological standard is assumed which will help saving water following the trend described in the draft for the next RBMP 2021-2027 (CHE 2018): As a result of the continuous modernisation of the irrigation techniques in the Ebro between 2004 and 2016 the highly water intensive surface irrigation has already been reduced from 64% to 45.8%. However, as it is further stated in this document, it is not always equal to water conservation since the cropping system is simultaneously intensified allowing a higher productivity per used m^3. For this reason, the SUSTAINABLE scenario additionally foresees cultivating less water intensive crops to reduce the water consumption. For the water use maps this means that the water consumption per pixel for *permanently irrigated land* and *fruit trees & olives* will be less in the SUSTAINABLE scenario than in the MYOPIC one, 85% vs. 90% of the current. The rather small reduction in both scenarios with respect to the present can be explained with the fact that the irrigation systems in the Ebro are already quite efficient and a stronger reduction would be unrealistic.

With regards to the factor for *complex cultivation patterns*, a 20% reduction in both scenarios is assumed to increase also the irrigation efficiency of small-scale agriculture.

As for the urban water consumption, it is expected to drop, by 15% in the MYOPIC and by 20% in the SUSTAINABLE while the population will increase slightly. This may seem contradictory at first glance. However, it is in line with the trend observed over the last decades in the Ebro and the whole Spanish territory where both the consumption per inhabitant and the total urban water supply has steadily gone down (CHE 2018). The assumption for the MYOPIC scenario is that urban sprawl will cause settlements to expand more than in the SUSTAINABLE one and consequently resulting in a lower population density per urban pixel, while the consumption per pixel will be reduced more in the latter scenario. This means that the consumption per person will be higher in a MYOPIC scenario.

5.5 Derivation of Water Use Maps - Evrotas River Basin

The derivation of water use maps for the Evrotas basin was carried out with statistics for the year 2001 from the MINISTRY OF DEVELOPMENT OF GREECE (2005) (MDG) for domestic uses and irrigation. Even if this source also provides information on the water consumption for livestock, the water use map for this sector was not calculated as it only makes up a small part of the total amount. The data are available at community level, the smallest Greek administrative unit at that time, and at municipality level, slightly larger units. While using the community data allows for a high spatial detail as already shown in HUBER GARCÍA et al. (2018), this fine disaggregation causes some problems when calculating the scenarios and water consuming pixels appear in communities where they were not present priorly. For this reason, the municipal data were used in this work to create a consistent set of water use maps for the Evrotas.

The CLC 2000 map served as basis to derive the reference scenario. As already described in HUBER GARCÍA et al. (2018), for calculations it was assumed that the land use class *permanently irrigated land* is dominated by citrus trees while irrigated olive trees are mainly distributed over the class *agriculture/olives*. This is in line with the data from the MDG (2005) which also provides data on the irrigated area and irrigation requirements per crop type at municipal level. According to this source, the irrigation requirements for citrus trees are approx. twice as high as for olive trees. Consequently, two times the amount of water per pixel of *agriculture/olives* was applied to *permanently irrigated land*.

TABLE 5.9: Factors applied to the water demand per pixel for the reference period to obtain values for the two future scenarios in the Evrotas.

FACTOR	MYOPIC	SUSTAINABLE
Sealed area	0.90	0.80
Perm. irrigated land	0.95	0.80
Agriculture/olives	1.2	0.68

The factors for adapting the water use in the future in table 5.9 show generally higher water use efficiencies except for olives in the MYOPIC scenario. It is assumed that the irrigation of olive trees will be further expanded and intensified in this scenario, both for economic reasons as well as climate change, resulting in a 20% increase. Meanwhile, the water consumption of *sealed areas* and *permanently irrigated land* is reduced by 10% and 5%, respectively. These adaptations result in an overall water use increase of approx. 15% for the MYOPIC scenario. To the contrary, the overall demand is reduced by 30% in the SUSTAINABLE scenario. Especially the irrigation efficiency for olive trees will be increased consuming 32% less per pixel. SKOULIKIDIS et al. (2011) report that the irrigation of olive trees has started only lately after a longer drought episode. Traditionally, most olive trees in the Evrotas were not irrigated. The SUSTAINABLE scenario aims at returning partly to the situation before the olive tree irrigation started. The water consumption of *sealed areas* and *permanently irrigated land* decreases by 20%.

Chapter 6

Estimating Water Availability

To be able to make a statement about the final water availability in the Ebro River basin, the attempt was made to compare the demand side, i.e. the resulting water use maps, to the water actually available. For this purpose, we contrasted the results of this study to 1) runoff simulations for the Ebro carried out in the context of GLOBAQUA by Stefanie Lutz from the Helmholtz-Zentrum für Umweltforschung (UFZ) (Centre for Environmental Research) in Halle (Saale), one of the project partners, and 2) the Climate Moisture Index (CMI) (WILLMOTT & FEDDEMA 1992) was calculated.

6.1 Runoff Modelling

The following section is taken from HUBER GARCÍA et al. (in prep.).

The mean annual water balance in the Ebro River basin was simulated with the mesoscale Hydrological Model (mHM) (KUMAR et al. 2013b, SAMANIEGO et al. 2010), which is a grid-based distributed hydrological model simulating canopy interception, snow accumulation and melting, soil moisture dynamics, infiltration, deep percolation, surface runoff, evapotranspiration, storage in the subsurface and groundwater, discharge generation, fast and slow interflow and baseflow. The model parameters are calibrated using a multi-scale parameter regionalization technique to account for the spatio-temporal distribution of catchment characteristics such as soil types, geological classes and land cover types (SAMANIEGO et al. 2010). The model has been successfully applied in various river basins including the Ebro (e.g. KUMAR et al. 2013a, KUMAR et al. 2013b, RAKOVEC et al. 2016a, RAKOVEC et al. 2016b, SAMANIEGO et al. 2010, VIGIAK et al. 2018, ZINK et al. 2017).

In this study, the model was run at a daily time step on a 6 km x 6 km grid for the periods 1981-2010 and 2036-2065, i.e. the GLOBAQUA reference and future period, using RCP 8.5 and RCP 4.5 climate data from one of the three selected model combinations, the RCA4, (interpolated to the 6 km x 6 km grid) and corresponding CLC maps at the original 100 m resolution, with land use before 1990 being set to the 1990 data. To obtain the model parameters for these scenario runs, mHM was first calibrated in a preliminary model run against daily discharge of the Ebro River at the Ascó Coca gauging station (41°11'9.24"N, 0°34'11.37"E) between 1991 and 2014 using CLC data (EEA 2013a, EEA 2013b, EEA 2013c, EEA 2016a) and the E-OBS temperature and precipitation dataset (HAYLOCK et al. 2008) as climate forcings. The interpolated station data from E-OBS was chosen for model parameter calibration due to their better representation of historical meteorological conditions compared to regional climate model output. Daily discharge at Asco Coca was provided by the CHE (`http://ceh-flumen64.cedex.es/anuarioaforos/afo/estaf-`

datos.asp?indroea=9163). The Dynamically Dimensioned Search (TOLSON & SHOEMAKER 2007) was applied for calibration using a combination of the Nash-Sutcliffe Efficiency (NSE) between observed and modelled discharges and their logarithm to capture high, average and low flow conditions. The runoff simulations do neither account for extractions nor for reservoirs and therefore represent the natural conditions in the Ebro basin.

The yearly runoffs for the reference period 1981-2010 and for both scenarios 2036-2065 were averaged and a difference map between each scenario and the reference was calculated to identify changes.

6.2 The Climate Moisture Index

The CMI after WILLMOTT & FEDDEMA (1992) is a modified version of Thornthwaite's Moisture Index (THORNTHWAITE 1948). It is calculated using precipitation *Prec* and potential evapotranspiration *ETpot* data as follows:

$$CMI = \begin{cases} 1 - ETpot/Prec & if \quad Prec > ETpot \\ Prec/ETpot - 1 & if \quad ETpot > Prec \end{cases} \tag{6.1}$$

Data originating from the EURO-CORDEX project for the RCA4 GCM-RCM-combination were used at the original 12 km^2 resolution to calculate the CMI. Analogous to the runoff, mean annual precipitation and potential evapotranspiration grids were averaged for the reference and future period of RCP 8.5 and RCP 4.5 data to eventually obtain the CMI for each scenario.

Chapter 7

Scenario Results & Discussion

7.1 Climate Scenarios

In order to satisfy the integrative approach of the present study, socio-economic scenarios need to be considered in combination with climate scenarios when projecting land and water use changes. The bias-adjusted and downscaled projections for mean annual air temperature and annual precipitation sum described in chapter 4.4 were included as dynamic drivers in iCLUE. Before running the model, the climate input was analysed in more detail.

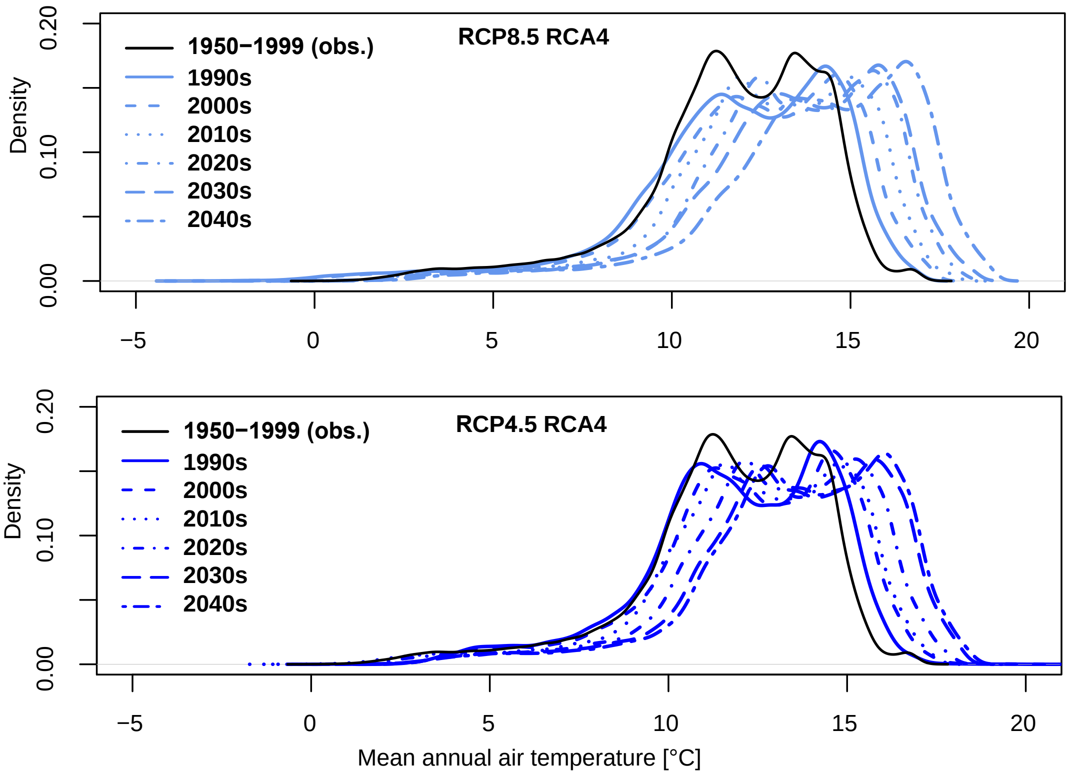

FIGURE 7.1: Density distributions of the decadal mean annual temperatures of the RCA4 climate model for the MYOPIC (top) and SUSTAINABLE (bottom) scenario. The black line represents the mean annual temperature for the period 1950 to 1999 according to observed data.

To take into account the uncertainties of climate projections each of the two GLOBAQUA scenarios was run with data from three different GCM-RCM-model combinations (see chapter 4.4 for details on the selection of the models) eventually resulting in six iCLUE scenarios. The density distributions of the yearly mean annual temperature maps for one of the three GCM-RCM-combinations, the RCA4 model combination, averaged over decades are compared in figure 7.1 to the distribution of observed temperatures. The observed data in this and also the following figures originate for the most part from the Digital Climate Atlas of the Iberian Peninsula 1950-1999 (NINYEROLA et al. 2005) completed with the Andorran Climate Digital Atlas (M. BATALLA et al. 2016) for the Andorran territory which represents the period 1981-2010. The fit between the observed curve and the decadal 1990s mean temperature is good considering the fact that they cover different periods and the latter ones originate from climate models. For both scenarios, there is a clear shift towards warmer temperatures until 2050. Each decade is projected to be warmer than the previous one, in total for six decades in a row. Even if thirty-year periods or longer are the standard time frames in climate science to analyse data, it is interesting to see that for the climate model data over the Ebro a trend can already be distinguished for ten-year intervals. The results are equally clear for the climate data from the models CCLM4 and RACMO22E (see chapter 4.4 for abbreviations), which is the reason they are not shown here.

What figure 7.1 also indicates is that there seems to be a slight difference between the climate projections for the two scenarios already for the historical period, which lasts until 2005 for the CMIP5 simulations used here, since the 1990s means for RCP 8.5 and RCP 4.5 have a slightly different shape, clearly visible around 10°C. There are two possible explanation for this effect: 1) It could be an artefact of the bias-adjustment applied to the data. For this means, the climate model simulations are compared to observed data, in this case the MESAN dataset (HÄGGMARK et al. 2000), to detect possible deviations. The period used to ascertain the delta was 1989 to 2010, which in case of the climate model data includes not only the historical period but with 2006 to 2010 also five years already under influence of the respective RCP. Since each RCP represents an independent model run, there is no relation between the results for RCP 8.5 and 4.5 for a specific year and they can deviate considerably. The data used here, both the RCP 8.5 as well as RCP 4.5 historical periods provided through the EURO-CORDEX ensemble (JACOB et al. 2014), already include a bias-adjustment which could be the reason the density distributions for the 1990s and 2000s of the two scenarios differ. 2) Each RCM is run with marginally different initial conditions which propagate through the climate system and produce different results (LEDUC et al. 2019).

The same effect can be observed for the precipitation data displayed in figure 7.2 originating from the CCLM4 model combination for the two scenarios. Also in this case, the solid lines in both graphs have a slightly different shape as a result from the bias-adjustment. Besides, compared with the observed data from the Digital Climate Atlas (NINYEROLA et al. 2005) the climate model underestimates considerably areas with approx. 350 to 550 mm yearly precipitation sum in both scenarios. In turn, according to the climate model data, a larger share of the Ebro basin is supposed to have more extreme annual precipitation sums below 350 mm and above 600 mm for all decades including past ones. Unlike the temperature, no clear trend can be recognised for the decadal precipitation means. This is certainly related to the high variability in space and time typical for the Ebro (CHE 2015) and other Mediterranean regions. In fact, RAMOS et al. (2012), who carried out a study on temperature and precipitation changes in Catalunya over the past 60 years, found that "the high variability observed from year to year hides any possible trend" in annual totals or the number of rainy days. Nevertheless, some trends could be identified for seasonal precipitation sums. As for the present study, the two decades showing highest densities at low precipitation values are the 2020s and 2030s, while the distribution curve for the 2040s moves back towards higher precipitation values. However, no assumptions on the total precipitation sum and water availability in the Ebro should be derived from the curves in figure 7.2 since the spatial and seasonal distribution of precipitation is equally variable and it was not considered here.

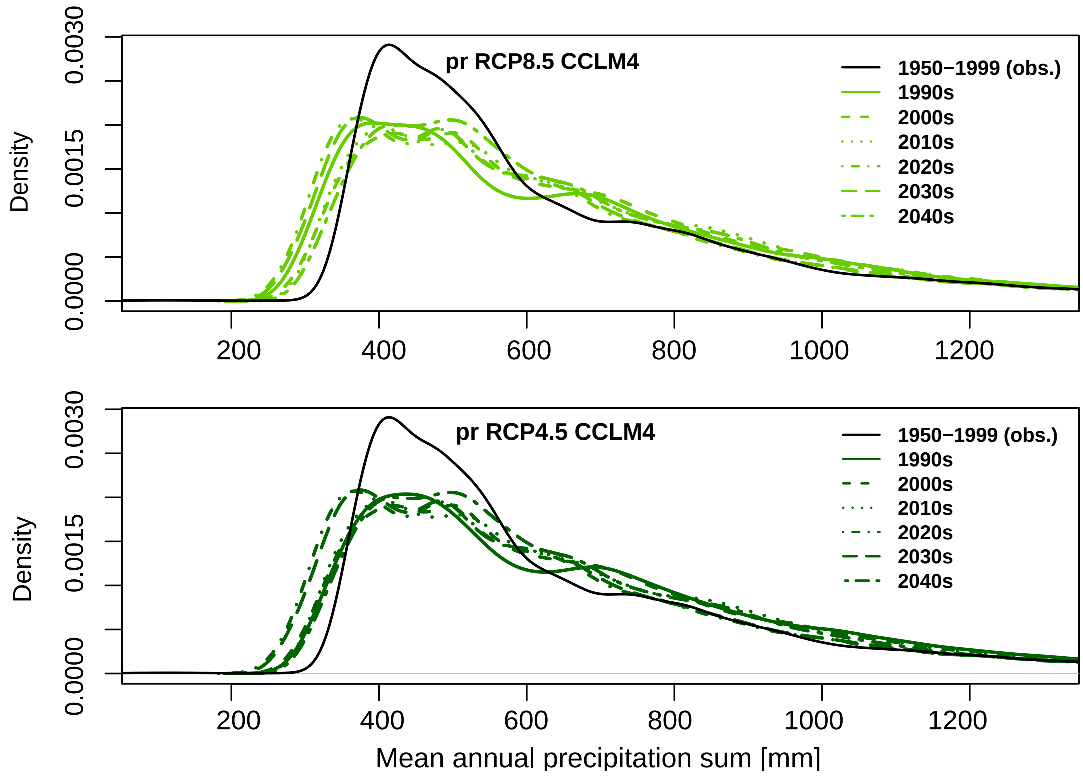

FIGURE 7.2: Density distributions of the decadal mean annual temperatures of the RCA4 climate model for the MYOPIC (top) and SUSTAINABLE (bottom) scenario. The black line represents the mean annual temperature for the period 1950 to 1999 according to observed data.

Comparing projections from different models, see figure 7.3, differences between the climate models exist. Looking at a thirty-year average from 2021 to 2050, RCA4 is the most extreme one, the RCP 8.5 run of this model combination reaching the highest temperatures followed by the RCP 4.5 of the same GCM-RCM combination. This means that the temperature in the SUSTAINABLE scenario with data from RCA4 tends to be higher than for the MYOPIC scenario of both RACMO22E and CCLM4. The latter two climate model combinations show more similarities. This agrees with findings from GAMPE et al. (2016) which compared the climate signals from many climate models over all four GLOBAQUA test sites and which identified RCA4 as being "hotter" then the other two models.

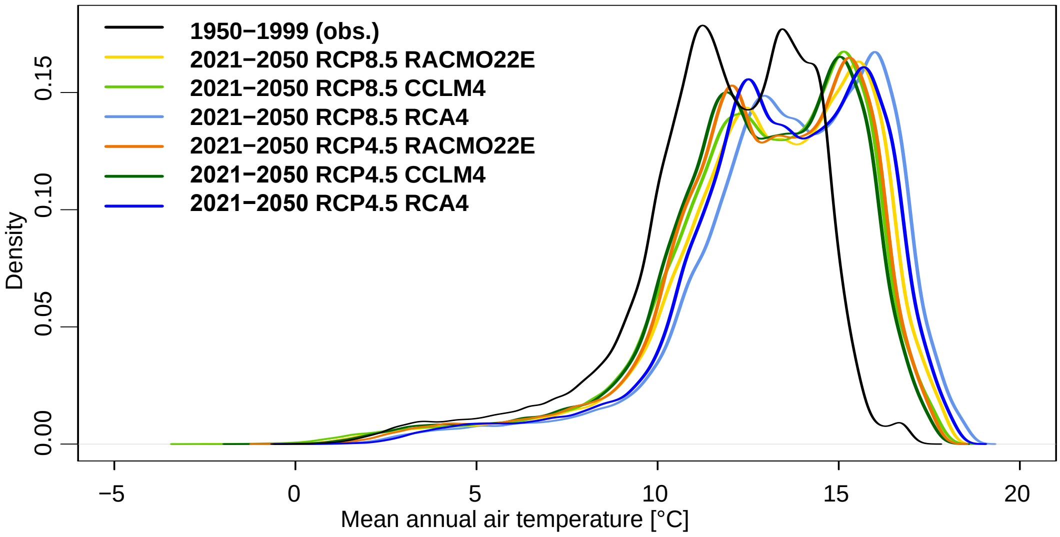

FIGURE 7.3: Density distributions of the 2021-2050 mean annual temperatures for all three climate models and both scenarios compared to observed data.

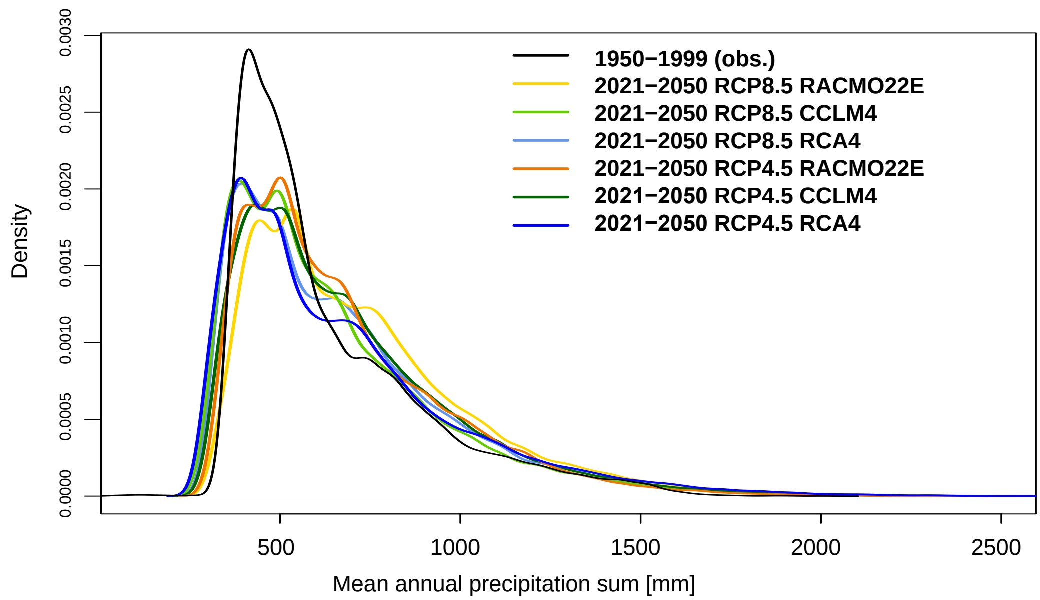

FIGURE 7.4: Density distributions of the 2021-2050 annual precipitation sums for all three climate models and both scenarios compared to observed data.

The thirty-year mean values for all six scenarios in figure 7.4 for precipitation do not deviate as much as the ones for temperature. Most climate simulations over Spain agree that the annual precipitation sum is not expected to change that much, but that seasonal precipitation shifts such as wetter autumns and drier summers might occur (CEDEX 2017). The black line in figure 7.4 represents again observed values originating from the two atlases mentioned above. For the model simulations, there is a slight trend towards more extreme values in both directions which means that in the future there could be regions with lower mean annual precipitation sums compared to the observed and areas with higher values. According to GAMPE et al. (2016), RCA4 is the GCM-RCM combination producing the "driest" climate out of the three used in GLOBAQUA.

To conclude, slight differences between the future temperature change in the two scenarios are visible but hard to deduce for precipitation. The constant decadal increase in temperature is noticeable and interesting per se. In case of temperature, the differences for the period 2021 to 2050 seem to be larger between climate models than scenarios. As mentioned by MOSS et al. (2010), deviations between the RCPs only start being significant after 2035 which might be the reason for similarities between RCP 8.5 and 4.5. The observed differences between data originating from various GCM-RCM-combinations show that it is important to take into account the uncertainty in climate modelling when running iCLUE. Due to the nature of this particular LULCC model following a top-down approach where the model is forced to allocate the complete land use demand, the influence of dynamic drivers is, however, restricted. Climate change is overruled by the demand allocation.

7.2 Change Detection Analysis

For obtaining information as input to the iCLUE model and assessing the model results it was necessary to analyse historical land use transitions first. Change detection is a common technique to identify such changes. The results described here have been published in HUBER GARCÍA et al. (2018). The procedure follows the one applied by FERANEC et al. (2007): A contingency table for CLC maps of two different points in time is calculated to spot the land use transitions that have taken place during the observed period. For the Ebro, the changes between the reclassified CLC maps 1990 (EEA 2013a) and 2000 (EEA 2013b) and 1990 and 2006 (version 17, EEA 2013c) were investigated for the whole study area including protected areas. The overall change detected for the calibration period of the model, 1990 to 2000, affected 3.2% of the study area, while 5.4% changed from 1990 to 2006, the model validation period, see chapter 7.3.

The results for the second period are summarised as a contingency table in table 7.1. The values indicate the percentage share of the total study area that was affected by change from one land use class to the other. The transition of *non-irrigated arable land* to more specialised uses such as *vineyards* (0.1%), *fruit trees & olives* (0.1%) and especially *permanently irrigated land* (0.9%) can be considered the most important change and the one with the largest impact on water resources. The change of *permanently irrigated land* to *complex cultivation patterns* is with 0.5% the second largest. However, it has to be analysed carefully. As will be explained in more detail in chapter 7.3.1 and in particular figure 7.8, parts of the large irrigation systems in the Ebro valley located in Aragón west of the Cinca River are classified as *complex cultivation patterns* in the CLC 2006 map while in the CLC maps of 1990 and 2000, and even more in

TABLE 7.1: Results of the change detection analysis in % of the total area of the Ebro basin for the validation period 1990 to 2006.

1990 \ 2006	Non-irrigated arable land	Permanently irrigated land	Vineyards	Fruit trees and olives	Grasslands & pastures	Complex cultivation	Agriculture with natural vegetation	Broad-leaved forest	Coniferous and mixed forest	Sealed area	Trans. woodland/ shrub/Sclerophyll.	Open spaces with little or no	Water
Non-irrigated arable land	0.0	0.9	0.1	0.1	0.0	0.2	0.0	0.0	0.0	0.1	0.0	0.0	0.0
Permanently irrigated land	0.2	0.0	0.0	0.0	0.0	0.5	0.0	0.0	0.0	0.1	0.0	0.0	0.0
Vineyards	0.0	0.0	0.0	0.0	0.0	0.0	0.0	0.0	0.0	0.0	0.0	0.0	0.0
Fruit trees and olives	0.0	0.0	0.0	0.0	0.0	0.0	0.0	0.0	0.0	0.0	0.0	0.0	0.0
Grasslands & pastures	0.0	0.0	0.0	0.0	0.0	0.0	0.0	0.0	0.0	0.0	0.2	0.0	0.0
Complex cultivation patterns	0.2	0.1	0.1	0.1	0.0	0.0	0.0	0.0	0.0	0.0	0.0	0.0	0.0
Agriculture with natural vegetation	0.0	0.0	0.0	0.0	0.0	0.0	0.0	0.0	0.0	0.0	0.1	0.0	0.0
Broad-leaved forest	0.0	0.0	0.0	0.0	0.0	0.0	0.0	0.0	0.0	0.0	0.1	0.0	0.0
Coniferous and mixed forest	0.0	0.0	0.0	0.0	0.0	0.0	0.0	0.0	0.0	0.0	0.4	0.0	0.0
Sealed area	0.0	0.0	0.0	0.0	0.0	0.0	0.0	0.0	0.0	0.0	0.0	0.0	0.0
Trans. woodland/shrub/Sclerophyllous	0.0	0.0	0.0	0.0	0.3	0.0	0.1	0.2	0.4	0.0	0.0	0.1	0.0
Open spaces with little or no vegetation	0.0	0.0	0.0	0.0	0.0	0.0	0.0	0.0	0.0	0.0	0.1	0.0	0.0
Water	0.0	0.0	0.0	0.0	0.0	0.0	0.0	0.0	0.0	0.0	0.0	0.0	0.0

a later version of the 2006 map (version 18.5.1, EEA 2016b), the CLC 2012 (version 18.4, EEA 2016a) and the unvalidated CLC 2018 (version 20, EEA 2018) they belong to *permanently irrigated land*. Consequently, it might well be that this transition does not represent an actual change in land use but rather an altered classification scheme. 0.4% of the study area are transformed from *coniferous & mixed forest* to *trans. woodland & shrubs & sclerophyllous vegetation* and the same percentage experienced the opposite change. The same happens for the change from *grasslands & pastures* to *trans. woodland & shrubs & sclerophyllous vegetation*, which affects 0.2% of the catchment, while the opposite transition accounts for 0.3%. Due to these opposed changes, the net change for the validation period is only 2.7% (2.3% for the calibration period), and therefore considerably smaller than the overall change. The reversed trends could be partly caused by diverging classifications between the observed years due to similarities between the classes. BÜTTNER & MAUCHA (2006) attribute in this respect a moderate reliability to the CLC classes *trans. woodland & shrubs* (CLC code 324) and even a low one for *sclerophyllous vegetation* (323) and *natural grassland* (321).
A reforestation trend in the Ebro is also expressed by the change from *trans. woodland & shrubs & sclerophyllous vegetation* to *broad-leaved forest*. With regards to urbanisation, *sealed area* gains 0.1% from *non-irrigated arable land*.

All in all, the observed changes confirm the overall trend in the Ebro, and in the Mediterranean region in general, described in many studies. They reveal the two main processes of land transformation that have taken place in the Mediterranean in the last decades: On the one hand, there has been a transformation from agricultural land to shrubs and forests caused by the abandonment of marginal farmland (i.e. DELGADO et al. 2010, GARCÍA-RUIZ et al. 2011, REY BENAYAS et al. 2007, SERRA et al. 2008). Frequently mentioned reasons for this development are social and economic changes that caused a rural exodus and made farming unprofitable under certain conditions (GARCÍA-RUIZ et al. 2011). The CHE lists the limited water supply guarantee, the low profitability and an ageing population as the main causes (CHE 2013, Annex III). As a consequence, natural vegetation succession to shrubs and forest

took place on abandoned fields and pastures. Reforestation was likewise fostered by the Spanish and European Government (DELGADO et al. 2010).
On the other hand, and contrary to the aforementioned process, lowlands and coastal areas have experienced a concentration of population and human activities as well as a strong increase in intensive and irrigated agriculture (AQUILUÉ et al. 2017, SERRA et al. 2008). This agrees with the above findings which helped setting the conversion rules of the iCLUE model realistically and assess future changes with respect to past trends.

7.3 Calibration & Validation of the Land Use Simulations

Model calibration and validation is crucial for all model types and LULCC models do not constitute an exception to that rule. It enables making a point on the applicability of the model and the quality of its output. In fact, there is broad agreement in land change science on the need for applying model calibration and validation, however, it differs from other research fields as no standard approach exists and a large number of different methods are in use (HAGEN-ZANKER & MARTENS 2008, PONTIUS et al. 2008).
As described by VAN VLIET et al. (2016), the calibration consists in fitting the model to a specific application by first setting the initial model parameters and then adjusting them "based on iterative comparison of the model output with observations". For the present study, the iCLUE model was calibrated to represent the Ebro case study as good as possible by adapting the parameters mentioned in chapter 5.2.5 and the drivers in chapter 5.2.4. The observational data used for the calibration was the CLC 2000 map, while the model was initiated using the CLC 1990 map. The model was calibrated manually. The validation, i.e. the assessment of the model output against observations (VAN VLIET et al. 2016), was carried out using the CLC 2006 map, version 17.
Following the practices discussed by VAN VLIET et al. (2016), the model results were assessed according to their location accuracy, pattern accuracy and uncertainty analysis. A climate sensitivity analysis was carried out for the final water use maps which is described in chapter 7.6.
Location accuracy, the most prevalent approach in land change sciences (PONTIUS et al. 2008, VAN VLIET et al. 2016), is a pixel-by-pixel comparison of the simulated and observed map which indicates whether the allocation of land changes happened at the correct location (VAN VLIET et al. 2016). For this purpose, the three-map-comparison came into use. This method was applied to different models in a combined study by PONTIUS et al. (2008) and its adoption to different versions of the CLUE model has proven successful. Observed land use maps for time t_0 (start of the simulation, 1990 in the present case) and t_1 (calibration year, here 2000) and the simulated land use maps for t_1 are necessary. A map of the differences between the two observed maps is calculated to identify the actual land use changes happened during the calibration period t_0 to t_1, see figure 7.5. The changes simulated by the model for the same time period are obtained by creating a difference map between the initial observed map for t_0 and the simulated map for t_1, also displayed in figure 7.5. To obtain the final map the two difference maps are overlaid which facilitates the distinction between correctly modelled pixels due to correctly modelled change versus correctly modelled persistence (PONTIUS et al. 2008). These two categories are represented by a green and grey colour, respectively, in figures 7.6, 7.7 and 7.9 displaying the calibration and validation results. As for the errors, the three-map-comparison allows to distinguish

between three types: I) pixels that did not change (persistence), but were simulated as change (yellow in the mentioned figures), II) the opposite, i.e. change pixels that were simulated as persistence (red), and III) change pixels where the model predicts a transition to the wrong land use class (pink). With CLC data being available for more than two points in time, a fortunate and rather rare situation in land use modelling, it was possible to carry out an independent validation applying the same method but using as observed map for time t_2 the CLC 2006 map.

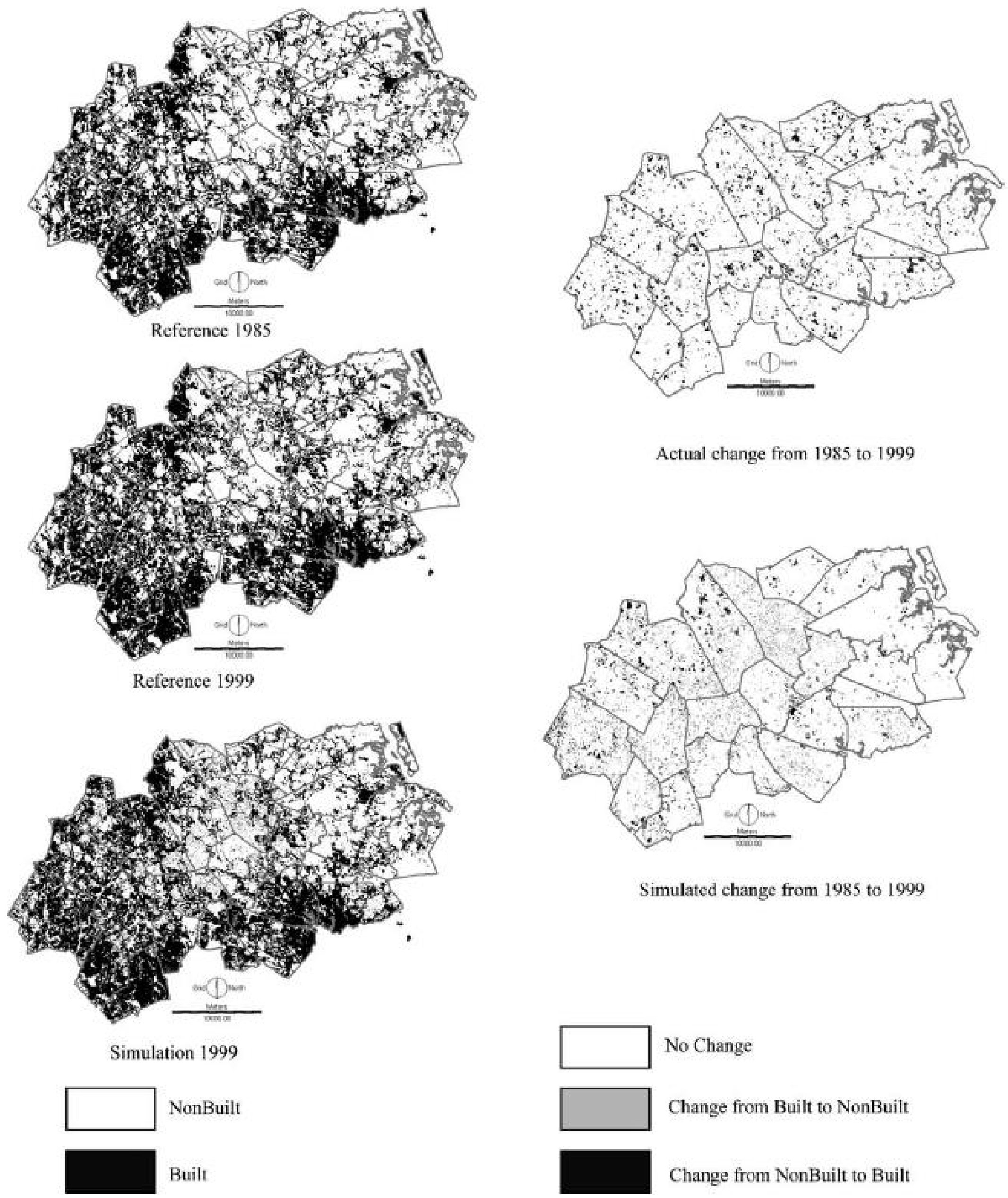

FIGURE 7.5: Maps necessary to carry out a three-map-comparison (left) and the two main difference maps representing the actual change and the simulated change (right). Source: PONTIUS et al. (2004).

A three-map-comparison was further carried out at various resolutions to assess the pattern accuracy of the model. The results of the location and pattern accuracy

have been published in HUBER GARCÍA et al. (2018), whereas the results presented here involve a slight improvement compared to the publication.
Regarding the uncertainty analysis, VAN VLIET et al. (2016) define it as an "analysis of the variation of model outputs without any changes in model parameters or variables". This measure was applied to quantify the effect of randomness of the model. Last, the model sensitivity with regard to different climate inputs was examined. The assessment of the quantity disagreement applied in other studies (PONTIUS et al. 2004) indicating whether the amount of the land use demand of each class is modelled correctly was not necessary since iCLUE follows a demand-allocation approach which means that the model fully allocates the demand of all classes for each model step whilst taking into account the allowed deviation described in chapter 5.2.5 (AQUILUÉ et al. 2017, PONTIUS et al. 2008). Since the results are very similar, all following calibration and validation exercises are only shown for the MYOPIC scenario run with RACMO22E data.

7.3.1 Location Accuracy

Figures 7.6 and 7.7 show the location accuracy results for the calibration and the validation for a specific model run, respectively. Only the results for one run are shown as the results for other runs do not show any substantial deviations.

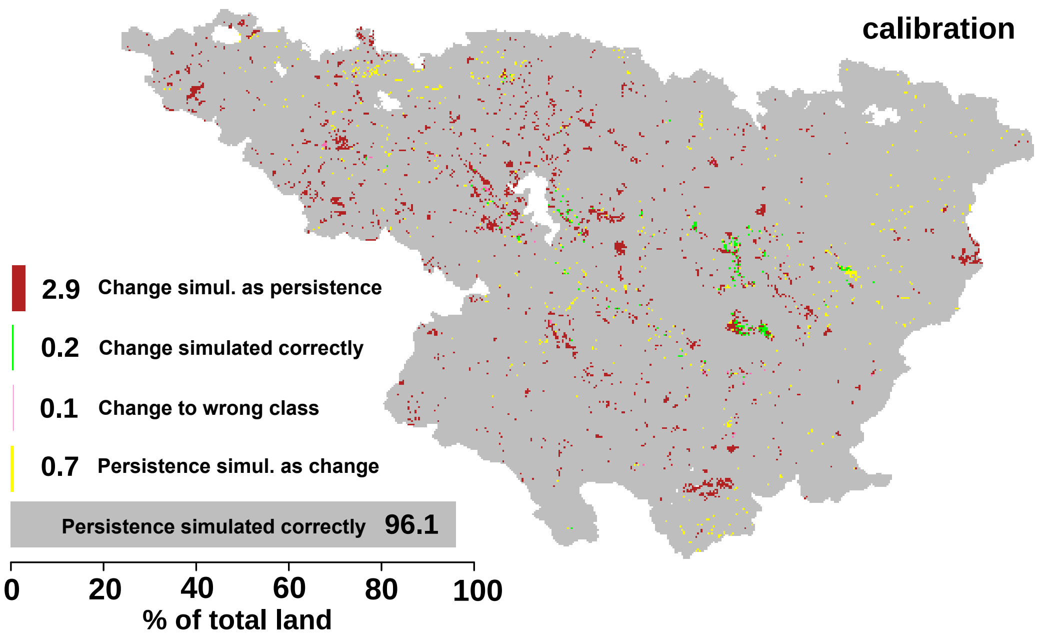

FIGURE 7.6: Calibration results of the iCLUE model for the Ebro setup.

As shown here, the calibration results are slightly better than the validation results. 96.1% of the study area is modelled correctly for the calibration year (2000) and 92.9% for the validation year (2006) due to the correct representation of persistence (grey colour), i.e. pixels not changing during the observed period. The large percentage of grey area has to be attributed to the generally little change during the observation period. The actual change taking place is correctly modelled (green) in 0.2% (calibration) and 0.3% (validation) of the basin area, but modelled to the wrong class for 0.1%

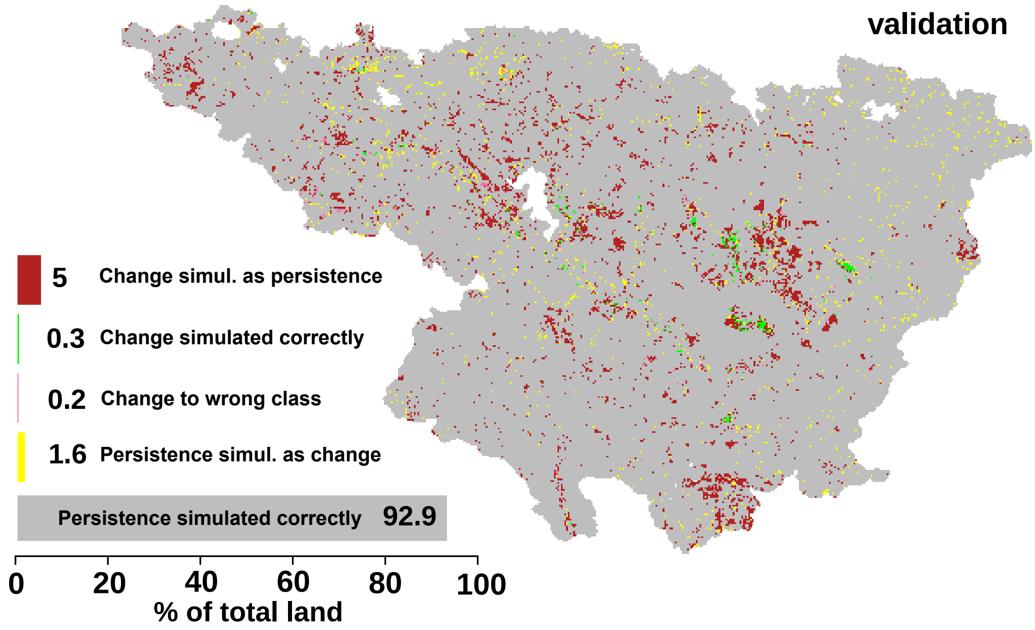

FIGURE 7.7: Validation results of the iCLUE model for the Ebro setup.

and 0.2% of the area, respectively. Persistence simulated as change (yellow) makes up 0.7% and 1.6% whereas misses, i.e. change simulated as persistence (red), accounts for the largest error both for the calibration (2.9%) as for the validation (5%). These latter error type occurs mainly in larger cohesive patches, visible in the two maps in figures 7.6 and 7.7, which coincide mainly with actual land use transformations that have taken place between the model initialisation map (1990) and the reference map. For iCLUE, and probably any other land change model, these "sudden" changes of many contiguous pixels are difficult to capture as they cannot be explained with the drivers supplied to the model. They may depend on personal decisions (e.g. a land owner decides to clear a large parcel of forest), government policies or unpredictable events such as wildfires. Besides, they are also caused to some extent by classification differences between the observed maps, as mentioned earlier in chapter 7.2.

Figure 7.8 shows a close up of the large irrigation systems (*permanently irrigated land* is displayed in turquoise) north of the Ebro main course and to the west of the Cinca River where the validation results are particularly poor due to an accumulation of missed land use transitions. It becomes clear that many patches are classified as *permanently irrigated land* in 1990, while in 2006 they are classified as *complex cultivation patterns* (orange). This, of course, cannot be predicted by iCLUE and consequently is responsible for the difference between the observed and the simulated map. However, in 2012 the same areas turn to be categorised as irrigated. It might well be that they were not irrigated in 2006 as this depends very much on the annual meteorology (THENKABAIL et al. 2009), but comparisons with different sources such as the Ebro RBMP, and particularly the map of existing irrigation systems in figure 5.3, make clear that they belong to the large irrigation systems in the Ebro since a long time. Consequently, the validation results here are misleading as they indicate that the land use simulated by iCLUE is wrong, although this error is caused by differing observations or interpretations of land use. This example illustrates well how deviations in the classification of the observed maps, either caused by errors or altered classification guidelines, affect the assessment of the model quality. PONTIUS et al. (2008), which compared the input, output and validation maps of several land change models in an extensive study, conclude that the most important lesson they learnt was "that the selection of the place, time, and format of the data must be taken into consideration when interpreting the model's performance, because these characteristics can have profound influence on the modelling results."

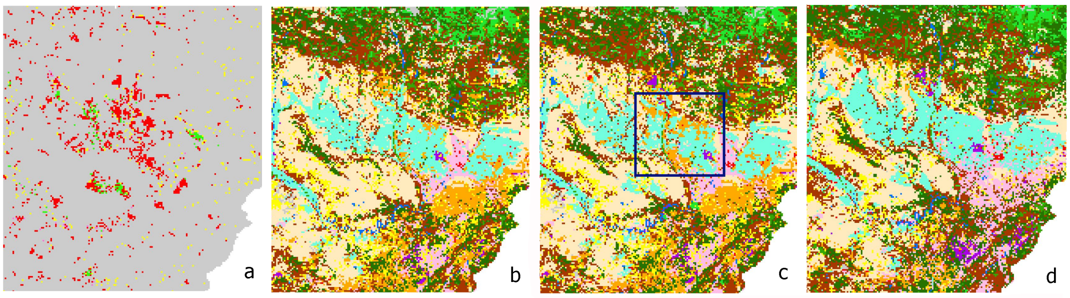

FIGURE 7.8: Close look at a) the validation results for the irrigation systems north of the Ebro main stream, b) the CLC 1990 map, c) CLC 2006 map and d) CLC 2012 map for the same area.

The fact that the calibration shows better results than the validation can be explained with the "conservative" behaviour of the model. It sticks to the initial input map (1990) and modifies it step by step, which is the reason it will always show a larger agreement with a reference map that is closer to the initial map. All in all, it can be considered a good result that also for the validation year, i.e. 16 years a head of the model input map, 93.2% of the study area are simulated correctly.
Looking closer into the errors, both for the calibration as for the validation year, the model produced more erroneously simulated change pixels than pixels showing the correct land use change. At first glance, this might be surprising. However, in the study by PONTIUS et al. (2008) twelve out of the 13 compared LULCC model applications showed similar proportions at the finest, i.e. the modelling resolution. According to the authors of this comparative study, the errors are reduced at coarser resolutions as it is also the case for the Ebro case study, see chapter 7.3.2.

7.3.2 Pattern Accuracy

Considering the complexity of land use systems, it cannot be expected that a land change model produces perfect results. Especially the pixel-by-pixel comparison described above is a very strict measure for evaluating model results. This is one reason why several authors agree on the necessity to perform model validations at multiple scales (KOK et al. 2001, VAN VLIET et al. 2016, VELDKAMP & LAMBIN 2001). Besides, and possibly more important, the processes taking place and the drivers of change are very scale dependent which is a further reason to apply a multi-resolution validation (KOK et al. 2001, VELDKAMP & LAMBIN 2001).

For the present study, the three-map-validation was carried out at different resolutions using the *lulcc* package (MOULDS et al. 2015) implemented in the R Statistics software (R DEVELOPMENT CORE TEAM 2008) which refers to PONTIUS et al. (2011). The results of the pattern accuracy in figure 7.9 for the validation year 2006 indicate that the overall agreement increases very slowly at first until a resolution of 4 km^2 and after that at a slightly faster constant rate until the maximum resolution of 256 km^2.

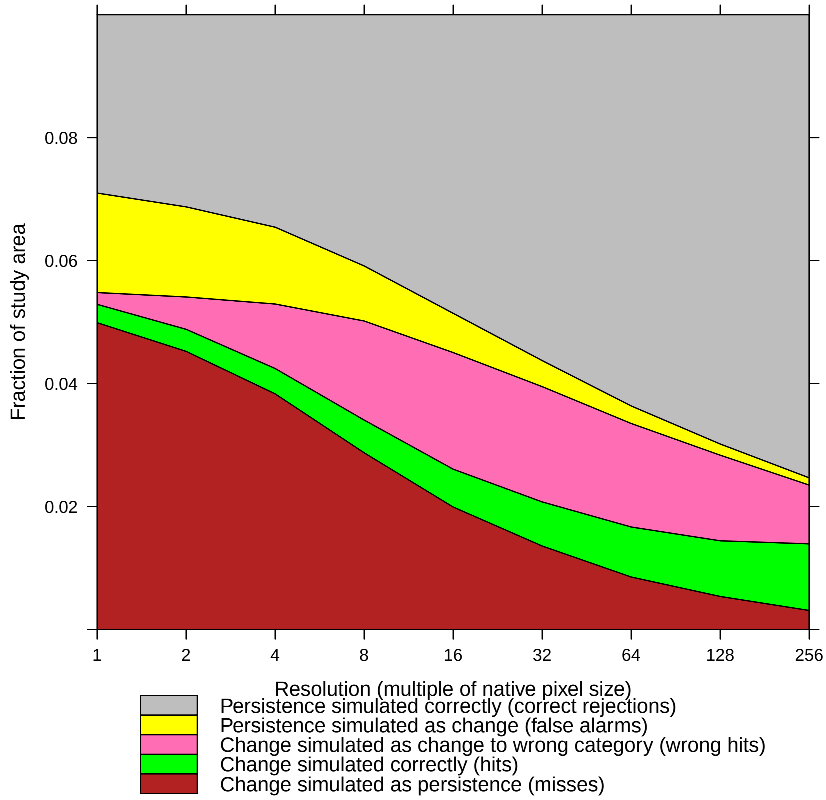

FIGURE 7.9: Results of the multi-scale validation in the Ebro basin for 2006.

PONTIUS et al. (2008) concluded in their study mentioned in chapter 7.3.1 that this is typical to happen "since near errors of location over small distances become resolved as resolution becomes slightly coarser". This would be the case if single erroneously classified pixels were spread across the study area as in another study by PONTIUS et al. (2011). However, for the present study, the reduction of change simulated as persistence (red) and persistence simulated as change (yellow) is mainly transformed to change simulated to the wrong class (pink). This is probably related to the large patches of missed change (red in figures 7.6, 7.7) which also at coarser resolutions do not represent the correct class. In addition, it has to be taken into account that a total of 13 land use classes are simulated at the same time for the Ebro setup. This large number allows for many wrong land use transitions. Furthermore, the observed change taken place between 1990 and 2006 affects only 5.4% of the total basin area. PONTIUS et al. (2008) state that simulations of study areas experiencing larger changes usually have a higher predictive accuracy. Small changes may be difficult to handle for land use change models like iCLUE since they are programmed to expect change. Moreover, PONGRATZ et al. (2008) further argue that study areas experiencing larger net changes offer a stronger statistical signal to be detected in the calibration procedure whereas simultaneous gains and losses of land use classes, which is the case in the Ebro as mentioned in chapter 7.2, are more difficult to predict. Following the argumentation by PONTIUS et al. (2011), the remaining 2.5% disagreement at a 256 km^2 resolution, which means that the whole study area would be represented by approx. 1.3 pixels, is entirely attributable to a quantity disagreement of the land use classes between the observed and simulated 2006 map caused here by the allowed deviation of the model from the targeted land use demand.

7.3.3 Uncertainty Analysis

As the developers of iCLUE Verweij et al. (2018) state, the random number generator included in the model inhibits the reproducibility of the results. However, model runs using exactly the same model parameters create similar results. To assess the uncertainty of the iCLUE model, 20 runs were analysed together.

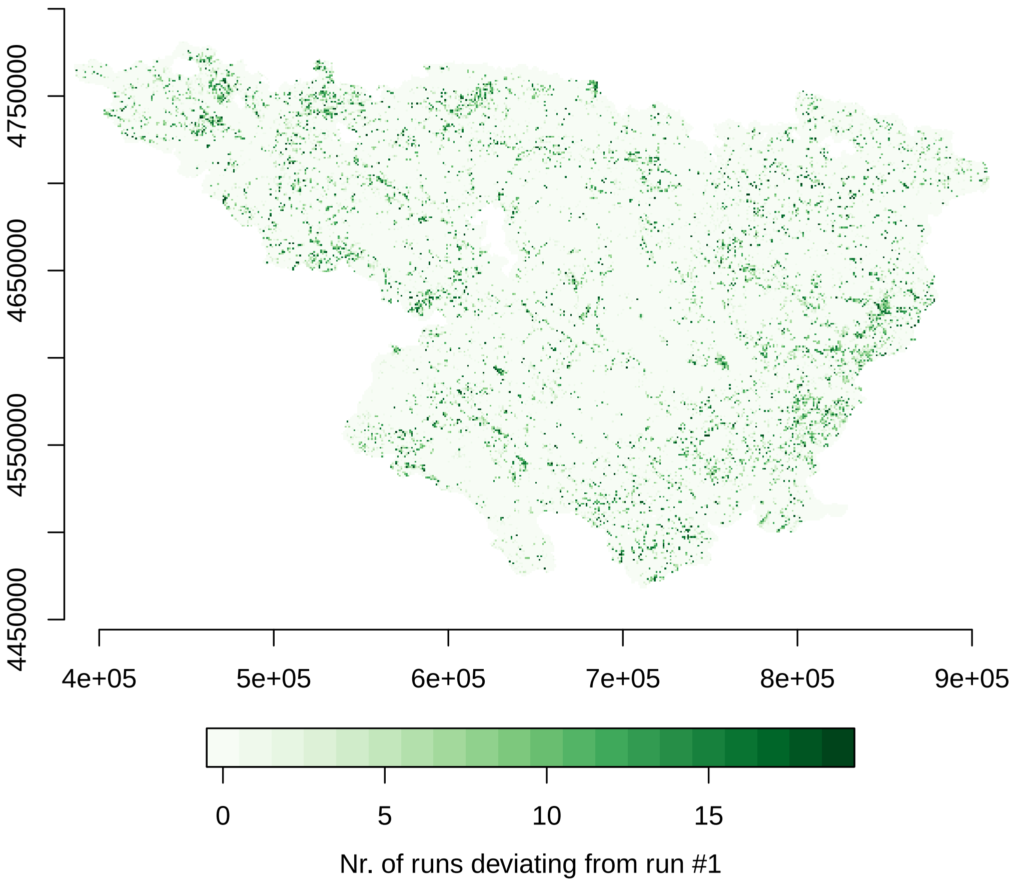

FIGURE 7.10: Visualisation of the spatial distribution of differences between iCLUE model runs. The darker the colour the more runs deviate from model run no. 1 at this exact location.

Figure 7.10 illustrates how the spatial distribution of land uses differs from run to run. An arbitrary simulation result for the MYOPIC scenario in 2050, let us call it run no. 1, was used as reference and its differences to 19 other result maps were calculated and summed up. The darker the green colour in figure 7.10, the higher the number of runs that predict a different land use than run no. 1 at this exact location. The analysis show that the randomness is not distributed homogeneously all over the catchment, but that differences occur more frequently in certain areas. These are mainly areas with a high land use heterogeneity, as visual comparison with the land use simulation in figure 7.14 shows, and which probably present high location probabilities for many land use classes. The spatial pattern does not change if another run is chosen as reference (not shown here).

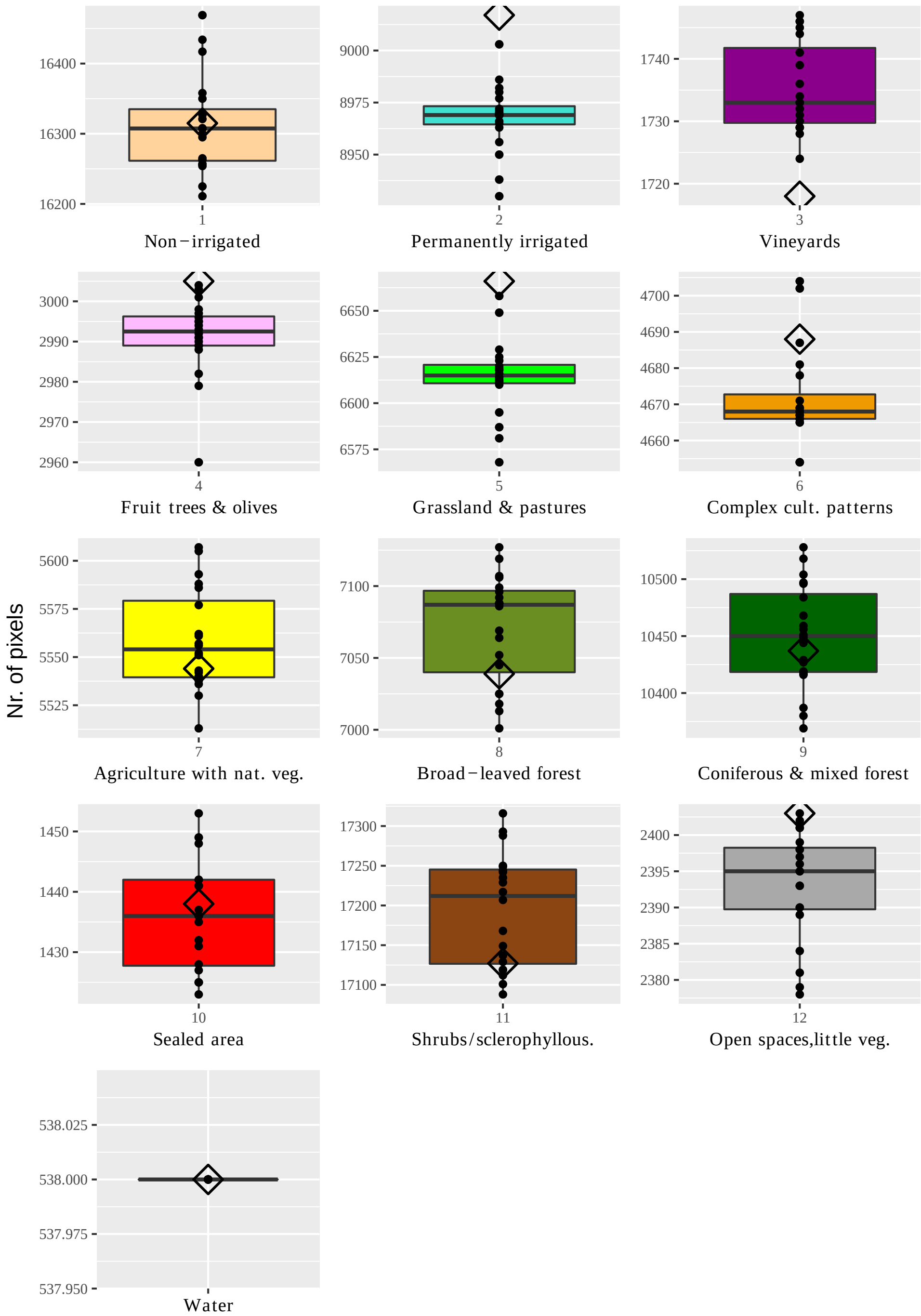

FIGURE 7.11: Boxplots representing the spread of amount of pixels for each land use class for 20 iCLUE model runs. The diamonds indicate the actual demand target passed to iCLUE.

In addition to the spatial distribution, also the quantity disagreement changes from model run to model run. This means, that the amount of pixels assigned to a certain land use class fluctuates slightly depending on the run, see the boxplots in figure 7.11. This is the case for all the classes except for *water* as it is not allowed to

change. The diamonds in figure 7.11 indicate the actual land use demand passed to iCLUE, i.e. the targeted demand, from which the model is allowed to deviate slightly, see percentages in table 5.4. Interestingly, for some land uses the simulated demand spreads more or less equally on both sides of the targeted demand, for example *non-irrigated arable land* or *sealed area*. For others, the target is over- or underestimated in all model runs (*permanently irrigated land, vineyards, grassland & pastures*). The reason is probably that some land uses are allocated more easily than others, so the model "prefers" to allocate more of it.
The uncertainty analysis visualise and quantify the effect of the random factor inherent to iCLUE. The magnitude of the deviations between model runs is small and might be negligible for the resulting land use simulations. For the calculated water use maps, however, it plays a role, as described later in chapter 7.7. The independent validation carried out and described above helps overcome an overfitting of the model to a specific run, as pointed out by VAN VLIET et al. (2016).

7.4 Land Use Scenarios for the Year 2050

For comparison, the CLC 1990 map used to initialise iCLUE is displayed in figure 7.12 while one realisation of the final land use simulation for the SUSTAINABLE and MYOPIC scenario using the RACMO22E climate input is exemplarily shown in figures 7.13 and 7.14, respectively. The protected areas excluded from modelling were included using the CLC 1990 map assuming that their land use is approximately constant which agrees with the observed changes between 1990 and 2012.

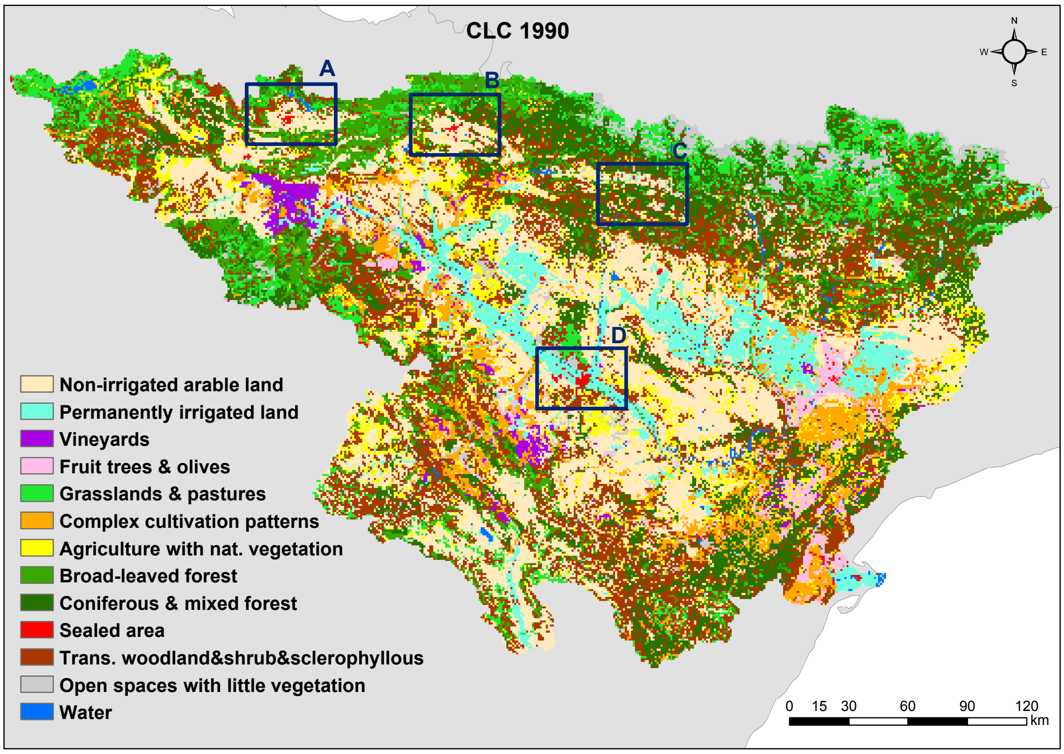

FIGURE 7.12: Land use in the Ebro basin according to CLC 1990.

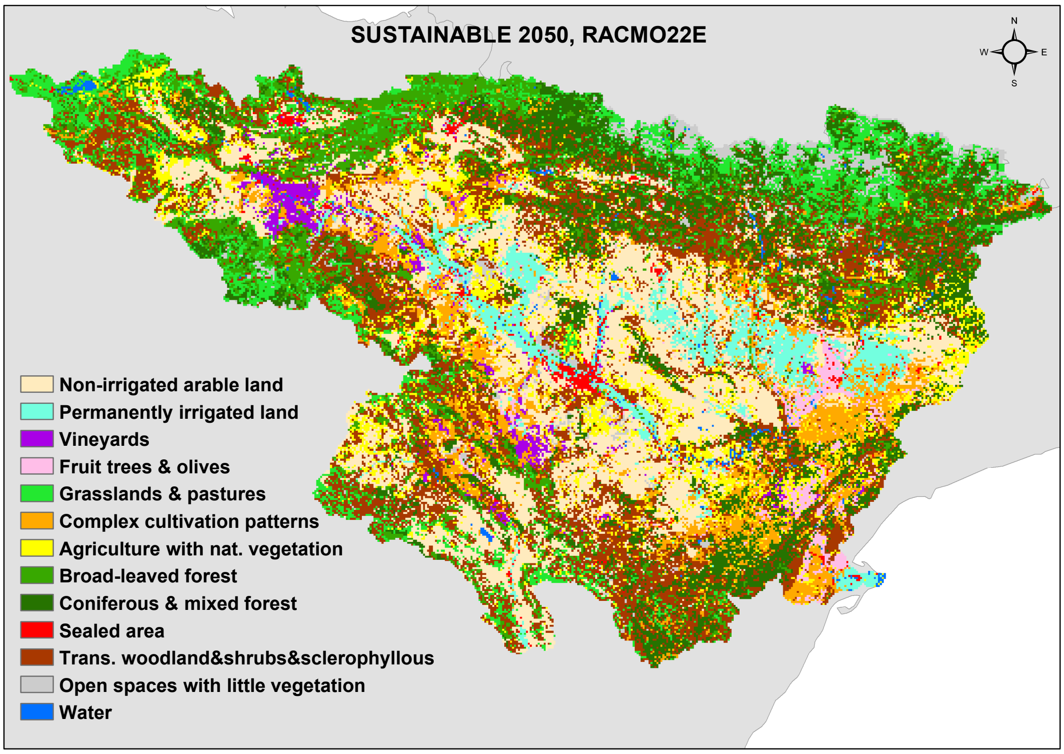

FIGURE 7.13: Land use simulation 2050 of the Ebro for the SUSTAINABLE scenario using the RACMO22E climate input.

The most striking difference between the two land use simulations is the prevalence of permanently irrigated land in the northern part of the Ebro lowlands in the MYOPIC scenario while this class has shrank in the SUSTAINABLE scenario compared to 1990. iCLUE also simulates large irrigated areas around the city of Vitoria-Gasteiz in the MYOPIC scenario, indicated in figure 7.12 by rectangle A. No permanent irrigation can be appreciated from the CLC 1990 map, neither it is the case for the CLC 2000 nor the 2006 data. However, more up to date CLC versions such as version 18.5.1 for 2006, the 2012 and also the - not yet validated - 2018 map show a significant area of irrigated land around the city of Vitoria-Gasteiz. In addition, an irrigation density map for the year 2004 provided by the CHE reports a medium irrigation density for this area, see also the existing irrigation systems in figure 5.3. The inclusion of the density irrigation map as driver in iCLUE probably plays a major role for the correct assessment of the suitability of this area for irrigation.

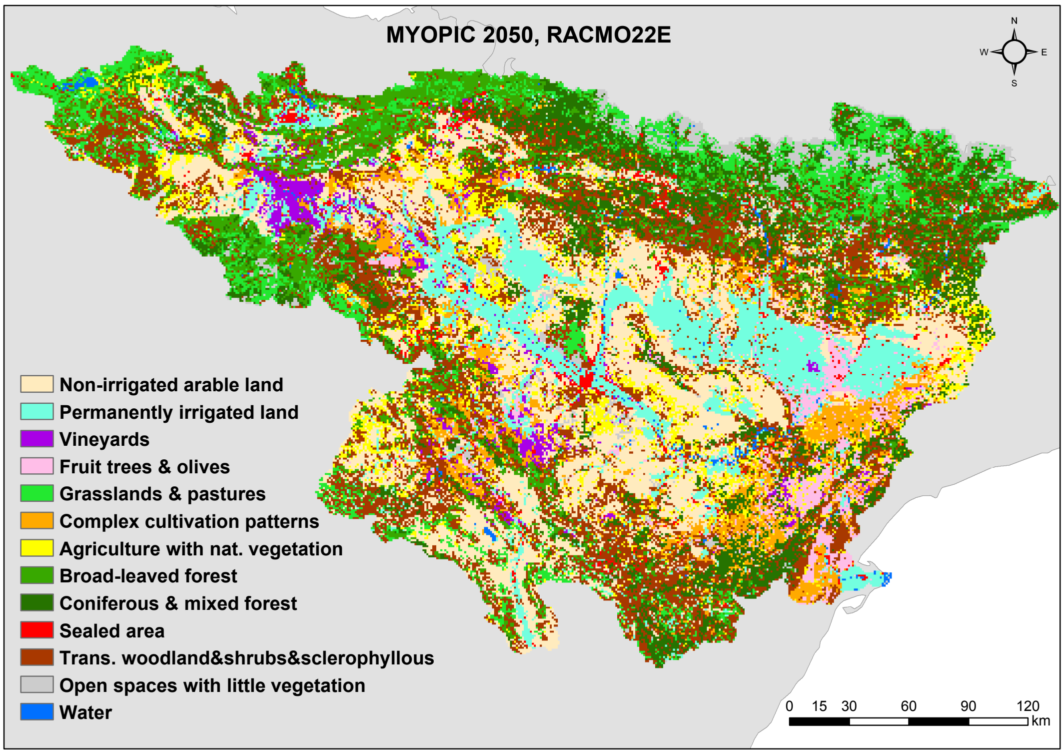

FIGURE 7.14: Land use simulation 2050 of the Ebro for the MYOPIC scenario using the RACMO22E climate input.

Noticeable in rectangle A in figure 7.12 is also the fact that the city itself was much smaller in 1990 as simulated for both scenarios in 2050. Again, the allocation of the demand for *sealed area* is distributed by iCLUE in a realistic way. Vitoria-Gasteiz has experienced a massive expansion since the 1990s and its area is currently much larger than back than. Consequently, it makes sense to distribute future urban demand in this area. The model setup includes several distance to cities and population density drivers which might influence the suitability for urban area.

In general, the model allocates the sealed area demand quite nicely around already existing agglomerations even though in reality the cities are more compact, as the direct comparisons for Pamplona in figure 7.15 show. iCLUE spreads urban pixels over a wider area around the cities and towns as compared to the observed development, see the changes from 1990 to 2006 in the upper row of figure 7.15. This effect might be caused by drivers with a spatial aggregation at municipality level such as the dynamic population density, the employment rate in agriculture or the manufacturing industry which only provide one value for the whole municipality and do not specify the correct location of settlements.

From visual inspection, urban areas seem to be more compact, and consequently more as one would expect them to look like, in the SUSTAINABLE scenario, see again the city of Pamplona in figure 7.15. However, the reason for this could be the generally lower demands of *sealed area* and hence simply less pixels of this class. Compared to reality, iCLUE introduces more pixels of other land uses in urban areas such as *vineyards*, *open spaces with little or no vegetation* and *broad-leaved forest*, which are rather unlikely to be found there, see figure 7.15.

Figure 7.15 finally also exemplifies the random differences between one run and

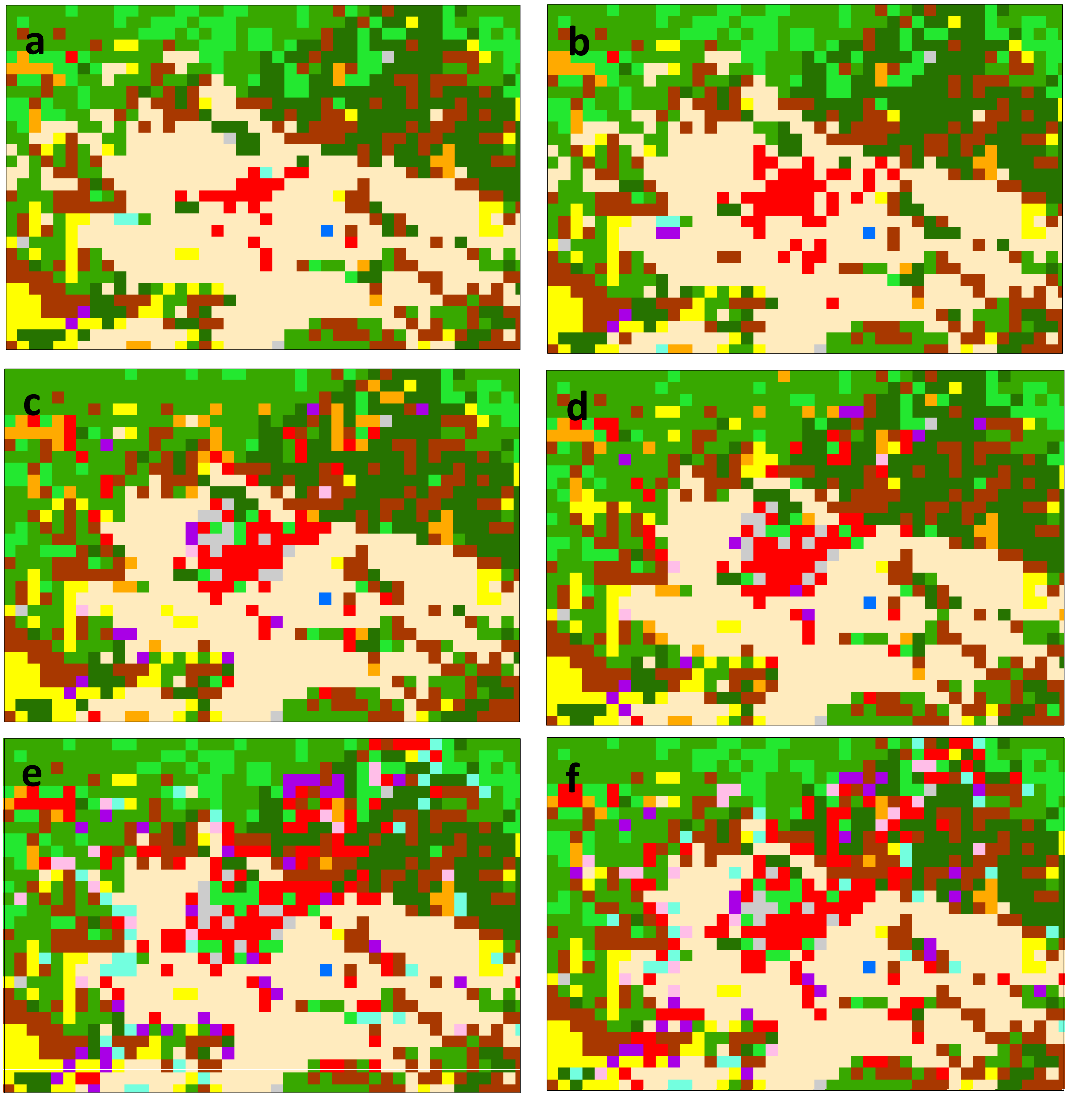

FIGURE 7.15: Comparison of iCLUE results for the greater area around the city of Pamplona (rectangle B in figure 7.12): a) CLC 1990, b) CLC 2006, c) SUSTAINABLE 2050 run 1, d) SUSTAINABLE 2050 run 2, e) MYOPIC 2050 run 1, f) MYOPIC 2050 run 2.

the other both for the SUSTAINABLE (central row) and MYOPIC scenario (bottom row). As can be observed, the two runs for each scenario are similar but not equal.

Rectangle C in figure 7.12 highlights an area where iCLUE allocates a substantial amount of urban pixels for the MYOPIC scenario, while according to the observed land use maps there are hardly any pixels. The two municipalities affected are Jaca and Sabiñánigo. Their population was approx. 13,000 and 10,000 for the year 2018 (INE 2015), respectively. Even if the medieval town of Jaca is a touristic place as it lies on one of the two main routes of the Way of Saint James crossing Spain (AYUNTAMIENTO DE JACA 2020), the uncontrolled urban sprawl simulated by iCLUE here is rather unrealistic. The reason for this artefact is not clear. It may be partly related to the input drivers of the model which assess a high suitability for urbanisation to this Pyrenean valley. However, the amount of sealed pixels allocated to this area is considerably less in the SUSTAINABLE scenario, see example in figure 7.13. The urban sprawl in this scenario is more realistic as already existing agglomerations such as Zaragoza in rectangle D (figure 7.12) grow. Surprisingly, the growth of this latter city is noticeably smaller in the MYOPIC scenario, see figure 7.14, whereas the overall urban demand for this scenario is higher.

However, also the demand for *permanently irrigated land* is very high and consequently also the pressure to allocate this class. This becomes clear when looking closer at the city of Zaragoza: In the MYOPIC scenario the city is nearly exclusively surrounded by permanently irrigated pixels, as it is the case in the observed map for 1990. The demand weight for *permanently irrigated land* seems to be very high so that this class is not transformed to *sealed area* in this region. This shows how the demand weight of a class can influence the total probability of a land use to occur at a certain location and that the suitability is not the only factor influencing the allocation process. To conclude, the remarkable small expansion of Zaragoza in the MYOPIC scenario and the uncontrolled urban sprawl in a rural mountain valley are likely to be linked. Due to the high overall demand of *permanently irrigated land*, this land use is kept in the municipality of Zaragoza where it has a high suitability and overall probability. This means that the high demand for *sealed area* has to be allocated somewhere else and the municipalities of Jaca and Sabiñánigo seem to be most suitable for it.

The described effect is not a singularity of a particular model run, but all MYOPIC runs show similar features and also all SUSTAINABLE scenarios resemble each other independently of the climate model used. This is visualised in figure 7.16 where each map shows the distribution of *sealed area* pixels for several model runs. The darker the reddish colour, the more model runs allocate urban land at this particular location. When comparing the patterns between the six maps it becomes clear that the three MYOPIC scenarios are very similar: Zaragoza, in the centre, does not grow as much as in the SUSTAINABLE scenario and the municipalities of Jaca and Sabiñánigo, North of Zaragoza, grow substantially. The similarities between the results with data from different climate model combinations were also found for other land uses, but they are not shown here. Regarding the land use maps, the influence of the climate model seems to be small compared to the random factor of iCLUE.

All in all, the results of the land use modelling are satisfactory. 96.3% of the case study area were modelled correctly for the calibration year and 93.2% in the validation year. The main problem regarding the calibration and validation is to differentiate between actual land use changes and altered classification schemes or classification errors. It should not be forgotten that CLC data is created by an automatic classification of satellite images, which is in itself just a model result with errors and misclassifications. This is also the reason why the CLC maps 1990, 2000 and 2006 version 17 used here could not be combined with the 2006 version 18.5.1, 2012 and soon also the 2018 map which would have allowed to have longer validation periods. Of a similar nature is also the non-representation of irrigated areas according to the official CHE registry, i.e. around Vitoria-Gasteiz. Obviously, classification differences between the two data sources exist.

Further factors influencing the calibration/validation results are the large amount of classes modelled, 13 in the case of the Ebro. Most comparable regional modelling exercises include less classes: 4 (AQUILUÉ et al. 2017), 4 (BASSE et al. 2014), 5 (BRINER et al. 2012), 9 (LÓPEZ-MORENO et al. 2014), 5 (LUO et al. 2010) or 10 (MEHDI et al. 2015). SOHL & SAYLER (2008) constitute rather an exemption with 16 classes.

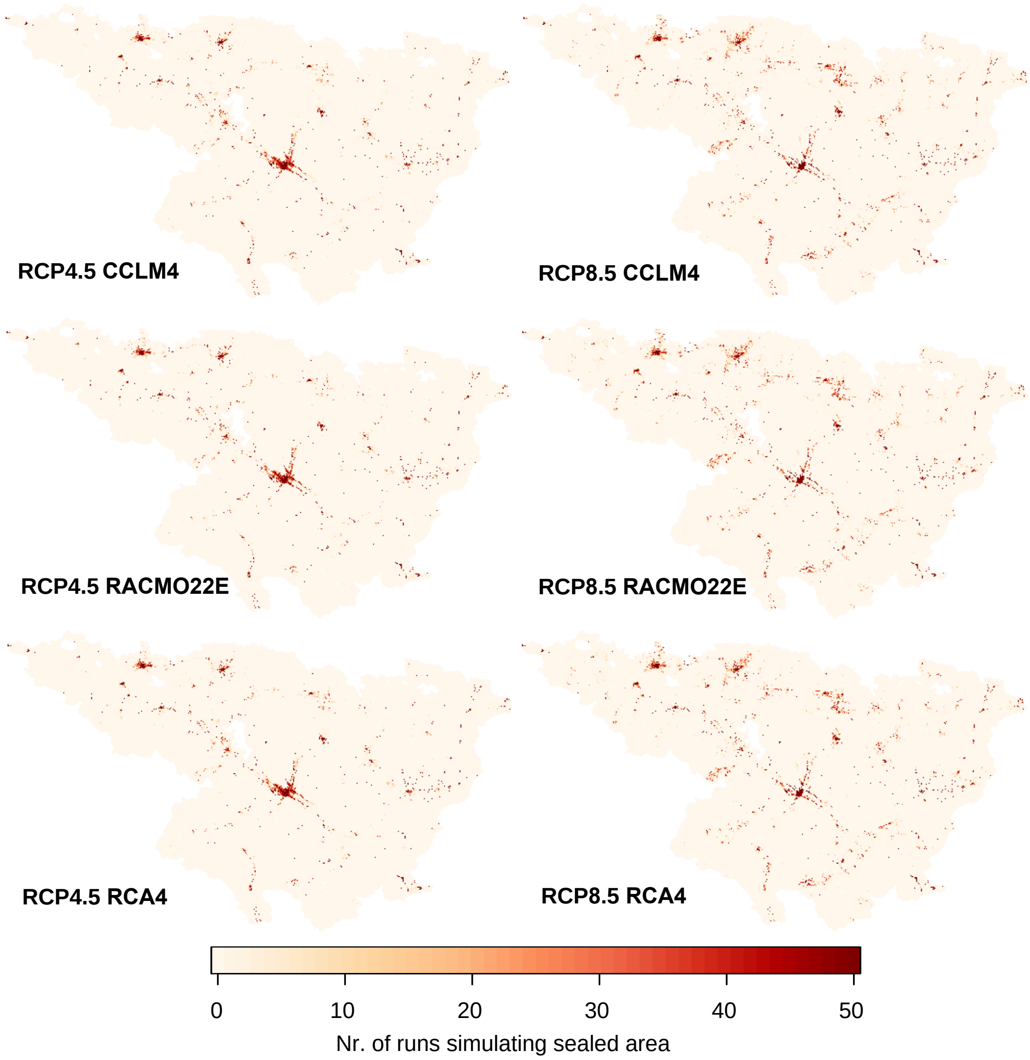

FIGURE 7.16: Distribution of urban pixels in numerous model runs and all six scenarios.

However, keeping 13 classes allowed to maintain a certain thematic detail to be able to spot changes which was one of the aims of this study. Obviously, the same happens for the spatial resolution. The results above show that modelling at a higher resolution and applying a pixel-by-pixel comparison seems to lead to more errors. A sufficient spatial detail can, however, only be obtained at a high resolution.

It has to be noticed here that in LULCC modelling a further source of uncertainty is the non-stationarity of land-change processes (VAN VLIET et al. 2016). The authors elaborate further that by extrapolating the calibrated model into the future one implicitly assumes that the same set of parameters is valid also in the future. However, political, economic or environmental conditions may change. This as a an important difference between empirical models such as iCLUE and physically based ones like hydrological models where the inputs may change but not the physics of the system. An attempt was made in the present iCLUE setup to overcome this non-stationarity by including dynamic drivers. Socio-economic dynamics of the scenarios are, however, not represented sufficiently in the model due to the lack of spatially distributed projections of GDP and population growth. Nonetheless, as much information as possible obtained from the stakeholder workshops was introduced through the conversion rules and the development of the land use demands. This is in line with the recommendation made by VAN VLIET et al. (2016), which underline that the credibility of a LULCC model should not be exclusively based on validation results but that it profits from interactions with stakeholders as applied here as part of the integrated approach of this study.

7.5 Assessment of the Water Use Estimations

Assessing the water use maps derived from the land use simulations is necessary but challenging at the same time. First, several variables have to be checked: 1) The irrigated area, 2) the water demand of different sectors and 3) the water applications per area. Secondly, it is difficult to define the reference situation since differing or even missing definitions of the variables limit the comparability of different data sources. MALEK & VERBURG (2018) report similar problems when setting the reference for irrigation efficiency. The variable "irrigated area" for instance, is defined in some databases or products (see the ones mentioned in chapter 2.5.3) as area equipped for irrigation (AEI), described also as *irrigable* area, in others as actually irrigated area (AIA) and still others give no precise definition. A further problem related to the fine spatial resolution of the statistics used here is that there are only very few independent sources reporting water uses at the same level of aggregation. Due to the lack of sufficient observed data, it was not possible to carry out a calibration and validation of the water use maps in a similar way as for the land use simulations. Alternative data sources such as the farm structure survey (FSS) of the European Union used by SALMON et al. (2015) to validate their global map of rainfed, irrigated and paddy cropland could not be used since the finest level of aggregation is the Nomenclature of Territorial Units for Statistics (NUTS) level 2 used by the European Union. For this reason, the following comparisons are referred to as "assessment" rather than calibration or validation.

7.5.1 Defining the Reference Scenario

Irrigated Area

The water use map representing the GLOBAQUA reference scenario 1980 to 2010 was calculated using the CLC 2006 map. Obviously, the irrigated area derived from this map cannot be calibrated to fit other sources of information. Still, the irrigated area per exploitation unit was compared to the estimations reported in the RBMP for around the year 2010 summing up to a total of 9657 km^2 (CHE 2013, Annex III). As mentioned before in chapter 5.4.2, this value is very high and needs to be interpreted as the AEI while the CLC 2006 map most likely represents the area actually irrigated. To align the water use estimations as good as possible to the values reported in the RBMP, also the land use classes *fruit trees & olives* and 20% of *complex cultivation patterns* were considered to be irrigated, as mentioned in chapter 5.4.3. The resulting irrigated area per exploitation unit from the CLC 2006 map and the estimated values from the RBMP are confronted in table 7.2.

The difference between the irrigable area reported in the RBMP and the actual irrigated area in the CLC 2006 map fluctuates strongly depending on the exploitation unit. The absolute deviation can be as small as only 3.2% but also as extreme as 276.1% in case of exploitation unit 10, the Matarraña subbasin. In this unit, the sum of the three irrigated classes in the CLC 2006 map exceeds the specifications in the

TABLE 7.2: Irrigable area [km^2] per exploitation unit in the Ebro according to estimations reported in the RBMP (CHE 2013, Annex III) for the year 2010 and irrigated area [km^2] of the CLC 2006 map taking into account *permanently irrigated land, fruit trees & olives* and 20% *complex cultivation patterns*.

Exploitation unit	Irrigable area RBMP	Irrigated area CLC 2006	Difference [%]	Difference scaled to total irrigable area [%]
1	1077	937	-13.0	-1.4
2	190	75	-60.4	-1.2
3	97	87	-10.0	-0.1
4	404	424	5.0	0.2
5	530	626	18.1	1.0
6	31	32	3.2	0.0
7	45	84	89.1	0.4
8	65	88	35.7	0.2
9	161	245	52.1	0.9
10	63	237	276.1	1.8
11	1117	948	-15.2	-1.8
12	1125	1226	9.0	1.1
13	1176	1009	-14.2	-1.7
14	1736	1622	-6.6	-1.2
15	1224	938	-23.3	-3.0
16	292	271	-7.1	-0.2
17	325	3	-99.1	-3.3
18	-	<1	-	-
Total	**9657**	**8853**	**-8.3**	**-8.3**

RBMP by far. As figure 7.17 shows, this overestimation is caused by the large area of *fruit trees & olives*, 148 km^2, and also *complex cultivation patterns*, 398 km^2, of which, however, only 20% (80 km^2) were considered for the calculation of the total irrigated area in unit 10. It seems that for this specific unit, assuming all three land use classes as being irrigated leads to incorrect results. Nevertheless, selecting only *permanently irrigated land* is neither a good approximation as the CLC 2006 map only locates 9 km^2 of this class in exploitation unit 10, which is considerably less than the targeted value of 63 km^2 from the RBMP.
Scaling, however, the individual differences of each unit with the total area of irrigable land (9657 km^2) as done in the last column of table 7.2, it becomes clear that the deviations do not carry so much weight. In case of exploitation unit 10, it means additional 1.8% of irrigable area for the whole catchment.
The differences for exploitation units 11 to 15, which include the large irrigation systems, are not that prominent at an individual level, only between -23.3 and 9.0%. Scaled to the total irrigable area, their deviations play a similar role than the one of unit 10, between -3.0 to 1.1%. In exploitation unit 18, the headwaters of the Garona River lying outside the hydrographic basin of the Ebro in France, the RBMP reports no irrigable area and only very little irrigation demand, 0.5 hm^3. For this reason and to avoid unrealistic low application values, it was assumed that no irrigation is taking place there.

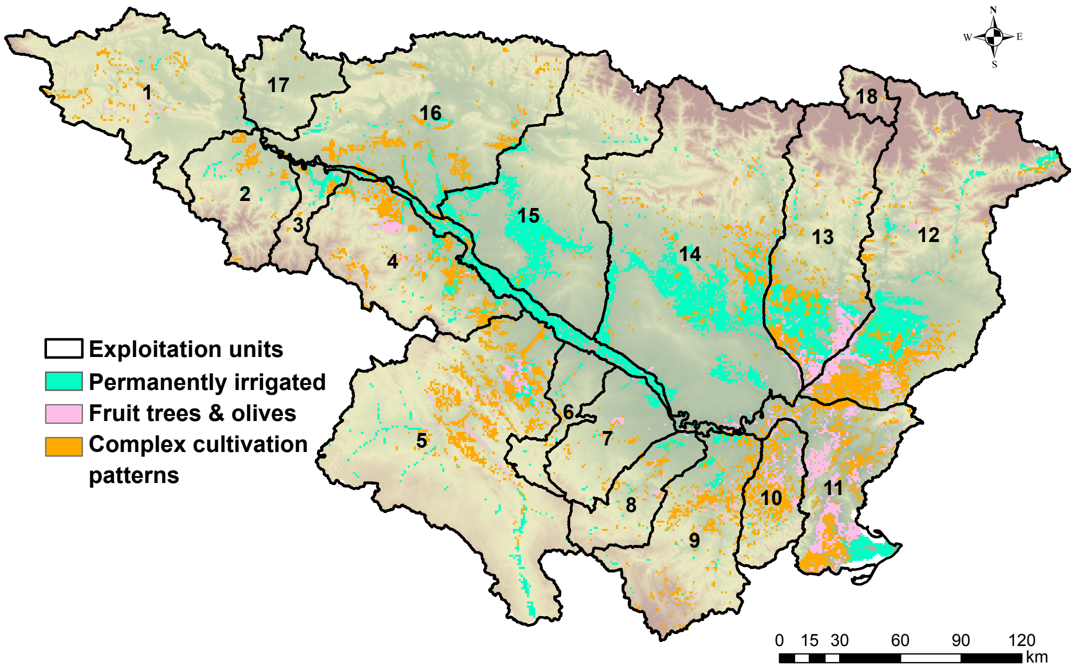

FIGURE 7.17: Distribution of the three irrigated land use classes across the exploitation units in the CLC 2006 map.

Water demand and application

As for the water demand values, the RBMP reports estimates for the water demanded per sector in each exploitation unit (CHE 2013, Annex III). The agricultural demands are confronted in table 7.3 to the values used hereafter to calculate the water demand per pixel.

TABLE 7.3: Agricultural water demand [hm^3] per exploitation unit according to the RBMP for approx. the year 2010 (CHE 2013, Annex III) and values used to calculate the water demand per pixel.

Exploitation unit	Water demand RBMP	Calculated water demand	Difference [%]	Application [hm^3/km^2]
1	737.4	737.4	0	0.79
2	110.7	54.6	-50.7	0.73
3	65.6	65.6	0	0.75
4	260.5	260.5	0	0.61
5	372.8	372.8	0	0.60
6	24.8	24.8	0	0.77
7	36.7	36.7	0	0.44
8	53.6	53.6	0	0.61
9	156.8	156.8	0	0.64
10	58.2	58.2	0	0.25
11	1194.6	1194.6	0	1.26
12	923.5	923.5	0	0.75
13	999.9	999.9	0	0.99
14	1564.6	1564.6	0	0.96
15	883.8	883.8	0	0.94
16	151.6	151.6	0	0.56
17	85.5	32.0	-97.6	0.73
18	0.5	0	0	0
Total	**7680.6**	**7541.0**	**-1.82**	**Mean: 0.73**

Unlike the irrigated area, the water demand values from the RBMP were directly adopted which is the reason for the exact matches in table 7.3. The only deviations occur for exploitation unit 2 and 17. This effect is caused by the introduction of a threshold described in chapter 5.4.4 to limit the maximum water consumption per pixel. The threshold is needed for exploitation units its water demand bears no proportion to the amount of irrigated pixels described by the CLC 2006 map. In the case of exploitation unit 17 no *permanently irrigated land* pixels can be found in the CLC map, only 1 *fruit trees & olives* and 9 *complex cultivation patterns* (reduced to 20%) pixels. At the same time, the RBMP reports a total agricultural water demand of 85.5 hm^3 for this area (CHE 2013, Annex III), which would result in an unrealistically high application of 30.54 hm^3/km^2. The RBMP 2015-2021 mentions, however, values around 7894 m^3/ha, which is equal to 0.79 hm^3/km^2 (CHE 2013, Annex III). The new RBMP 2021-2027 says that the modern irrigation systems are even rather close to 0.65 hm^3/km^2 (CHE 2018). The discrepancy is due to the fact that already existing irrigation systems around the city of Vitoria-Gasteiz in exploitation unit 17 are not captured by the CLC 2006 map, while they are visible in the map of irrigation systems from the RBMP in figure 5.3 representing the situation in 2004 and also in other CLC maps, as described earlier. By introducing a threshold, the water application per pixel adopt more realistic values ranging from 0.25 to 1.26 hm^3/km^2, see table 7.3. It prevents, however, the water use of the affected exploitation units to reach the value they are assigned to in the RBMP and consequently the modelled overall water demand for the present is lower than the one reported in the plan: 7541 hm^3 compared to 7681.6 hm^3 in the RBMP (CHE 2013, Annex III). The same happens for the urban demand where 483 instead of 506 hm^3 are modelled (359 hm^3 urban plus 147 hm^3 industrial demand are reported), an underestimation of -4.6%. For this sector, the only difference between RBMP and calculated urban water demand per exploitation unit happens for unit 3 since it is the only unit where the threshold is effective. It is the smallest unit and urban areas are under-represented in the CLC 2006 map, especially at the rather coarse modelling resolution of 1 km^2. A table listing the urban demands per exploitation unit according to the RBMP can be found in Appendix D.

It is important to notice that water from the Ebro catchment is diverted to the metropolitan area of Bilbao (82 hm^3 urban + 38 hm^3 industrial uses) out of exploitation unit 17, to the coastal areas of the province of Tarragona (41 hm^3 urban + 31 hm^3 industrial) from unit 11 and approx. 14 hm^3 unspecified further extractions (CHE 2013, Annex III; CHE 2015), see table D.1. This adds approx. 1.4 million inhabitants that are supplied with water from the Ebro (CHE 2015). The transferred amounts were not considered for calculations.

The presented assessment reveals that there are some differences between the land use map used for modelling and the irrigable area as described in the RBMP. As for the validation of the land use maps, it is important to take into account the quality of the reference data. In this case, it is well known that CLC maps are subject to errors or classification differences. Besides, the values specified in the RBMP are explicitly called "estimations" which are based on simulations without providing any detailed information, so they also have to be used with much care.

7.5.2 Comparison with other Water Use Maps

Agricultural Water Demand

The attempt was made to compare the final water use maps for the reference period to other freely available water use products. As mentioned in the introduction chapter 2.5.3, numerous global and European irrigation maps exist. Figure 7.18 compares the irrigation density of registered irrigated areas in the Ebro basin in 2004 according to the CHE, considered to be the reference hereafter, to the GIAM by THENKABAIL et al. (2009) describing the situation around the year 2000, the GMIA of 2005 by SIEBERT et al. (2013) and finally also to the derived agricultural water use map for the reference period based on the CLC 2006 map. This example clearly shows how difficult it is to compare these products and to quantify the differences. First, the resolution varies strongly, from 5′ (GMIA) to very detailed vector data in case of the reference, and second, they all show different variables: an ordinal irrigation density scale, land use classes specifying the source of irrigation water and the crop type, the percentage of AEI on the total pixel area and, in case of the results of this study, the quantitative water demand in mm per year. It has to be pointed out that other products providing absolute irrigation applications in mm exist, such as the ones produced by AUS DER BEEK et al. (2010), SCHALDACH et al. (2012) and WRIEDT et al. (2009a). However, they are not directly downloadable and, what is more, their resolution is course: 5′, 5′ and 10 km^2, respectively.

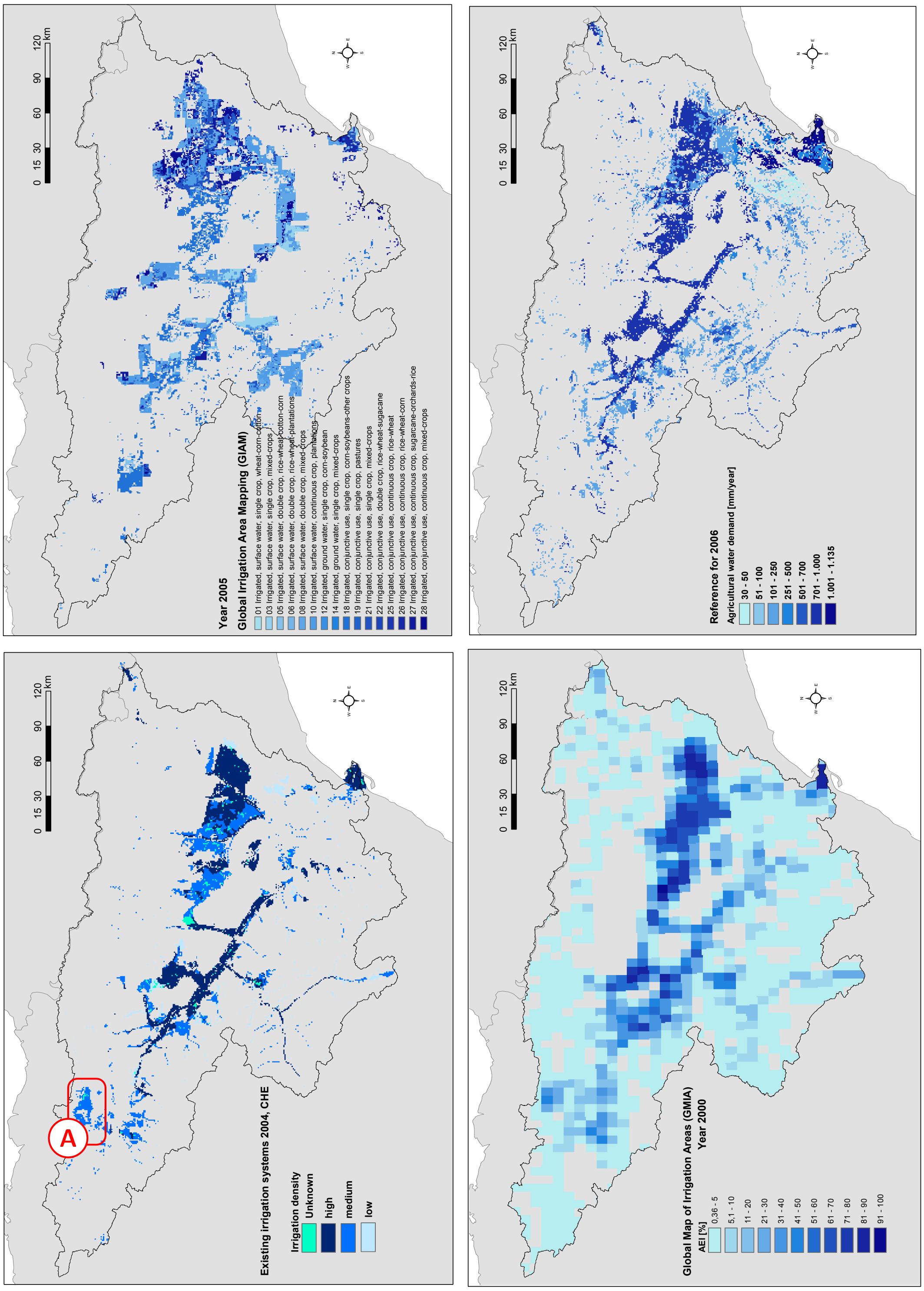

FIGURE 7.18: Comparison of various irrigation maps for the reference period. Lower left: Irrigation intensity according to the CHE (`http://iber.chebro.es/geoportal/`), upper left: GIAM (THENKABAIL et al. 2009), lower right: GMIA (SIEBERT et al. 2013), upper right: Modelled agricultural water use map based on CLC 2006.

The visual inspection of the four maps reveals that all roughly follow the same patterns: The extensive irrigation systems of the Alto Aragón and Catalunya in the northern part of the basin are easily recognisable as well as the irrigated areas along the main coarse of the Ebro River and the rice production in the Delta region. Due to the fine resolution of 1 ha of the underlying data the water use map produced for the purpose of this study is the one best capturing the fine patterns. It therefore gets closest to the irrigation density map from the CHE. Besides, by applying less water to *complex cultivation* pixels, it is possible to capture differences in the irrigation intensity following the range of the CHE reference map. Nevertheless, the consideration of *complex cultivation patterns* increases the total irrigated area compared to the reference, especially in the southern part and the Northwest of the basin, adding areas that are not irrigated according to the reference map. The same happens for the GMIA at approximately the same locations. The comparison with this map reveals that it is mainly about areas with only small shares of irrigation, at maximum 20% of the area, many even below 5%. This is in line with the absolute values of the here presented results, which attribute only small values below 250 mm/year to these pixels. But whom to trust here? Is the reference missing parts of the irrigated areas? The irrigation density map from the CHE probably captures the large irrigation systems, while it does not consider scattered small scale irrigation.

At the same time, there is one particular patch visible in the reference map but not captured by the water use maps derived from CLC data, see rectangle A, the irrigated area around the city of Vitoria-Gasteiz mentioned already several times. While newer CLC maps do identify this area as being irrigated, older versions like the ones used in this study do not. Neither the GIAM, which is based on remote sensing as the CLC datasets, does. The reason could be that in this part of the basin, where the annual precipitation is still relatively high (the long-term mean annual sum is 749 mm for the period 1981-2010 (AEMET 2020a)), irrigation is only taking place sporadically and at a lower intensity, maybe not captured by the remote sensing acquisitions underlying the CLC maps and the GIAM. In fact, the RBMP 2015-2021 characterises the whole exploitation unit 17 as humid according to the UNESCO humidity index while the central Ebro valley hosting the large irrigation systems is classified as semi-arid (CHE 2015). Besides, it could be that irrigation is being applied more often in the last years due to climate change or a cultivation shift to other crop types, even if the equipment is in place already at least since 2004, as the reference dataset suggests.

Regarding the absolute amounts applied per pixel, the highest values of 1261 mm are applied in the delta region where rice cultivation plays a major role. This is in line with GARCÍA-RUIZ et al. (2011) which state that rice consumes up to 1000 mm in one summer. According to NOGUÉS & HERRERO (2003), the net water requirement of rice in a small study area in the Ebro river basin may be even as high as 1590 mm. The range of values also fits to the water demand calculations carried out by BOITHIAS et al. (2014) which reach values of 500 to over 1000 mm in the intensively irrigated areas of the Alto Aragón. A further source to compare is the map of mean annual net irrigation requirement by SCHALDACH et al. (2012). Here, large parts of the intensively irrigated areas in the Ebro are assumed to need between 50-250 mm per year, some areas also more than 250 mm. Since SCHALDACH et al. (2012) focus on the net requirements rather than on the gross demand, which is the case for the present study, their values have to be lower by definition. In the modelled water use map for the present, the large irrigation systems excluding the delta all lie between 700 to 1000 mm, see colour scheme in figure 7.18. The mean of all irrigated pixels is 552 mm.

According to the new RBMP 2021-2027, the average water provision is 7953 m^3/ha, which is equal to 795,3 mm (CHE 2018). Considering that small scale agriculture is not considered in the plan, the comparison of these values shows that the range of the newly derived water use map is in line with other sources.

Urban water demand
The availability of urban, domestic or industrial water use maps is considerably smaller than the one for agricultural ones. The JRC provides European water abstraction maps for different sectors for 2006 and 2030. The domestic and industrial abstractions for the year 2006 are confronted in figure 7.19 to the urban water use map, which is the sum of domestic and industrial, for the reference period.

The most striking difference is the wide-spread distribution of water uses in the JRC maps, especially regarding domestic uses, compared to the results of this study where the demand is concentrated in some points. Obviously, the JRC estimations also take into account small scattered settlements while the derived map only considers agglomerations large enough to be represented by a 1 km x 1 km pixel. All the larger urban areas can be appreciated also in the domestic JRC and the here presented urban water use map, while they are less pronounced in the industrial JRC map. This is in line with the RBMP where the purely urban demand (which includes industries supplied by urban supply networks, though) is higher than the industrial demand in all exploitation units. In terms of the whole Ebro basin, the total demand for the year 2010 is 359 hm^3 and 147 hm^3 for urban and industrial demand, respectively (CHE 2013, Annex III).

Regarding the absolute values, the range in all three maps is similar. For the JRC maps, Pamplona, the eastern agglomeration located close to the northern border of the basin, consumes most with approx. 1160 mm/year when domestic and industrial uses are summed up. For the map based on the CLC 2006 data, the maximum values are found in Zaragoza with 1068 mm/year apart from a few scattered pixels to the east of the city. The high values of these pixels are caused by the method for deriving water use maps per se. The exploitation unit they are located in, unit 13, reports a relatively high water demand in the RBMP compared to the amount of urban pixels resulting in an high application per pixel. Vitoria-Gasteiz, the westerly city visible close to the northern catchment border, reaches values around 690 mm/year and Pamplona lies around 787 mm/year. The mean consumption per pixel over the whole study area is 662 mm.

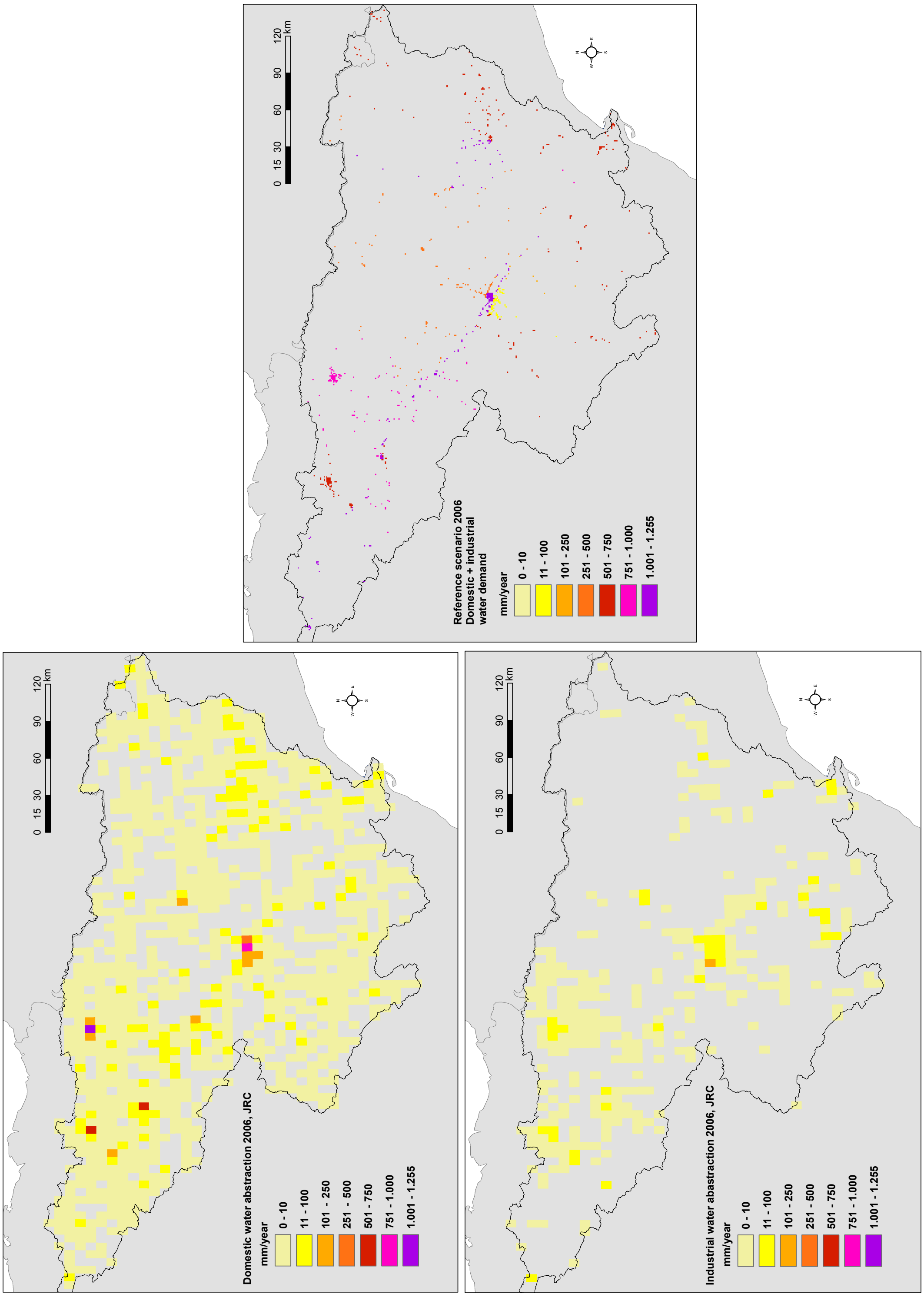

FIGURE 7.19: Comparison of various urban water use maps for the reference period. Lower left: JRC domestic water abstraction 2006, lower right: JRC industrial water abstraction 2006, top: Urban (domestic + industrial) water use map based on CLC 2006.

7.5.3 Assessment of Future Scenario Results

The future is uncertain, so no need to say that scenario simulations cannot be validated. Nevertheless, the MYOPIC scenario is used to specify the current CHE plans and therefore follows approximately the indications in the RBMP 2015-2021 which is the reason the MYOPIC simulation results for 2050 were contrasted with the estimations from that plan.

Irrigated Area
With regards to the irrigated area, the various versions of the RBMP do not report numbers per exploitation unit, they merely provide estimations of the increase for the whole Ebro basin or plans to expand the area in each autonomous community, which do, however, not coincide with the exploitation units. Since the actual irrigated reference area differs according to the source of information, also the total future area varies significantly: The older RBMP 2015-2021 is the first one to mention the long-term irrigation plans of the autonomous communities, without specifying any time horizon, displayed in figure 5.3 which sum up to additional 4567 km^2. Added to the 9657 km^2 considered above for the reference scenario, this means a future irrigable area of 14224 km^2, and consequently an increase of approx. 47% (CHE 2013, Annex III). As mentioned earlier, the environmental organisation FEDERACIÓ ECOLOGISTES EN ACCIÓ DE CATALUNYA (2012) mentions very similar number, 14100 km^2. This very high value has to be interpreted as the absolute maximum of potentially irrigable area. More representative for the actually irrigated area is the sum of 7000 km^2 estimated for the present in the RBMP 2015-2021 with half of the long-term plans, i.e. 2284 km^2, to take into account the simultaneous abandonment of unprofitable irrigated farmland and large annual differences as done in the newest RBMP 2021-2027, resulting in 9284 km^2. This latest version of the RBMP is more prudent and estimates the actually irrigated area at 8316 km^2 for 2033 considering the development of irrigated area taken place between 2008 and 2016 (CHE 2018). The total irrigated area modelled with iCLUE for the MYOPIC scenario 2050 summing *permanently irrigated land*, *fruit trees & olives* and 20% *complex cultivation patterns* is 12960 km^2. This clearly overestimates the last estimations by the CHE, however, still lies noticeably below the maximum value including the long-term plans from the former RBMP. As the estimations of agricultural water demands reported in this document refer to the already high value of 9657 km^2 irrigable around the year 2010, it is consistent to consider the totality of additional 4567 km^2 as reference.

TABLE 7.4: Agricultural water demand [hm^3] per exploitation unit according to the RBMP for approx. the year 2010 and 2033 (CHE 2013, Annex III) and values for the MYOPIC scenario 2050.

Exploitation unit	Water demand RBMP 2010	Water demand RBMP 2033	Water demand MYOPIC 2050	Difference [%]
1	737.4	821.1	849.1	3.4
2	110.7	161.3	188.6	16.9
3	65.6	99.8	60.6	-39.3
4	260.5	301.4	393.3	30.5
5	372.8	410.2	489.2	19.3
6	24.8	24.8	36.0	44.9
7	36.7	49.7	56.2	13.2
8	53.6	53.6	80.3	49.9
9	156.8	193.1	239.1	23.8
10	58.2	59.1	69.3	17.3
11	1194.6	1559.4	1412.7	-9.4
12	923.5	1292.0	1127.6	-12.7
13	999.9	1136.3	1386.7	22.0
14	1564.6	1991.7	1839.3	-7.7
15	883.8	1037.4	950.3	-8.4
16	151.6	490.7	224.8	-54.2
17	85.5	95.0	213.3	124.5
18	0	0.0	0	0
Total	**7680.6**	**9776.5**	**9616.4**	**-1.6**

Water demand
With regards to the future water demand, the RBMP 2015-2021 (CHE 2013, Annex III) provides estimations at exploitation unit level reproduced in table 7.4 for agricultural uses and in table 7.5 for urban and industrial uses together which were confronted to the results from the derived water use maps for 2050. Unlike the specifications for irrigated area, the time horizon for the water demand estimations in the RBMP is clearly defined at 2033. This time lag of 17 years has to be taken into account when interpreting the data.
The differences between RBMP estimations and own simulation results can vary substantially for individual units. The largest deviation for the agricultural water demand is registered, again, for exploitation unit 17 where the water use maps simulate more than twice the amount estimated by the CHE, 124.5% compared to the RBMP. If only the sum over the whole catchment is considered, the difference is merely -1.6%, the simulated total agricultural water demand for 2050 being slightly lower than the estimation for 2033 reported in the RBMP 2015-2021. The simulation is therefore quite close to the reference, especially taking into account that the total irrigated area is supposed to keep growing in the MYOPIC scenario also after 2033 by another 4.3%. The new RBMP 2021-2027 states that implementing the long-term irrigation plans mentioned above would mean an additional water demand of 2096 hm^3 per year without specifying a time horizon (CHE 2018). In another section of the document they estimate the total water demand for the year 2027 at 10626 hm^3. This gets very close to and lies even above the simulated total water demand in the MYOPIC scenario for 2050, more then 20 years ahead, which lies at 10424 hm^3 for the year 2050 summing both agricultural and urban demands.

The situation for urban demand simulations is similar, see table 7.5: At basin scale, the difference between RBMP estimations and own simulations is only -5%. Also here, the water use maps underestimate the values provided by the CHE. The regional differences, however, may sum up to 194.2% as it is the case for exploitation unit 8. Also for unit 9 the deviation lies above 150%. iCLUE locates many isolated urban pixels in this area for 2050 while the CLC 2006 shows only very few causing the demand to increase more than expected. In case of unit 10, the Matarraña subbasin, the urban area increases from 2 pixels in 2006 vs. up to 7 pixels in 2050 depending on the iCLUE run. For unit 8, the Martía subbasin, the difference is 7 to approx. 48 pixels, i.e. 48 km^2. At the same time, the unexpected urban sprawl modelled by iCLUE in exploitation unit 14, the subbasins of the Gállego and Cinca, around the municipalities of Jaca and Sabiñánigo mentioned in chapter 7.4, do not cause such a large difference, only 33.2% above the estimations in the RBMP. Since unit 14 is quite large, their influence on the urban water demand of this unit might be less pronounced. Finally, it has to be mentioned that not knowing the assumptions made by the CHE to estimate the individual demands an in-depth analysis of the differences is not possible.

TABLE 7.5: Urban water demand [hm^3] per exploitation unit according to the RBMP for approx. the year 2010 and 2033 (CHE 2013, Annex III) and values for the MYOPIC scenario 2050.

Exploitation unit	**Water demand RBMP 2010**	**Water demand RBMP 2033**	**Water demand MYOPIC 2050**	**Difference [%]**
1	141.1	254.7	162.6	-36.2
2	10.8	16.4	17.6	7.5
3	29.5	49.6	6.5	-86.9
4	22.4	35.3	62.2	76.2
5	21.0	32.2	46.9	45.8
6	0.9	1.5	0.4	-73.2
7	1.3	2.0	1.7	-14.6
8	4.8	9.5	27.8	194.2
9	8.2	10.7	27.3	155.1
10	2.0	2.5	4.2	65.4
11	26.1	41.9	35.1	-16.1
12	37.2	56.1	61.5	9.7
13	42.6	64.8	58.6	-9.6
14	31.9	57.1	76.0	33.2
15	14.7	23.1	30.5	32.0
16	70.9	123.9	126.5	2.1
17	39.4	66.4	60.0	-9.6
18	1.3	2.0	1.7	-13.7
Total	**506.2**	**849.5**	**807.1**	**-5.0**

7.6 Random Factor vs. Climate Sensitivity

VAN VLIET et al. (2016) state that sensitivity analysis should be part of the assessment process applied to land use models. In this case, the most interesting question is how the use of climate data originating from different GCM-RCM-combinations affects the land use simulation results and, in this specific case, the final water use maps. At

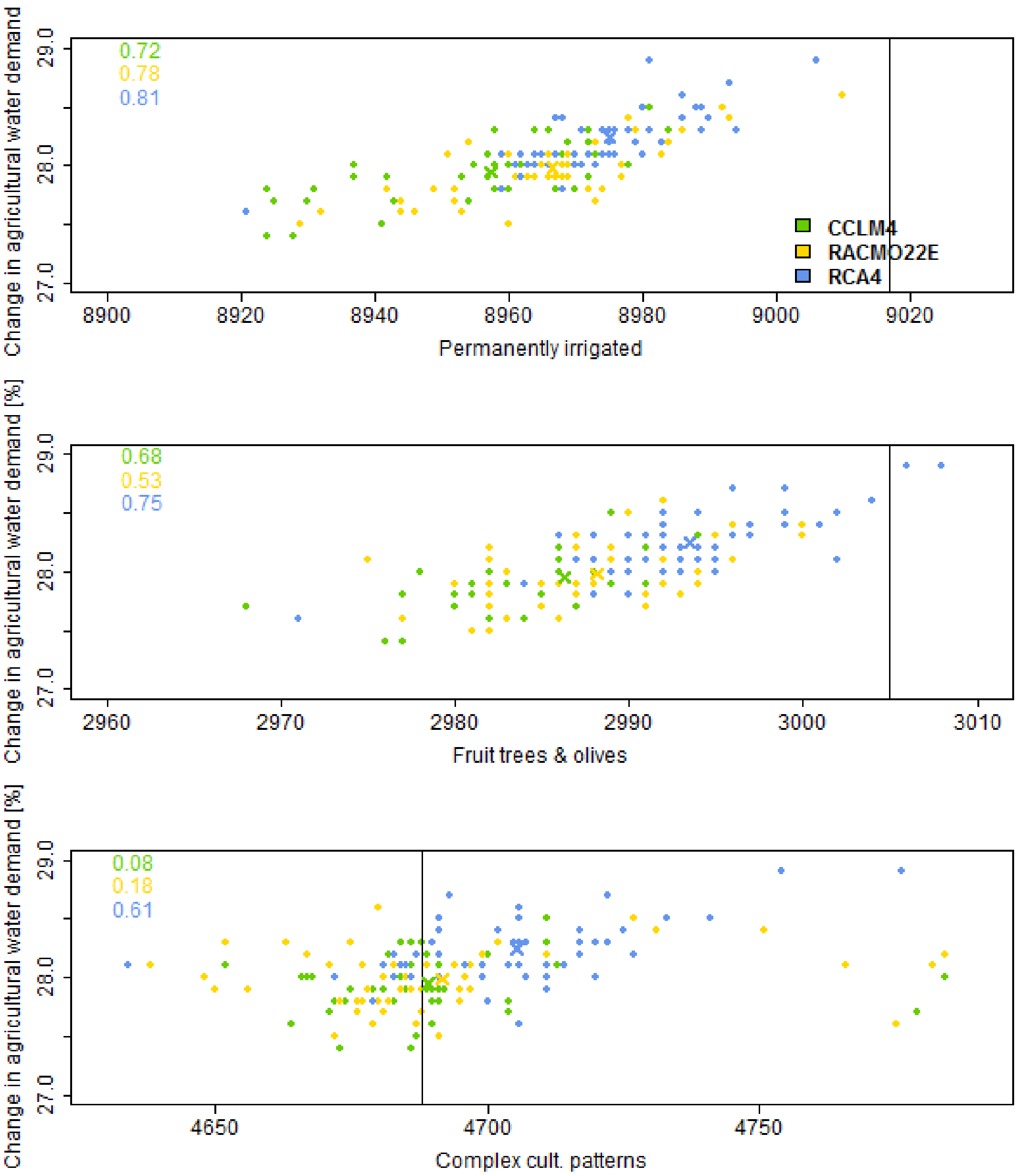

FIGURE 7.20: Changes of the agricultural water demand vs. the total number of pixels of three land use classes for the MYOPIC scenario. The colours represent the iCLUE model runs carried out with different climate inputs. The black line marks the pixel target.

the same time, iCLUE simulations are influenced by a random factor. Its effect on the model results was compared to the climate sensitivity of iCLUE.

As mentioned previously, iCLUE distributes land uses slightly differently for each model run due to the the randomness inherent in the model. Besides, also the number of pixels of a land use class fluctuates around the target value within the allowed deviation range. Both phenomena affect the final water use maps as the total calculated water demand changes depending on the amount of water consuming pixels and, not to be neglected, their location. If more irrigated pixels are simulated in an exploitation unit with high water application rates, they contribute stronger to the overall water demand. The random factor of iCLUE causes the point clouds displayed in figures

7.20 to 7.23 where the amount of pixels in each water consuming class was plotted against the changes either in the agricultural or urban water demand in the future for 150 model runs. As a consequence, the change of the agricultural water demand in the MYOPIC scenario with respect to the reference scenario varies from 27.4 to 29.2%. For urban uses the future increase lies between 56.3 and 63.7%. This results in a 29.4 to 31% increase of the total water demand in the Ebro, whereas the target value is 30%. For the SUSTAINABLE scenario, the changes are a reduction of -34.3 to -32.3% of the agricultural water demand, an 16.3 to 21.7% increase of the urban demand and, finally, a shrinkage of -29.2 to -31% of the overall water demand (target: -30%). These deviations capture the impact of iCLUE's randomness on subsequent processing steps, but may also be caused to some extent by the sensitivity to the climate input as discussed later. The effect, however, is small and certainly negligible compared to the great number of sources of uncertainty in the modelling chain and assumptions made.

Figures 7.20 and 7.21 further reveal that for some classes a correlation between the total amount of pixels and the total sectoral water demand exists. This is mainly the case for *permanently irrigated land*, followed by *fruit trees & olives*, in both scenarios: The more pixels, the higher the water demand increase or the smaller the decrease. The correlation coefficients displayed in the figures, each colour indicating one of the six scenarios (MYOPIC or SUSTAINABLE combined with climate data from one of the three GCM-RCM-combinations), confirm this. For *permanently irrigated land*, the three MYOPIC model setups reach correlation coefficients above 0.72, two out of the SUSTAINABLE scenarios even above 0.89, the third one is 0.69. The relationship is less strong for *complex cultivation patterns* independently of the scenario. The reason for it could be that this class has only a reduced influence on the agricultural water demand as the water applied to these pixels is only 20% compared to the other two agricultural classes.

For the MYOPIC scenario, also the correlation between increase in urban water demand, see figure 7.22, and *sealed area* is relatively high (0.62, 0.68, 0.71), while the relationship is less pronounced for the SUSTAINABLE scenario. The existence of these correlations shows that the total water demand is clearly influenced by the number of water consuming pixels, while their location may have a subordinate effect. However, it is not possible to quantify the influence of each variable.

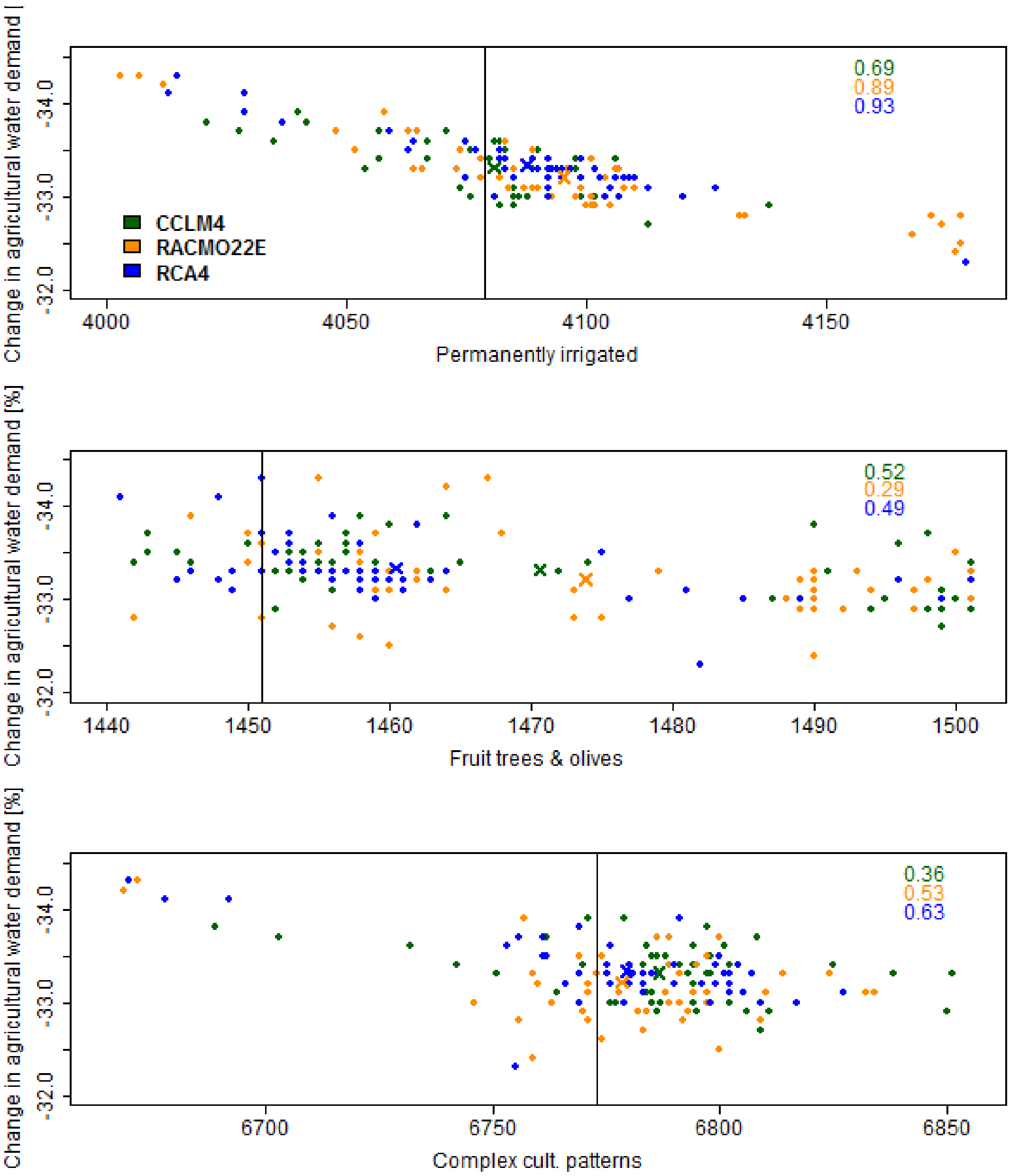

FIGURE 7.21: Changes of the agricultural water demand vs. the total number of pixels of three LU classes for the SUSTAINABLE scenario. The colours represent the iCLUE model runs carried out with different climate inputs. The black line marks the pixel target.

With respect to the targeted amount of pixels passed to iCLUE represented in figures 7.20 to 7.23 by a black line, the value for *permanently irrigated land* and *fruit trees & olives* in the MYOPIC scenario is nearly always smaller than the target. The value varies only to one side of the allowed deviation range. This could indicate that iCLUE has difficulties allocating so many irrigated pixels. The total probability of other land use classes might be higher for many locations which is the reason irrigated pixels are overruled. Direct comparisons of the simulated amount of pixels of *permanently irrigated land* and *fruit trees & olives* with land use classes which tend to be overrepresented by the model, see figure 7.11, did not reveal any direct connection. This means, that there is no specific land use class gaining from the under-representation of the

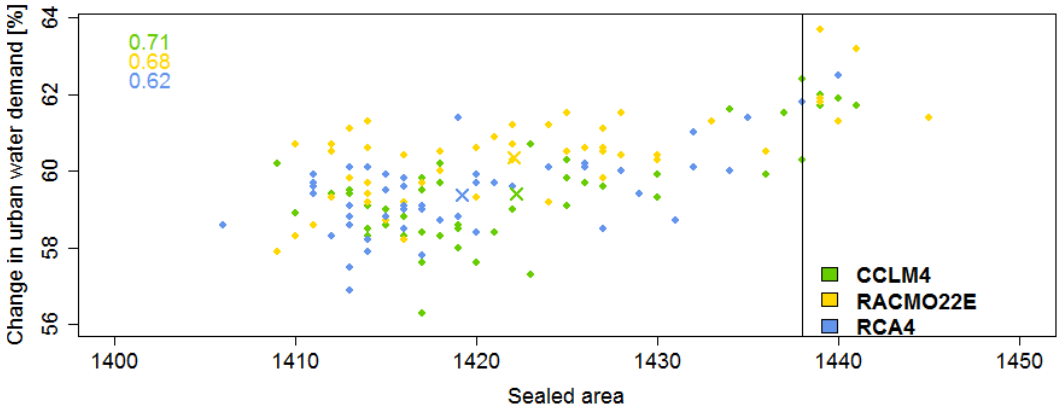

FIGURE 7.22: Changes of the urban water demand vs. the total number of urban pixels for the MYOPIC scenario.

irrigated classes, but that the gain might be distributed across all land uses.
The systematic under-representation does not apply to *complex cultivation patterns* in the MYOPIC scenario or any of the three irrigated classes in the SUSTAINABLE scenario, see figure 7.21, where the pixel sums fluctuate to both sides of the target or even over-represent them. Neither it is the case for *sealed area* in the SUSTAINABLE scenario, where the value to be achieved is both over- and under-estimated. In the MYOPIC scenario, *sealed area* is mainly under-represented. As for the irrigated classes, the cause could be the fast and strong growth of these classes in the MYOPIC scenario resulting in a strong competition for land with other land use classes. The SUSTAINABLE scenario, in contrast, foresees a reduction of *permanently irrigated land* and *fruit trees & olives* which leads to the opposite effect where both classes are mainly overestimated, especially the second one. As regards *complex cultivation patterns* in the SUSTAINABLE scenario, most runs allocate more pixels than the target value, even it experiences a slight increase of 10% between 2017 and 2050. The total probability for allocating this class seems to be high and higher than for other classes.

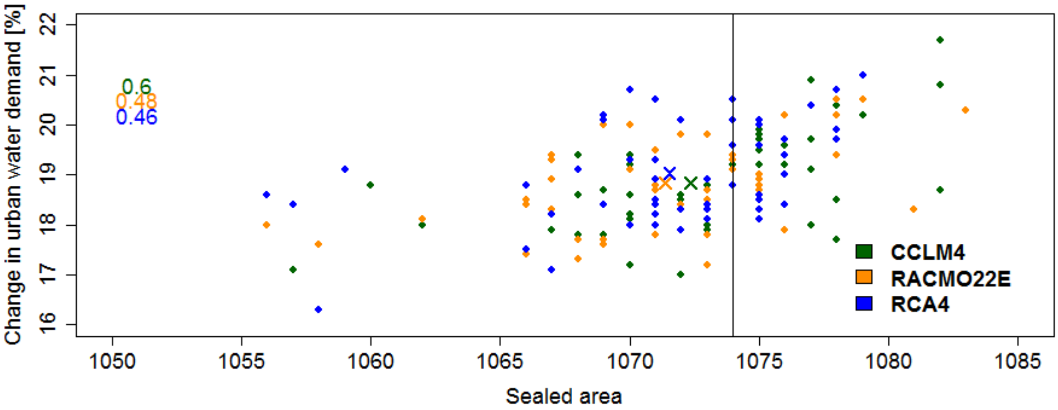

FIGURE 7.23: Changes of the urban water demand vs. the total number of urban pixels for the SUSTAINABLE scenario.

Finally, emphasising the climate sensitivity of iCLUE, how does the use of different climate inputs influence the land use simulations and consequently the water use maps? To answer this question, the model was run 50 times for each of the six scenarios and climate data combinations resulting in 300 independent model runs. In figures 7.20 to 7.23 they are coloured according to their combination. Besides, the diagrams include crosses indicating the spatial centre of the point cloud of each combination. For the irrigated classes in the MYOPIC scenario, see figure 7.20, there is a small but clear trend: Runs using the RCA4 climate data simulate larger amount of pixels for the three classes and consequently, due to the correlation analysed above, also a slightly stronger increase of the agricultural water demand. The lowest mean values for both variables are obtained by running iCLUE with the CCLM4 combination. At close look, it can be appreciated that the CCLM4 and RCA4 runs have only little overlap while the RACMO22E runs cover a wider range. For this particular case, the average values for water demand and pixel sums of the three climate scenarios are ordered like the density distributions in figure 7.3: RCA4 will reach highest values for the mean annual temperature, followed by RACMO22E and finally CCLM4. Although one could be tented to say "the hotter it gets, the more irrigation is allocated", this deduction cannot be made since there is no casual link between the climate data and the land use distribution but only a statistical one. No trend is visible for *sealed area* in the MYOPIC scenario (figure 7.22). Runs with RACMO22E data reach highest urban demand values. In addition, no trend at all can be appreciated neither for the irrigated nor urban pixels in the SUSTAINABLE scenario, see figures 7.21 and 7.23.

Even the casual connection is missing, one could argue that in a MYOPIC scenario, where climate changes are more pronounced, the altered temperature and precipitation values of the input drivers have a stronger impact on the suitability of a land use for a certain location than in the SUSTAINABLE scenario. Besides, the distribution of *sealed area* may be explained rather by drivers like distance to cities and roads than climate variables and consequently changes in the latter ones affect them less.

To sum up, both the random factor as well as the different climate datasets have an effect on the land use and water use maps. A weak relation between climate model and number of pixels/total water demand can be deduced for the MYOPIC scenario. However, the resulting absolute differences in the sectoral and total water demand are so small that they can be neglected as it is the case for the random factor discussed above. It can be concluded that the resulting water use maps are robust and nearly neither affected by differences in each individual iCLUE model run nor noticeably sensible to the uncertainty inherent in climate model projections. To confirm this, the MYOPIC scenario was run also 20 times using RCP 4.5 as climate input. The results did not show any susbtantial difference to the entirely myopic runs.

7.7 Water Use Scenarios for the Year 2050

The analysis in chapter 7.6 revealed that the differences between individual model runs and different climate inputs can be neglected considering the overall scenario uncertainty. For this reason, only results derived from one single iCLUE simulation driven with RCA4 climate data are discussed hereafter.

Agricultural Water Demand

Figures 7.24 and 7.25 show the final agricultural water use maps for the MYOPIC and SUSTAINABLE scenario. Their overall water demand modelled is approx. 10455 hm^3 and 5655 hm^3, respectively. As expected, the irrigated area is expanded in the MYOPIC scenario and also the applications per pixel are higher than in the other map. Compared to the reference scenario, see chapter 7.5.2, the maximum applications per pixel are 1135 mm for the MYOPIC and 1072 mm for the SUSTAINABLE scenario and therefore slightly below the maximum of the reference (1261 mm). This is obviously caused by the higher irrigation efficiency in both scenarios achieved by reducing the future water applications per pixel by the factors described in table 5.8. The mean values for all irrigated pixels are as follows: MYOPIC: 580 mm, SUSTAINABLE: 408 mm and reference: 552 mm. Even if the water use efficiency is applied to all pixels in both scenarios, the mean consumption per pixel rises in the MYOPIC scenario with respect to the reference since irrigation is intensified while small-scale agriculture is pushed back, characterised by a reduction of *complex cultivation patterns* in this scenario by -22.2% from 2006 to 2050. As mentioned earlier, the increasing water efficiency observed in the Ebro over the past years has not let to the same amount of water savings since the saved water is often used to increase the productivity per m^3 (CHE 2018). Meanwhile in a SUSTAINABLE world, not only the maximum consumption per pixel but also the average values are reduced by both improving the water efficiency and cultivating less water consumptive crops.

As mentioned earlier, by introducing the irrigation density map of the CHE as a driver iCLUE is able to allocate the already existing irrigated areas around the city of Vitoria-Gasteiz in the MYOPIC scenario and by this means "improves" the map and brings it closer to the inventory of present irrigation according to the CHE, see figure 5.3. Interestingly, this does not happen in the SUSTAINABLE one. A look into simulation results of earlier years shows that the model distributes a few irrigated pixels around Vitoria in both scenarios already before 2018, the year the deviation between the scenarios starts, but than does not add any new ones in the SUSTAINABLE scenario as there seem to be other more suitable regions that are sufficient to accommodate the demand for irrigated land. In general, the distribution of different consumption values in the latter scenario resembles the reference scenario more, see figure 7.18. The distribution is more heterogeneous due to large amounts of

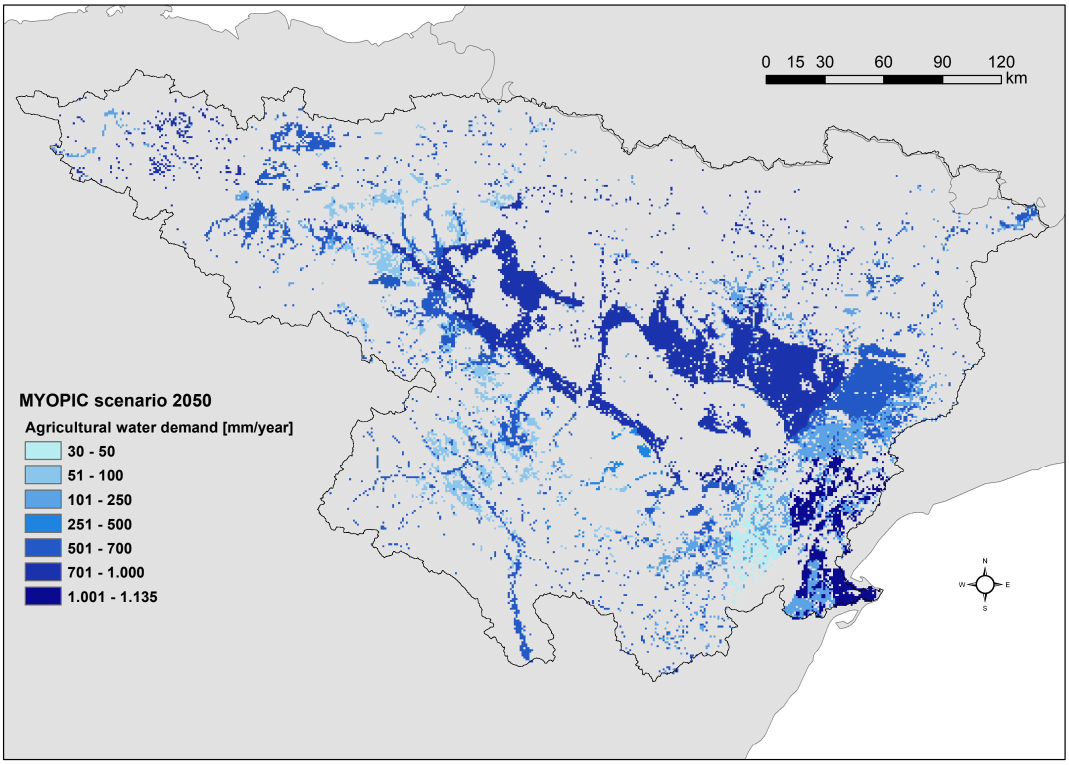

FIGURE 7.24: Derived agricultural water use map [mm/year] for the MYOPIC scenario, horizon 2050.

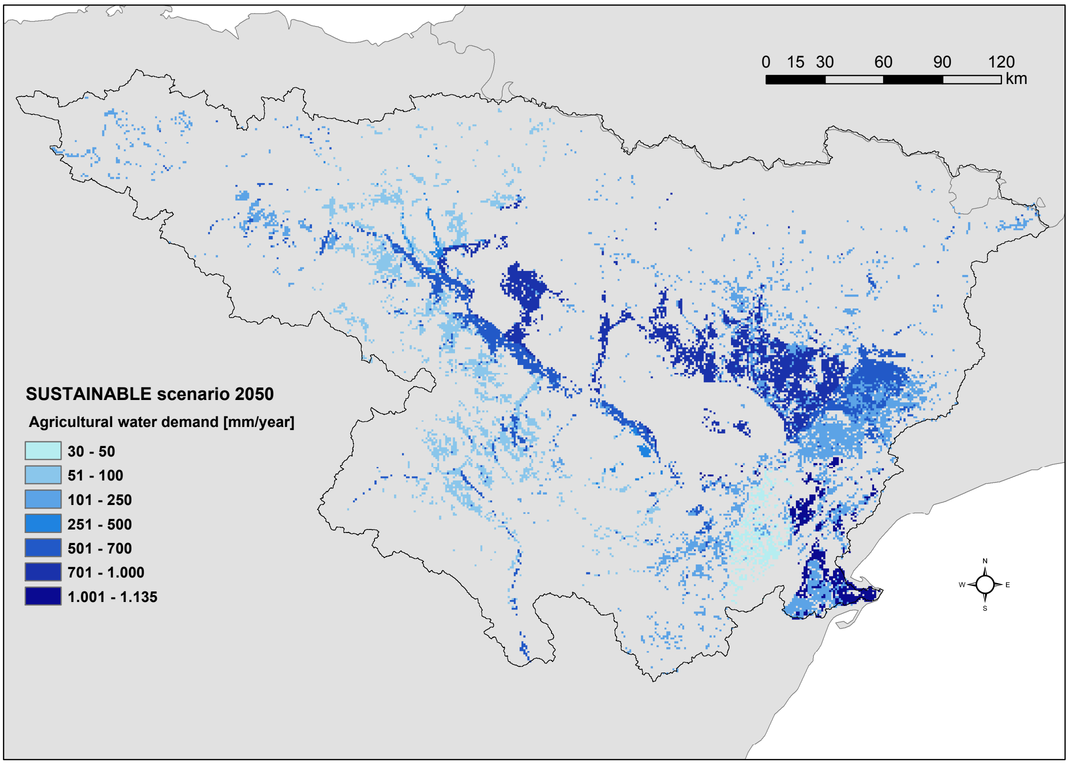

FIGURE 7.25: Derived agricultural water use map [mm/year] for the SUSTAINABLE scenario, horizon 2050.

complex cultivation patterns that need to be allocated and which receive only 20% of the water compared to the other pixels. In the MYOPIC scenario, the irrigation patches are more homogeneous, *complex cultivation patterns* pixels are obviously replaced by *permanently irrigated land* or *fruit trees & olives* and "wholes" are filled.

Urban Water Demand

The final urban water use maps are shown in figures 7.26 and 7.27. Compared to the reference urban water use map in figure 7.19, both the maximum and the average demand per pixel decreases as intended by the application of the factors in table 5.8. The highest values are still reached in exploitation unit 13, 1066 mm (MYOPIC) and 1023 mm (SUSTAINABLE). Due to the coarse modelling resolution, many small settlements do not appear in the land use map or are underestimated in size. In this particular unit, the urban agglomerations do not grow substantially in any of the scenarios so the total demand is still distributed to a small area. The mean urban water consumption in the SUSTAINABLE scenario is 558 mm, very close to the 569 mm in the MYOPIC scenario. The small difference is due to the fact that in the latter scenario urban areas grow also more in units with lower consumption values per pixel than in the SUSTAINABLE one, as it is the case for the noticeably growing towns Jaca and Sabiñánigo mentioned earlier with 382 mm.

As mentioned earlier, the city of Zaragoza in the central valley grows substantially more in the SUSTAINABLE scenario than in the MYOPIC one. In both scenarios, the area directly outside the city is used for irrigated agriculture. While the MYOPIC scenario sticks more to the patterns as in the 1990 initialisation map with a small urban nucleus and irrigation around it, the city has grown in the SUSTAINABLE scenario but still being surrounded by irrigation. It seems that the pressure for allocating irrigated pixels is so high in the MYOPIC scenario that they are distributed to areas also suitable for urban uses, as the SUSTAINABLE map shows.

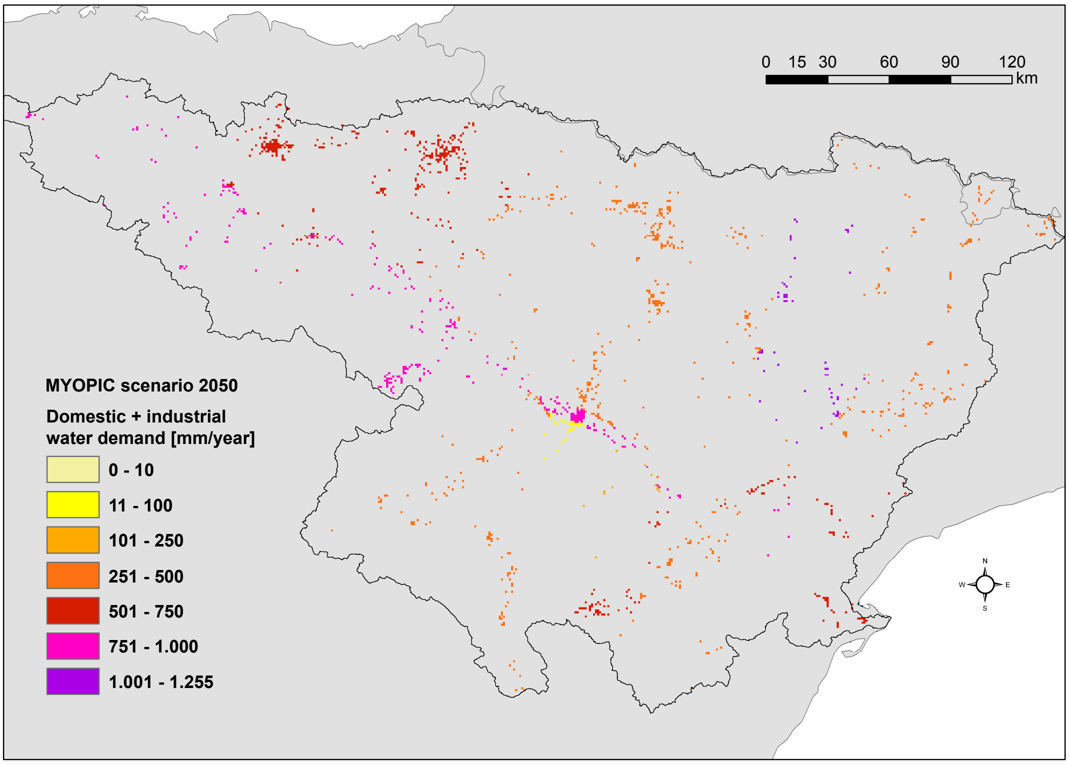

FIGURE 7.26: Derived urban water use map [mm/year] for the MYOPIC scenario, horizon 2050.

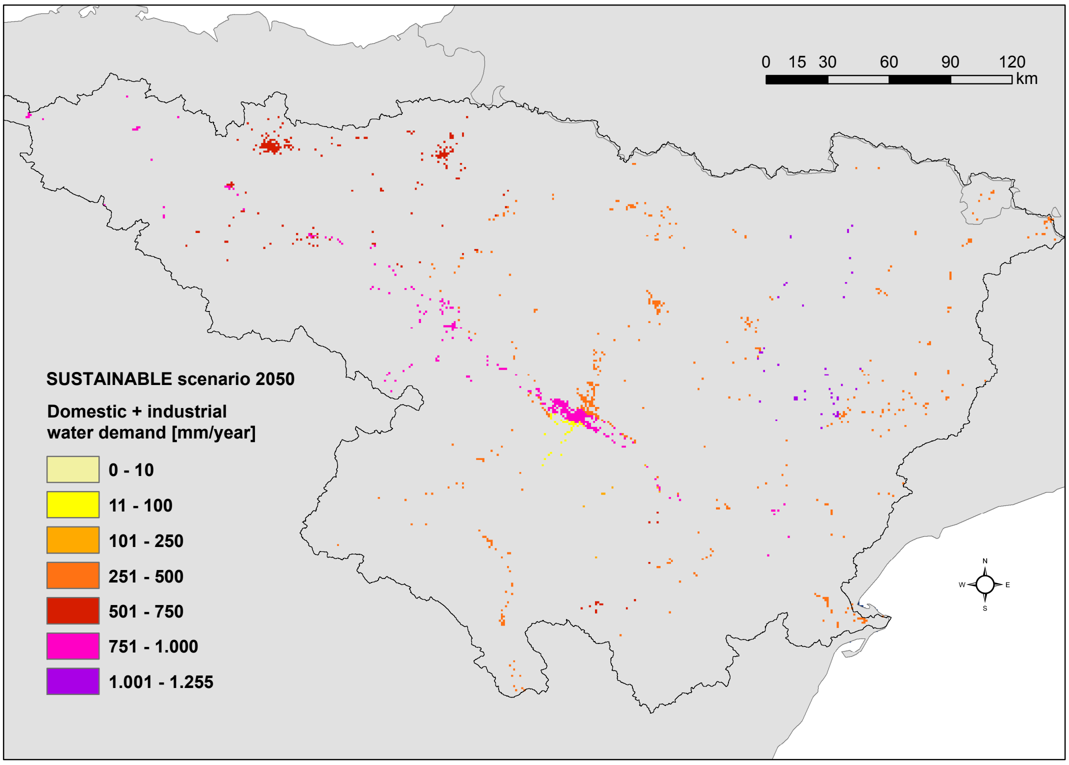

FIGURE 7.27: Derived urban water use map [mm/year] for the SUSTAINABLE scenario, horizon 2050.

Overall, there is more uncontrolled urban sprawl in the MYOPIC scenario, as one would expect for this kind of scenario, meaning that there are many more isolated urban pixels across the whole basin. This is particularly true for the area around the city of Pamplona, its shape is distinctly fuzzier in the MYOPIC scenario than in the SUSTAINABLE. As regards the absolute values, Pamplona reaches 669 mm per year in the MYOPIC scenario, Vitoria-Gasteiz 588 mm and the heart of Zaragoza 908 mm. The yellow areas adjacent to Zaragoza visible in all urban water use maps are located in another exploitation unit with a very low urban demand. However, since iCLUE allocates urban pixels of the periphery of Zaragoza to this unit, they have to adapt the mean value for this unit which is 12 mm. This is unrealistically low and could be overcome by using another spatial segmentation that does not split urban areas. The same happens at the northern part of the city for both scenarios.

7.8 Future Water Availability

The analysis of the iCLUE climate input in chapter 7.1 has shown that there is a clear trend towards warmer temperatures in both scenarios until 2050 over the Ebro catchment independently of the climate model combination while it is hard to make a statement about changes in annual precipitation sums. But what about variables representing the future water availability? And how is the situation for the climate reference period of GLOBAQUA, 2036-2065, where the RCPs start deviating more clearly at a global level? The Climate Moisture Index (CMI) and runoff for the future scenarios discussed hereafter were calculated for this time frame over the Ebro basin as part of the GLOBAQUA project.

7.8.1 Climate Moisture Index

The CMI for the reference period 1980-2010 in figure 7.28 makes clear that large parts of the Ebro basin have a negative CMI, meaning that the potential evapotranspiration is larger than the precipitation, already nowadays. This is mainly the case for the inner Ebro valley where the CMI adopts the lowest values between -0.8 and -0.6. These areas coincide with the intensively used agricultural areas. Meanwhile, the mountainous areas at the northern and western edges of the watershed have still positive CMI values being highest in the Pyrenees reaching values of up to 0.8 to 1. The mean value over the whole catchment is, however, -0.18 and therefore negative already for the reference scenario.

As it regards the future scenarios in figures 7.29 and 7.30, already from visual inspection it becomes clear that there is a shift towards more negative values, i.e. drier conditions, both for RCP 8.5 and RCP 4.5. The "wetter" regions bordering the catchment are reduced to a narrow edge and their values drop while the dry areas with CMI of -0.6 or below grow in the central valley. The differences between the two scenarios are, however, marginal. The spatial mean for the CMI of RCP 8.5 is -0.29 while it is -0.28 for RCP 4.5. One can conclude that both RCPs project a similar reduction in water availability over the Ebro for 2036-2065 compared to the reference scenario. It has to be noticed that the CMI was only calculated using data of the RCA4 GCM-RCM-combination, which according to GAMPE et al. (2016) is the "driest" climate model combination out of the three chosen for the GLOBAQUA project.

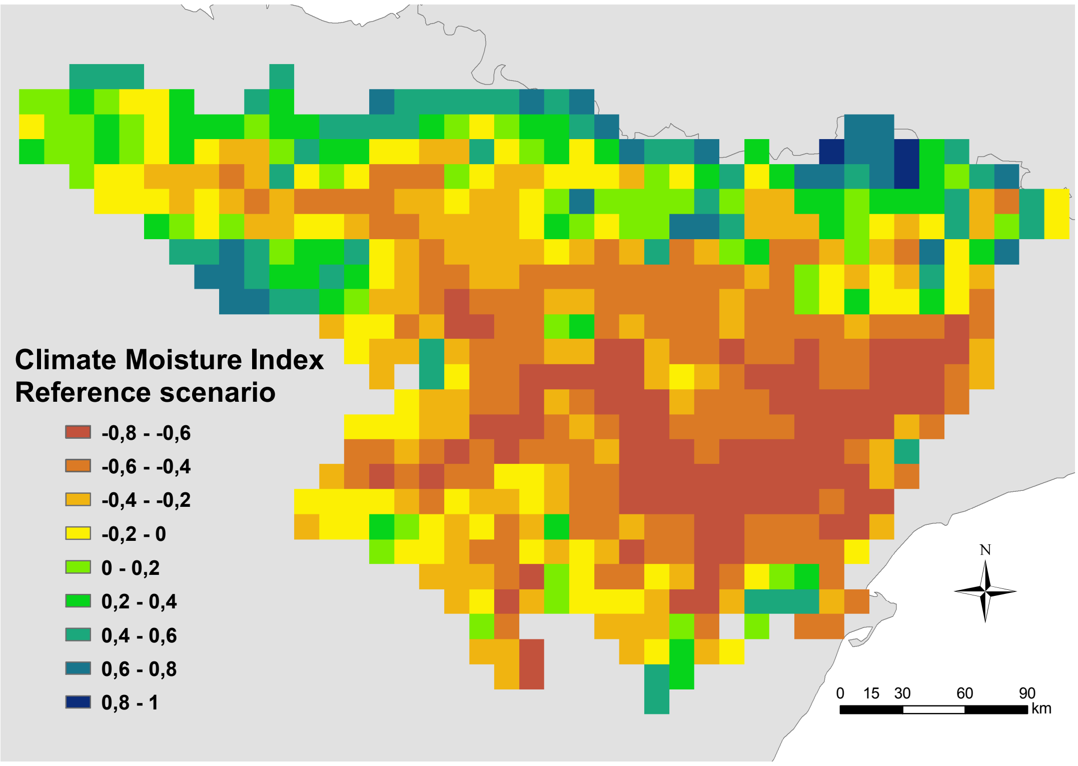

FIGURE 7.28: Climate Moisture Index calculated for the reference scenario, 1980-2010.

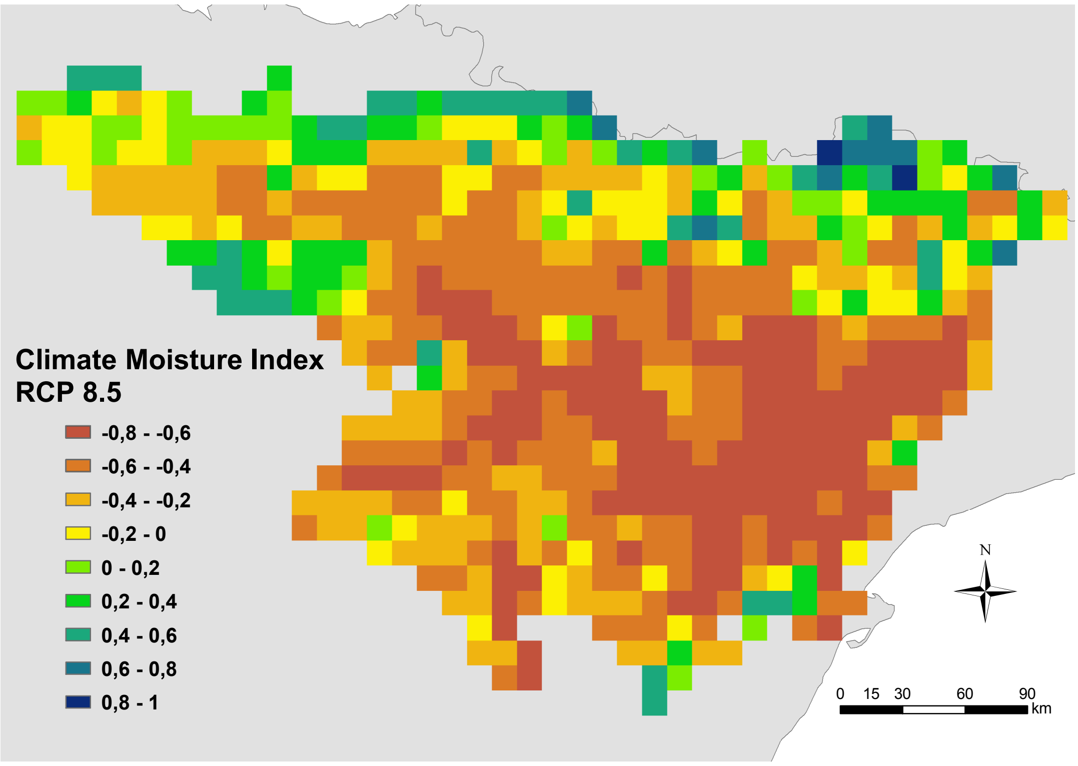

FIGURE 7.29: Climate Moisture Index calculated for RCP 8.5, 2036-2065.

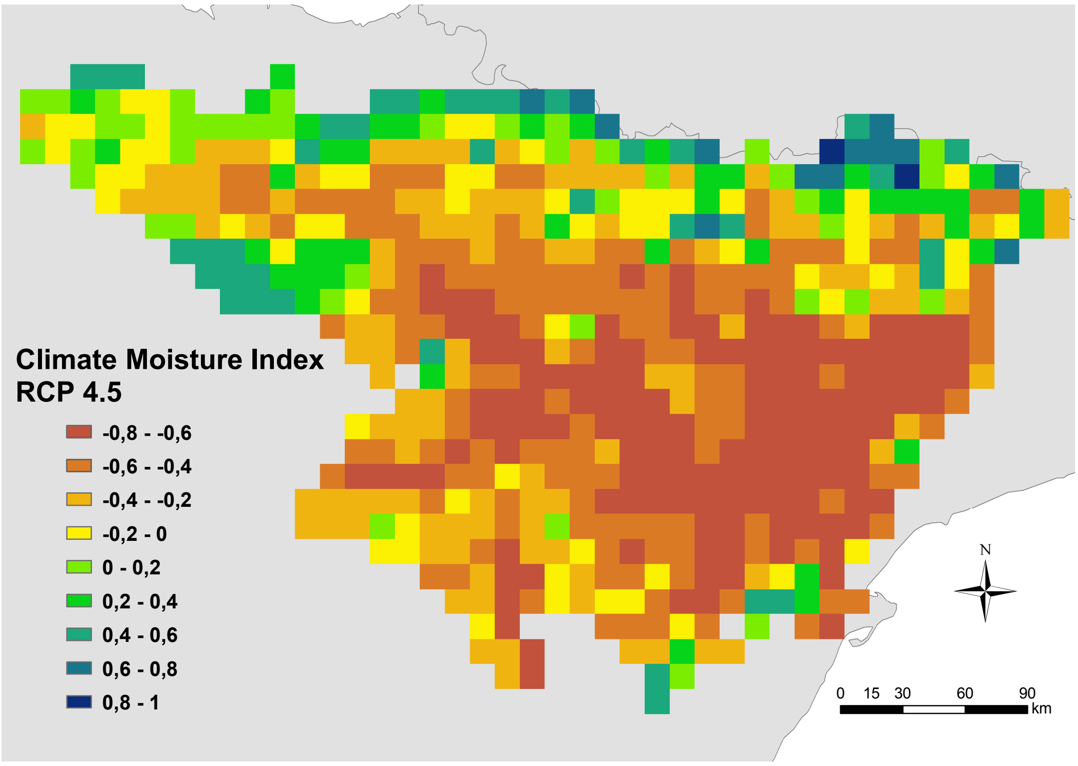

FIGURE 7.30: Climate Moisture Index calculated for RCP 4.5, 2036-2065.

7.8.2 Runoff Modelling

Also the runoff simulations carried out with the mHM model by the UFZ used RCA4 climate data and the land use maps for the MYOPIC and SUSTAINABLE scenario produced as part of the present thesis. No water management information was included in the model since it is supposed to represent the total natural runoff conditions in the Ebro. Consequently, neither reservoirs nor irrigation was considered.

The resulting changes in runoff between the reference and future scenarios in figures 7.31 and 7.32 show that in both cases the runoff will decrease in the largest part of the Ebro basin. This reduction is strongest in the mountainous areas decreasing by more than 300 mm/year on average. Since the largest part of precipitation occurs in the mountains and in particular the Pyrenees (CHE 2015) and they therefore constitute the areas producing most runoff, these are also the areas were the largest absolute runoff reductions can take place. The decrease in mountain areas is more pronounced in the MYOPIC scenario than in the SUSTAINABLE one. Regarding the lowlands of the Ebro, the runoff will remain more or less constant, between -49 to +50 mm/years on average, in both scenarios. There is a larger coherent patch of runoff increase in the MYOPIC scenario, see figure 7.31, to the east of the catchment located in the lower coarse of the Segre River. As the headwaters of the Segre reach the highest elevations within the Ebro basin above 2500 m a.s.l., the runoff increase downstream could be connected to the expected shift from snow to liquid precipitation (CEDEX 2017) leading to more direct runoff and a reduced storage effect.

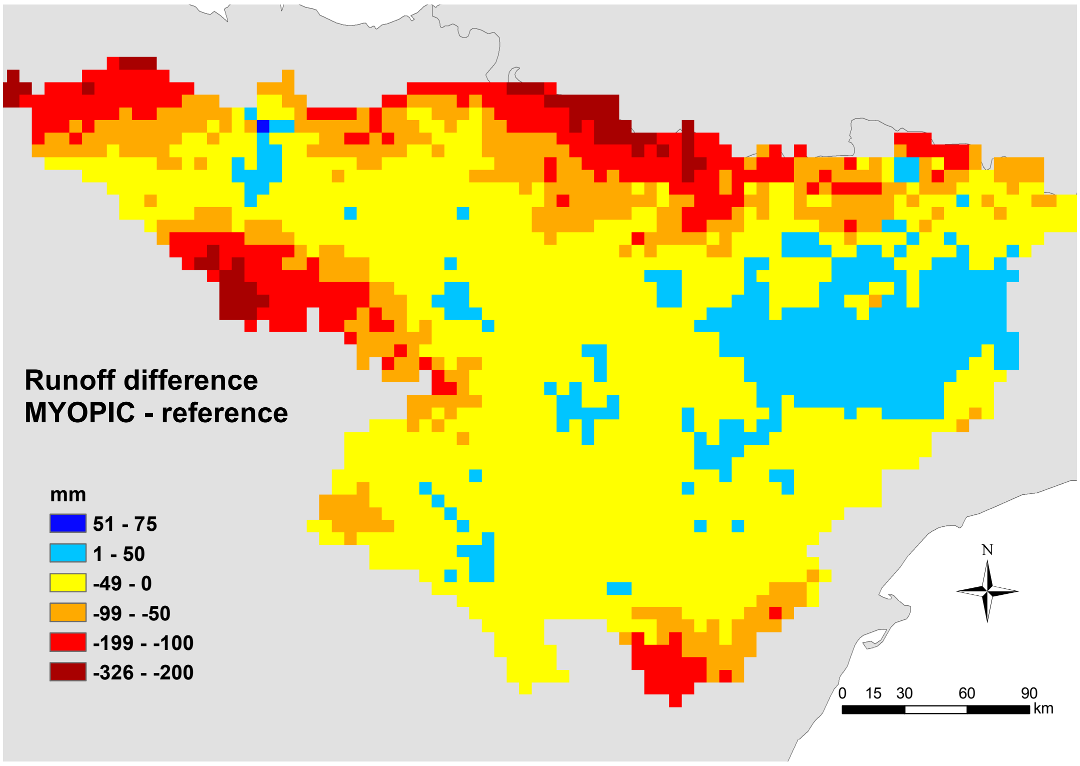

FIGURE 7.31: Runoff difference MYOPIC - reference modelled with the mHM model.

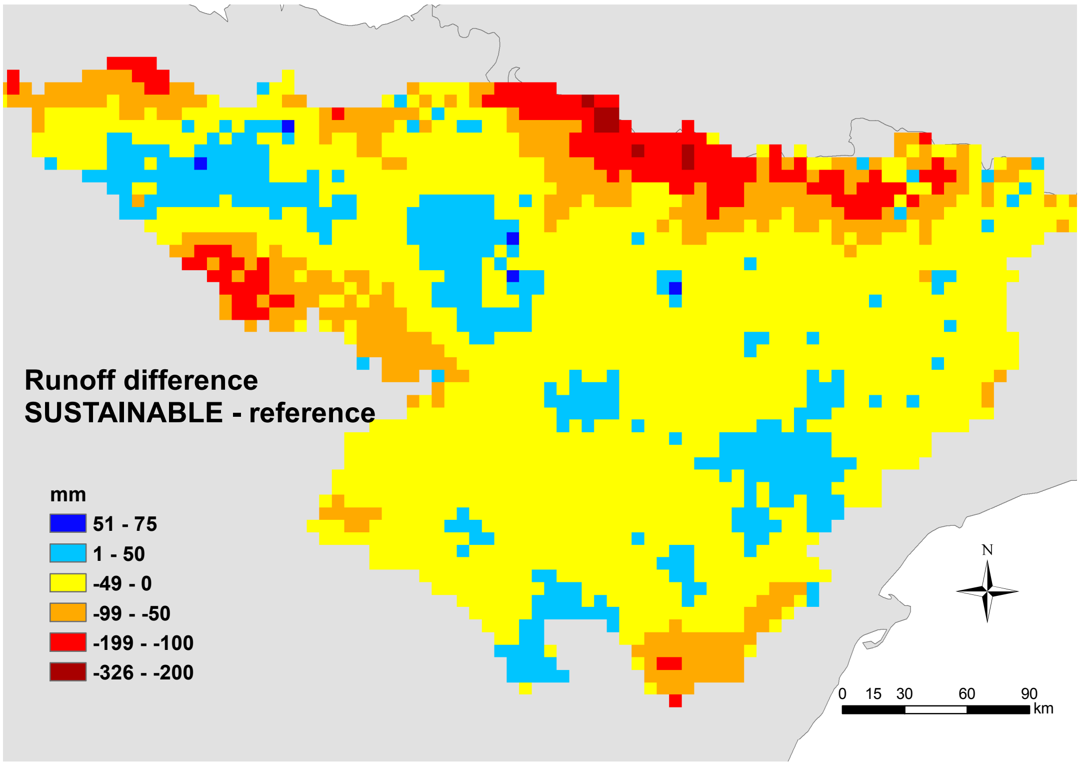

FIGURE 7.32: Runoff difference SUSTAINABLE - reference modelled with the mHM model

The mean difference in runoff over the whole Ebro basin is -39 mm/year in the MYOPIC and -28 in the SUSTAINABLE scenario. As expected, the reduction is slightly stronger in the MYOPIC scenario even if the values lie very close to each other. When looking at percentages, the runoff decreases in the MYOPIC scenario with respect to the reference by 20% and by 15% in the SUSTAINABLE scenario, which constitute substantial changes.

Chapter 8

Validation Experiment - Application to The Evrotas River Basin

In order to validate the methods proposed in this thesis, the procedure to derive consistent land and water use maps was applied also to the Evrotas River basin, Greece. Due to its limited extent, the modelling resolution for this case study is 100 m x 100 m compared to the 1 km x 1 km in case of the Ebro. In light of the low sensitivity of the iCLUE model to different climate data inputs observed for the Ebro, the Evrotas setup was only run with RCA4 climate data.

8.1 Results for the Evrotas River Basin

8.1.1 Change Detection Analysis

The change detection analysis was already described in HUBER GARCÍA et al. (2018): According to the reclassified CLC maps with only seven classes, there was nearly an absence of land use change in the Evrotas between 1990 and 2000 (0.5% of the total area). From 1990 to 2012 3.1% of the catchment area experienced change. The transformation of *coniferous forests* to *shrubs/semi-natural vegetation* accounts for the largest change (1.1% of the study area), see table 8.1. Also in case of the Evrotas, the differentiation between these two classes is difficult and classification differences between the CLC 2012 map and the prior ones may play a significant role, as it is the case for the Ebro. *Agriculture* gained 0.8% from *shrubs/semi-natural vegetation* but was in turn also transformed to it (0.5%). The urbanisation process proceeds slowly in the Evrotas characterised by a transformation of 0.1% of agricultural land to sealed area. In general, the visible land use changes are considered to be small and have only very limited influence on the water uses in the Evrotas.
Due to the coarse thematic resolution chosen for modelling with only seven land use classes, the change detection analysis for the Evrotas was also carried out with the original CLC classes (results not shown here). The total change for the same period sums up to 9%. This is the case as it includes transitions between very similar categories such as *sclerophyllous vegetation* and *transitional woodlands & shrubs* regrouped to the same class in the final map. Transitions between these categories do not influence the water use in the region and can be consequently neglected for the present study. Besides, it has to be noted that these two classes are those associated to large classification errors in the CLC datasets since their distinction is difficult (FERANEC et al. 2007).

TABLE 8.1: Results of the change detection analysis for the Evrotas between 1990 and 2012 in % of the total basin area.

1990 \ 2012	Sealed area	Agriculture	Shrubs/ semi-natural vegetation	Coniferous forest	Mixed & broadleaved forest	Permanently irrigated	Water
Sealed area	0.0	0.0	0.0	0.0	0.0	0.0	0.0
Agriculture	0.0	0.0	0.5	0.0	0.1	0.1	0.0
Shrubs/semi-nat. vegetation	0.1	0.8	0.0	0.1	0.0	0.0	0.0
Coniferous forest	0.0	0.0	1.1	0.0	0.0	0.0	0.0
Mixed & broadleaved forest	0.0	0.1	0.0	0.0	0.0	0.0	0.0
Permanently irrigated	0.1	0.0	0.0	0.0	0.0	0.0	0.0
Water	0.0	0.0	0.0	0.0	0.0	0.0	0.0

8.1.2 Calibration & Validation of the Land Use Simulations

The three-map-comparison of the Evrotas land use simulations reveals similarly good results as for the Ebro. For the calibration with CLC 2000 data more than 99.5% of the basin are modelled correctly as persistence (not shown here). This high value may be related to the general little change taking place in this case study. According to the results for the validation year 2012 presented in figure 8.1, 96% (95.9% persistence and 0.1% change) of the land uses in the catchment are modelled correctly. Only 0.1% of the area is transformed to the wrong class. 2.9% of the changes that actually happened between 1990 and 2012 - concentrated mainly in a few larger patches - are not captured. These patches could be related to large wild fires that occurred in the Evrotas basin during heat waves in 2007 (SKOULIKIDIS et al. 2011). The sudden land cover change between 2007 and 2008 in some of these areas is visible from optical satellite time series in the Google Earth Engine, which confirms this assumption. Such events may cause big areas of land to change within a very short time frame and at unpredictable locations, which constitute changes that cannot be captured by a land use change model (HUBER GARCÍA et al. 2018). Overall, the land use modelling results for the Evrotas are satisfying.

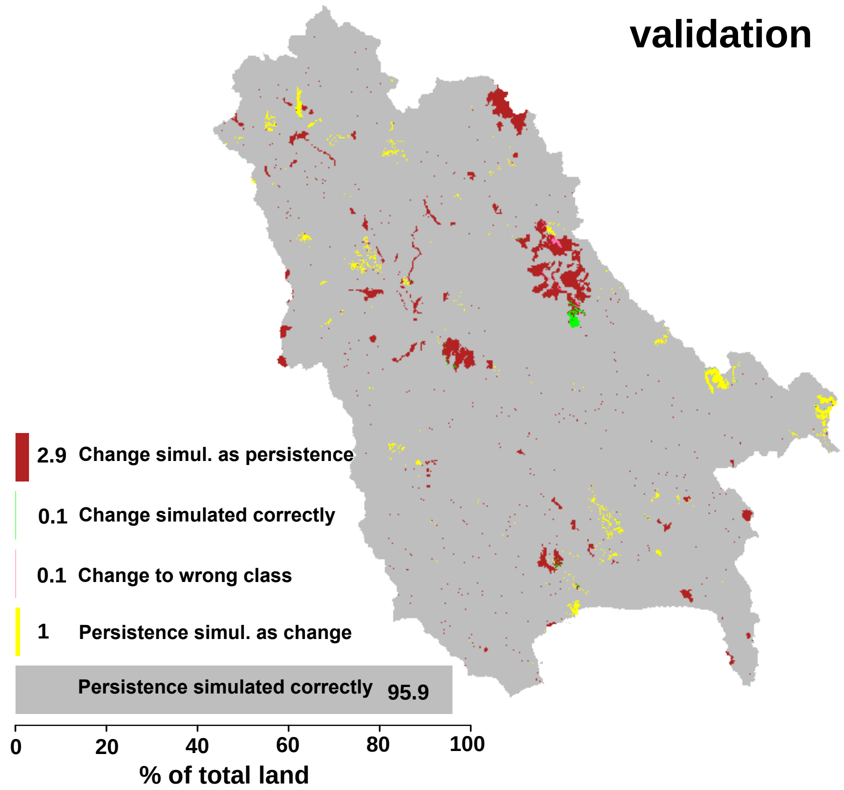

FIGURE 8.1: Validation results of the iCLUE model for the Evrotas setup 2012.

8.1.3 Land Use Scenarios for the Year 2050

The land use map for the reference period (CLC 2000) and the two scenarios are displayed in figure 8.2. At first glance the future land use maps seem identical and also differences to the CLC 2000 map are hard to detect. There is an increase of semi-natural shrubs in both scenarios with respect to the reference. As for forested areas, they decrease in the MYOPIC while they increase in the SUSTAINABLE one. The implementation of riparian forests below 500 m .a.s.l. is clearly visible in the latter one. Agricultural areas covered mainly by olives are nearly the same in both scenarios whereas there is a marked increase of *permanently irrigated land* in the MYOPIC scenario of +14% and a 6% decrease in the SUSTAINABLE one.

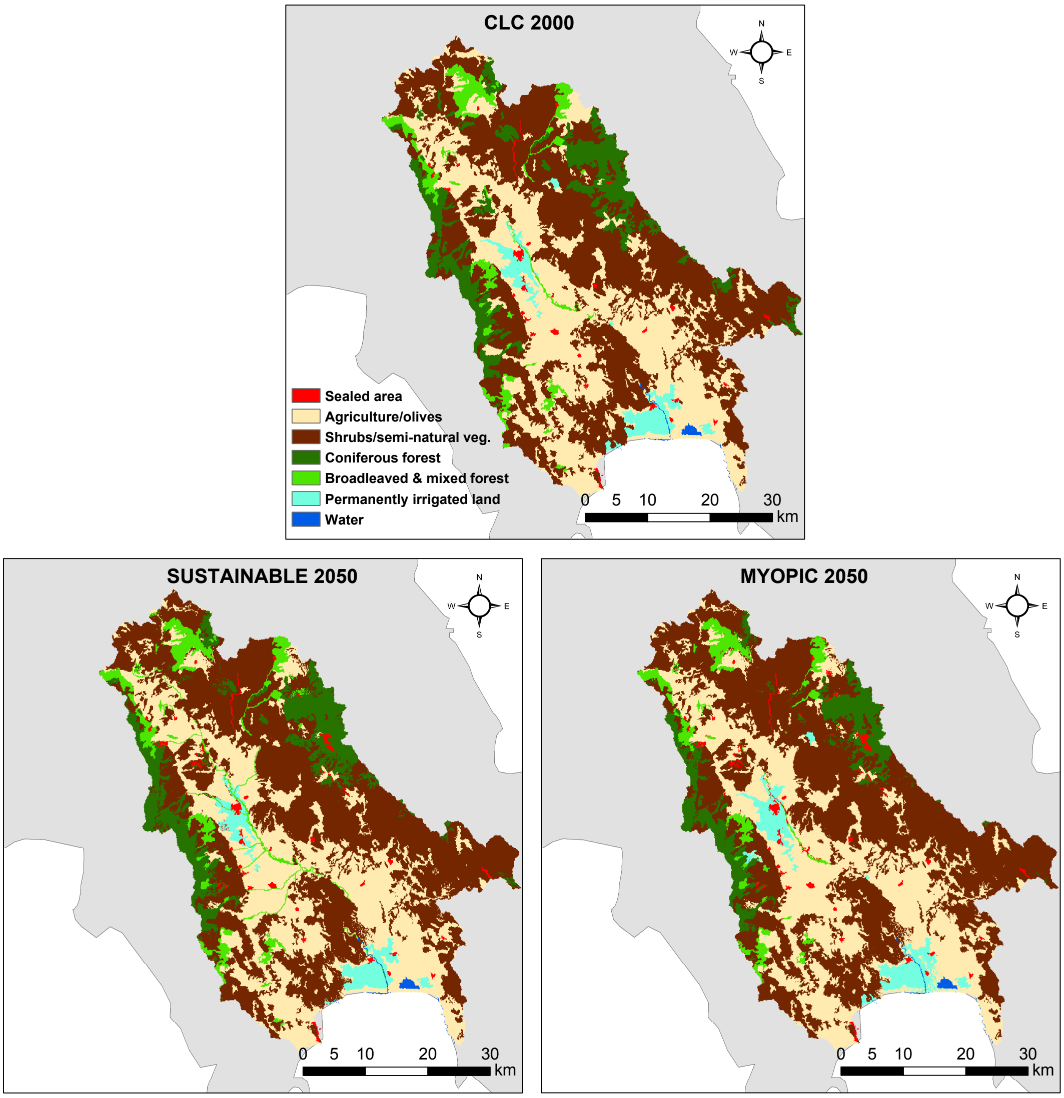

FIGURE 8.2: Land use maps of the Evrotas for the reference scenario (CLC 2000, top), SUSTAINABLE (bottom left) and MYOPIC scenario (bottom right).

8.1.4 Assessment of Water Use Estimations

8.1.4.1 Defining the Reference Scenario

As for the Ebro, the statistics from the Ministry of Development of Greece (MDG) (2005) used for deriving the water use maps and also the final results were checked for reliability and consistency comparing them with other datasets. Table 8.2 summarises the available sources and values. Generally speaking, it is difficult to determine the precise water demand for irrigation in the Evrotas River basin due to insufficient water meters and an unknown number of illegal water abstractions (NIKOLAIDIS et al. 2009). As a consequence, the range of values is wide. The number ascertained by the MDG (2005), used as basis for deriving the water use maps, sums up to 76.8 hm^3 for all communities lying inside the Evrotas River basin for the year 2001, very close to the 77 hm^3 estimated by GAMVROUDIS et al. (2015) which, however, relates to the largest part of the basin. The 174 hm^3 estimated by NIKOLAIDIS et al.

(2009) on typical plant water needs is considerably higher. The authors state that hydrological modelling revealed that the actual demand used by farmers might be even three times as high. Finally, SKOULIKIDIS et al. (2011) calculated the irrigation water uses from the area and the water needs of each cultivation type and obtained 287 hm^3 including the irrigation of olives. The water use prior to olive irrigation was estimated at 84 hm^3. The Evrotas basin is part of the Eastern Peloponnese River Basin District and the existing RBMP reports only data for the whole district covering an area of 8442 km^2 (SSW 2013). A rough approximation for the irrigation demand of this basin is therefore obtained by assuming that the percentage area covered by the Evrotas, 28.6% of the whole district, is equal to the share of irrigation demand used in the Evrotas which results in 94.4 hm^3. Obviously, without knowing the real distribution of irrigated areas within the Eastern Peloponnese district this remains a rough estimation. The comparison shows that it is difficult to know which value gets closer to reality. Since one aim of the present study is to validate official statistics, the data from the MDG (2005) were used as its magnitude coincides with the ones from the RBMP and also with GAMVROUDIS et al. (2015).

Table 8.2 also includes the total sums of the calculated water use maps. Similar to the Ebro, they lie slightly below the values from the MDG (2005) they are based on. This happens when the water demand of a subunit is discarded for calculations because no irrigated or urban pixel is located in this unit. The underestimation is stronger for urban water demand which is probably related to the small settlement sizes in the Evrotas which are assumed to be under-represented even in the CLC 2000 map at a 100 m x 100 m resolution.

TABLE 8.2: Total and sectoral water demands [hm^3] in the Evrotas according to various sources. [1]Sum for all communities lying inside the Evrotas basin, data for 2001. [2]Percentage share of the Evrotas of the Eastern Peloponnese River Basin District.

Source	Irrigation	Domestic/Industrial	Livestock	Total
NIKOLAIDIS et al. (2009)	174	-	-	-
SKOULIKIDIS et al. (2011)	287	-	-	-
MDG (2005)[1]	76.8	6.4	<0.1	83.2
GAMVROUDIS et al. (2015)	77	-	-	-
Evrotas RBMP (SSW 2013)[2]	94.4	39	5	373
Own calculation based on MDG (2005)	72.6	5.3	-	77.9

8.1.4.2 Comparison with other Water Use Maps

Figure 8.3 compares various available irrigation maps with the water use map for the reference period based on CLC 2000. Apart from the JRC irrigation map, which only provides information on the location of irrigation but not on the amount, the GIAM and GMIA deviate greatly from the calculated water use map. The spatial resolution of 5′ of the latter is not able to capture the heterogeneous pattern of irrigation in the Evrotas, while the GIAM misses several irrigated areas. Since this product is based on remote sensing, it could be that the irrigation of olive trees is hard to detect from satellite images. The water use map calculated as part of this thesis differentiates between various water demand rates, as is from below 25 mm/y to up to 310 mm/y. The intensively irrigated areas, i.e. mainly citrus trees, are also visible in the irrigation

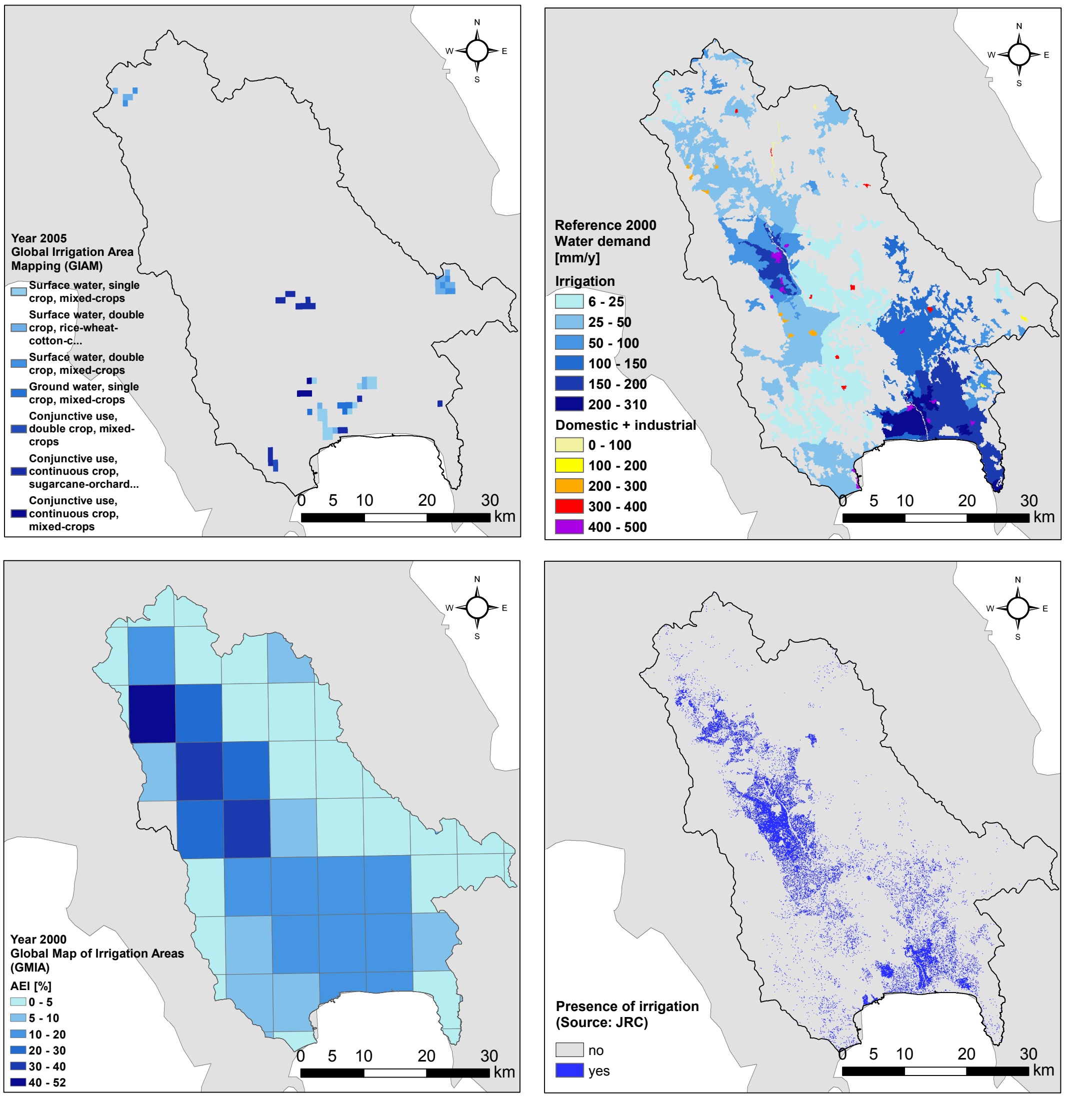

FIGURE 8.3: Comparison of various irrigation maps for the reference period for the Evrotas. Upper left: GIAM (THENKABAIL et al. 2009), upper right: calculated water use map (irrigation and domestic+industrial) for the reference period based on CLC 2000, lower right: presence of irrigation provided by the JRC (`http://data.jrc.ec.europa.eu/collection/water`), lower left: GMIA (SIEBERT et al. 2013).

map from the JRC around the city of Sparta in the basin centre and in the coastal part of the basin.

8.1.5 Water Use Scenarios for the Year 2050

The resulting water use maps in figure 8.4 show that the distribution of irrigation is very similar in both scenarios. The difference, however, is the management of land and therefore the higher application rates in the MYOPIC scenario. Following the assumption that the irrigation of olive trees will be intensified in this scenario, both for maximising the economic profit and also due to a higher expected water scarcity

in the region caused by climate change (GAMPE et al. 2016), the water demand of this class was set to rise by 20%. At the same time, the cultivated area is reduced as more marginal farmland is abandoned. This results in a higher water application per pixel on *agriculture & olives* with respect to the reference scenario all over the catchment. The largest volumes are still applied in the intensively irrigated areas around the city of Sparta (150 - 200 mm/y) and in the southern part of the basin close to the sea (150 - 310 mm/y) where mainly citrus trees are cultivated.
In contrast to that, the areas dominated by olives would need less water in a SUSTAINABLE world, a large share of land even below 25 mm/y. Also the largest part of the intensively irrigated citrus orchards around Sparta would reduce their demand from 150 - 200 mm/y to 100 - 150 mm/y. Even the area of irrigated land is very similar in all three scenarios, the total demand for irrigation would be 49.5 hm^3 in the SUSTAINABLE scenario, approx. 32% less than in the reference scenario (72.6 hm^3). Meanwhile, the water demand for irrigation in the MYOPIC scenario would increase by 14.5% resulting in 83.1 hm^3.

The trends for the urban demands are in line with expectations. Due to the higher water efficiency in both scenarios, the application rates per pixel are generally reduced in both scenarios, whereas stronger in the SUSTAINABLE scenario. For Sparta for example, the demand in the reference scenario lies at 447 mm/y, for the MYOPIC at 403 and for the SUSTAINABLE at 356 mm/y. The total urban water demand rises, however, in both future scenarios by 40.8% (to 7.4 hm^3) and 10.9% (to 5.9 hm^3) in the MYOPIC and SUSTAINABLE scenario, respectively. This is caused by the expansion of *sealed area* in both scenarios, which is stronger for the MYOPIC scenario. iCLUE locates urban pixels in both future scenarios mainly around settlements in the mountainous areas north-west and north-east of Sparta and less around the city itself.

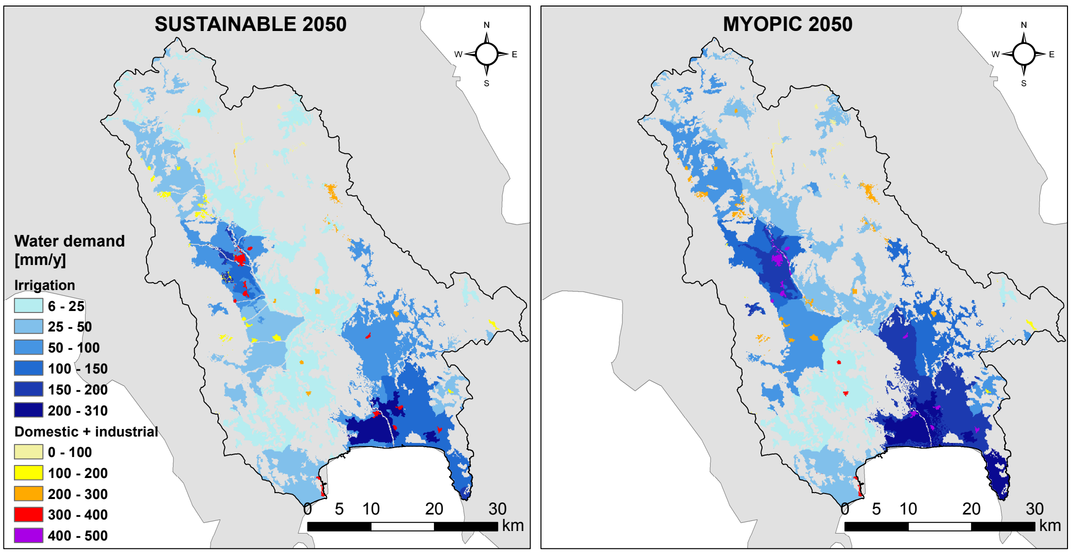

FIGURE 8.4: Derived combined irrigation and domestic+industrial water use maps for the SUSTAINABLE (left) and MYOPIC (right) scenarios for the Evrotas, horizon 2050.

Chapter 9

Conclusion

9.1 Reflection on Research Objectives and Hypotheses

9.1.1 The Ebro River Basin

To hypothesis 1:
"Under conditions of climate and land use change, current water management practices and even long-term RBMPs are insufficient to meet the goals of the EU-WFD in Mediterranean river basins."

The concerns regarding the sustainability of the water use in the Ebro are severe. To recall the points mentioned in the introduction, the long-term irrigation plans reported in the RBMP 2015-2021 sum up to additional 4567 km^2 of irrigated area, an increase of about 47%. The current draft for the RBMP of the 3rd cycle (2021-2027) is more prudent regarding the future expansion of irrigation due to the simultaneously abandonment of other irrigated areas. Still, the estimated water demand is equally high as in previous plans, i.e. 10626 hm^3 already for 2027 and therefore 30% more than at present.

At the same time, the probability of a reduced water availability in the future in the Ebro, as well as in other Mediterranean catchments, is very high. Also the CMI, calculated in chapter 6.2 exemplarily with data from one GCM-RCM combination, shows once more that the future amount of available water is very likely to decrease, independently of the selected RCP. This is equally true for the runoff simulations presented in chapter 6.1, which implemented the land use scenarios developed as part of this thesis: For the SUSTAINABLE scenario a runoff decrease of 15% is projected for 2050, for the MYOPIC scenario even 20%.
Similar results are obtained by the Spanish Centre for Studies and Experiments on Public Works (CEDEX) using the hydrological SIMPA model to simulate the natural flow conditions for each Spanish river basin (CEDEX 2017). To account for the uncertainty in climate modelling they used data from six different GCMs to run the model for RCP 8.4 and 4.5. This is also the modelling exercise providing recommendations on expected runoff reductions for 2039 to the RBMPs expressed already in chapter 1.2. For the period 2040 to 2070, which is only shifted by five years from the future period used in GLOBAQUA (2036-2065), the simulated changes for the Ebro are -11% for RCP 4.5 and -13% for RCP 8.5 taking the mean over all model runs. Consequently, the results of the CEDEX study are of similar magnitude as the simulation with the mHM model.

The MYOPIC scenario, which constitutes the hypothetical implementation of the RBMP, will therefore be marked by the clash between an increased water demand and a reduced water availability. Coming back to the WEI+ referred to in the beginning, the development in this scenario will find expression in a higher WEI+. At present, the ratio between water consumption (5080 hm^3 according to CHE 2015) and actual water demand (8186 hm^3, CHE 2015) lies at 62%. Assuming that the future ratio stabilises at approximately 60%, the WEI+ for the MYOPIC scenario would rise to 54% supposing a 20% reduction of renewable water resources as simulated with the mHM model for the total runoff (i.e. 11698 hm^3 compared to the 1980-2006 average of 14623 hm^3, CHE 2018) and a total water demand increase of 30% to 10423.5 hm^3 as modelled above for this scenario. To recall, the mHM model was run with climate data from the RCA4 model combination, which is the driest out of the three GCM-RCM combinations selected for GLOBAQUA, so a 20% reduction might seem extreme. Nevertheless, applying the -13% obtained in the study by CEDEX as a multi-model mean for RCP 8.5, the WEI+ would lie just slightly below at 49%.

Taking all this in consideration, it proves *hypothesis 1* correct for the Ebro case study, stating that the current but also future long-term RBMPs are not in line with the sustainability goals of the EU-WFD. The directive clearly states that sustainable water abstraction regimes should be supported "even in water stress and shortage situations" (EUROPEAN COMMISSION 2007) which are likely to occur more often in the future due to climate and land use change. Opposed to that, the above estimations show that the current plan is in the truest sense of the word 'myopic' and that it will add to the already now experienced water scarcity.
One may argue that the water use efficiency may increase in the future. However, past developments in Spain have shown that this increase has been accompanied by a rebound effect leading in turn to an increased water consumption (DUMONT et al. 2013, GONZÁLEZ-CEBOLLADA 2016, LECINA et al. 2010). A MYOPIC world would amplify this mechanism.
A further negative effect of the modernisation of irrigation systems over the past decades has been the strong increase in energy use making irrigated agriculture the second largest electricity consumer in Spain (GONZÁLEZ-CEBOLLADA 2016). The new pressurised irrigation systems now strongly depend on electricity to keep them going. If no alternative sources are found, the energy consumption is likely to rise even more for a MYOPIC pathway.

As regards the SUSTAINABLE scenario, the water availability will be equally reduced. It foresees, however, also a more sustainable water management as postulated by the EU-WFD, increasing the irrigation efficiency and shifting the cultivation to less water consumptive crops or applying deficit irrigation (GONZÁLEZ-CEBOLLADA 2016). By this means, the WEI+ could be kept down despite the simultaneous reduction in water availability. For a scenario as simulated with the mHM model with a 15% runoff reduction and the simulated approx. 5655 hm^3 total water demand in the SUSTAINABLE scenario, the WEI+ would be 27%, which nonetheless indicates water scarcity but to a considerably lower level than in the MYOPIC scenario. Applying the average -11% reduction obtained by the SIMPA model for RCP 4.5 (CEDEX 2017), the WEI+ would lie at 26%.

To hypothesis 2:
"The future projection of land and water uses at the basin-scale requires the downscaling of global change narratives and the modelling of integrated scenarios of climate and land use change."

The downscaling applied in this study to bridge the gap between the global RCPs and SSPs and the scale of the case study was successful in producing, for the first time, high-resolution land use and water use maps for the Ebro for various future scenarios. They provide a spatial and thematic resolution useful both for subsequent IAV studies as well as for water authorities, water managers and policy makers. Only by downscaling of global scenarios to the basin-scale it was possible to include stakeholders's opinions on the future developments in the two scenarios and adapt the land use model to local characteristics. This further allowed to design the MYOPIC scenario on the one hand to fit SSP 5 and RCP 8.5 and on the other hand to shape it according to the declarations in the RBMP described above. The result maps have already been used in a series of GLOBAQUA related studies such as JORDA-CAPDEVILA et al. (2019), HERRERO et al. (2018) and also the modelling with the mHM model mentioned above (HUBER GARCÍA et al. in prep.).

Regarding the quality of the results, the land use modelling simulations could be improved by introducing more dynamic socio-economic drivers. Downscaled projections for the various SSPs at municipal or at least provincial resolution were, however, missing. Furthermore, also an increase of the modelling resolution to 500 m^2 or even 100 m^2, which would be easily possible with CLC data, could provide more accurate results. It should be further investigated if using more up to date CLC maps, i.e. starting with CLC 2006 version 18.5.1 and using 2012 and 2018 as soon as the validation has finished, would lead to a better representation of irrigated areas and higher accordance with the CHE reference map of irrigated areas. All in all, the validation of the land use modelling revealed that the results are satisfying.
One limitation of the integrated modelling presented here is the lack of feedback loops. For this reason, it is neither possible to consider the impact of LULCC on the local climate nor the the impact of climate induced water scarcity on the distribution of the vegetation. Nevertheless, the integration of downscaled climate data in the modelling chain makes the scenarios more complete, even though its effect on the actual distribution of land uses may be small for the scenario horizon 2050. In any case, the influence of different climate scenarios keeps getting larger beyond that date and therefore it is important to consider climate change.

The downscaling of scenarios from global projections includes many sources of uncertainty, as there are the RCPs and SSPs per se, the use of downscaled climate data, the land use modelling, the translation of the global narratives by experts and local stakeholders or the water use statistics. The results presented in chapter 7.6 show that the concerns regarding the uncertainty introduced by the random factor of the iCLUE model and its sensitivity to climate data could be overcome. Other sources of uncertainty, however, remain difficult to quantify.
Nevertheless, downscaling is the only way of producing concise and reasonable scenarios at the basin-scale which are still in line with the global change narratives and by this means add a small piece to the large picture. The approach proved to be successful for the present study and consequently *hypothesis 2* can be confirmed.

To hypothesis 3:
"Combining sectoral water use statistics with land use change models provides an efficient and transferable method to deliver projected water use maps as planning tools for users and policy makers."

Regarding the *third hypothesis* of this study, the combination of land use modelling results with water use statistics has revealed to be a relatively easy to use method to obtain water use maps in accordance both with the spatial distribution of land use and official statistics. The most time consuming part of the study relates to the land use model, mainly the data preparation and calibration while the setup of an additional water use model is not necessary.
The applied method further allows for high flexibility. First, one is free to adapt the modelling resolution to the needs and size of the study area. While 1 km^2 was used in the Ebro, finer resolutions might be more appropriate for other study sites such as the Evrotas, see chapter 8. As mentioned earlier, also for the Ebro a finer modelling resolution could be applied combining the land use maps with water statistics at a finer reporting level. Second, the method allows to take into account and relate to very basin-specific data such as the statistics from the RBMP or other official sources. This in turn allows to visualise the data, which is usually not possible in a spatially explicit way, and offers ways of validation.
Without applying a specific water use model and being bound to the CLC classes, it is not possible to simulate the cultivation and irrigation of selected crop types as done by other authors. Still, the flexibility also relates to the fact that one is free to decide which land use classes are consuming water and to what extend. In case of the Ebro, also *complex cultivation patterns* were included with a reduced application rate. The approach further allowed to derive also urban water use maps.

The assessment of the water use maps above has revealed that large differences and uncertainties exist regarding water statistics and spatial products due to varying definitions or unmonitored activities making comparisons difficult. As an example, the newest RBMP 2021-2027 differentiates the total water demand for the hydrological year 2016/2017 into controlled demand, 5516 hm^3, and estimated, 2745 hm^3 (CHE 2018). The latter part might be simply unrecorded in the absence of a water meter but with an official concession or due to illegal abstractions. Nevertheless, the range of values obtained in the present study are in line with other studies, which are estimations themselves, and the differences to the reference are acceptable. A satisfactory balance was found to obtain realistic values for the irrigated area, the water demand and the application per pixel. The maps show only little deviations from the reference at the basin scale while for the exploitation units larger deviations have to be admitted. This could be partly overcome by either reducing the modelling resolution or using statistics at a finer administrative level which for the Ebro exist, however, only for agricultural uses. Comparing to other available water use products, the results of this study capture the details of the Ebro at least as good as other products while providing enhanced quantitative information directly relating to the RBMP. The results could be further refined by combining the LU maps with monthly water use statistics if available, since the water demand in Mediterranean basin varies strongly throughout the year.

It has to be noticed that due to the underlying data the results of the present study need to be interpreted as the upper possible margin. In case of the irrigated area, the maps represent rather the area equipped for irrigation than the actually irrigated area. As for the total water demand, it is higher than the actual water consumed. Still, the expected water demand for 2027 from the RBMP 2021-2027 used here for the horizon 2050 could underestimate the value for 2050. This has to be considered when using or interpreting the water use maps. Besides, the resulting maps disregard the actual availability of water which is the reason they were confronted to the CMI and runoff modelling. Nevertheless, they provide important information for policy makers and the basis for further IAV studies which are clearly necessary: As the RBMP 2015-2021 states, the long-term irrigation plans were projected only considering if sufficient water would be available, which the CHE affirms, but possible economic, social or environmental effects were neglected (CHE 2015).

All in all, also *hypothesis 3* can be confirmed as the combination of land use modelling results and water use statistics to obtain spatially distributed water use maps was successful.

9.1.2 The Evrotas River Basin

Several authors state that the expansion of irrigation to olives has been accompanied by a general precipitation and runoff reduction observed in the Evrotas for the period 1989-2011 compared to 1970-1989 (GAMVROUDIS et al. 2015, SKOULIKIDIS et al. 2011). The study by GAMPE et al. (2016), where future climate projections from the EURO-CORDEX model ensemble were analysed over the GLOBAQUA case studies, revealed that this trend is likely to continue in the Evrotas. The strongest negative precipitation changes out of the four investigated river basins are projected over the Evrotas basin. Up to 30% less precipitation are simulated over the summer months for the period 2035-2065 compared to 1981-2010; this causes also decreased evaporation rates in spring, summer and autumn and a 20% runoff reduction for the ensemble mean. It seems therefore very certain that the water availability in the Evrotas basin will be less in the future.

Meanwhile, on the water demand side, GAMVROUDIS et al. (2015) estimated that already the current irrigation practices consume twice the recommended amount of water in the Evrotas. This is in line with *hypothesis 1* which states that already current water management practices are insufficient to meet the sustainability goals of the EU-WFD.
For the MYOPIC scenario modelled here, which comprises a further expansion of the irrigation of olive trees, an extra 15% water demand was estimated for the horizon 2050. Having in mind the already existing pressure on water resources, there is no doubt that a future MYOPIC scenario would severely exacerbate the situation. Improved water efficiencies for urban uses and irrigation systems would not be able to compensate the increased water demand in the MYOPIC scenario. Besides, as the example of the Ebro shows, improved irrigation technologies do not always lead to water savings but rather to a higher water consumption (CHE 2018).

Regarding water quality, a higher water scarcity would also imply a reduced dilution capacity of agrochemicals and agro-industrial wastes (KARAOUZAS et al. 2018), in case of the Evrotas mainly from olive oil presses and orange juice factories. DEMETROPOULOU et al. (2010) identified these problems as the main EU-WFD related pressures for the basin together with the over-exploitation of water resources for irrigation. Following the assumption of growing settlements, the resulting increase in urban water demand would also lead to higher point source pollution through urban waste water if not more Waste Water Treatment Plants (WWTPs) are built. By now, only one WWTP exists in the Evrotas basin next to the city of Sparta (SKOULIKIDIS et al. 2011).

In contrast to that, the SUSTAINABLE scenario could be a step towards a more sustainable land and water management. In this scenario the irrigation of olive trees is partially reduced going back to the cultivation without irrigation that has been applied in the region for centuries. Of course, this should be achieved without affecting agricultural production. KARAOUZAS et al. (2018) point out that significant reductions in water abstractions could be achieved by alternative irrigation systems such as drip irrigation which consumes less water. Besides, in their study, NIKOLAIDIS et al. (2009) suggest the use of non-conventional water resources. Water from the WWTP and from agro-industrial facilities such as oil mills could be reused for irrigation particularly during dry periods.
The SUSTAINABLE scenario emphasises the importance of river bank protection and restoration in the catchment, necessary for preventing erosion, floods and for filtering pollutants entering the water course (KARAOUZAS et al. 2018, NIKOLAIDIS et al. 2009, SKOULIKIDIS et al. 2011). It depicts an alternative way in which the riparian zones are restored. The implementation of this important measure in the land and water use maps are helpful for studies using these maps as input for subsequent environmental assessment studies. The only way of providing this level of detail in the scenarios was by downscaling them to the catchment level which allows to include these local peculiarities, as *hypothesis 2* suggests.

All in all, the two alternative scenarios presented here show that it is not the land use change per se, but a change in land management that makes the difference and is decisive for achieving a sustainable future. Out of the two simulated integrated scenarios, the SUSTAINABLE one takes up the measures already proposed in several priorly mentioned studies that would allow the successful implementation of the EU-WFD giving priority to environment conservation as the directive seeks for (EUROPEAN COMMISSION 2007). Besides, the increase in water use in the MYOPIC scenario is opposed to the trend in water availability that is becoming apparent. Furthermore, one should not neglect that the actual irrigation demands may be even higher than the ones considered in this study. Consequently, a major and important step forward in the Evrotas would be to estimate the real irrigation needs and adapt the charges for water abstractions which currently are calculated on the areal extend of the farm rather than on the actual water use (NIKOLAIDIS et al. 2009).

9.2 Implications for Transferability and Scaling

As the previous chapters show, the hypotheses could be corroborated and also the transferability of the approach to a different case study proved to be successful in case of the Evrotas. The validation experiment further confirmed that the applied methods can be transferred to a different scale, both in extend and resolution: The Evrotas basin (approx. 2413 km^2) is considerably smaller than the Ebro (85600 km^2) and the modelling resolution is a 100 times smaller, 100 m x 100 m vs. 1 km x 1 km. The iCLUE results for both case studies were satisfying and the resulting land and water use maps are plausible and provide important information relevant for water management. Still, a few points have to be considered when transferring the methods to another region and scale.

First of all, any modeling setup for a given study area, requires river basin specific modifications. This includes obviously the collection of iCLUE drivers matching the characteristics of the area and the modelling resolution. Local singularities such as past land use transitions, history of water uses, restrictions etc. have to be researched as they are needed for the general setup of the model and the development of future land use demands. This includes also the selection of water consuming land use classes and the link to the appropriate and most accurate water statistics.

Secondly, the aggregation level of available water statistics has to be chosen with great care. At a coarse resolution the values in the final water use maps would be very homogeneous and local differences would be missed. At the same time, a high resolution of the statistics, i.e. choosing the lowest administrative level, may augur very detailed results while it also can cause problems: The water demands of units without any water consuming pixel are dropped from calculations. Consequently, having larger units increases the chances to find a few pixels in a unit. This becomes even more important when developing scenarios as the future distribution of water consuming pixels may look very different. Both in case of the Ebro and the Evrotas, neither the finest water statistics level was chosen nor the coarsest but an intermediate one which still allowed to spatially differentiate water use amounts. This yielded a good approximation at basin scale, for more local studies the information might be, however, still too coarse. Modelling at finer resolution could be a possible solution.

It has to be pointed out that the successful application of the approach developed in this thesis depends completely on the availability of reliable data. As the application to the Adige and Sava River basin, two further GLOBAQUA case studies, show, this is not always the case, see HUBER GARCÍA et al. (2018).
The main obstacle in case of the Adige River basin in Northern Italy was that the provided water statistics differ substantially between administrative units. The watershed is located to its largest parts in the provinces of Bolzano and Trentino, which however, report different variables: While Bolzano reports actual sectoral water demands, the values for Trentino represent the maximum possible water supply for each sector, which is substantially higher. The lower coarse of the Adige River basin, located in the Veneto region, had to be excluded from calculations. For this part, it is neither possible to know the exact volumes nor the location of the water consumption since the area supplied by the Adige receives water also from several other rivers, as the basin authority states. Consequently, the discrepancy between the reported variables complicates comparisons and renders the derivation of meaningful water use maps impossible.
The situation is similar for the Sava River basin as its tributaries traverse several countries (Slovenia, Croatia, Bosnia-Herzegovina, Montenegro and Albania) and their statistics are not harmonised. A further factor limiting the applicability of the approach to the Sava is that the linkage between land and water uses is more difficult. Irrigation plays only a very minor role, while livestock consumes more water. While irrigation can be easily distributed in space as the examples of the Ebro and Evrotas show, the spatial location of livestock is, however, very difficult. This is even more the case as the modelling resolution for the Sava had to be coarser than the original CLC resolution, 1 km x 1 km, as the basin is considerably larger (approx. 97506 km^2). Agricultural water uses were attributed to the CLC class *complex cultivation patterns* which resulted in very low application rates per pixel. The reason for the low values could be that the selected land use class does not correctly represent agricultural water uses which is distributed to too many pixels. For these reasons, the results for the Adige and Sava were discarded from the analyses in this thesis.

Regarding the application of the developed method to the Evrotas, it can be concluded that for small study areas where a fine modelling resolution can be applied, the development of river basin specific land and water use scenarios is even more important than for larger sites. As the comparison with other water use maps carried out in chapter 8.3 reveals, continental or global products are not able to capture the patterns at such a small resolution like the GMIA (SIEBERT et al. 2013) or even miss large parts of the irrigated areas due to their low application rates or little importance at larger scale as the GIAM (THENKABAIL et al. 2009).
In case of the Evrotas, it was possible to create water use maps based on existing water statistics and local information applying the same approach as in the Ebro. This confirms the transferability of the method and consequently also *hypothesis 3*.

9.3 Recommendations for the EU-WFD

The results presented here constitute an approximation, but reveals clear trends: Water scarcity is undoubtedly going to increase in the Mediterranean in the future due to climate change and an unsustainable water management will add to aggravate the situation. In light of the looming problems, it is more than clear that present and future water management needs to be adapted.
The work presented in this thesis provides support for an improved understanding of related interconnections and possible management strategies: Modelling downscaled integrated scenarios can be used as tool to better analyse the relationships between impacts, causes and measures taken. The integrative approach further allows to take into account dynamic changes in climate, land use and water management, in line with the holistic view of the EU-WFD. Coming back to the quote from MOSS et al. (2010) in the introduction, this allows to test the robustness of measures under various conditions. By this means, simulations like the ones presented here can contribute to a more sophisticated assessment of truly applicable and efficient Programmes of Measures (PoMs), avoiding unsustainable planning.
A further necessity of implementing integrated scenario analyses as standard procedure in the selection of PoMs is that it allows to include also scientific knowledge in the decision process. The directive further explicitly states the need for public involvement which can be achieved by engaging stakeholders in the scenario development process as done here.
It is already a substantial progress that the directive implemented river basin districts organising the management within natural watersheds and across national boundaries. The EU-WFD should, however, go even a step further and demand for a compulsory and standardised reporting on water uses at river basin level, as this is already the case for crop, fertilizer or pesticide statistics at the EU NUTS level. This, of course, requires also the metering of water coordinated by the river basin authorities, which in many cases is not all-encompassing. The standardised collection and reporting of statistics is important since it provides the basis for accurate planning and it facilitates studies like the one presented here allowing for more comparability across Europe.
Finally, even though the EU-WFD is not target based, it should consider to set quantitative targets such as the adherence to a certain WEI+ level. This would allow to better assess the sustainability of water management practices and, hopefully, promote the targeted implementation of the directive.

Summary

In order to satisfy future demands for water, food, fibre and energy, it is necessary to develop management strategies that find a balance between ecological, economical and societal needs. This is particularly true for regions that are likely to be negatively affected by climate change, such as the Mediterranean. Many studies agree that altered precipitation patterns and higher mean temperatures will increase water scarcity in this region, which is already prone to water stress. At the same time, irrigation is by far the major water consumer in Mediterranean countries. Still, many river basin authorities plan to expand the irrigation activities consuming even more water while the natural supply diminishes.

The work presented here concentrates on two Mediterranean river basins, the Ebro in Spain and the Evrotas in Greece. In case of the Ebro, the River Basin Management Plan (RBMP) foresees an expansion of approx. 50% of the irrigated area for the future and a related rise of the water demand by 30% until 2033. The irrigation in the Evrotas has been expanded to olive trees over the last decades increasing the water demand for irrigation substantially. Consequently, the reduced water availability caused by a changing climate in combination with an expected water demand increase are very likely to aggravate the situation in the future.

Both river basins constitute case studies of the EU-FP7 project GLOBAQUA, which builds the thematic frame of this thesis. With a focus on aquatic ecosystems, one of the project aims was to investigate how future water-related management practices and policies, in particular the Water Framework Directive of the European Union (EU-WFD), have to be adapted to be able to cope with the impacts of multiple stressors, such as climate and land use change, under increased water scarcity in the future.

One of the objectives of the work presented here was to analyse if the current and future official water management strategies in the study areas adhere to the EU-WFD, which promotes the sustainable use of water, and to sketch alternatives.

For this purpose, integrated, spatially explicit land and water use scenarios were developed that reflect the water management practices of the individual study areas. The scenarios are, at the same time, in line with the global Representative Concentration Pathways (RCPs) and Shared Socio-economic Pathways (SSPs), a scenario framework widely used in climate change impact studies. Integration in this respect means that climate, socio-economic and environmental future projections were taken into account.

To be able to apply these global storylines to regional study areas, they had to be downscaled first. Within the GLOBAQUA project, several project-specific scenarios were developed based on RCPs and SSPs for the time horizon 2050. Out of these, the MYOPIC and the SUSTAINABLE scenario were investigated in detail as part of this

thesis. For both case studies the MYOPIC scenario represents the continuation of the 'business as usual'; in case of the Ebro it is parametrised according to the plans reported in the RBMP mentioned above. The downscaling to the basin-scale was achieved by including the knowledge of experts and local stakeholders and combining it with quantitative values gathered through an extensive literature review. This information was further used to parametrise the land use change model iCLUE. Eventually, this resulted in land use maps for the MYOPIC and SUSTAINABLE scenario for the year 2050 for the Ebro and Evrotas.

In order to obtain also spatially distributed water use maps, official water use statistics were combined with the spatially explicit land use simulations. Urban and industrial uses were linked to urban areas and agricultural uses, irrigation for the largest part, to all irrigated land use classes. For the future, the water consumption of each land use class was adapted with a factor to fit the overall water demand which was priorly specified for each scenario.
In case of the Ebro, the final water use scenarios were compared to the Climate Moisture Index (CMI) to evaluate also the water availability under both scenarios.

The validation of the land use simulations revealed that the performance of iCLUE in both case studies is good. Also the water use maps, which were compared to already existing similar products, are satisfying.
The concerns regarding water management were confirmed: Already the current practices demand substantially more water than what could be considered sustainable. The long-term mean Water Exploitation Index Plus (WEI+) for the Ebro indicates water scarcity already for the present. The CMI projects a future reduction of available water independently of the scenario. If the RBMP is implemented as planned, it is certain that water scarcity will increase dramatically, resulting in a higher WEI+. Applying, however, a SUSTAINABLE scenario, the WEI+ would only rise marginally compared to the present. The situation is very similar for the Evrotas.

The downscaling of the scenarios appeared to be not only useful but necessary to obtain the spatial and thematic resolution to support planning decisions on a river basin level. The proposed method for deriving water use maps based on local statistics rather than through modelling proved to be an easy to use tool. Its transferability in space, scale and resolution was confirmed by the application to the Evrotas basin.

The work presented in this thesis describes a procedure that can help to better implement the Water Framework Directive of the European Union (EU-WFD). Such integrated modelling exercises, which address the systemic view of the directive, should be established as standard procedure to better assess the efficiency and applicability of Programmes of Measures (PoMs). The final recommendations of this thesis to the EU-WFD are to demand for a compulsory and standardised reporting on water related variables and to set quantitative targets such as the adherence to a certain WEI+ level. This would allow to better assess the sustainability of water management practices and facilitate the comparability across Europe.

Zusammenfassung

Um auch in Zukunft den Bedarf an Wasser, Nahrungsmitteln, Faserstoffen und Energie decken zu können, ist es notwendig Ressourcenmanagement so zu betreiben, dass das Gleichgewicht zwischen ökologischen, ökonomischen und sozialen Bedürfnissen sichergestellt ist. Dies betrifft besonders Regionen wie den Mittelmeerraum, in denen die Folgen des Klimawandels mit hoher Wahrscheinlichkeit negativ sein werden. Viele Studien stimmen darin über ein, dass veränderte Niederschlagsmuster und höhere Jahresmitteltemperaturen die Wasserknappheit in dieser ohnehin schon betroffenen Region verstärken werden. Gleichzeitig wird das meiste Wasser in vielen Ländern um das Mittelmeer zur Bewässerung verwendet. Nichtsdestotrotz geht man in den Bewirtschaftungsplänen vieler Flusseinzugsgebiete von einer Ausweitung der Bewässerung aus, was einen noch höheren Wasserverbrauch mit sich bringt, während die natürliche Wasserverfügbarkeit schrumpft.

Die vorliegende Arbeit befasst sich mit zwei mediterranen Flusseinzugsgebieten, dem Ebro in Spanien und dem Evrotas in Griechenland. Im Falle des Ebro sieht der Bewirtschaftungsplan eine Zunahme der bewässerten Fläche um ca. 50% vor, während der damit verbundene erwartete Anstieg des Wasserbedarfs ca. 30% bis zum Jahr 2033 beträgt. Im Einzugsgebiet des Evrotas wurde die Bewässerung im Laufe der letzten Jahrzehnte auf Oliven ausgeweitet, was den Wasserbedarf deutlich erhöht hat. Im Folge der durch den Klimawandel hervorgerufenen geringeren Wasserverfügbarkeit könnte sich demnach, in Kombination mit einer erhöhten Nachfrage nach Wasser, die Situation zuspitzen.

Sowohl Ebro als auch Evrotas waren Untersuchungsgebiete im EU-FP7-Projekt "GLOBAQUA", welches den thematischen Rahmen dieser Dissertation bildet und dessen Hauptaugenmerk auf aquatischen Ökosystemen lag. Eines der Hauptziele GLOBAQUAs bestand darin herauszufinden wie Managementpraktiken und Richtlinien, die einen Bezug zu Wasser haben, - insbesondere die Wasserrahmenrichtlinie der Europäischen Union (EU-WRRL) - angepasst werden müssen um mit den Auswirkungen multipler Stressoren auch unter zukünftig verstärkter Wasserknappheit zurecht zu kommen. Solche Stressoren sind unter anderem der Klimawandel aber auch der Landnutzungswandel.

Eines der Ziele der vorliegenden Arbeit war es zu untersuchen ob die aktuellen und zukünftigen offiziellen Bewirtschaftungspläne der Untersuchungsgebiete sich an die EU-WRRL halten, welche eine nachhaltige Wassernutzung fördert. Des Weiteren sollten Alternativen aufgezeigt werden.

Zu diesem Zweck wurden integrierte und räumlich explizite Land- und Wassernutzungsszenarien entwickelt, in denen die Wassermanagementstrategien der einzelnen Untersuchungsgebiete eingebaut wurden. Gleichzeitig stimmen die Szenarien mit den globalen Repräsentativen Konzentrationspfaden (engl.: Representative

Concentration Pathways, RCPs) und den Gemeinsamen Sozioökonomischen Entwicklungspfaden (engl.: Shared Socio-economic Pathways, SSPs) überein, die in der Klimafolgenforschung eine weitverbreitete Grundstruktur für Szenarien bilden. Der Begriff "Integration" bezieht sich in diesem Zusammenhang auf die gleichzeitige Berücksichtigung zukünftiger Klima-, Umwelt- und sozioökonomischer Projektionen.

Um diese globalen Szenarien auf der regionalen Ebene anwenden zu können, wurden sie zunächst herunterskaliert. Für GLOBAQUA wurden mehrere projektspezifische Szenarien auf Grundlage der RCPs und SSPs für das Jahr 2050 entwickelt. Das sogenannte "kurzsichtige Szenario" und das nachhaltige Szenario wurden im Rahmen dieser Arbeit genauer untersucht. In beiden Einzugsgebieten beschreibt das kurzsichtige Szenario die Fortführung des "business as usual", im Falle des Ebro ist dieses gemäß den Angaben im oben genannten Bewirtschaftungsplan parametrisiert. Die Herunterskalierung auf die Einzugsgebietsebene gelang mit Hilfe des Wissens von Experten und lokalen Interessensvertretern und der Kombination dieser Information mit quantitativen Angaben, die in einer umfangreichen Literaturrecherche ermittelt wurden. Diese Informationen wurden ferner dazu verwendet das Landnutzungsmodel iCLUE zu parametrisieren. Daraus ergaben sich schließlich Landnutzungskarten für das kurzsichtige und nachhaltige Szenario im Ebro und Evrotas für das Jahr 2050.

Um räumlich verteilte Wassernutzungskarten zu erhalten, wurden diese Landnutzungssimulationen mit offiziellen Wasserstatistiken kombiniert. Der Wasserbedarf für Industrie und Haushalte wurde mit versiegelten Flächen verknüpft, der landwirtschaftliche Bedarf, zum Großteil zur Bewässerung, wurde allen bewässerten Landnutzungsklassen zugeschrieben. Der zukünftige Bedarf wurde mit Hilfe eines Faktors an den für das jeweilige Szenario zuvor festgelegten gesamten Wasserbedarf angepasst.
Für das Ebroeinzugsgebiet wurden die endgültigen Wassernutzungskarten noch mit dem Climate Moisture Index (CMI), d.h. einem klimatischen Feuchteindikator, verglichen um auch die Wasserverfügbarkeit in beiden Szenarien abschätzen zu können.

Die Validierung der Landnutzungssimulationen ergab, dass die iCLUE-Ergebnisse in beiden Untersuchungsgebieten von guter Qualität sind. Auch die Güte der Wassernutzungskarten, die mit ähnlichen bereits existierenden Produkten verglichen wurden, war zufriedenstellend.

Die Bedenken bezüglich des Wassermanagements haben sich bestätigt: Bereits die aktuellen Praktiken verbrauchen deutlich mehr Wasser als nachhaltig wäre. Das langjährige Mittel des Wassernutzungsindikators WEI+ (engl.: Water Exploitation Index Plus) bescheinigt dem Ebro bereits jetzt Wasserknappheit. Der CMI prognostiziert eine verringerte Wasserverfügbarkeit in der Zukunft, unabhängig vom Szenario. Falls der Bewirtschaftungsplan wie geplant umgesetzt wird, wird die Wasserknappheit ohne Zweifel zunehmen, was sich in einem höheren WEI+ äußern würde. Wenn allerdings ein nachhaltiges Szenario angewendet wird, würde der WEI+ nur leicht über den heutigen Wert steigen. Für den Evrotas ist die Situation sehr ähnlich.

Das Herunterskalieren der Szenarien stellte sich nicht nur als hilfreich sondern auch als notwendig heraus um die räumliche und thematische Auflösung zu erhalten, die zur Unterstützung von Entscheidungen auf Einzugsgebietsskala notwendig ist. Die hier vorgestellte Methode, bei der Wassernutzungskarten auf Grundlage von lokalen Statistiken anstatt durch Modellierung erstellt werden, erwies sich als leicht anwendbar. Die Übertragbarkeit auf andere Skalen, Auflösungen und Gebiete konnte durch die Anwendung auf den Evrotas gezeigt werden.

Die vorliegende Arbeit beschreibt eine Vorgehensweise, die zur besseren Umsetzung der EU-WRRL beitragen kann. Solche integrierten Modellierungsansätze, die die systemische Sicht der Richtlinie wiedergeben, sollten standardmäßig eingesetzt werden um die Wirksamkeit und Anwendbarkeit von Maßnahmenprogrammen zu bewerten. Die abschließenden Empfehlungen dieser Arbeit an die EU-WRRL beinhalten zum einen die verpflichtende und standardisierte Berichterstattung wasserbezogener Variablen. Des Weiteren sollte eine quantitative Zielvorgabe eingeführt werden, beispielsweise die Einhaltung eines gewissen WEI+-Wertes. Das würde die Einschätzung von Wassermanagementpraktiken bezüglich ihrer Nachhaltigkeit erleichtern und die Vergleichbarkeit innerhalb Europas verbessern.

Bibliography

AGENCIA ESTATAL DE METEOROLOGÍA, (AEMET) (2020a). *Valores climatológicos normales. Foronda-Txokiza*. URL: http://www.aemet.es/es/serviciosclimaticos/datosclimatologicos/valoresclimatologicos?l=9091O&k=pva (visited on 17/01/2020).

— (2020b). *Valores climatológicos normales. Tortosa*. URL: http://www.aemet.es/es/serviciosclimaticos/datosclimatologicos/valoresclimatologicos?l=9981A&k=cat (visited on 17/01/2020).

— (2020c). *Valores climatológicos normales. Zaragoza Aeropuerto*. URL: http://www.aemet.es/es/serviciosclimaticos/datosclimatologicos/valoresclimatolo%20gicos?l=9434&k=arn (visited on 17/01/2020).

ALCAMO, J.; VAN VUUREN, D. P.; RINGLER, C.; ALDER, J.; BENNETT, E.; LODGE, D.; MASUI, T.; MORITA, T.; ROSEGRANT, M.; SALA, O.; SCHULZE, K. & ZUREK, M. B. (2005). 'Methodology for Developing the MA Scenarios'. In: *Ecosystems and Human Well-Being: Scenarios: Findings of the Scenarios Working Group*. Ed. by S. R. CARPENTER; R. HASSAN; MILLENIUM ECOSYSTEM ASSESSMENT, SCHOLES, R. & N. ASH. Island Press, pp. 145–172.

ALEXANDER, P.; PRESTELE, R.; VERBURG, P. H.; ARNETH, A.; BARANZELLI, C.; BATISTA E SILVA, F.; BROWN, C.; BUTLER, A.; CALVIN, K.; DENDONCKER, N.; DOELMAN, J. C.; DUNFORD, R.; ENGSTRÖM, K.; EITELBERG, D.; FUJIMORI, S.; HARRISON, P. A.; HASEGAWA, T.; HAVLIK, P.; HOLZHAUER, S.; HUMPENÖDER, F.; JACOBS-CRISIONI, C.; JAIN, A. K.; KRISZTIN, T.; KYLE, P.; LAVALLE, C.; LENTON, T.; LIU, J.; MEIYAPPAN, P.; POPP, A.; POWELL, T.; SANDS, R. D.; SCHALDACH, R.; STEHFEST, E.; STEINBUKS, J.; TABEAU, A.; VAN MEIJL, H.; WISE, M. A. & ROUNSEVELL, M. D. A. (2017). 'Assessing uncertainties in land cover projections'. In: *Global Change Biology* vol. 23, no. 2, pp. 767–781.

ANTOÑANZAS VILLAR, F.; BARCO ROYO, E.; EGUÍA PEÑA, M. B.; MURÚA MÚGICA, J. R.; NAVARRO PÉREZ, M. C.; PINDADO TAPIA, E.; PINILLOS GARCÍA M. & SÁNCHEZ GARCÍA, M. M. (2015). *Estudio de las posibilidades de crecimiento de la superficie de viñedo en la DOC Rioja: Parte primera. Resumen ejecutivo*. Ed. by ORGANIZACIÓN INTERPROFESIONAL DEL VINO DE RIOJA. Logroño, Spain.

AQUILUÉ, N.; CÁCERES, M. de; FORTIN, M.-J.; FALL, A. & BROTONS, L. (2017). 'A spatial allocation procedure to model land-use/land-cover changes: Accounting for occurrence and spread processes'. In: *Ecological Modelling* vol. 344, pp. 73–86.

ARAÚJO, M. B. & NEW, M. (2007). 'Ensemble forecasting of species distributions'. In: *Trends in Ecology & Evolution* vol. 22, no. 1, pp. 42–47.

AUS DER BEEK, T.; FLÖRKE, M.; LAPOLA, D. M.; SCHALDACH, R.; VOSS, F. & TEICHERT, E. (2010). 'Modelling historical and current irrigation water demand on the continental scale: Europe'. In: *Advances in Geosciences* vol. 27, pp. 79–85.

AYUNTAMIENTO DE JACA (2020). *Jaca y el Camino de Santiago*. URL: https://www.jaca.es/cultura/santiago/jaca-y-el-camino-de-santiago.html (visited on 21/01/2020).

BASSE, R. M.; OMRANI, H.; CHARIF, O.; GERBER, P. & BÓDIS, K. (2014). 'Land use changes modelling using advanced methods: Cellular automata and artificial neural networks. The spatial and explicit representation of land cover dynamics at the cross-border region scale'. In: *Applied Geography* vol. 53, pp. 160–171.

BATALLA, M.; NINYEROLA, M. & TRAPERO, L. (2016). *ACDA: Andorran Climate Digital Atlas (period 1981-2010). Map server.* URL: `http://opengis.uab.es/wms/ACDA/index.htm` (visited on 23/01/2020).

BATALLA, R. J.; GÓMEZ, C. M. & KONDOLF, G. (2004). 'Reservoir-induced hydrological changes in the Ebro River basin (NE Spain)'. In: *Journal of Hydrology* vol. 290, no. 1-2, pp. 117–136.

BISWAS, A. K. & TORTAJADA, C. (2003). 'An assessment of the Spanish national hydrological plan'. In: *International Journal of Water Resources Development* vol. 19, no. 3, pp. 377–397.

BOITHIAS, L.; ACUÑA, V.; VERGOÑÓS, L.; ZIV, G.; MARCÉ, R. & SABATER, S. (2014). 'Assessment of the water supply: demand ratios in a Mediterranean basin under different global change scenarios and mitigation alternatives'. In: *The Science of the Total Environment* vol. 470-471, pp. 567–577.

BOLETÍN OFICIAL DEL ESTADO 161 (06/07/2001). *Ley 10/2001, de 5 de julio, PLAN HIDROLÓGICO NACIONAL.*

BOSSARD, M.; FERANEC, J. & OTAHEL, J. (2000). *CORINE land cover technical guide - Addendum 2000*. Ed. by EUROPEAN ENVIRONMENT AGENCY. Copenhagen, Denmark.

BRINER, S.; ELKIN, C.; HUBER, R. & GRÊT-REGAMEY, A. (2012). 'Assessing the impacts of economic and climate changes on land-use in mountain regions: A spatial dynamic modeling approach'. In: *Agriculture, Ecosystems & Environment* vol. 149, pp. 50–63.

BRITISCH GEOLOGICAL SURVEY (2020). *The Anthropocene*. URL: `http://www.bgs.ac.uk/anthropocene/` (visited on 05/02/2020).

BRITZ, W.; VERBURG, P. H. & LEIP, A. (2011). 'Modelling of land cover and agricultural change in Europe: Combining the CLUE and CAPRI-Spat approaches'. In: *Agriculture, Ecosystems & Environment* vol. 142, no. 1-2, pp. 40–50.

BROVKIN, V.; BOYSEN, L.; ARORA, V. K.; BOISIER, J. P.; CADULE, P.; CHINI, L.; CLAUSSEN, M.; FRIEDLINGSTEIN, P.; GAYLER, V.; VAN DEN HURK, B. J. J. M.; HURTT, G. C.; JONES, C. D.; KATO, E.; NOBLET-DUCOUDRÉ, N. de; PACIFICO, F.; PONGRATZ, J. & WEISS, M. (2013). 'Effect of Anthropogenic Land-Use and Land-Cover Changes on Climate and Land Carbon Storage in CMIP5 Projections for the Twenty-First Century'. In: *Journal of Climate* vol. 26, no. 18, pp. 6859–6881.

BÜTTNER, G. & MAUCHA, G. (2006). *The thematic accuracy of Corine land cover 2000*. Ed. by EUROPEAN ENVIRONMENT AGENCY. Copenhagen, Denmark.

CENTRO DE ESTÚDIOS Y EXPERIMENTACIÓN DE OBRAS PÚBLICAS (2017). *Evaluación del impacto del cambio climático en los recursos hídricos y sequías en España: Informe Técnico para el Ministerio de Agricultura y Pesca, Alimentación y Medio Ambiente*. Madrid, Spain.

CGIAR-CONSORTIUM FOR SPATIAL INFORMATION (2015). *CGIAR-SRTM data*. URL: `http://srtm.csi.cgiar.org/srtmdata/` (visited on 31/10/2019).

CHAUDHURI, G. & CLARKE, K. (2013). 'The SLEUTH land use change model: A review'. In: *International Journal of Environmental Resources Research* vol. 1, no. 1.

CONFEDERACIÓN HIDROGRÁFICA DEL EBRO (CHE) (July 2013). 'Anejo II Inventario de recursos hídricos'. In: *Propuesta de proyecto de Plan Hidrológico 2010-2015 de la cuenca del Ebro. Memoria*.

— (2013). 'Anejo III Usos y demandas de agua'. In: *Propuesta de proyecto de Plan Hidrológico 2010-2015 de la cuenca del Ebro. Memoria*.

— (2015). *PLAN HIDROLÓGICO de la parte española de la DEMARCACIÓN HIDROGRÁFICA DEL EBRO 2015-2021. Memoria*.

— (2018). *Plan Hidrológico de la Demarcación Hidrográfica del Ebro. Revisión de tercer ciclo (2021-2027): Documentos iniciales. Programa, calendario, estudio general sobre la demarcación y fórmulas de consulta*. Ed. by CONFEDERACIÓN HIDROGRÁFICA DEL EBRO.

CROLS, T.; WHITE, R.; ULJEE, I.; POELMANS, L.; ENGELEN, G. & CANTERS, F. (2017). 'High-resolution of population-density change with an activity-based cellular automata land-use model.' In: *Proceedings of GeoComputation 2017*.

CRUTZER, P. J. & STOERMER, E. F. (2000). 'The Anthopocene'. In: *International Geosphere-Biosphere Programme Newsletter*, no. 41, pp. 17–18.

DANG, A. N. & KAWASAKI, A. (2016). 'A Review of Methodological Integration in Land-Use Change Models'. In: *International Journal of Agricultural and Environmental Information Systems* vol. 7, no. 2, pp. 1–25.

DE ROO, A.; BISSELINK, B.; BECK, H.; BERNHARD, J.; BUREK, P.; REYNAUD, A.; PASTORI, M.; LAVALLE, C.; JACOBS-CRISTIONI, C.; BARANZELLI, C.; ZAJAC, Z. & DOSIO, A. (2016). *Modelling water demand and availability scenarios for current and future land use and climate in the Sava River Basin: Addressing the water-food-energy-ecosystem nexus*. Ed. by JOINT RESEARCH CENTRE. (Visited on).

DE ROO, A.; BUREK, P.; GENTILE, A.; UDIAS, A.; BOURAOUI, F.; ALOE, A.; BIANCHI, A.; LA NOTTE, A.; KUIK, O.; ELORZA TENREIRO, J.; VANDECASTEELE, I.; MUBAREKA, S.; BARANZELLI, C.; DER PERK, M. V. & BIDOGLIO, G. (2012). *A multi-criteria optimisation of scenarios for the protection of water resources in Europe: RC Scientific and Policy Reports*. Ed. by JOINT RESEARCH CENTRE.

DELGADO, J.; LLORENS, P.; NORD, G.; CALDER, I. R. & GALLART, F. (2010). 'Modelling the hydrological response of a Mediterranean medium-sized headwater basin subject to land cover change: The Cardener River basin (NE Spain)'. In: *Journal of Hydrology* vol. 383, no. 1-2, pp. 125–134.

DEMETROPOULOU, L.; NIKOLAIDIS, N.; PAPADOULAKIS, V.; TSAKIRIS, K.; KOUSSOURIS, T.; KALOGERAKIS, N.; KOUKARAS, K.; CHATZINIKOLAOU, A. & THEODOROPOULOS, K. (2010). 'Water framework directive implementation in Greece: Introducing participation in water governance - the Case of the Evrotas River Basin management plan'. In: *Environmental Policy and Governance* vol. 20, no. 5, pp. 336–349.

DESER, C.; PHILLIPS, A.; BOURDETTE, V. & TENG, H. (2012). 'Uncertainty in climate change projections: the role of internal variability'. In: *Climate Dynamics* vol. 38, no. 3-4, pp. 527–546.

DOSIO, A. (2016). 'Projections of climate change indices of temperature and precipitation from an ensemble of bias-adjusted high-resolution EURO-CORDEX regional climate models'. In: *Journal of Geophysical Research: Atmospheres* vol. 121, no. 10, pp. 5488–5511.

DOUGHERTY, T. C.; HALL, A. W. & WALLINGFORD, H. R. (1995). *Environmental Impact Assessment of Irrigation and Drainage Projects: FAO Irrigation and Drainage Paper 53*. Ed. by FOOD AND AGRICULTURE ORGANIZATION OF THE UNITED NATIONS.

DU, T.; KANG, S.; ZHANG, X. & ZHANG, J. (2014). 'China's food security is threatened by the unsustainable use of water resources in North and Northwest China'. In: *Food and Energy Security* vol. 3, no. 1, pp. 7–18.

DUMONT, A.; MAYOR, B. & LÓPEZ-GUNN, E. (2013). 'Is the Rebound Effect or Jevons Paradox a Useful Concept for better Management of Water Resources? Insights from the Irrigation Modernisation Process in Spain'. In: *Aquatic Procedia* vol. 1, pp. 64–76.

European Commission (2007). *Mediterranean water scarcity and drought report. Technical report on water scarcity in the Mediterranean and the Water Framework Directive*. (Visited on 26/11/2019).

— (2019a). *5th Report from the Commission to the European Parliament and the Council on the implementation of the Water Framework Directive (2000/60/EC) and the Floods Directive (2007/60/EC).*

— (2019b). *Introduction to the EU Water Framework Directive*. URL: `http://ec.europa.eu/environment/water/water-framework/info/intro_en.htm` (visited on 18/07/2019).

— (2019c). *The EU Water Framework Directive - integrated river basin management for Europe*. URL: `https://ec.europa.eu/environment/water/water-framework/index_en.html` (visited on 24/10/2019).

— (2019d). *WFD and FD Implementation Reports*. URL: `https://ec.europa.eu/environment/water/water-framework/impl_reports.htm` (visited on 18/07/2019).

European Commission & Joint Research Centre (2011). *Annual water abstraction irrigation 2030 (dataset)*. URL: `https://data.jrc.ec.europa.eu/dataset/5f4e4d2b-8706-4bf2-9faa-af7e648e6e69` (visited on 23/01/2020).

European Environment Agency (2013a). *CORINE Land Cover 1990 raster data (Version 17)*. Copenhagen, Denmark. URL: `https://land.copernicus.eu/pan-european/corine-land-cover/clc-1990?tab=metadata` (visited on 23/01/2020).

— (2013b). *CORINE Land Cover 2000 raster data (Version 17)*. Copenhagen, Denmark. URL: `https://www.eea.europa.eu/data-and-maps/data/clc-2000-raster` (visited on 23/01/2020).

— (2013c). *CORINE Land Cover 2006 raster data (Version 17)*. Copenhagen, Denmark. URL: `https://www.eea.europa.eu/data-and-maps/data/clc-2006-raster-3` (visited on 23/01/2020).

— (2014a). *Nationally designated areas (CDDA). Version 12*. URL: `https://www.eea.europa.eu/data-and-maps/data/nationally-designated-areas-national-cdda-9` (visited on 23/01/2020).

— (2014b). *Natura 2000 data - the European network of protected sites (Version 22 May 2014*. URL: `https://www.eea.europa.eu/data-and-maps/data/natura-5` (visited on 23/01/2020).

— (2016a). *CORINE Land Cover 2006 raster data (Version 18.5.1)*. Copenhagen, Denmark. URL: `https://land.copernicus.eu/pan-european/corine-land-cover/clc-2006?tab=metadata` (visited on 23/01/2020).

— (2016b). *CORINE Land Cover 2012 raster data (Version 18.4)*. Copenhagen, Denmark. URL: `https://land.copernicus.eu/pan-european/corine-land-cover/clc-2012?tab=metadata` (visited on 23/01/2020).

— (2018a). *CORINE Land Cover 2018 raster data (Version 20)*. Copenhagen, Denmark. URL: `https://land.copernicus.eu/pan-european/corine-land-cover/clc2018?tab=metadata` (visited on 23/01/2020).

— (2018b). *River basin districts with a WEI+ greater than 20 % in summer*. URL: `https://www.eea.europa.eu/data-and-maps/daviz/averaged-water-exploitation-index-at-1#tab-chart_1` (visited on 04/02/2020).

European Topic Centre on Inland, Coastal and Marine Waters (2016). *Use of freshwater resources in Europe 2002–2012. Supplementary document to the European Environment Agency's core set indicator 018: ETC/ICM Technical Report 1/2016,* Magdeburg, Germany.

Fader, M.; Shi, S.; Bloh, W. von; Bondeau, A. & Cramer, W. (2016). 'Mediterranean irrigation under climate change: more efficient irrigation needed to compensate for increases in irrigation water requirements'. In: *Hydrology and Earth System Sciences* vol. 20, no. 2, pp. 953–973.

FAERGEMANN, H. (2012). *Update on Water Scarcity and Droughts indicator development*.

FEDERACIÓ ECOLOGISTES EN ACCIÓ DE CATALUNYA (2012). *Alegaciones a la "propuesta de proyecto del plan hidrológico de la cuenca en la parte española de la demarcación hirdográfica del Ebro" publicado en el BOE N 114 de 12 de mayo de 2012*. URL: `https://spip.ecologistasenaccion.org/IMG/pdf/Alegaciones_Ecologistes_en_Accio.pdf` (visited on 03/11/2016).

FERANEC, J.; HAZEU, G.; CHRISTENSEN, S. & JAFFRAIN, G. (2007). 'Corine land cover change detection in Europe (case studies of the Netherlands and Slovakia)'. In: *Land Use Policy* vol. 24, no. 1, pp. 234–247.

FOOD AND AGRICULTURE ORGANIZATION (2016a). *AQUASTAT website. Did you know...? Facts and figures about irrigation areas, irrigated crops, environment*. URL: `http://www.fao.org/nr/water/aquastat/didyouknow/index3.stm` (visited on 23/10/2019).

— (2016b). *AQUASTAT website. Did you know...? Facts and figures about water withdrawal and pressure on water resources*. URL: `http://www.fao.org/nr/water/aquastat/didyouknow/index2.stm` (visited on 23/10/2019).

FORZIERI, G.; FEYEN, L.; ROJAS, R.; FLÖRKE, M.; WIMMER, F. & BIANCHI, A. (2014). 'Ensemble projections of future streamflow droughts in Europe'. In: *Hydrology and Earth System Sciences* vol. 18, no. 1, pp. 85–108.

FOX, J.; VOGLER, J. B.; SEN, O. L.; GIAMBELLUCA, T. W. & ZIEGLER, A. D. (2012). 'Simulating Land-Cover Change in Montane Mainland Southeast Asia'. In: *Environmental management* vol. 49, no. 5, pp. 968–979.

FRAME, B.; LAWRENCE, J.; AUSSEIL, A.-G.; REISINGER, A. & DAIGNEAULT, A. (2018). 'Adapting global shared socio-economic pathways for national and local scenarios'. In: *Climate Risk Management* vol. 21, pp. 39–51.

FRANQUET I BERNIS, J. M. (2009). *El caudal mínimo medioambiental del tramo inferior del río Ebro*. Tortosa, Spain: UNED-Tortosa.

GAMPE, D.; NIKULIN, G. & LUDWIG, R. (2016). 'Using an ensemble of regional climate models to assess climate change impacts on water scarcity in European river basins'. In: *The Science of the Total Environment*.

GAMVROUDIS, C.; NIKOLAIDIS, N. P.; TZORAKI, O.; PAPADOULAKIS, V. & KARALEMAS, N. (2015). 'Water and sediment transport modeling of a large temporary river basin in Greece'. In: *The Science of the Total Environment* vol. 508, pp. 354–365.

GARCÍA-RUIZ, J. M.; LÓPEZ-MORENO, J. I.; VICENTE-SERRANO, S. M.; LASANTA, T. & BEGUERÍA, S. (2011). 'Mediterranean water resources in a global change scenario'. In: *Earth-Science Reviews* vol. 105, no. 3-4, pp. 121–139.

GEOFABRIK GMBH (2018). *OpenStreetMap Download for Greece*. URL: `http://download.geofabrik.de/europe/greece.html` (visited on 31/10/2019).

GIORGI, F.; JONES, C. & ASRAR, G. R. (2009). 'Addressing climate information needs at the regional level: the CORDEX framework'. In: *WMO Bulletin* vol. 58, no. 3, pp. 175–183.

GONZÁLEZ-CEBOLLADA, C. (2016). 'Water and energy consumption after the modernization of irrigation in Spain'. In: *Sustainable development*. Ed. by C. A. BREBBIA. Vol. 1. WIT Transactions on The Built Environment. Southampton: WIT Press, pp. 457–465.

GRAHAM, L. P.; ANDRÉASSON, J. & CARLSSON, B. (2007). 'Assessing climate change impacts on hydrology from an ensemble of regional climate models, model scales and linking methods – a case study on the Lule River basin'. In: *Climatic Change* vol. 81, no. S1, pp. 293–307.

GREEK SPECIAL SECRETARIAT FOR WATER (2013). *River Basin Management Plan - Summary. Management Plan for the River Basins of Eastern Peloponnese River Basin District*.

HAGEN-ZANKER, A. & MARTENS, P. (2008). 'Map Comparison Methods for Comprehensive Assessment of Geosimulation Models'. In: *Computational Science and Its Applications – ICCSA 2008*. Ed. by O. GERVASI; B. MURGANTE; A. LAGANÀ; D. TANIAR; Y. MUN & M. L. GAVRILOVA. Berlin, Heidelberg: Springer Berlin Heidelberg, pp. 194–209.

HÄGGMARK, L.; IVARSSON, K.-I.; GOLLVIK, S. & OLOFSSON, P.-O. (2000). 'Mesan, an operational mesoscale analysis system'. In: *Tellus A: Dynamic Meteorology and Oceanography* vol. 52, no. 1, pp. 2–20.

HALLMANN, C. A.; SORG, M.; JONGEJANS, E.; SIEPEL, H.; HOFLAND, N.; SCHWAN, H.; STENMANS, W.; MÜLLER, A.; SUMSER, H.; HÖRREN, T.; GOULSON, D. & KROON, H. de (2017). 'More than 75 percent decline over 27 years in total flying insect biomass in protected areas'. In: *PloS one* vol. 12, no. 10.

HARRISON, P. A.; DUNFORD, R.; SAVIN, C.; ROUNSEVELL, M. D. A.; HOLMAN, I. P.; KEBEDE, A. S. & STUCH, B. (2015). 'Cross-sectoral impacts of climate change and socio-economic change for multiple, European land- and water-based sectors'. In: *Climatic Change* vol. 128, no. 3-4, pp. 279–292.

HAWKINS, E. & SUTTON, R. (2009). 'The Potential to Narrow Uncertainty in Regional Climate Predictions'. In: *Bulletin of the American Meteorological Society* vol. 90, no. 8, pp. 1095–1108.

HAYLOCK, M. R.; HOFSTRA, N.; KLEIN TANK, A. M. G.; KLOK, E. J.; JONES, P. D. & NEW, M. (2008). 'A European daily high-resolution gridded data set of surface temperature and precipitation for 1950–2006'. In: *Journal of Geophysical Research: Atmospheres* vol. 113.

HEDDERICH, J. & SACHS, L. (2012). *Angewandte Statistik: Methodensammlung mit R*. 14. Springer.

HELLENIC STATISTICAL AUTHORITY (2001). *Population and Housing Census 2001. Economic Characteristics*. URL: `https://www.statistics.gr/el/statistics/-/publication/SAM04/2001` (visited on 23/01/2020).

— (2009a). *Hotels, rooms for rent and tourist campsites / 2009*. URL: `https://www.statistics.gr/en/statistics/-/publication/STO12/2009` (visited on 31/10/2019).

— (2009b). *The Agricultural and Livestock Census of Greece 2009*.

— (2011). *Population and Housing Census 2011*. URL: `https://www.statistics.gr/el/statistics/-/publication/SAM04/2011` (visited on 23/01/2020).

HERRERO; GUTIÉRREZ-CÁNOVAS, C.; VIGIAK, O.; LUTZ, S.; KUMAR, R.; GAMPE, D.; HUBER GARCÍA, V.; LUDWIG, R.; BATALLA, R. & SABATER, S. (2018). 'Multiple stressor effects on biological quality elements in the Ebro River: Present diagnosis and predicted responses'. In: *Science of The Total Environment* vol. 630, pp. 1608–1618.

HERTEL, T. W. & TSIGAS, M. E. (1997). 'Structure of GTAP'. In: *Global Trade Analysis Modeling Applications*. Ed. by T. W. HERTEL. Cambridge: Cambridge University Press, pp. 13–73.

HSIANG, S.; KOPP, R.; JINA, A.; RISING, J.; DELGADO, M.; MOHAN, S.; RASMUSSEN, D.; MUIR-WOOD, R.; WILSON, P.; OPPENHEIMER, M.; LARSEN, K. & HOUSER, T. (2017). 'Estimating economic damage from climate change in the United States'. In: *Science* vol. 356, pp. 1362–1369.

HUANG, Z.; HEJAZI, M.; LI, X.; TANG, Q.; VERNON, C.; LENG, G.; LIU, Y.; DÖLL, P.; EISNER, S.; GERTEN, D.; HANASAKI, N. & WADA, Y. (2018). 'Reconstruction of global gridded monthly sectoral water withdrawals for 1971–2010 and analysis of their spatiotemporal patterns'. In: *Hydrology and Earth System Sciences* vol. 22, no. 4, pp. 2117–2133.

Huber García, V.; Lutz, S.; Wood, R. & Ludwig, R. (in prep.). 'Assessing water scarcity in the Ebro River Basin under scenarios of climate and land use change'. In: *Water*.

Huber García, V.; Meyer, S.; Kok, K.; Verweij, P. & Ludwig, R. (2018). 'Deriving spatially explicit water uses from land use change modelling results in four river basins across Europe'. In: *Science of The Total Environment* vol. 628-629, pp. 1079–1097.

Hurtt, G. C.; Chini, L. P.; Frolking, S.; Betts, R. A.; Feddema, J.; Fischer, G.; Fisk, J. P.; Hibbard, K.; Houghton, R. A.; Janetos, A.; Jones, C. D.; Kindermann, G.; Kinoshita, T.; Klein Goldewijk, K.; Riahi, K.; Shevliakova, E.; Smith, S.; Stehfest, E.; Thomson, A.; Thornton, P.; van Vuuren, D. P. & Wang, Y. P. (2011). 'Harmonization of land-use scenarios for the period 1500–2100: 600 years of global gridded annual land-use transitions, wood harvest, and resulting secondary lands'. In: *Climatic Change* vol. 109, no. 1-2, pp. 117–161.

Hurtt, G. C.; Chini, L. P.; Sahajpal, S. & Frolking, S. (in prep.). 'Harmonization of global land-use change and management for the period 850-2100'. In: *Geoscientific Model Development*.

IIASA (2016). *SSP Database (Shared Socioeconomic Pathways) - Version 1.1*. URL: `https://tntcat.iiasa.ac.at/SspDb/dsd?Action=htmlpage&page=about` (visited on 11/12/2018).

Institut d'Estudis Andorrans (1995). *Mapa de Cobertes del Sòl d'Andorra (1995)*.

Instituto Nacional de Estadística (2015). *Censos de Población y Viviendas 2011. Resultados Municipales*.

Intergovernmental Science-Policy Platform on Biodiversity and Ecosystem Services (2019). *Report of the Plenary of the Intergovernmental Science-Policy Platform on Biodiversity and Ecosystem Services on the work of its seventh session. Addendum: Summary for policymakers*.

IPCC (2013). 'Summary for Policymakers'. In: *Climate Change 2013: The Physical Science Basis. Contribution of Working Group I to the Fifth Assessment Report of the Intergovernmental Panel on Climate Change*. Ed. by T. F. Stocker; G.-K. Plattner; M. Tignor; S. K. Allen; J. Boschung; A. Nauels; Y. Xia; V. Bex & P. M. Midgley. Cambridge, United Kingdom & New York, NY, USA: Cambridge University Press.

— (2014a). *Climate Change 2014: Impacts, Adaptation and Vulnerability. Part A: Global and Sectoral Aspects. Contribution of Working Group II to the Fifth Assessment Report of the Intergovernmental Panel on Climate Change*. Cambridge, United Kingdom & New York, NY, USA: Cambridge University Press.

— (2014b). 'Summary for Policy Makers'. In: *Climate Change 2014: Mitigation of Climate Change. Contribution of Working Group III to the Fifth Assessment Report of the Assessment Report of the Intergovernmental Panel on Climate ChangeIntergovernmental Panel on Cliamte Change*. Ed. by Intergovernmental Panel on Climate Change. Cambridge, United Kingdom & New York, NY, USA: Cambridge University Press.

Jacob, D.; Petersen, J.; Eggert, B.; Alias, A.; Christensen, O. B.; Bouwer, L. M.; Braun, A.; Colette, A.; Déqué, M.; Georgievski, G.; Georgopoulou, E.; Gobiet, A.; Menut, L.; Nikulin, G.; Haensler, A.; Hempelmann, N.; Jones, C.; Keuler, K.; Kovats, S.; Kröner, N.; Kotlarski, S.; Kriegsmann, A.; Martin, E.; van Meijgaard, E.; Moseley, C.; Pfeifer, S.; Preuschmann, S.; Radermacher, C.; Radtke, K.; Rechid, D.; Rounsevell, M. D. A.; Samuelsson, P.; Somot, S.; Soussana, J.-F.; Teichmann, C.; Valentini, R.; Vautard, R.; Weber, B. & Yiou, P. (2014). 'EURO-CORDEX: new high-resolution climate change projections for European impact research'. In: *Regional Environmental Change* vol. 14, no. 2, pp. 563–578.

Jorda-Capdevila, D.; Gampe, D.; Huber García, V.; Ludwig, R.; Sabater, S.; Vergoñós, L. & Acuña, V. (2019). 'Impact and mitigation of global change on freshwater-related ecosystem services in Southern Europe'. In: *Science of The Total Environment* vol. 651, pp. 895–908.

Kankaanpää, S. & Carter, T. R. (2004). *Construction of European forest land use scenarios for the 21st century*. Vol. 707. Helsinki, Finnland: Finnish Environment Institute.

Karaouzas, I.; Theodoropoulos, C.; Vardakas, L.; Kalogianni, E. & Th. Skoulikidis, N. (2018). 'A review of the effects of pollution and water scarcity on the stream biota of an intermittent Mediterranean basin'. In: *River Research and Applications* vol. 34, no. 4, pp. 291–299.

KC, S. & Lutz, W. (2017). 'The human core of the shared socioeconomic pathways: Population scenarios by age, sex and level of education for all countries to 2100'. In: *Global environmental change : human and policy dimensions* vol. 42, pp. 181–192.

Kebede, A. S.; Nicholls, R. J.; Allan, A.; Arto, I.; Cazcarro, I.; Fernandes, J. A.; Hill, C. T.; Hutton, C. W.; Kay, S.; Lázár, A. N.; Macadam, I.; Palmer, M.; Suckall, N.; Tompkins, E. L.; Vincent, K. & Whitehead, P. W. (2018). 'Applying the global RCP-SSP-SPA scenario framework at sub-national scale: A multi-scale and participatory scenario approach'. In: *The Science of the total environment* vol. 635, pp. 659–672.

Ker Rault, P. (2017). 'Down-scaling IPCC Climate Change Scenarios at River scale Level'. In: *7th GLOBAQUA project newsletter*, p. 5. URL: `http://www.globaqua-project.eu/files/repository/20170828125350_GLOBAQUA_NEWSLETTER_JUL_2017_WEB_HR_v6.pdf` (visited on 29/11/2018).

Ker Rault, P.; Koundouri, P.; Akinsete, E.; Ludwig, R.; Huber-Garcia, V.; Tsani, S.; Acuna, V.; Kalogianni, E.; Luttik, J.; Kok, K.; Skoulikidis, N. & Froebrick, J. (2018). 'Down scaling of climate change scenarii to river basin level: A transdisciplinary methodology applied to Evrotas river basin, Greece'. In: *Science of The Total Environment* vol. 660, pp. 1623–1632.

Kim, J.; Choi, J.; Choi, C. & Park, S. (2013). 'Impacts of changes in climate and land use/land cover under IPCC RCP scenarios on streamflow in the Hoeya River Basin, Korea'. In: *The Science of the total environment* vol. 452-453, pp. 181–195.

Klein Goldewijk, K.; Beusen, A. & Janssen, P. (2010). 'Long-term dynamic modeling of global population and built-up area in a spatially explicit way: HYDE 3.1'. In: *The Holocene* vol. 20, no. 4, pp. 565–573.

Kok, K. (2004). 'The role of population in understanding Honduran land use patterns'. In: *Journal of environmental management* vol. 72, no. 1-2, pp. 73–89.

Kok, K.; Farrow, A.; Veldkamp, A. T. & Verburg, P. H. (2001). 'A method and application of multi-scale validation in spatial land use models'. In: *Agriculture, Ecosystems & Environment* vol. 85, no. 1-3, pp. 223–238.

Konzmann, M.; Gerten, D. & Heinke, J. (2013). 'Climate impacts on global irrigation requirements under 19 GCMs, simulated with a vegetation and hydrology model'. In: *Hydrological Sciences Journal* vol. 58, no. 1, pp. 88–105.

Kotlarski, S.; Keuler, K.; Christensen, O. B.; Colette, A.; Déqué, M.; Gobiet, A.; Goergen, K.; Jacob, D.; Lüthi, D.; van Meijgaard, E.; Nikulin, G.; Schär, C.; Teichmann, C.; Vautard, R.; Warrach-Sagi, K. & Wulfmeyer, V. (2014). 'Regional climate modeling on European scales: a joint standard evaluation of the

EURO-CORDEX RCM ensemble'. In: *Geoscientific Model Development* vol. 7, no. 4, pp. 1297–1333.

KOUNDOURI, P.; SOULIOTIS, I. & LEVANTIS, E. (2016). 'Sub-Deliverable 9.2 Integration of the GARB-specific results of STEPS 1A and 1B of the implementation of the WFD: Integrating the results on the assessment of the importance of water resources ecosystem services to the economy and socio-economic development of the GARBs and socio-economic scenarios'. In: *GLOBAQUA Deliverable 004: Importance of ecosystem services to the economy and socio-economic development*. Ed. by V. ACUÑA; L. VERGONYOS; M. TERRADO; R. LUDWIG; V. HUBER GARCÍA; S. MEYER; P. KOUNDOURI; I. SOULIOTIS; E. LEVANTIS; P. KER RAULT; J. LUTTIK & A. PISTOCCHI.

KRIEGLER, E.; EDMONDS, J. A.; HALLEGATTE, S.; EBI, K. L.; KRAM, T.; RIAHI, K.; WINKLER, H. & VAN VUUREN, D. P. (2014). 'A new scenario framework for climate change research: the concept of shared climate policy assumptions'. In: *Climatic Change* vol. 122, no. 3, pp. 401–414.

KUMAR, R.; LIVNEH, B. & SAMANIEGO, L. (2013a). 'Towards computationally efficient large-scale hydrologic predictions with a multiscale regionalization scheme'. In: *Water Resources Research* vol. 49, no. 9, pp. 5700–5714.

KUMAR, R.; SAMANIEGO, L. & ATTINGER, S. (2013b). 'Implications of distributed hydrologic model parameterization on water fluxes at multiple scales and locations'. In: *Water Resources Research* vol. 49, no. 1, pp. 360–379.

KUMMU, M.; WARD, P. J.; MOEL, H. de & VARIS, O. (2010). 'Is physical water scarcity a new phenomenon? Global assessment of water shortage over the last two millennia'. In: *Environmental Research Letters* vol. 5, no. 3.

LASANTA-MARTÍNEZ, T.; VICENTE-SERRANO, S. M. & CUADRAT-PRATS, J. M. (2005). 'Mountain Mediterranean landscape evolution caused by the abandonment of traditional primary activities: a study of the Spanish Central Pyrenees'. In: *Applied Geography* vol. 25, no. 1, pp. 47–65.

LAVALLE, C.; BATISTA E SILVA, F.; BARANZELLI, C.; JACOBS-CRISIONI, C.; VANDECASTEELE, I.; BARBOSA, A. L.; MAES, J.; ZULIAN, G.; PERPIÑA, C.; BARRANCO, R. & VALLECILLO, S. (2016). 'Land Use and Scenario Modeling for Integrated Sustainability Assessment'. In: *European Landscape Dynamics. CORINE Land Cover Data*. Ed. by J. FERANEC; T. SOUKUP; G. HAZEU & G. JAFFRAIN. Vol. 24. CRC Press, pp. 237–262.

LAWRENCE, D. M.; HURTT, G. C.; ARNETH, A.; BROVKIN, V.; CALVIN, K. V.; JONES, A. D.; JONES, C. D.; LAWRENCE, P. J.; NOBLET-DUCOUDRÉ, N. de; PONGRATZ, J.; SENEVIRATNE, S. I. & SHEVLIAKOVA, E. (2016). 'The Land Use Model Intercomparison Project (LUMIP) contribution to CMIP6: rationale and experimental design'. In: *Geoscientific Model Development* vol. 9, no. 9, pp. 2973–2998.

LECINA, S.; ISIDORO, D.; PLAYÁN, E. & ARAGÜÉS, R. (2010). 'Irrigation Modernization in Spain: Effects on Water Quantity and Quality—A Conceptual Approach'. In: *International Journal of Water Resources Development* vol. 26, no. 2, pp. 265–282.

LEDUC, M.; MAILHOT, A.; FRIGON, A.; MARTEL, J.-L.; LUDWIG, R.; BRIETZKE, G. B.; GIGUÈRE, M.; BRISSETTE, F.; TURCOTTE, R.; BRAUN, M. & SCINOCCA, J. (2019). 'The ClimEx Project: A 50-Member Ensemble of Climate Change Projections at 12-km Resolution over Europe and Northeastern North America with the Canadian Regional Climate Model (CRCM5)'. In: *Journal of Applied Meteorology and Climatology* vol. 58, no. 4, pp. 663–693.

LEVIS, S.; BADGER, A.; DREWNIAK, B.; NEVISON, C. & REN, X. (2018). 'CLMcrop yields and water requirements: avoided impacts by choosing RCP 4.5 over 8.5'. In: *Climatic Change* vol. 146, no. 3-4, pp. 501–515.

LIU, X.; LIANG, X.; LI, X.; XU, X.; OU, J.; CHEN, Y.; LI, S.; WANG, S. & PEI, F. (2017). 'A future land use simulation model (FLUS) for simulating multiple land use scenarios by coupling human and natural effects'. In: *Landscape and Urban Planning* vol. 168, pp. 94–116.

LÓPEZ-MORENO, J. I.; VICENTE-SERRANO, S. M.; ZABALZA, J.; BEGUERÍA, S.; LORENZO-LACRUZ, J.; AZORIN-MOLINA, C. & MORÁN-TEJEDA, E. (2013). 'Hydrological response to climate variability at different time scales: A study in the Ebro basin'. In: *Journal of Hydrology* vol. 477, pp. 175–188.

LÓPEZ-MORENO, J. I.; ZABALZA, J.; VICENTE-SERRANO, S. M.; REVUELTO, J.; GIL-ABERTE, M.; AZORIN-MOLINA, C.; MORÁN-TEJEDA, E.; GARCÍA-RUIZ, J. M. & TAGUE, C. (2014). 'Impact of climate and land use change on water availability and reservoir management: scenarios in the Upper Aragón River, Spanish Pyrenees'. In: *The Science of the Total Environment* vol. 493, pp. 1222–1231.

LUO, G.; YIN, C.; CHEN, X.; XU, W. & LU, L. (2010). 'Combining system dynamic model and CLUE-S model to improve land use scenario analyses at regional scale: A case study of Sangong watershed in Xinjiang, China'. In: *Ecological Complexity* vol. 7, no. 2, pp. 198–207.

LUYSSAERT, S.; JAMMET, M.; STOY, P. C.; ESTEL, S.; PONGRATZ, J.; CESCHIA, E.; CHURKINA, G.; DON, A.; ERB, K.; FERLICOQ, M.; GIELEN, B.; GRÜNWALD, T.; HOUGHTON, R. A.; KLUMPP, K.; KNOHL, A.; KOLB, T.; KUEMMERLE, T.; LAURILA, T.; LOHILA, A.; LOUSTAU, D.; MCGRATH, M. J.; MEYFROIDT, P.; MOORS, E. J.; NAUDTS, K.; NOVICK, K.; OTTO, J.; PILEGAARD, K.; PIO, C. A.; RAMBAL, S.; REBMANN, C.; RYDER, J.; SUYKER, A. E.; VARLAGIN, A.; WATTENBACH, M. & DOLMAN, A. J. (2014). 'Land management and land-cover change have impacts of similar magnitude on surface temperature'. In: *Nature Climate Change* vol. 4, no. 5, pp. 389–393.

MALEK, Ž. & VERBURG, P. H. (2018). 'Adaptation of land management in the Mediterranean under scenarios of irrigation water use and availability'. In: *Mitigation and adaptation strategies for global change* vol. 23, no. 6, pp. 821–837.

MALLAMPALLI, V. R.; MAVROMMATI, G.; THOMPSON, J.; DUVENECK, M.; MEYER, S.; LIGMANN-ZIELINSKA, A.; DRUSCHKE GOTTSCHALK, C.; HYCHKA, K.; KENNEY, M. A.; KOK, K. & BORSUK, M. E. (2016). 'Methods for translating narrative scenarios into quantitative assessments of land use change'. In: *Environmental Modelling & Software* vol. 82, pp. 7–20.

MARCOS FERNÁNDEZ, A. de (2016). *River Basins and Water Management in Spain. Tagus and Ebro River Basin Districts: an account of their current situation and main problems*. Ed. by EUROPEAN PARLIAMENT'S POLICY DEPARTMENT FOR CITIZENS' RIGHT AND CONSTITUTIONAL AFFAIRS.

MARKE, T. (2008). 'Development and Application of a Model Interface to couple Land Surface Models with Regional Climate Models for Climate Change Risk Assessment in the Upper Danube Watershed'. Dissertation. Munich, Germany: Fakultät für Geowissenschaften, Ludwig-Maximilians-Universität München.

MAS, J.-F.; KOLB, M.; PAEGELOW, M.; CAMACHO OLMEDO, M. T. & HOUET, T. (2014). 'Inductive pattern-based land use/cover change models: A comparison of four software packages'. In: *Environmental Modelling & Software* vol. 51, pp. 94–111.

MEEHL, G. A.; COVEY, C.; DELWORTH, T.; LATIF M.; MCAVANEY, B.; MITCHELL, J. F. B.; STOUFFER, R. J. & TAYLOR, K. E. (2007). 'The WCRP CMIP3 Multimodel Dataset: A new Era in Climate Change Research'. In: *Bulletin of the American Meteorological Society* vol. 88, pp. 1383–1394.

MEHDI, B.; LUDWIG, R. & LEHNER, B. (2015). 'Evaluating the impacts of climate change and crop land use change on streamflow, nitrates and phosphorus: A modeling study in Bavaria'. In: *Journal of Hydrology: Regional Studies* vol. 4, pp. 60–90.

MEIER, J.; ZABEL, F. & MAUSER, W. (2018). 'A global approach to estimate irrigated areas - a comparison between different data and statistics'. In: *Hydrology and Earth System Sciences* vol. 22, no. 2, pp. 1119–1133.

MINISTERIO DE AGRICULTURA Y PESCA, ALIMENTACIÓN Y MEDIO AMBIENTE (2007). *Cuencas hidrográficas de los principales ríos definidos en el artículo 3 de la Directiva Marco del Agua (DMA)*. Madrid, Spain. URL: https://www.mapama.gob.es/ide/metadatos/index.html?srv=main.search&category=CategAgua&sortBy=title&sortOrder=descending (visited on 07/2019).

MINISTERIO PARA LA TRANSICIÓN ECOLÓGICA (2018). *Informe de seguimiento de los planes hidrológicos de cuenca y de los recursos hídricos en España. Año 2017*.

MINISTRY OF DEVELOPMENT OF GREECE (2005). *Development of systems and management tools for the water resources of the West Peloponnese, North Peloponnese and East Peloponnese water districts (01, 02, 03), B Phase Infrastructure Analysis - Uses, Water Resources Management and Development Plans (in Greek)*.

MOSS, R. H.; EDMONDS, J. A.; HIBBARD, K. A.; MANNING, M. R.; ROSE, S. K.; VAN VUUREN, D. P.; CARTER, T. R.; EMORI, S.; KAINUMA, M.; KRAM, T.; MEEHL, G. A.; MITCHELL, J. F. B.; NAKICENOVIC, N.; RIAHI, K.; STOUFFER, R. J.; THOMSON, A. M.; WEYANT, J. P. & WILBANKS, T. J. (2010). 'The next generation of scenarios for climate change research and assessment'. In: *Nature* vol. 463, no. 7282, pp. 747–756.

MOULDS, S.; BUYTAERT, W. & MIJIC, A. (2015). 'An open and extensible framework for spatially explicit land use change modelling: the lulcc R package'. In: *Geoscientific Model Development* vol. 8, no. 10, pp. 3215–3229.

NAJAFI, M. R. & MORADKHANI, H. (2015). 'Multi-model ensemble analysis of runoff extremes for climate change impact assessments'. In: *Journal of Hydrology* vol. 525, pp. 352–361.

NAKICENOVIC, N.; ALCAMO, J.; DAVIS, G.; VRIES, B. d.; FENHAM, J.; GAFFIN, S.; GREGORY, K.; GRUEBLER, A.; JUNG, T. Y.; KRAM, T.; LA ROVERE, E. L.; MICHAELIS, L.; MORI, S.; MORIT, T.; PEPPER, W.; PITCHER, H.; PRICE, L.; RIAHI, K.; ROEHRL, A.; ROGNER, H.-H.; SANKOVSKI, A.; SCHLESINGER, M.; SHUKLA, P.; SMITH, S.; SWART, R.; VAN ROOIJEN, S.; VICTOR, N. & DADI, Z. (2000). *Special report on emissions scenarios*. New York: Cambridge University Press.

NAVARRO-ORTEGA, A.; ACUÑA, V.; BELLIN, A.; BUREK, P.; CASSIANI, G.; CHOUKR-ALLAH, R.; DOLÉDEC, S.; ELOSEGI, A.; FERRARI, F.; GINEBREDA, A.; GRATHWOHL, P.; JONES, C.; RAULT, P. K.; KOK, K.; KOUNDOURI, P.; LUDWIG, R. P.; MERZ, R.; MILACIC, R.; MUÑOZ, I.; NIKULIN, G.; PANICONI, C.; PAUNOVIĆ, M.; PETROVIC, M.; SABATER, L.; SABATERB, S.; SKOULIKIDIS, N. T.; SLOB, A.; TEUTSCH, G.; VOULVOULIS, N. & BARCELÓ, D. (2015). 'Managing the effects of multiple stressors on aquatic ecosystems under water scarcity. The GLOBAQUA project'. In: *The Science of the Total Environment* vol. 503-504, pp. 3–9.

NEWBOLD, T.; HUDSON, L. N.; HILL, S. L. L.; CONTU, S.; LYSENKO, I.; SENIOR, R. A.; BÖRGER, L.; BENNETT, D. J.; CHOIMES, A.; COLLEN, B.; DAY, J.; PALMA, A. de; DÍAZ, S.; ECHEVERRIA-LONDOÑO, S.; EDGAR, M. J.; FELDMAN, A.; GARON, M.; HARRISON, M. L. K.; ALHUSSEINI, T.; INGRAM, D. J.; ITESCU, Y.; KATTGE, J.; KEMP, V.; KIRKPATRICK, L.; KLEYER, M.; CORREIA, D. L. P.; MARTIN, C. D.; MEIRI, S.; NOVOSOLOV, M.; PAN, Y.; PHILLIPS, H. R. P.; PURVES, D. W.; ROBINSON, A.; SIMPSON, J.; TUCK, S. L.; WEIHER, E.; WHITE, H. J.; EWERS, R. M.; MACE, G. M.; SCHARLEMANN, J. P. W. & PURVIS, A. (2015). 'Global effects of land use on local terrestrial biodiversity'. In: *Nature* vol. 520, no. 7545, pp. 45–50.

NIKOLAIDIS, N. P.; SKOULIKIDIS, N. T.; KALOGERAKIS, N. & TSAKIRIS, K. (2009). *Environmental Friendly Technologies for Rural Development. Final Report 2005-09*.

NINYEROLA, M.; PONS, X. & ROURE, J. M. (2005). *Atlas Climático Digital de la Península Ibérica. Metodología y aplicaciones en bioclimatología y geobotánica*. Bellaterra.

NOGUÉS, J. & HERRERO (2003). 'The impact of transition from flood to sprinkler irrigation on water district consumption'. In: *Journal of Hydrology* vol. 276, no. 1-4, pp. 37–52.

O'NEILL, B. C.; KRIEGLER, E.; EBI, K. L.; KEMP-BENEDICT, E.; RIAHI, K.; ROTHMAN, D. S.; VAN RUIJVEN, BAS J.; VAN VUUREN, D. P.; BIRKMANN, J.; KOK, K.; LEVY, M. & SOLECKI, W. (2017). 'The roads ahead: Narratives for shared socioeconomic pathways describing world futures in the 21st century'. In: *Global Environmental Change* vol. 42, pp. 169–180.

O'NEILL, B. C.; KRIEGLER, E.; RIAHI, K.; EBI, K. L.; HALLEGATTE, S.; CARTER, T. R.; MATHUR, R. & VAN VUUREN, D. P. (2014). 'A new scenario framework for climate change research: the concept of shared socioeconomic pathways'. In: *Climatic Change* vol. 122, no. 3, pp. 387–400.

O'NEILL, B. C.; TEBALDI, C.; VAN VUUREN, DETLEF P.; EYRING, V.; FRIEDLINGSTEIN, P.; HURTT, G.; KNUTTI, R.; KRIEGLER, E.; LAMARQUE, J.-F.; LOWE, J.; MEEHL, G. A.; MOSS, R.; RIAHI, K. & SANDERSON, B. M. (2016). 'The Scenario Model Intercomparison Project (ScenarioMIP) for CMIP6'. In: *Geoscientific Model Development* vol. 9, no. 9, pp. 3461–3482.

PIJANOWSKI, B. C.; SHELLITO, B.; PITHADIA, S. & ALEXANDRIDIS, K. (2002). 'Forecasting and assessing the impact of urban sprawl in coastal watersheds along eastern Lake Michigan'. In: *Lakes and Reservoirs: Research and Management* vol. 7, no. 3, pp. 271–285.

PIÑOLS, A. (2016). 'Miles de personas se manifiestan contra el Plan hidrológico del Ebro'. In: *El País*. URL: `https://elpais.com/ccaa/2016/06/05/catalunya/1465128257_975061.html` (visited on 23/01/2020).

PONGRATZ, J.; REICK, C.; RADDATZ, T. & CLAUSSEN, M. (2008). 'A reconstruction of global agricultural areas and land cover for the last millennium'. In: *Global Biogeochemical Cycles* vol. 22, no. 3.

PONGRATZ, J.; DOLMAN, H.; DON, A.; ERB, K.-H.; FUCHS, R.; HEROLD, M.; JONES, C.; KUEMMERLE, T.; LUYSSAERT, S.; MEYFROIDT, P. & NAUDTS, K. (2018). 'Models meet data: Challenges and opportunities in implementing land management in Earth system models'. In: *Global change biology* vol. 24, no. 4, pp. 1470–1487.

PONTIUS, R. G.; BOERSMA, W.; CASTELLA, J.-C.; CLARKE, K.; NIJS, T. d.; DIETZEL, C.; DUAN, Z.; FOTSING, E.; GOLDSTEIN, N.; KOK, K.; KOOMEN, E.; LIPPITT, C. D.; MCCONNELL, W.; SOOD., A. M.; PIJANOWSKI, B.; PITHADIA, S.; SWEENEY, S.; TRUNG, T. N.; VELDKAMP, A. T. & VERBURG, P. H. (2008). 'Comparing the input, output, and validation maps for several models of land change'. In: *The Annals of Regional Science* vol. 42, no. 1, pp. 11–37.

PONTIUS, R. G.; HUFFAKER, D. & DENMAN, K. (2004). 'Useful techniques of validation for spatially explicit land-change models'. In: *Ecological Modelling* vol. 179, no. 4, pp. 445–461.

PONTIUS, R. G.; PEETHAMBARAM, S. & CASTELLA, J.-C. (2011). 'Comparison of Three Maps at Multiple Resolutions: A Case Study of Land Change Simulation in Cho Don District, Vietnam'. In: *Annals of the Association of American Geographers* vol. 101, no. 1, pp. 45–62.

POPP, A.; CALVIN, K.; FUJIMORI, S.; HAVLIK, P.; HUMPENÖDER, F.; STEHFEST, E.; BODIRSKY, B. L.; DIETRICH, J. P.; DOELMANN, J. C.; GUSTI, M.; HASEGAWA, T.; KYLE, P.; OBERSTEINER, M.; TABEAU, A.; TAKAHASHI, K.; VALIN, H.; WALDHOFF,

S.; WEINDL, I.; WISE, M.; KRIEGLER, E.; LOTZE-CAMPEN, H.; FRICKO, O.; RIAHI, K. & VAN VUUREN, D. P. (2017). 'Land-use futures in the shared socio-economic pathways'. In: *Global Environmental Change* vol. 42, pp. 331–345.

PORTMANN, F. T.; SIEBERT, S. & DÖLL, P. (2010). 'MIRCA2000-Global monthly irrigated and rainfed crop areas around the year 2000: A new high-resolution data set for agricultural and hydrological modeling'. In: *Global Biogeochemical Cycles* vol. 24, no. 1.

R DEVELOPMENT CORE TEAM (2008). *R: A language and environment for statistical computing.* Vienna, Austria.

RAKOVEC, O.; KUMAR, R.; ATTINGER, S. & SAMANIEGO, L. (2016a). 'Improving the realism of hydrologic model functioning through multivariate parameter estimation'. In: *Water Resources Research* vol. 52, no. 10, pp. 7779–7792.

RAKOVEC, O.; KUMAR, R.; MAI, J.; CUNTZ, M.; THOBER, S.; ZINK, M.; ATTINGER, S.; SCHÄFER, D.; SCHRÖN, M. & SAMANIEGO, L. (2016b). 'Multiscale and Multivariate Evaluation of Water Fluxes and States over European River Basins'. In: *Journal of Hydrometeorology* vol. 17, no. 1, pp. 287–307.

RAMOS, M. C.; BALASCH, J. C. & MARTÍNEZ-CASASNOVAS, J. A. (2012). 'Seasonal temperature and precipitation variability during the last 60 years in a Mediterranean climate area of Northeastern Spain: a multivariate analysis'. In: *Theoretical and Applied Climatology* vol. 110, no. 1-2, pp. 35–53.

RASKIN, P.; GLEICK, P. H.; KIRSHEN, P.; PONTIUS JR., G. & STRZEPEK, K. (1997). *Comprehensive Assessment of the Freshwater Resources of the World*.

REGINSTER, I. & ROUNSEVELL, M. (2006). 'Scenarios of future urban land use in Europe'. In: *Environment and Planning B: Planning and Design* vol. 33, no. 4, pp. 619–636.

REY BENAYAS, J. M.; MARTINS, A.; NICOLAU, J. M. & SCHULZ, J. J. (2007). 'Abandonment of agricultural land: an overview of drivers and consequences'. In: *CAB Reviews: Perspectives in Agriculture, Veterinary Science, Nutrition and Natural Resources* vol. 2, no. 057.

RIAHI, K.; VAN VUUREN, D. P.; KRIEGLER, E.; EDMONDS, J. A.; O'NEILL, B. C.; FUJIMORI, S.; BAUER, N.; CALVIN, K.; DELLINK, R.; FRICKO, O.; LUTZ, W.; POPP, A.; CUARESMA, J. C.; KC, S. LEIMBACH, M.; JIANG, L.; KRAM, T.; RAO, S.; EMMERLING, J.; EBI, K. L.; HASEGAWA, T.; HAVLIK, P.; HUMPENÖDER, F.; DA SILVA, L. A.; SMITH, S.; STEHFEST, E.; BOSETTI, V.; EOM, J.; GERNAAT, D.; MASUI, T.; ROGELJ, J.; STREFLER, J.; DROUET, L.; KREY, V. LUDERER, G.; HARMSEN, M.; TAKAHASHI, K.; BAUMSTARK, L.; DOELMAN, J. C.; KAINUMA, M.; KLIMONT, Z.; MARANGONI, G.; LOTZE-CAMPEN, H.; OBERSTEINER, M.; TABEAU, A. & TAVONI, M. (2017). 'The Shared Socioeconomic Pathways and their energy, land use, and greenhouse gas emissions implications: An overview'. In: *Global Environmental Change* vol. 42, pp. 153–168.

RICHTER, S.; VÖLKER, J.; DWORAK, T.; FREIEDL; BORCHARDT, D.; DÖRR; R.-D; IRMER; JEKEL; KIRSCHBAUM; MATHAN; MEHLHORN; MOHAUPT; NAUMANN; RECHENBERG; STRATENWERTH; ROHRMOSER; WOLTER; BUSSKAMP & KIRCHMEYER (2010). *Water Framework Directive - The way towards healthy waters. Results of the German River Basin Management Plans 2009*. Ed. by GERMAN FEDERAL MINISTRY FOR THE ENVIRONMENT, NATURE CONSERVATION AND NUCLEAR SAFETY.

ROUNSEVELL, M. & METZGER, M. (2010). 'Developing qualitative scenario storylines for environmental change assessment'. In: *Wiley Interdisciplinary Reviews: Climate Change* vol. 1, no. 4, pp. 606–619.

SALMON, J.; FRIEDL, M. A.; FROLKING, S.; WISSER, D. & DOUGLAS, E. M. (2015). 'Global rain-fed, irrigated, and paddy croplands: A new high resolution map derived from remote sensing, crop inventories and climate data'. In: *International Journal of Applied Earth Observation and Geoinformation* vol. 38, pp. 321–334.

SAMANIEGO, L.; KUMAR, R. & ATTINGER, S. (2010). 'Multiscale parameter regionalization of a grid-based hydrologic model at the mesoscale'. In: *Water Resources Research* vol. 46, no. 5.

SCHALDACH, R.; KOCH, J.; AUS DER BEEK, T.; KYNAST, E. & FLÖRKE, M. (2012). 'Current and future irrigation water requirements in pan-Europe: An integrated analysis of socio-economic and climate scenarios'. In: *Global and Planetary Change* vol. 94-95, pp. 33–45.

SCHALDACH, R.; ALCAMO, J.; KOCH, J.; KÖLKING, C.; LAPOLA, D. M.; SCHÜNGEL, J. & PRIESS, J. A. (2011). 'An integrated approach to modelling land-use change on continental and global scales'. In: *Environmental Modelling & Software* vol. 26, no. 8, pp. 1041–1051.

SERRA, P.; PONS, X. & SAURÍ, D. (2008). 'Land-cover and land-use change in a Mediterranean landscape: A spatial analysis of driving forces integrating biophysical and human factors'. In: *Applied Geography* vol. 28, no. 3, pp. 189–209.

SIEBERT, S.; DÖLL, P.; HOOGEVEEN, J.; FAURES, J.-M.; FRENKEN, K. & FEICK, S. (2005). 'Development and validation of the global map of irrigation areas'. In: *Hydrology and Earth System Sciences* vol. 9, no. 5, pp. 535–547.

SIEBERT, S.; HENRICH, V.; FRENKEN, K. & BURKE, J. (2013). *Update of the digital global map of irrigation areas to version 5*. (Visited on).

SIEBERT, S.; KUMMU, M.; PORKKA, M.; DÖLL, P.; RAMANKUTTY, N. & SCANLON, B. R. (2015). 'A global data set of the extent of irrigated land from 1900 to 2005'. In: *Hydrology and Earth System Sciences* vol. 19, no. 3, pp. 1521–1545.

SIMPSON, N. P.; SHEARING, C. D. & DUPONT, B. (2019). 'Climate gating: A case study of emerging responses to Anthropocene Risks'. In: *Climate Risk Management* vol. 26.

SKOULIKIDIS, N. T.; VARDAKAS, L.; KARAOUZAS, I.; ECONOMOU, A. N.; DIMITRIOU, E. & ZOGARIS, S. (2011). 'Assessing water stress in Mediterranean lotic systems: insights from an artificially intermittent river in Greece'. In: *Aquatic Sciences* vol. 73, no. 4, pp. 581–597.

SOHL, T. & SAYLER, K. L. (2008). 'Using the FORE-SCE model to project land-cover change in the southeastern United States'. In: *Ecological Modelling* vol. 219, no. 1-2, pp. 49–65.

SOHL, T.; SLEETER, B. M.; SAYLER, K. L.; BOUCHARD, M. A.; REKER, R. R.; BENNETT, S. L.; SLEETER, R. R.; KANENGIETER, R. L. & ZHU, Z. (2012). 'Spatially explicit land-use and land-cover scenarios for the Great Plains of the United States'. In: *Agriculture, Ecosystems & Environment* vol. 153, pp. 1–15.

SUBRAMANIAN, M. (2019). *Anthropocene now: influential panel votes to recognize Earth's new epoch*. URL: `https://www.nature.com/articles/d41586-019-01641-5` (visited on 04/02/2020).

TAYLOR, K. E.; STOUFFER, R. J. & MEEHL, G. A. (2012). 'An Overview of CMIP5 and the Experiment Design'. In: *Bulletin of the American Meteorological Society* vol. 93, no. 4, pp. 485–498.

THENKABAIL, P. S.; BIRADAR, C. M.; NOOJIPADY, P.; DHEERAVATH, V.; LI, Y.; VELPURI, M.; GUMMA, M.; GANGALAKUNTA, O. R. P.; TURRAL, H.; CAI, X.; VITHANAGE, J.; SCHULL, M. A. & DUTTA, R. (2009). 'Global irrigated area map (GIAM), derived from remote sensing, for the end of the last millennium'. In: *International Journal of Remote Sensing* vol. 30, no. 14, pp. 3679–3733.

THOBER, S.; KUMAR, R.; WANDERS, N.; MARX, A.; PAN, M.; RAKOVEC, O.; SAMANIEGO, L.; SHEFFIELD, J.; WOOD, E. F. & ZINK, M. (2017). 'Multi-model ensemble projections of European river floods and high flows at 1.5, 2, and 3 degrees global warming'. In: *Environmental Research Letters* vol. 13, no. 1.

THORNTHWAITE, C. W. (1948). 'An approach toward a rational classification of climate.' In: *Geographical Review* vol. 38, no. 1, pp. 55–94.

TOLSON, B. A. & SHOEMAKER, C. A. (2007). 'Dynamically dimensioned search algorithm for computationally efficient watershed model calibration'. In: *Water Resources Research* vol. 43, no. 1.

TURNER, B. L.; LAMBIN, E. F. & REENBERG, A. (2007). 'The emergence of land change science for global environmental change and sustainability'. In: *Proceedings of the National Academy of Sciences of the United States of America* vol. 104, no. 52, pp. 20666–20671.

TZORAKI, O.; MORAETIS, D.; STAMATI, F.; NAVROZIDIS, S.; KOUSERI, E.; KALOGERAKIS, N. & NIKOLAIDIS, N. P., eds. (2008). *Fate of Olive Mill Wastewater in Evrotas River Basin*.

TZORAKI, O.; COOPER, D.; KJELDSEN, T.; NIKOLAIDIS, N. P.; GAMVROUDIS, C.; FROEBRICH, J.; QUERNER, E.; GALLART, F. & KARALEMAS, N. (2013). 'Flood generation and classification of a semi-arid intermittent flow watershed: Evrotas river'. In: *International Journal of River Basin Management* vol. 11, no. 1, pp. 77–92.

UNITED NATIONS ENVIRONMENT PROGRAMME (2004). *Global Environment Outlook Scenario Framework: Background Paper for UNEP's Third Global Environment Outlook Report (GEO-3)*.

VALDEMORO, H. I.; SÁNCHEZ-ARCILLA, A. & JIMÉNEZ, J. A. (2007). 'Coastal dynamics and wetlands stability. The Ebro delta case'. In: *Hydrobiologia* vol. 577, no. 1, pp. 17–29.

VAN ASSELEN, S. & VERBURG, P. H. (2013). 'Land cover change or land-use intensification: simulating land system change with a global-scale land change model'. In: *Global change biology* vol. 19, no. 12, pp. 3648–3667.

VAN VLIET, J.; BREGT, A. K.; BROWN, D. G.; VAN DELDEN, H.; HECKBERT, S. & VERBURG, P. H. (2016). 'A review of current calibration and validation practices in land-change modeling'. In: *Environmental Modelling & Software* vol. 82, pp. 174–182.

VAN VUUREN, D. P. & CARTER, T. R. (2014). 'Climate and socio-economic scenarios for climate change research and assessment: reconciling the new with the old'. In: *Climatic Change* vol. 122, no. 3, pp. 415–429.

VAN VUUREN, D. P.; EDMONDS, J.; KAINUMA, M.; RIAHI, K.; THOMSON, A.; HIBBARD, K.; HURTT, G. C.; KRAM, T.; KREY, V.; LAMARQUE, J.-F.; MASUI, T.; MEINSHAUSEN, M.; NAKICENOVIC, N.; SMITH, S. J. & ROSE, S. K. (2011). 'The representative concentration pathways: an overview'. In: *Climatic Change* vol. 109, no. 1-2, pp. 5–31.

VAN VUUREN, D. P.; KRIEGLER, E.; O'NEILL, B. C.; EBI, K. L.; RIAHI, K.; CARTER, T. R.; EDMONDS, J. A.; HALLEGATTE, S.; KRAM, T.; MATHUR, R. & WINKLER, H. (2014). 'A new scenario framework for Climate Change Research: scenario matrix architecture'. In: *Climatic Change* vol. 122, no. 3, pp. 373–386.

VASSOLO, S. & DÖLL, P. (2005). 'Global-scale gridded estimates of thermoelectric power and manufacturing water use'. In: *Water Resources Research* vol. 41, no. 4, p. 317.

VAUTARD, R.; GOBIET, A.; SOBOLOWSKI, S.; KJELLSTRÖM, E.; STEGEHUIS, A.; WATKISS, P.; MENDLIK, T.; LANDGREN, O.; NIKULIN, G.; TEICHMANN, C. & JACOB, D. (2014).

'The European climate under a 2C global warming'. In: *Environmental Research Letters* vol. 9.

Veldkamp, A. T. & Fresco, L. O. (1996). 'CLUE-CR: an integrated multi-scale model to simulate land use change scenarios in Costa Rica'. In: *Ecological Modelling* vol. 91, pp. 231–248.

Veldkamp, A. T. & Lambin, E. F. (2001). 'Predicting land use change'. In: *Agriculture, Ecosystems & Environment* vol. 85, pp. 1–6.

Verburg, P. H. (2010). *The CLUE model. Hands-on exercises*.

Verburg, P. H. & Overmars, K. P. (2007). 'Dynamic simulation of land-use change trajectories with the CLUE-s model'. In: *Modelling land-use change*. Ed. by E. Koomen. The GeoJournal library. Dordrecht: Springer.

— (2009). 'Combining top-down and bottom-up dynamics in land use modeling: exploring the future of abandoned farmlands in Europe with the Dyna-CLUE model'. In: *Landscape Ecology* vol. 24, no. 9, pp. 1167–1181.

Verburg, P. H.; Schulp, C. J. E.; Witte, N. & Veldkamp, A. T. (2006). 'Downscaling of land use change scenarios to assess the dynamics of European landscapes'. In: *Agriculture, Ecosystems & Environment* vol. 114, no. 1, pp. 39–56.

Verburg, P. H.; Soepboer, W.; Veldkamp, A. T.; Limpiada, R.; Espaldon, V. & Mastura, S. S. A. (2002). 'Modeling the spatial dynamics of regional land use: the CLUE-S model'. In: *Environmental Management* vol. 30, no. 3, pp. 391–405.

Vernooij, M.; Querner, E. P.; Jacobs, C. & Froebrich, J. (2011). *Flow characterization temporary streams: Using the model SIMGRO for the Evrotas basin, Greece*. Wageningen, The Netherlands.

Verweij, P. (June 2015). *About the iCLUE model calibration. Direct communication to Verena Huber García*.

Verweij, P.; Cormont, A.; Kok, K.; van Eupen, M.; Janssen, S.; te Roller, J.; Winter, W. d.; Pérez-Soba, M. & Staritisky, I. (2018). 'Improving the applicability and transparency of land use change modelling: The iCLUE model'. In: *Environmental Modelling & Software*.

Verweij, P.; Janssen, S.; Braat, L.; van Eupen, M.; Pérez-Soba, M.; Winograd, M.; Winter, W. d. & Cormont, A. (2016). 'QUICKScan as a quick and participatory methodology for problem identification and scoping in policy processes'. In: *Environmental Science & Policy* vol. 66, pp. 47–61.

Vigiak, O.; Lutz, S.; Mentzafou, A.; Chiogna, G.; Tuo, Y.; Majone, B.; Beck, H.; Roo, A. de; Malagó, A.; Bouraoui, F.; Kumar, R.; Samaniego, L.; Merz, R.; Gamvroudis, C.; Skoulikidis, N. T.; Nikolaidis, N. P.; Bellin, A.; Acuňa, V.; Mori, N.; Ludwig, R. & Pistocchi, A. (2018). 'Uncertainty of modelled flow regime for flow-ecological assessment in Southern Europe'. In: *Science of The Total Environment* vol. 615, pp. 1028–1047.

von Thünen, J. H. (1826). *Der isolierte Staat in Beziehung auf Landwirthschaft und Natinoalökonomie: oder Untersuchungen über den Einfluß, den Getreidepreise, der Reichthum des Bodens und die Abgaben auf den Ackerbau ausüben*. 1st edition. Hamburg: Perthes.

Wada, Y.; Wisser, D. & Bierkens, M. F. P. (2014). 'Global modeling of withdrawal, allocation and consumptive use of surface water and groundwater resources'. In: *Earth System Dynamics* vol. 5, no. 1, pp. 15–40. (Visited on 04/02/2020).

Wilcke, R. A. & Bärring, L. (2016). 'Selecting regional climate scenarios for impact modelling studies'. In: *Environmental Modelling & Software* vol. 78, pp. 191–201.

Willmott, C. J. & Feddema, J. J. (1992). 'A More Rational Climatic Moisture Index*'. In: *The Professional Geographer* vol. 44, no. 1, pp. 84–87.

WRIEDT, G.; VAN DER VELDE, M.; ALOE, A. & BOURAOUI, F. (2009a). 'Estimating irrigation water requirements in Europe'. In: *Journal of Hydrology* vol. 373, no. 3-4, pp. 527–544.

WRIEDT, G.; VAN DER VELDE, M.; ALOE, A. & BOURAOUI, F. (2009b). 'A European irrigation map for spatially distributed agricultural modelling'. In: *Agricultural Water Management* vol. 96, no. 5, pp. 771–789.

YANG, W.; ANDRÉASSON, J.; PHIL GRAHAM, L.; OLSSON, J.; ROSBERG, J. & WETTERHALL, F. (2010). 'Distribution-based scaling to improve usability of regional climate model projections for hydrological climate change impacts studies'. In: *Hydrology Research* vol. 41, no. 3-4, pp. 211–229.

ZAL, N.; BARIAMIS, G.; BALTAS, E. & MIMIKOU, M. (2017). *Use of Freshwater Resources in Europe 2002-2014 - An assessment based on water quantity accounts: ETC/ICM Technical Report 1/2017*. Ed. by A. KÜNTZER. Magdeburg, Germany.

ZINK, M.; KUMAR, R.; CUNTZ, M. & SAMANIEGO, L. (2017). 'A high-resolution dataset of water fluxes and states for Germany accounting for parametric uncertainty'. In: *Hydrology and Earth System Sciences* vol. 21, no. 3, pp. 1769–1790.

ZOMLOT, Z.; VERBEIREN, B.; HUYSMANS, M. & BATELAAN, O. (2017). 'Trajectory analysis of land use and land cover maps to improve spatial–temporal patterns, and impact assessment on groundwater recharge'. In: *Journal of Hydrology* vol. 554, pp. 558–569.

Appendix A

Appendix A: Storylines of SSP 1 & SSP 5

A.1 SSP 1: Sustainability—Taking the Green Road

The world shifts gradually, but pervasively, toward a more sustainable path, emphasizing more inclusive development that respects perceived environmental boundaries. Increasing evidence of and accounting for the social, cultural, and economic costs of environmental degradation and inequality drive this shift. Management of the global commons slowly improves, facilitated by increasingly effective and persistent cooperation and collaboration of local, national, and international organizations and institutions, the private sector, and civil society. Educational and health investments accelerate the demographic transition, leading to a relatively low population. Beginning with current high-income countries, the emphasis on economic growth shifts toward a broader emphasis on human well-being, even at the expense of somewhat slower economic growth over the longer term. Driven by an increasing commitment to achieving development goals, inequality is reduced both across and within countries. Investment in environmental technology and changes in tax structures lead to improved resource efficiency, reducing overall energy and resource use and improving environmental conditions over the longer term. Increased investment, financial incentives and changing perceptions make renewable energy more attractive. Consumption is oriented toward low material growth and lower resource and energy intensity. The combination of directed development of environmentally friendly technologies, a favorable outlook for renewable energy, institutions that can facilitate international cooperation, and relatively low energy demand results in relatively low challenges to mitigation. At the same time, the improvements in human well-being, along with strong and flexible global, regional, and national institutions imply low challenges to adaptation. Source: O'NEILL et al. (2017).

A.2 SSP 5: Fossil-Fueled Development—Taking the Highway

Driven by the economic success of industrialized and emerging economies, this world places increasing faith in competitive markets, innovation and participatory societies to produce rapid technological progress and development of human capital as the path to sustainable development. Global markets are increasingly integrated, with interventions focused on maintaining competition and removing institutional barriers to the participation of disadvantaged population groups. There are also strong investments in health, education, and institutions to enhance human and social capital. At the same time, the push for economic and social development is coupled with the exploitation of abundant fossil fuel resources and the adoption of resource and energy intensive lifestyles around the world. All these factors lead to rapid growth of the global economy. There is faith in the ability to effectively manage social and ecological systems, including by geo-engineering if necessary. While local environmental impacts are addressed effectively by technological solutions, there is relatively little effort to avoid potential global environmental impacts due to a perceived tradeoff with progress on economic development. Global population peaks and declines in the 21st century. Though fertility declines rapidly in developing countries, fertility levels in high income countries are relatively high (at or above replacement level) due to optimistic economic outlooks. International mobility is increased by gradually opening up labor markets as income disparities decrease. The strong reliance on fossil fuels and the lack of global environmental concern result in potentially high challenges to mitigation. The attainment of human development goals, robust economic growth, and highly engineered infrastructure results in relatively low challenges to adaptation to any potential climate change for all but a few. Source: O'NEILL et al. (2017).

Appendix B

Appendix B: GLOBAQUA Scenario Descriptors

TABLE B.1: Descriptor table for the GLOBAQUA scenarios.

Descriptor	MYOPIC	SUSTAINABLE
Society & Economy		
Growth per Capita	+++	++
Unemployment	—	—
Inequality Index	–	—
International trade or globalisation index	+++	++
Population growth (%)	-	-
Urbanisation	+++	+
Energy		
Use of fossil fuel (%)	+++	—
Hydropower production	0	+
Use of renewable resources (%)	0	+++
Efficiency index (% RE/FF)	—	+++
Oil price	0	+++
Environmental Effects		
Air Quality	—	++
Biodiversity	—	++
Invasive species	+++	-
Deforestation	++	-
Soil Degradation	++	–
Water Scarcity (quantity/quality)	+++	–
Water management		
Technical Measures	–	+
Non-Technical Measures	–	+++
Economic Measures	—	+++
Agriculture		
Irrigated surface area (ha)	++	–
Industrial agriculture (yield levels)	++	-
Irrigation efficiency (ha/m^3)	+++	+++
Organic agriculture (yield levels)	–	+++
Meat production	+	–
Farms with public vs. private irrigation	0	++
Use of pesticides	++	–
New pesticides' Env Effect	–	+
Area covered with water intensive crops (ha)	–	—

TABLE B.1: Descriptor table for the GLOBAQUA scenarios.

Descriptor	**MYOPIC**	**SUSTAINABLE**
Self-sufficiency	++	++
Organic fertilisers	–	–
Mineral fertilisers	++	—
Reuse of manure and by-products	+	++
Abandonment of land	+	-
Controlled drainage	+	+
Genetically modified crops	++	—
Crop rotation	+	+++
Erosion prevention	+	+++
Soil Salinisation	+	–
Subsistence agriculture	—	++
Industry		
Number of industries connected to WWT	++	+++
Investment emission reduction technology	0	++
Employees with higher education	+++	+++
Level of emissions	+++	–
Residential		
Water consumption/demand	0	–
Density urban – rural	++	+
Access to sanitation	+	+++
Equal participation in employment (gender)	++	++
Tourism & recreation		
Mass tourism	++	–
Selected tourism	0	+++
Policies		
Supports innovation	+	++
Investment in infrastructure	+	++
Protected areas	0	+++
Use of resources in alternative ways	-	+
Water quality standards	0	+++
Planning horizon	–	+++
Food security	+	++
Desalination for irrigation	+	–
Institutions International cooperation	+	+++
Focused on environmental issues	—	+++
Well-defined property rights	++	+++

Appendix C

Appendic C: Relevance of Scenario Descriptors - Ebro

TABLE C.1: Relevance of scenario descriptors as stressors in the Ebro according to case study experts.

Descriptor	Relevance
Society & Economy	
Growth per Capita	yes
Unemployment	no
Inequality Index	no
Urbanisation	yes
Energy	
Use of fossil fuel (%)	yes
Use of renewable resources (%)	yes
Environmental Effects	
Air Quality	no
Biodiversity	no
Invasive species	yes, key stressor
Deforestation	yes
Soil Degradation	yes
Water Scarcity (quantity/quality)	yes, key stressor
Water management	
Technical Measures	yes
Non-Technical Measures	yes
Agriculture	
Irrigated surface area (ha)	yes
Industrial agriculture (yield levels)	yes
Organic agriculture (yield levels)	(yes)
Meat production	yes, specially pigs
Use of pesticides	yes
Area covered with water intensive crops (ha)	yes
Organic fertilisers	yes
Mineral fertilisers	yes
Reuse of manure and by-products	(yes)
Abandonment of land	yes
Crop rotation	no
Erosion prevention	yes
Soil Salinisation	yes
Industry	

TABLE C.1: Relevance of scenario descriptors as stressors in the Ebro according to case study experts.

Descriptor	Relevance
Investment emission reduction technology	yes, if it is to the water
Level of emissions	(yes)
Residential	
Water consumption/demand	yes
Tourism & recreation	
Mass tourism	no
Selected tourism	yes, negative effects from fishing
Policies	
Protected areas	yes
Water quality standards	yes
Food security	no
Desalination for irrigation	no

Appendix D

Appendix D: Urban Water Demand - Ebro

TABLE D.1: Urban and industrial water demand [hm^3] per exploitation unit according to the RBMP for around the year 2010 (CHE 2013, Annex III) and values used to calculate the water demand per pixel.

Exp. unit	**Urban demand RBMP**	**Industrial demand RBMP**	**Sum urban +industrial**	**Calculated demand**	**Diff. [%]**
1	94.4	46.7	141.1	141.1	0.0
2	7.4	3.4	10.8	10.8	0.0
3	22.2	7.3	29.5	6.4	-78.4
4	14.9	7.6	22.4	22.4	0.0
5	14.4	6.6	21.0	21.0	0.0
6	0.8	0.2	0.9	0.9	0.0
7	1.0	0.3	1.3	1.3	0.0
8	2.3	2.5	4.8	4.8	0.0
9	7.1	1.1	8.2	8.2	0.0
10	1.7	0.3	2.0	2.0	0.0
11	17.4	8.8	26.1	26.1	0.0
12	28.1	9.1	37.2	37.2	0.0
13	35.3	7.3	42.6	42.6	0.0
14	22.2	9.7	31.9	31.9	0.0
15	10.5	4.2	14.7	14.7	0.0
16	53.3	17.6	70.9	70.9	0.0
17	24.6	14.8	39.4	39.4	0.0
18	1.3	0.0	1.3	1.3	0.0
Total	**358.9**	**147.3**	**506.2**	**483.1**	**Mean: -4.6**
Tranfers:					
Bilbao (unit 17)	81.7	37.8	119.5		
Tarragona (unit 11)	40.7	31.27	72.0		
others	12.5	1	13.5		
Total			**711.2**		